Effectiveness of Electrochemical Treatment of Municipal Sewage

Walaa Hirzallah

A Thesis

in

The Department

of

Building, Civil and Environmental Engineering

Presented in Partial Fulfillment of the Requirements
for the Degree of Master of Applied Science (Civil Engineering) at
Concordia University
Montreal, Quebec, Canada

March 2011

CONCORDIA UNIVERSITY

School of Graduate Studies

This is to certify that the thesis prepared

By: Walaa Hirzallah

Entitled: Effectiveness of Electrochemical Treatment of Municipal Sewage

and submitted in partial fulfillment of the requirements for the degree of

M.A.Sc in Civil Engineering

complies with the regulations of the University and meets the accepted standards with respect to originality and quality.

Signed by the final examining committee:

Dr. C. Mulligan Chair

Dr. S. Li Examiner

Dr. S. Williamson Examiner

Dr. C. Mulligan Examiner

Dr. M. Elektorowicz Co- Supervisor

Dr. J. Oleszkiewicz Co- Supervisor

Approved by: Dr. S. Alkass
Chair of Department or Graduate Program Director

Robin Drew
Dean of Faculty

Date 15th of April 2011

Abstract

Effectiveness of Electrochemical Treatment of Municipal Sewage

Walaa Hirzallah

Municipal wastewater was treated in four phases, using electrocoagulation batch reactors. In Phase I, a comparison between electrocoagulation (EC) and chemical coagulation showed enhanced effluent quality when EC is used. In Phase II, two concentrations of a conditioner were added to four-hour EC experiments at two different voltage gradients to increase conductivity and initiate electroflotation, thus improving solid-liquid separation. Complete phosphorus removal was observed in Phase II. However, the four-hour duration resulted in higher operating costs, especially given that flotation was achieved within the first 45 minutes.

Tests of Phase III were run using current densities of 10, 20 and 40 A/m^2 and treatment durations of 30, 60 and 120 minutes. In each run, four 1.5 L electrokinetic reactors were operated in parallel, with continuous and intermittent exposure to DC current. Wastewater samples from two treatment plants (WWTP1 and WWTP2), with different initial characteristics, were used to evaluate the treatment efficiency.

Phosphorus was entirely removed for all runs for WWTP1 and above 90% for WWTP2. Final COD concentrations after treatment were below 40 mg/L for both wastewater samples. Intermittent exposure prevented excess dissolution of the anodes, while allowing mixing and enhancing flocculation. Operating costs of the treated samples started at the level of 16 $CAD/1000m^3$ and depended on material and energy costs. The final phase compared flat and perforated electrodes in terms of material and energy consumption, as well as operating costs. It was demonstrated that the use of perforated anodes can reduce operating costs by 50-75%.

Acknowledgments

I earnestly thank Dr. Maria Elektorowicz and Dr. Jan Oleszkiewicz for their supervision and continuous support. I acknowledge the financial support from the NSERC STPGP 350666 Grant entitled "Submerged electrokinetic membrane bioreactor for excellent quality effluent" (awarded to Dr. M. Elektorowicz and Dr. J. Oleszkiewicz) and the "Graduate Students Support Program" of the Faculty of Engineering and Computer Science at Concordia University.

I would also like to thank my friends and laboratory colleagues for the great team work spirit that we shared, in addition to the help and support of the BCEE and HSE lab technicians and BCEE staff; namely Ms. Claire Therrien, Mr. Joe Hrib, Ms. Lorena Boju, Ms. Debbie Walker and Ms. Olga Soares.

This thesis couldn't have been possible without the support, help and love of my husband Tareq, and the unconditional love and prayers of my parents Wedad and Mohammed, and my brothers and sisters (Wisam, Muayyad, Helena, Muhannad, Ilknur, Wiaam, Fateen and Moath); I am sincerely grateful to them all for being the support and driving force that I needed.

Table of Contents

List of Figures

List of Tables

List of Symbols

$A_{effective}$: Effective surface area of electrode (m^2)

BOD: Biological oxygen demand (mg/L)

$C_{electrode}$: Electrode consumption (kg/ m^3treated wastewater)

$C_{electrolyte}$: Concentration of electrolyte (mole/L)

C_{energy}: Energy consumption (kWh/m^3treated wastewater)

COD: Chemical oxygen demand (mg/L)

d_b: Bubble diameter (length, μm)

DDL: Diffuse double layer

e_0: Electric charge (1.602 x 10^{-19} C)

E: Potential gradient/ Voltage gradient (V/cm)

EC: Electrocoagulation

EF: Electroflotation

F: Faraday's number (96485 Coulombs/mole)

F/M: Food to microorganisms ratio

F_B: Buoyancy forces (N)

F_D: Frictional force (N)

F_E: Electric filed force (N)

F_P: Pressure forces (N)

F_σ: Surface tension forces (N)

H: Number of hydrogen molecules generated per electron involved in redox reactions

H^+: Hydrogen ion

H_2O: Water

I: Electric current (Amps)

I: Ionic strength (mole/L)

J: Current density (A/m^2)

k: Boltzmann constant (1.381×10^{-23} J/K)

MBR: Membrane bioreactor

MLSS: Mixed liquor suspended solids (mg/L)

M_w: Molecular weight (g/mole)

n_{H_2}: Amount of hydrogen gas produced during EC-EF treatment (moles)

Q: Flow rate (Volume/time- m^3/ hour)

Q_{Joule} : Heat generated (Joules)

r: Radius of spherical particle (length)

SRT: Sludge retention time (hours)

t: EC Exposure duration (minutes, hours)

T: Temperature (K, C)

U: Voltage (V)

ΔU : Voltage drop (V)

V: Volume of reactor or of treated water (m^3)

Wt%: weight %

X_v: Volatile suspended solids concentration (mg/L)

z - z_{ion}: Ion valence

5'ON-5'OFF: 5 minutes ON - 5 minutes OFF

5'ON-10'OFF: 5 minutes ON - 10 minutes OFF

5'ON-20'OFF: 5 minutes ON- 20 minutes OFF

Greek Symbols

ε: Dielectric permittivity of solvent (dimensionless)

ε_0: Dielectric permittivity of vacuum ($8.854 \times 10^{-12} C^2 J^{-1} m^{-1}$)

ε_{gas}: Gas hold up (%)

κ^{-1} :Double layer thickness- Debye Length

ε_r: Dielectric permittivity of medium

F_σ: Surface tension forces (N)

ρ_{ion} :Number density of ions (m^{-3})

θ: Hydraulic retention time (hours)

μ: Viscosity (kg/ms)

v: Velocity of ion (m/s)

v_{H2O}: Flow of water due to electro-osmosis (m/s)

υ_{max}: Maximum ion velocity (m/s)

υ_p: Particle velocity/mobility (m/s)

v_{rise}: Bubble rise velocity (m/s)

ζ: Zeta potential (V)

Chapter 1 – Problem Statement

The process of treating wastewater involves many challenges that are not limited to the technical goals of maximizing water quality and solid/liquid separation. In developing a wastewater treatment method, one must also consider its overall environmental impact, usefulness in various industrial applications, ease of installation and operation, energy-efficiency, and cost-effectiveness. Today, many wastewater treatment units are employed all over the world, each having its advantages and disadvantages. This study aims to explore the use of electrocoagulation, a process that was developed over a century ago for treating wastewater and which can be applied to novel operation units these days.

Conventional treatment methods often induce a chemical reaction through the use of coagulants, flocculants, and other additives that aid in the removal or sedimentation of contaminants. In physical-chemical treatment units, sludge conditioning also requires the addition of polymers which change the properties of the wastewater and might decrease biodegradability (Bratby, 2006). Moreover, these treatment methods result in high sludge production, which in turn increases treatment cost. An alternative to that is to apply a treatment that yields similar or higher effluent quality but with lower sludge production.

The suggested alternative process is electrocoagulation. This process (i) requires no addition of chemicals that might contribute to increase the initial pollution level, (ii) is known for its low sludge production, (iii) generates dense flocs that are easily separable from the liquid phase, and (iv) achieves high quality effluents. Furthermore, the equipment used in the process is simple and readily operable equipment. This makes EC

an environmentally-friendly alternative to chemical coagulation and other treatment processes that require large serving areas for treatment facilities and staff.

Electrocoagulation can also be combined with other treatment units to improve the solid-liquid separation process. When coupled with membrane bioreactor processes, it has proven its effectiveness in removing colloids and suspended solids, hence avoiding fouling and increasing membrane filtration efficiency (Bani-Melhem & Elektorowicz, 2010).

The study is being conducted on wastewater sampled from different municipalities in the province of Quebec, where hydroelectric power is an essential natural resource. In 2008, hydroelectric power accounted for 96.75% of the total power available in Quebec (MNR, Quebec, 2008); therefore, it makes economic and practical sense to use it in treating the province's wastewater, in lieu of using chemicals that require storage, transportation, specific handling practices, in addition to producing secondary pollution.

Past investigations have focused on wastewaters with high contaminant and solid loads; meanwhile, the wastewater sampled for the purpose of this study was considered diluted. This characteristic encourages the investigation into the efficiency of electrocoagulation treatment for dilute water systems. The study focuses on phosphorus, nitrates, ammonia, COD, and turbidity of an effluent. Increased phosphorus levels in the wastewater can be reduced at the source by banning phosphate-based detergents; nevertheless, adequate treatment is required to avoid eutrophic conditions, which are created through excessive algal growth due to high consumption of phosphate and nitrogenous nutrients.

Eutrophication is a serious problem, especially in stagnant waters where most of the dissolved oxygen is depleted by algal growth, thus killing aquatic life (Thomann & Mueller, 1987). Phosphorus concentration is an indication of the status of a water body. Removal of nutrients such as nitrate and phosphorus before wastewater discharge is therefore necessary to avoid creating eutrophic conditions in the open water sources (Thomann & Mueller, 1987; Sincero & Sincero, 2003).

Nitrate removal is also important because high concentrations of nitrate in drinking water can cause irritability, muscle stiffness and pain, loss of appetite and nausea (Sabzali et al. 2006). Moreover, nitrate present in drinking water is converted by the body to nitrite, which then reacts with ferrous iron in the hemoglobin, oxidizing it to methomoglobin and thereby impairing the body's ability to transfer oxygen (Morris et al. 2009).

Electrocoagulation is a straightforward process that requires a short treatment time, making it ideal for treatment facilities with a very high flow rate. Time-intensive treatment processes require large reactors, especially when wastewater flow rates are high. The additional land and space requirements contribute significantly to the treatment's overall operating costs. This study is therefore targeted to investigate EC's potential to produce a high-quality effluent and a good solid-liquid separation in the shortest time, leaving the smallest possible financial and environmental footprints.

Chapter two - Literature Review

2. Wastewater

In the context of this thesis, wastewater is used water that is discharged by residential, industrial, and institutional buildings, as well as any other facility used by humans. The wastewater should be collected and treated before being discharged to surface waters. Each source of wastewater might contain different types of pollutants or impurities, each one contributing to its characteristics.

2.1 Wastewater Characteristics

Understanding wastewater treatment methods requires knowledge about different wastewater characteristics and components as defined by physical, chemical, or biological properties.

2.1.1 Physical Properties

Physical properties include color, odor, temperature, and the presence of solids. Before explaining the importance of these properties, brief information will be given about their sources in wastewater.

Solids: The presence of solids can have a positive or a negative impact, depending on the type of treatment used. In cases where biological treatment is used, solids concentrations are sometimes considered a design parameter of the reactor. When treated wastewater is discharged to receiving water bodies, high concentrations of solids, especially colloids, can cause turbidity (Metcalf & Eddy, 1979). Turbidity is defined as the cloudiness of the solution and is caused by the presence of particles, colloids, clays, organics, inorganics or

microorganisms (Shidong et al. 2009; Merzouk et al. 2010). High turbidity impedes the penetration of sunlight into the water, therefore inhibiting plant growth, which is a food source for aquatic organisms (Peavy et al. 1985). Moreover, sight-dependent fish face greater difficulty in finding their food when turbidity is extremely high (Missouri DC, 2001).

When suspended solids are discharged in aquatic environments without treatment, accumulation of solids can form a thick sludge that contributes to the creation of anaerobic conditions that will harm aquatic life. Anaerobic conditions are produced when oxygen is not available in sufficient quantity to sustain life.

Excess solids such as salts should also be monitored because a high concentration of salt in treated effluents can contribute to corrosion in the pipes transporting the water. Corrosion is a phenomenon that usually occurs when metals react with their surrounding environment and get oxidized releasing metallic cations. Moreover, if the water is to be reused domestically, the high salt concentrations, especially those of magnesium and calcium salts and carbonates, contribute to hardness of the water. Hardness is traditionally defined as the water's incapacity to react with soap; soap does not readily lather with hard water, making it impractical for domestic use (Metcalf & Eddy, 1979). However, scientifically, hardness is the quantity of multivalent cations present in solution. When present in excess concentrations, these cations react with ions in solution to produce insoluble solids (Peavy et al. 1985). Therefore, it is very important to manage solids during wastewater treatment and in treated effluents.

Odor: Odor results from decomposition of organic wastes and due to the presence of industrial wastes, contributing to the unpleasant smell. Odors from wastewater are usually very repulsive; if the odor sources are not eliminated before the wastewater is discharged to receiving bodies, especially if these are located near inhabited areas, various repulsive consequences can result. Bad odors result in several physical and psychological stresses on human beings, causing nausea, vomiting, loss of appetite, minimal water intake, respiratory problems, and mental disturbances (Metcalf & Eddy, 1979).

Color: Color in wastewater usually comes from the presence of colored constituents, the decomposition of organic matter, discharge of untreated wastes, septic discharge or surface runoffs (Peavy et al. 1985; Sincero & Sincero, 2003). Both color and odor give an indication of the water quality and source.

Temperature: Wastewater temperature is affected by the influents' temperatures and discharges, as well as infiltration and runoffs in cases of heavy rain or snowmelt (Metcalf & Eddy, 1979). Temperature is an important parameter that affects the efficiency of most treatment processes (Sincero & Sincero, 2003).

Temperature variations in receiving bodies have a big effect on aquatic life, since the solubility of oxygen in water decreases with increasing temperature. Dissolved oxygen is necessary for almost all organisms; the respiration process in aquatic living organisms and aerobic microorganisms requires dissolved oxygen. Therefore, monitoring water temperatures and dissolved oxygen is very important during the treatment processes and before discharge.

2.1.2 Chemical characteristics

Chemical characteristics of wastewater are defined by the chemical components such as organic and inorganic matter and characteristics such as pH and alkalinity. pH is a measure of how acidic or basic a medium is; pH is log of the concentration of hydrogen ions present in solution, which is determined by the degree of dissociation of water molecules, expressed in Equation 1:

$$H_2O \leftrightarrow H^+ + OH^- \quad (1)$$

When the concentrations of hydrogen ions are known, the pH can be calculated directly:

$$pH = -log_{10}[H^+] \quad (2)$$

pH is a very important parameter because it affects many reactions in addition to its effects on microorganisms and aquatic organisms. pH values during wastewater treatment are adjusted or maintained within a specific range, depending on the treatment process. Effluent discharge standards for pH vary between 6 and 9 (Environmental Commissioner of Ontario , 2010).

Alkalinity on the other hand represents the amount of ions present in the wastewater that can react with and neutralize hydrogen ions (Sincero & Sincero, 2003). Examples of such ions are carbonates, hydroxides, phosphates and ammonia. Although ammonia is not an ion, it contributes to alkalinity. Monitoring alkalinity of treated effluents is essential to avoid reactions between alkalinity and cations that can result in undesired precipitates (Peavy et al. 1985).

Organic compounds are composed of carbon, hydrogen and oxygen, which are sometimes combined with nitrogen, as is the case in proteins (Sincero & Sincero, 2003). Organics are often referred to as the carbon source, and can be classified as biodegradable or non-biodegradable. Biodegradable organics are mainly proteins, carbohydrates, and fats, which can be used up by living organisms and transformed into simpler forms. An example of such a process is aerobic degradation, where aerobic bacteria (aerobes) use oxygen to degrade or metabolize organic matter, usually producing carbon dioxide and water (LaGrega et al. 2001; Sincero & Sincero, 2003).

Biodegradable organic compounds are also degraded by anaerobic processes. As the name alludes to, this process occurs in the absence of oxygen, with methane gas as the main byproduct. Dissolved oxygen concentration in water reaches saturation at 8 mg/L, and aerobic conditions are present when dissolved oxygen levels are greater than 2 mg/L. Concentrations lower than 2 mg/L create anoxic conditions, whereas absence of dissolved oxygen leads to anaerobic conditions. The presence of organics is usually expressed in terms of biochemical oxygen demand (BOD) or chemical oxygen demand (COD). BOD represents the amount of oxygen needed by microorganisms to oxidize the organic matter biologically; meanwhile COD represents the amount of oxygen required to oxidize the organic matter through biological or chemical processes. Both measurements give an indication of the amount of organic compounds present (Metcalf & Eddy, 1979).

High BOD and COD in discharged wastewater indicate oxygen depletion in the natural system, potentially causing anaerobic conditions and affecting oxygen dependent living organisms. Although COD and BOD are measures of oxygen requirements, they are considered as pollutants and regulations are set by governments with respect to their

discharge to surface waters (Moreno-Casillas et al. 2007). Both BOD and COD are important parameters when designing wastewater treatment processes because they are used to estimate the process treatment efficiency (Sincero & Sincero, 2003).

Inorganic compounds include nutrients, heavy metals, salts, etc. Phosphorus and nitrogen are the most common nutrients in wastewater. Both are also important growth nutrients for microorganisms and should be treated before the effluent is discharge to water bodies to avoid conditions that stimulate algal growth in receiving water bodies. Algae grow on surface water when there is an excess of nutrient supply, resulting in decreased light penetration and oxygen solubility in water (Metcalf & Eddy, 1979). Algal presence can also create odor and taste problems in drinking water, and efforts must be taken to avoid creating conditions that encourage its growth close to drinking water supply sources.

Table 1 - Phosphorus Concentrations and Water Body Status (Environment Canada, 2007)

Status	Phosphorus Concentrations (mg/L)
Oligotrophic	**0.004–0.010**
Mesotrophic	**0.010–0.020**
Meso-eutrophic	**0.020-0.035**
Eutrophic	**0.035–0.100**

Water bodies with a high nutrient content are referred to as eutrophic; moderate concentrations result in what is known as mesotrophic conditions, and poor nutrient concentrations are known as oligotrophic conditions. Concentrations higher than 0.1 mg/L are considered hypereutrophic and require immediate remedial measures. To avoid

eutrophic conditions in water stream, it is recommended that total phosphorus concentrations in treated effluents do not exceed the standards set by the Ministry of Sustainable Development in Quebec.

Table 2 - Treatment Methods and Total Phosphorus Limits in Effluents (MDDEP-Quebec, 2002)

Treatment Method	Total Phosphorus Limits (mg/L)
Membrane Filtration	0.1
Physical-Chemical	0.5
Activated sludge	0.6
Biofiltration	0.6
Aerated Lagoons	0.8

The common phosphorus forms are orthophosphate, polyphosphate and organic phosphate; as for nitrogen, it is present in water as proteins, urea, ammonia, nitrates and nitrites. Ammonia is transformed to nitrate through the nitrification process and denitrification reduces nitrates to nitrites and nitrogen gas. Nitrogen transformation is mainly carried out biologically in the environment and in treatment plants, but chemical and physical removal also take place during treatment processes (Bratby, 2006).

2.1.3 Biological constituents

Viruses, bacteria, protozoa, algae, and fungi constitute the biological constituents of domestic wastewater (Metcalf & Eddy, 1979; Sincero & Sincero, 2003). These microorganisms exist in various sizes; therefore, the wastewater treatment should be chosen based on the type of microorganisms present. Bacteria play a major role in

decomposition of organic material and wastes, both in the environment and in wastewater treatment. Some bacteria are useful in wastewater treatment, such as the *nitrosomonas* and *nitrobacter*, which are responsible for nitrification and denitrification respectively (Mulligan, 2002). Meanwhile, other bacteria like *Escherichia Coli* or other coliform bacteria, which originate in colons of humans and animals, are often indicators of human and animal pollution. Human consumption of water or food contaminated with coliform bacteria can cause severe health problems such as gastroenteritis, bloody diarrhea, and death. Such was the case in Walkerton, Ontario in 2000, when drinking water became contaminated, causing over 2500 cases of illness and seven fatalities (Aylesworth-Spink, 2009).

Knowing the characteristics of wastewater and their importance during the treatment process, as well as in the ecosystem, is necessary before exploring the various types of treatment methods.

2.2 Wastewater Treatment

Wastewater treatment, like wastewater characteristics, is divided into biological, physical and chemical categories; in many cases, processes include more than one of these types. The following section will elaborate on each category, its design characteristics, and applications.

2.2.1 Biological Treatment

Biological treatment processes are also referred to as secondary treatment units, and as their name indicates, they always involve living organisms, mostly microorganisms.

Microorganisms need carbon, nitrogen and phosphorus as sources of energy. Since many types of wastewater already have high biodegradable organic content, wastewater is the perfect source of energy for microorganisms. Biological removal of these organics is done through their oxidation or transformation to less polluting compounds, or to structures that are easily separated by settling. Examples of biological treatment units are activated sludge, aerated lagoons, trickling filters, and anaerobic digesters. Wastewater treatment using activated sludge, aerated lagoons, and membrane bioreactors (MBR) is discussed below.

2.2.1.1 Activated sludge

The activated sludge process is a process that has been in use since the beginning of the 20th century. The process can be described as an aeration basin where microorganisms and wastewater are present together, forming what is known as mixed liquor. The aerobic bacteria culture and the wastewater stay in contact for a specific period of time, known as the hydraulic retention time (HRT), defined as the time that the water stays in a specific reactor (LaGrega et al. 2001). The hydraulic retention time is a design parameter in water treatment, and is controlled by two factors: the reactor volume and the flow rate into the reactor, as seen from Equation 3:

$$\boldsymbol{\theta = \frac{V}{Q}} \qquad \textbf{(3)}$$

Where θ is the HRT, V is the volume of the reactor and Q is the influent flow rate.

The HRT is chosen in order to allow the microorganisms to oxidize most of the organic matter. The wastewater then leaves the activated sludge reactor and enters a secondary

clarifier, or a settling tank (Figure 1). In the settling tank, heavy particles and colloids sink, leaving clean water at the top and heavy sludge in the bottom. The sludge from the settling tank is usually recycled back to the activated sludge reactor to maintain a microorganism balance in the reactor.

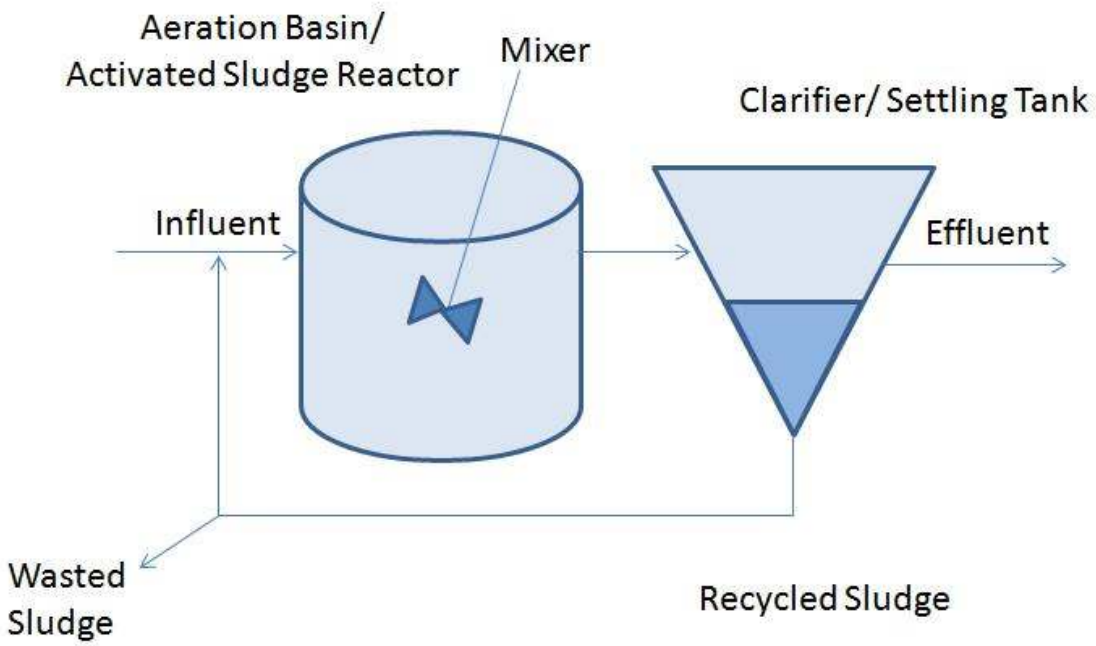

Figure 1 - Activated Sludge Reactor

Aeration and mixing are very important to maintain the mixed liquor in that state and to ensure enough oxygen to sustain the microorganisms, thus increasing treatment efficiency. The recycle stream contains microorganisms that have already been in the aeration basin; hence, recycling the sludge can improve the efficiency of the process, since the recycled microorganisms will have already adapted to the components to be treated.

The amount of sludge produced during the process increases as the concentration of the influent streams increases. The amount of sludge wasted and recycled depends on the

influent concentration, desired effluent concentration, and concentration inside the reactor. The microorganisms in the formed sludge need time to reproduce and consume substrates present in the reactor; this time is known as the sludge age. Sludge age is a very important design parameter in activated sludge reactors because it affects the concentration of microorganisms in the reactor and the properties of the flocs in the sedimentation basin (LaGrega et al. 2001). The time in the sedimentation tank or clarifier is not considered part of the sludge age, because in the anaerobic conditions of the clarifiers, the sludge becomes inactive. Sludge age is also known as sludge retention time (SRT) and is expressed in Equation 4

$$\boldsymbol{SRT} = \frac{\boldsymbol{V\,X_v}}{\boldsymbol{Rate\ of\ solid\ wasting}} \quad \textbf{(4)}$$

V= volume of reactor (m^3)

X_v= volatile suspended solids concentration (g/m^3)

Another important parameter when designing the activated sludge process is the sludge load, often known as food to microorganism ratio (F/M) (Sperling, 2007).

$$\frac{\boldsymbol{F}}{\boldsymbol{M}} = \frac{\boldsymbol{Q.BOD_5}}{\boldsymbol{V\,X_v}} \quad \textbf{(5)}$$

Typical F/M ratios are listed in Table 3.

Table 3 – Typical food to microorganisms ratio – F/M (Grimm, 2002)

Process	F/M range
Extended Aeration BOD	0.02 – 0.1 mg/L
Conventional F/M BOD	0.1 to 0.5 mg/L
High Rate Range BOD	0.5 – 2.5 mg/L

F/M ratio refers to the relationship between energy sources available in the influent and the amount of microorganisms in the reactor. Although the activated sludge process has proved efficient in the removal of BOD, COD and nutrients, the process is only applicable to high initial concentrations of suspended solids and BOD. As seen in Table 3, even with low F/M ratios extended aeration is required, thus resulting in elevated operating costs.

2.2.1.2 Aerated Lagoons

Aerated lagoons are natural or artificial bodies of water allowing for inflow and outflow of wastewater after a defined retention period. Treatment relies solely on the natural processes of biological purification that occurs in any natural water body. Organic wastes in aerated lagoons are decomposed by oxidation, synthesis, and endogenous respiration. Organic matter oxidizes to produce carbon dioxide, water and ammonia. Energy produced through oxidation converts some organic waste to new cell tissue (GNL, 2009).

Aerated lagoons retain wastewater for an extended period of time, thus stabilizing wastewater as heavier particles sink to the bottom and lighter ones rise to the surface. The hydraulic retention time gives microorganisms time to feed on the nutrients and trace elements in the water (Virginia Tech, 1996). Treatment is optimized by selecting the appropriate organic loading, hydraulic retention time (HRT) and pond depth in order to promote the maximum growth of organisms beneficial to the treatment process (Mara et al. 1992).

Aerated lagoons are built into or above the ground and lined with clay or other impervious materials to prevent groundwater contamination. The number and size of each lagoon, if more than one is required, depend on the wastewater inflow flow rate. However, systems that use several small lagoons have proven more effective than a single large lagoon.

Aerated lagoons create aerobic conditions through mechanical means. External energy is required to ensure sufficient oxygen supply through mechanical aerators. Mechanical mixers may also be required to ensure adequate distribution of oxygen throughout the lagoon and prevent conditions that lead to the creation of anaerobic zones. Mechanical aeration allows these lagoons to use 60% to 90% less land area than other natural wastewater treatment systems. Lagoons can be best applied for small communities, nevertheless, limitations of surface space or cold winter temperatures are two major limitations of the process (Metcalf & Eddy, 1979; Virginia Tech, 1996). Moreover, the accumulation of nutrients in the lagoons can results in lower removal when compared to other processes (Table 2).

2.2.1.3 MBR

Membrane bioreactors (MBRs) are units that combine membrane filtration with biological treatment units. They combine activated sludge with a membrane filtration unit to achieve superior effluent quality due to the simultaneous biological treatment of biodegradable pollutants and the total solid/liquid separation through filtration (Merz et al. 2007; Tian et al. 2009). MBRs therefore have the advantage of using less space, making them practical in areas with high population density. Furthermore, the use of a membrane results in improved solid/liquid separation, independently of sludge settleability (Artiga et al. 2007; Meng et al. 2007). Although MBRs have several advantages over conventional biological units, the operating costs are very high (Merz et al. 2007); therefore, thorough investigation should be carried out before installing an MBR unit to ensure feasibility and cost-efficiency of the project.

The membrane in the MBR reactor replaces the clarifier in the conventional activated sludge process train (Merlo et al. 2004; Ng et al. 2006; Sun et al. 2007; Mohammed et al. 2008). This technology is controlled by various parameters, such as hydraulic retention time (HRT), sludge retention time (SRT), mixed liquor suspended solids concentration (MLSS), reactor volume, flow rate, depth of membrane in the reactor and membrane pore size.

An advantage that MBRs have over other biological treatment units is the ability to operate at the range of high MLSSs (10- 40g/L), while typical biological units operate at a maximum of 6g/L. This is due to weaker settling at higher MLSS concentrations (Khor et al. 2006; Meng et al. 2007; Sun et al. 2007). Several studies were conducted to examine the effect of changing the MLSS concentration or SRT on the performance of

membrane bioreactors. A prolonged SRT, where almost no sludge is produced, has been investigated by various researchers. The advantage of that would be an extended retention of biomass, thus increased adaptation of microorganisms to the system; however, accumulation of inorganic compounds, inhibiting compounds or other by-products could be a limitation of prolonged SRTs (Han et al. 2005; Khor et al. 2006).

Khor et al. (2006) designed an MBR reactor consisting of a big reactor divided by a barrier into three segments naming them a C-Tank, an N-tank, and an M-tank. The C-tank was responsible for COD removal, whereas the N-tank was responsible for nitrogen removal and the M-tank for filtration. The team tested three different SRTs: 5days, 10 days, and prolonged; organic removal, inorganic accumulation and microbial activities were also tested. All three reactors showed more than 97% removal of organic compounds and no sign of inorganic accumulation.

Although the proposed design achieved high removal efficiencies; the investigations conducted by Khor et al. (2006) did not show the performance of a fully submerged membrane bioreactor. The separation in the design made it similar to a sequential batch reactor with a membrane filtration unit at the end; thereby increasing the space needed for such an installation.

Applications of submerged membrane bioreactors vary widely, and they can be used for the treatment of various types of wastewater; Tian et al. (2009) investigated treating drinking water with a submerged membrane bioreactor, and used powdered activated carbon as a source of energy for the microorganisms. Artiga et al. (2007) tested submerged membrane bioreactor treatment on winery waste which has properties

completely different than drinking water. The tests yielded high COD removal efficiencies higher than 97%, regardless of the initial concentration.

What determines the efficiency of a membrane bioreactor, other than contaminant and impurities removal efficiency is the ability of the membrane to operate under a constant flux. Darcy's law defines flux as the rate of volume flow rate per unit area, making it a function of volume, time and area. The flow rate of permeate through the membrane decreases with time as the pores become blocked. The blocking of the membrane pores is known as fouling.

The major limitation of the MBR technology is the fouling of the membrane, and research has been conducted over the past decade to improve the operational parameters and avoid fouling. Membrane fouling is caused by the depositing of particles on the membrane surface, blocking its pores (Bani-Melhem & Elektorowicz, 2010); therefore the amount of water passing through the membrane decreases. Different researchers investigated different foulants; but the major two contributing to fouling are suspended solids and colloids (Yang et al. 2006). Fouling of membranes decreases the membrane permeability and increases energy demand for pumping the water across the membrane (Tian et al. 2009). The energy for pumping results from the increase in trans-membrane pressure (TMP) which results from the decrease in permeate flux (Yang et al. 2006).

Suggestions to avoid membrane fouling include aeration (Ji & Zhou, 2006; Yang et al. 2006; Meng et al. 2007), back flushing of membrane with permeate (Ng et al. 2006); and operating at a flux lower than the critical flux (Ng et al. 2006; Yang et al. 2006; Wang et al. 2006). Aeration prevents fouling because the air pumped into the reactor helps to detach particles from the membrane surface and maintains sludge in suspension (Ji &

Zhou, 2006; Meng et al. 2007). Although aeration is thought of as a fouling alleviator, high aeration intensities could break big flocs into smaller flocs and increase the probability of fouling (Ji & Zhou, 2006); moreover, continuous aeration means that the dissolved oxygen in the reactor increases, therefore impeding the denitrification process, which needs anoxic conditions (Yang et al. 2006). The last and most important limitation of aeration is its high energy requirement; Meng et al. (2007) stated that more than 90% of energy consumption of a membrane bioreactor process is due to aeration.

The aforementioned suggestions involved controlling operating conditions in a reactor; however, some researchers have suggested modifying sludge characteristics as a solution to fouling problems. Common solutions applied are the addition of coagulants that help in improving aggregation and producing large flocs, the addition of powdered activated carbon to increase porosity, which helps adsorb and remove small colloids, or zeolites addition to improve sludge compressibility. To improve aggregate formation, Han et al. (2008) and Bagga et al. (2008) pretreated the water with chemical coagulation and electrocoagulation, and sent the effluent from pretreatment to the MBR reactor. Bani-Melhem & Elektorowicz (2010) investigated the alleviation of membrane fouling by electrocoagulation, where dense aggregates form and prevent membrane fouling. Their novel design involved a submerged membrane bioreactor in addition to immersed electrodes connected to an electric field. Results of the investigation showed significant decrease in membrane fouling with the addition of electrokinetic treatment. Coagulation and electrocoagulation processes are discussed in sections 2.2.2.2 and 2.2.2.3 respectively. Despite the good solid liquid separation and the high removal efficiencies discussed, biological processes are not practical for dilute water systems and have energy

intensive requirements due to aeration and membrane operations. A realistic alternative is the physical-chemical treatment.

2.2.2 Physical - Chemical Treatment

Physical- Chemical treatment of wastewater involves physical processes, where constituents do not undergo a chemical change, and chemical processes, where a chemical reaction or transformation takes place. The use of the word physical refers to the movement of particles or contaminants during the treatment process (Sincero & Sincero, 2003).

Conventional wastewater treatment is preceded by a pretreatment phase. After passing through the screening, the water is sent to a primary clarifier, where large sized particles that were not retained by screening would settle.

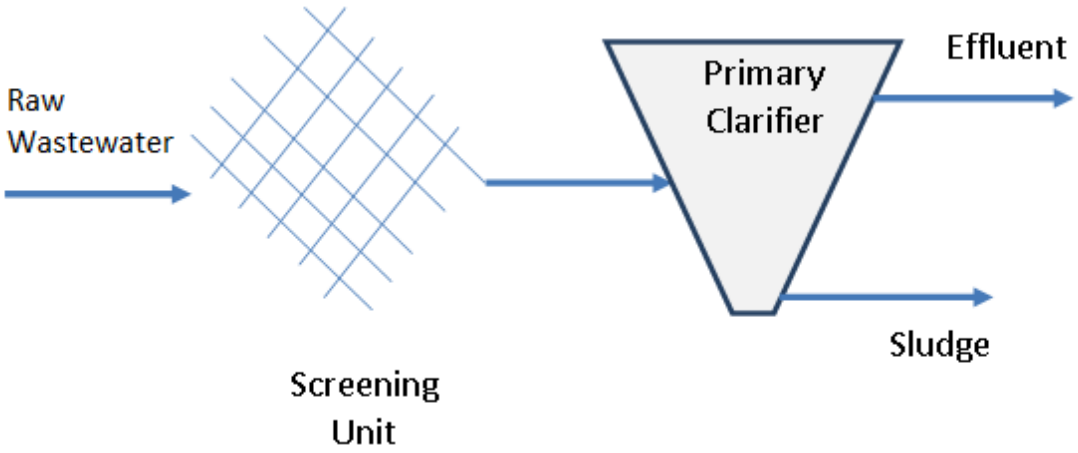

Figure 2 - Primary and Pretreatment Phases

The type of treatment seen in Figure 2 is entirely physical, there are no chemical interferences, and separation is mainly due to the movement of particles due to filtration

or gravity. The process demonstrated can be a pretreatment to biological treatment. However, if the treatment process is solely primary, then chemicals are added before the primary clarifier. Solids are separated from liquids by three processes: screening, settling and flotation.

Settling is another physical process that results in solids moving by gravity if it was a gravitational settling tank, or in many cases if centrifugal settling is employed, solids will move towards the driving forces (Sincero & Sincero, 2003). In settling tanks, the velocity and size of particles vary as the particles move down due to the adsorption and agglomeration of particles to form bigger settlable structures (Bratby, 2006). However, repulsive forces between particles in the settling tank can prevent the agglomeration phenomenon and retard the settling process.

Floatation is the rise of particles in a reactor under the influence of gas bubbles that rise to the surface. Usually fine air bubbles are introduced in a solution, forcing light solids to be carried to the surface. To separate the solids from the liquids, a skimmer can be used to separate the floated particles; alternatively the reactor walls can be leveled. Leveling is having a reactor that has a side adjacent to a reservoir for collection of floating material. Floating particles will be collected when they overflow over the wall of the tank into the reservoir as seen in Figure 3. Limitations of flotation process are the expenses resulting from introducing the gases to lift solid particles to the surface. Moreover, the repulsive forces existing between particles and colloids in the solution can hinder the proper solid liquid separation.

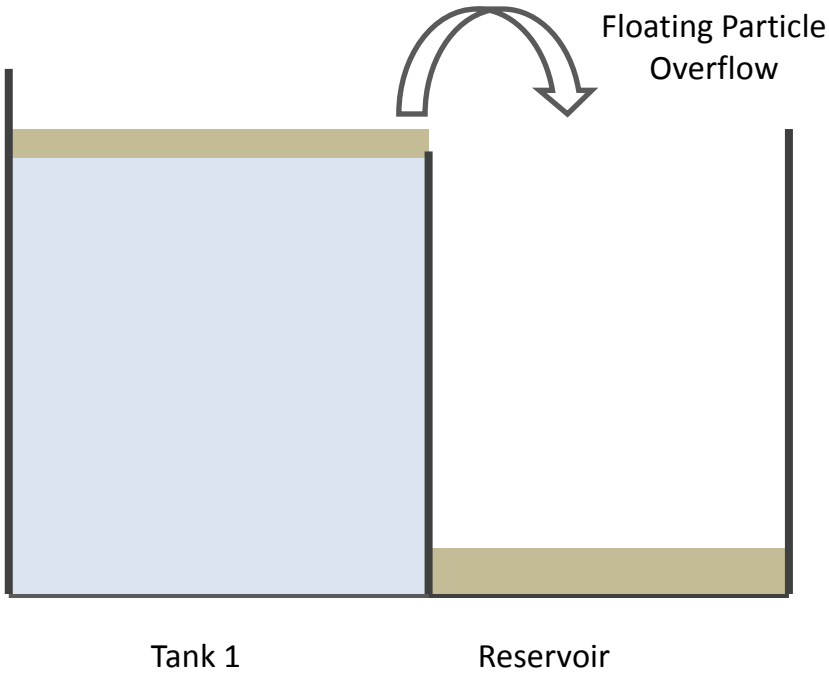

Figure 3 - Floating Particle Overflow

As noted so far, physical treatment does not convert contaminants to simpler, safer compounds before discharge into the environment; therefore, chemical treatment is needed to actually treat the wastewater (Sincero & Sincero, 2003). Conventional primary wastewater treatment plants usually remove nutrients and other impurities from the influent by the addition of chemical coagulants. This process involves destabilization of charge on colloids and weakening the attractive forces present in wastewater. It is important to destabilize the forces between colloids because stable colloids remain dispersed in the wastewater and are not readily separated (Bratby, 2006). When a coagulant is added, it reacts with functional groups on colloid surfaces, and reduces the surface charges. The destabilization results in colloid aggregation to form flocs which are then separated from water by settling, floatation, or precipitation (Holt et al. 2002; Wang

et al. 2005). The forces that affect floatation and settling are surface tension, bouyancy, and gravity as will be explained in section 2.2.2.3.

2.2.2.1 Surface Charge and Destabilization

Colloids in wastewater have mostly negative surface charges (Duan & Gregory, 2003; Bratby, 2006). The negative charges, along with the bipolarity of water molecules, result in water binding at the colloid-water interface, in addition to water molecule arrangements around the charged surface. The destabilization of the charge results in reduction of:

- surface charge
- number of adsorbed water molecules
- zone of influence of surface charge

Particles of opposite charges attract meanwhile those of same charges repel. Overlapping of the attraction and repulsion creates a charge separation were charges repel on each side and give a net charge of zero (point zero charge) – pzc (Bratby, 2006). The pzc of ions and charged particles have a capacitor- like structure that is the electrical double layer (Cosgrove, 2010). Gouy and Chapman introduced a model for the electrical double layer and defined it as “a charged surface and a diffused region of ions around the surface”. Stern then followed with a developed model including “a region in which ions are adsorbed and held to the surface” (Bratby, 2006). The Stern model divides the Electric Double Layer into Stern’s layer and the Diffuse Double Layer (DDL). Stern’s layer is the distance between the radii of hydrated positive ions and the negatively charged surface. The molecules in the DDL show Maxwell-Boltzmann distribution, which relates the

number of molecules present in the plane to the energy possessed by these molecules. Figure 4 shows the fixed Stern layer and the diffuse double layer explained by Stern and Gouy-Chapman (Bratby, 2006; Cosgrove, 2010).

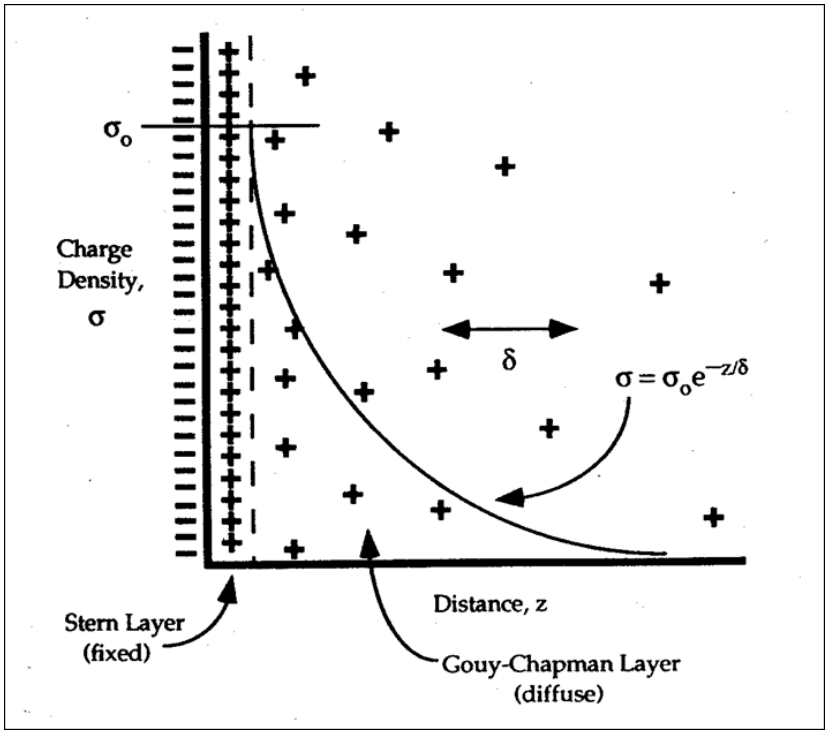

Figure 4 - Diffuse Double Layer (Texas A & M, 2009)

Electric Double layer: thickness of double layer is measure by the Debye Length κ^{-1} (Cosgrove, 2010)

$$\boldsymbol{\kappa^{-1} = \left(\frac{e^2 \sum \rho_{ion} z_{ion}^2}{\varepsilon_0 \varepsilon_r kT}\right)^{-1/2}} \quad \textbf{(6)}$$

- Where *e (Electronic charge)* = -1.609 x 10 $^{-19}$ C,
- ρ_{ion} is the number density of ions
- z_{ion} is the ion's valence
- ε_0 is dielectric permittivity of vacuum, 8.854x 10 $^{-12}$C^{2}J^{-1}m^{-1}.

- ε_r is the dielectric constant of medium (dimensionless),
- k is Boltzmann constant1.381 x10^{-23}JK^{-1}
- T is absolute temperature in Kelvin.

Therefore, the colloids start moving toward each other, and can be maintained in close proximity by Van der Waals forces of attraction (Zanello, 2003; Cosgrove, 2010). These forces are explained by a strong attraction between the electron cloud of an atom and the nucleus of an adjacent atom. Van der Waals forces can hold the atoms close together because they are stronger than repulsion forces when DDL has an adequately low thickness. The adsorption of polymers and ions, in addition to the formation of precipitate, contribute to destabilization (Bratby, 2006). Another force of attraction that helps in keeping molecules clustered is hydrogen bonding. Hydrogen sites from one molecule are attracted electrostatically to the oxygen sites of an adjacent molecule; holding them close together as a pair (Taniguchi et al. 2002).

Derjaguin, Landau, Verwey and Overbeek, introduced the DLVO theory, which estimates the total force between colloidal particles as a sum between the Van der Waal's forces and the double layer forces (Cosgrove, 2010). Charged ions in solution move under the influence of thermal agitation; as the ions move, they will most likely collide with stable colloids in suspension. This collision disturbs the stability of the colloids, causing them to move randomly known as the Brownian motion. Brownian motion allows the particles to be adsorbed on colloid surfaces.

Measuring the potential between the moving particle and the supporting liquid allows the quantification of the DDL, yielding a value known as zeta potential (Den & Huang, 2006). Zeta potential is the potential at the shear plane of the solid/liquid interface

(Cosgrove, 2010); it gives a good indication of colloid stability, ion adsorption, and the efficiency of coagulation and flocculation processes as will be shown in the next section.

$$\zeta = \frac{3v_p\mu}{2E\,\varepsilon_0\varepsilon} \quad (7)$$

Where ζ is the zeta potential (V)

μ is electrolyte viscosity (kg/ms)

ε_0 and ε are the permittivity of the vacuum and solvent respectively $C^2J^{-1}m^{-1}$

E is the potential gradient applied (V/m)

v_p is the particle velocity/mobility (m/s)

2.2.2.2 Coagulation

Destabilization of the electric double layer and the surface charge during coagulation is a result of the addition of metal coagulants (metal salts) and polymers (Bratby, 2006; Al-Amoudi et al. 2007). When metal salts are added, the ionic strength of the solution increases, leading to a thinning of the double layer and reduction in zeta potential (Duan & Gregory, 2003). The most common metal salts used in water treatment are aluminum sulphate $(Al_2 (SO_4)_3. xH_2O)$ and ferric chloride $(FeCl_3)$ because they have a high valance, readily available, and are cheaper than other chemical coagulants (Duan & Gregory, 2003; Ahmad et al. 2007). The hydrolysis of the salt and release of metal cations leads to neutralization of surface charge in negatively charged colloids, decreases DDL thickness followed by formation of insoluble hydroxides on which impurities can adsorb (Duan & Gregory, 2003; Ahmad et al. 2007).

Aluminum sulphate salt is known as alum and can be used in industry in its liquid or dry form. Liquid aluminum sulphate is corrosive and needs to be stored in corrosion- resistant tanks made of lead, plastic-lined steel, or 316 stainless steel (Bratby, 2006). When hydroxides are present in water, the following reactions take place upon addition of alum:

$$Al_2(SO_4)_3.14H_2O + 6\,OH^- \rightarrow 2Al(OH)_3 + 3SO_4^{2-} + 14H_2O \quad (8)$$

If carbonates are present in water, carbon dioxide will be produced:

$$Al_2(SO_4)_3.14H_2O + 6\,Ca(HCO_3)_2 \rightarrow 2Al(OH)_3 + 3CaSO_4 + 6\,CO_2 + 14H_2O \quad (9)$$

The hydroxides formed are insoluble and form the basis of floc formation; however, hydrolyzed sulphates are released in solution. The same reactions take place when ferric chloride is added; except that iron has two oxidation states, therefore both ferrous and ferric hydroxides form ($Fe(OH)_2$ and $Fe(OH)_3$) in addition to the chlorides being released in solution. Equations 8 and 9 describe the simple reactions that take place; however, upon hydrolysis of the coagulants, the hydroxides formed could polymerize to form metal hydroxide polymers, especially aluminum. Examples of aluminum hydroxide polymers are $Al_3(OH)_4^{5+}$, $Al_8(OH)_{20}^{4+}$, $Al_{13}O_4(OH)_{24}(H_2O)_{12}^{7+}$, etc. (Bratby, 2006).

Impurities and colloids can be adsorbed onto the hydroxide precipitate. The colloids present in the solution can be either entrapped inside the hydroxide flocs formed, or enmesh to the surface of hydroxides. The enmeshment is defined as sweep coagulation (Peavy et al. 1985). As the flocs get bigger, they start settling due to gravity; hence, adsorbing more particles from the solution. The settling velocity of the flocs increases as flocs become larger. Mixing is a vital step in the chemical coagulation treatment for it

ensures uniform coagulation, in addition to increasing the collisions between charged particles, hence, promoting flocculation (Peavy et al. 1985).

Treatment using chemical coagulation has been used on a variety of wastewaters such as dairy effluents (Tchamango et al. 2010), textile wastewater (Zongo et al. 2009), industrial wastewater (Meas et al. 2010), dye- polluted water (Canizares et al. 2006), pulp and paper wastewater (Ahmad et al. 2007), personal care product wastewater (El-Gohary et al. 2010), and soil leachate (Meunier et al. 2006). The main parameters studied were COD, turbidity, color, total solids (TS) and phosphorus.

TS removal occurs through physical and chemical processes, namely the coagulation and flocculation as aggregates form settleable structures. Turbidity removal is a consequence of the decrease in the concentration of total solids concentration. On the other hand, phosphorus in the form of phosphates is removed through a chemical reaction between phosphate ions and the metal cations in solution, which results in the formation of insoluble metal phosphates.

$$(Al_2(SO_4)_3).14\,H_2O + 2\,PO_4^{3-} \rightarrow 2\,AlPO_4 + 3\,SO_4^{2-} + 14\,H_2O \qquad (10)$$

$$4\,FeCl_3 + 3\,PO_4^{3-} \rightarrow FePO_4 + Fe_3(PO_4)_2 + 12\,Cl^- \qquad (11)$$

Both $FePO_4$ and $AlPO_4$ are insoluble, with solubility products of $10^{-21.9}$ and 10^{-21} respectively. However, alum is the recommended coagulant for phosphorus removal because ferric ion in $FePO_4$ can be reduced to ferrous ion, Fe^{2+} under anoxic or anaerobic conditions. Ferrous phosphate is soluble in water, thus re-releasing phosphates back into solution, or to a water body if released from sediments (Bratby, 2006).

Kabdasli et al. (2007) investigated the efficiency of three different coagulants in the treatment of dye-bath effluents: ferrous sulphate, ferric chloride, and alum. COD removal efficiencies were 61.6%, 66.1% and 62.8% respectively starting at an initial concentration of 310 mg/L. Kabdasli et al. (2007) concluded that ferric chloride is a better coagulant salt with respect to COD removal; nevertheless, the differences can be considered negligible. Similar comparisons were carried out by El- Gohary et al. (2010), using the same coagulant salts for COD removal on personal care products wastewater with an initial COD concentration of 2300 mg/L, as well as comparing the removal efficiencies for precipitation and flotation techniques for solid/liquid separation. Results for precipitation tests were 75.8%, 77.5 %, and 76.7% for ferric chloride, ferrous sulphate and alum respectively; differences were therefore not very significant. Flotation results were highest for alum 77.5 % and lowest for ferrous sulphate 67.7 %. Sludge volume index (SVI) measures were done after the experiments to evaluate the settleability of the sludge. Ferric chloride had the lowest SVI, while the poorest settling was with alum treatment. Alum treatment yielded the biggest volume of sludge and the lowest sludge solid content, therefore indicating high water retention of sludge produced. Tchamango et al. (2010) used alum to treat dairy effluents, and investigated the removal efficiencies of turbidity, phosphorus, nitrogen and COD. The highest removal rate was for turbidity (100%), followed by phosphorus (94%) and nitrogen (81%), and finally COD (63%). Results were based on a 30- minutes treatment and a coagulant dose of 0.414g/L; the pH of the solution dropped significantly upon addition of the coagulant, while conductivity increased. Bagga et al. (2008) also investigated the removal of solids and colloids to improve the filtration process and avoid fouling, using chemical coagulation as a

pretreatment to surface water microfiltration. The investigation findings showed an increase in fouling in the pH range of 6.4 – 8.3, and that low concentrations of coagulants (< 10 mg/L) did not produce flocs large enough to avoid fouling. Fouling decreased with iron concentrations greater than 10 mg/L; therefore, pH and the coagulant dose are very important parameters for efficiency of a coagulation/flocculation treatment process.

The most important parameters in the chemical coagulation process are the pH and the coagulant dose, as seen from the findings of the aforementioned researchers (Duan & Gregory, 2003; Sincero & Sincero, 2003; Bratby, 2006). The formed metal hydroxides show a point of zero charge, and that is the pH, where the hydroxides exhibit a zero surface charge (Duan & Gregory, 2003). Particle aggregation is enhanced as pH increases towards the i.e.p. due to a decrease in stability. Correct coagulant dosage is important for many reasons:

- An excessive dose can contribute to charge reversal, increasing colloid stability (Duan & Gregory, 2003; Mouedhen et al. 2008)
- Excess salt can contribute to increasing conductivity of the treated solution
- An excessive dose can contribute to increasing turbidity of solution (Duan & Gregory, 2003)
- An excessive dose can contribute to increasing TSS content (Ahmad et al. 2007)
- An excessive dose directly contributes to an excess of chemicals that will pollute receiving bodies if not treated further
- An excessive dose drives up the overall cost due to an increase in coagulant cost
- An excessive dose leads to larger settled sludge volumes, contributing to increase sludge handling costs

- An insufficient dose will result in an incomplete treatment process
- An insufficient dose does not release enough cations to destabilize charges

The right coagulant dosage is determined by evaluating the change in zeta potential; the optimal coagulant dose is found when the zeta potential value approaches zero mV. Achieving better flocculation without the risk of excess coagulant dosage, synthetic polymers with high molecular weight are added to help produce heavier flocs (Das et al. 2009). Since the step that follows coagulation and flocculation is usually sedimentation, it is important to produce flocs that will readily settle. Dense flocs are desirable in water treatment because they have better settling and less water retention properties, therefore enhancing the dewatering process (Wang et al. 2006; Ni'am et al. 2007). Polymers bring about two types of interactions: bridging interactions and charge neutralization, both of which help in aggregation and production of dense flocs (Bratby, 2006; Cosgrove, 2010).

The chemical coagulation studies presented showed that a significant amount of chemicals, namely coagulant salts, polymers, and buffers, is necessary to be added to the wastewater treatment process; therefore increasing both the environmental footprint and costs of the treatment. Particularly considering that chemicals needed for the treatment are not fully consumed during the process, and that the unused portion remains in the treated wastewater, which is in some cases directly discharged to water bodies. Moreover, the chemicals used in the treatment require special transportation, handling and storage; subsequently, adding to the costs of the treatment. Another drawback of using chemical coagulants is the high amount of chemical sludge produced during the treatment which contributes to more dewatering costs (Sincero & Sincero, 2003). These limitations encourage exploring an alternative treatment process that eliminates high sludge

production (Khoufi et al. 2007), the addition of coagulant salts, polymers, and buffers, and yields superior effluent quality.

2.2.2.3 Electrocoagulation

Interest in improving physical- chemical treatment, along with increasing environmental awareness, is fuelling the drive to minimize the use of chemical products in water treatment. Electrocoagulation (EC) is a process that does not require the addition of any chemical coagulants; the coagulation- flocculation process is very similar to chemical coagulation, except that the coagulant is generated in-situ through the dissolution of sacrificial anodes that are connected to an electric current (Can˜izares et al. 2005; Hansen et al. 2005, 2007; Meunier et al. 2006; Drouiche et al. 2008).

The EC process eliminates contaminants through several steps: (i) electro-oxidation of the anode and release of metallic cations in solution, (ii) electro-migration and electrophoresis, which are the movements of charged ions and colloids, respectively, in the direction of electrodes of opposite charge resulting in destabilization of charges in solution, (iii) collisions and interactions between moving particles causing compression of the double layer, hence coagulation, (iv) adsorption of the solids, colloids and other contaminants on the coagulated particles, forming bigger aggregates, (v) separation of aggregates by settling or flotation as a result of hydrogen gas generation at the cathode (Kobya et al. 2006; Ni'am et al. 2007; Ghernaout et al. 2008; Liu et al. 2010).

The process involves connecting metal electrodes to a direct current generator. The chosen metal should be suitable for use as sacrificial anodes; that is, it should produce metal cations in the solution (Meunier et al. 2006; Hansen et al. 2007). Aluminum and

iron are the materials of choice because they produce a higher valence (Merzouk et al. 2010). Hydroxyl ions and hydrogen gas form at the cathode, and metal ions are released at the anode by electrolytic oxidation of the metal electrode.

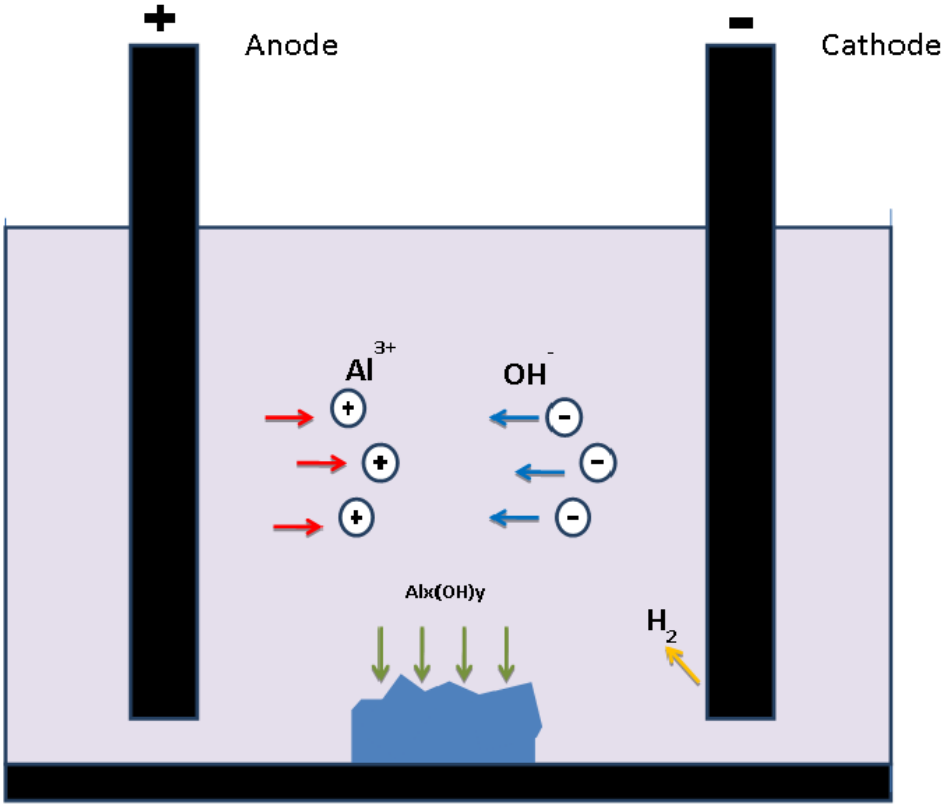

Figure 5 – Schema of Electrocoagulation Process in Wastewater

To further elaborate on the mechanism described above, the REDOX reactions at the anode and cathode are as follows:

Example 1: Aluminum anode

$$\boldsymbol{Anode}: \boldsymbol{Al \rightarrow Al^{3+} + +3e^{-}} \quad \textbf{(12)}$$

$$\boldsymbol{Cathode}: \boldsymbol{3H_2O + 3e^{-} \rightarrow 1.5\,H_2 + 3OH^{-}} \quad \textbf{(13)}$$

$$\boldsymbol{Overall}: \boldsymbol{Al + 3\,H_2O \rightarrow 1.5\,H_2 + Al(OH)_3} \quad \textbf{(14)}$$

Example 2: Iron anode

$$\boldsymbol{Anode: Fe \rightarrow Fe^{2+} + 2e^{-}} \quad \textbf{(15)}$$

$$\boldsymbol{Cathode: 2H_2O + 2e^{-} \rightarrow H_2 + 2OH^{-}} \quad \textbf{(16)}$$

$$\boldsymbol{Overall: Fe + 2H_2O \rightarrow H_2 + Fe(OH)_2} \quad \textbf{(17)}$$

Or

$$\boldsymbol{Anode: Fe \rightarrow Fe^{3+} + 3e^{-}} \quad \textbf{(18)}$$

$$\boldsymbol{Cathode: 3H_2O + 3e^{-} \rightarrow 1.5\, H_2 + 3OH^{-}} \quad \textbf{(19)}$$

$$\boldsymbol{Overall: Fe + 3H_2O \rightarrow 1.5\, H_2 + Fe(OH)_3} \quad \textbf{(20)}$$

Therefore, the general equations to describe the reactions occurring during the EC process are:

$$\boldsymbol{Anode: M \rightarrow M^{n+} + ne^{-}} \quad \textbf{(21)}$$

$$\boldsymbol{Cathode: 2H_2O + 2e^{-} \rightarrow H_2 + 2OH^{-}} \quad \textbf{(22)}$$

As mentioned earlier, the charged particles move toward the oppositely charged electrodes. Concentrations of charged particles in addition to the strength of electric field control the thickness of the double layer which is numerically represented as zeta potential. Ionic strength of the solution is related to both the concentration of electrolyte and the valence of the ion (Bratby, 2006).

$$\boldsymbol{I = \frac{C_{electrolyte} z^2}{2}} \quad \textbf{(23)}$$

$$\boldsymbol{\frac{1}{\kappa} = \frac{2.0\, x\, 10^{-8}}{\sqrt{I}}} \quad \textbf{(24)}$$

Where I = Ionic strength

κ^{-1}= Double layer thickness,

z= valence of ion

$C_{electrolyte}$ = Concentration of electrolyte (moles/L)

Concentration of moving charged particles from the bulk of solution to the electrode surface are affected by the distance of the particle from the electrode and the time needed for the movement of particles (Zanello, 2003). Although ions or molecules of the same charge can be present close to the electrode surface, the forces of attraction between the charged particles and electrode surface are stronger than the repulsive forces. Movement of ions and charged particles under the influence of electric field is demonstrated in Figure 6.

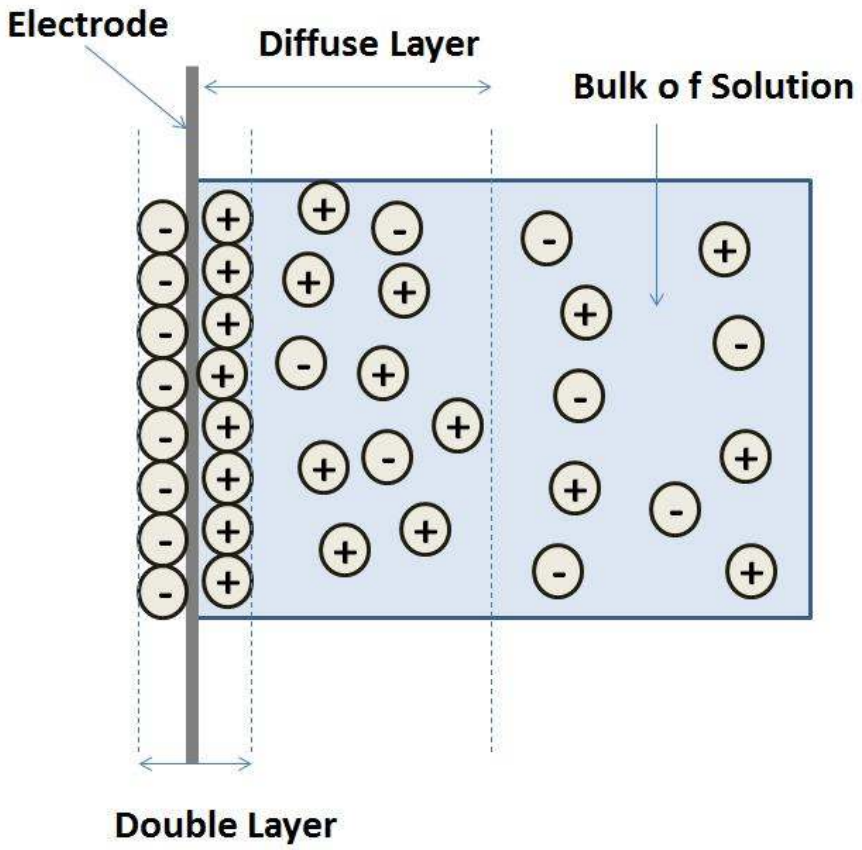

Figure 6 - Electrode/Solution interface

When setting electric parameters in an electrocoagulation experiment, voltage gradient or current density should be fixed. Electrical conductivity represents the amount of electrons available to carry charges and allow the passing of the current; thus, it is the measure of the mobility of ions in a solution (Valenzuela et al. 2002). Once an electric field is applied to a conductor material, electric forces act on charged particles in solution, causing them to move to electrodes of opposite charge, producing an electric current. Two forces act on ions in solution in an electrochemical cell: electric field forces and frictional forces. These forces can be expressed as:

$$F_E = ze_oE \tag{25}$$

$$F_D = 6\pi\mu r v \quad (26)$$

WhereF_E = electric field force

F_D= frictional force

E= electric field – voltage gradient (V/m)

e_o=electric charge = 1.602×10^{-19} Coulombs

μ = viscosity (kg/ms)

r= radius of a spherical ion (m) – spherical assumption

v= velocity of ion (m/s)

z = ion valence

The maximum ion velocity is derived by balancing the equations of both forces, as shown in equation 26

$$zE = 6\pi\mu r v \rightarrow v_{max} = \frac{ze_oE}{6\pi\mu r} \quad (27)$$

Ion mobility in an EC treatment process depends on ion size, its valence, the solution viscosity, the applied voltage, the spacing between the electrodes, and the solution temperature. The solution temperature influences ion mobility indirectly as it affects viscosity (Valenzuela et al. 2002).

During EC treatment, positively charged ions are generated then stabilized by the negatively charged particles in the solution, producing heavy flocs (Merzouk et al. 2010). The metal cations and the hydroxyl anions form metal hydroxide coagulants on which solids, metals and other impurities are adsorbed (Bagotsky, 2006). Moreover, the electroflocculation process can be enhanced due to the increased particles collisions resulting from the generation of gases at the cathode and anode and the movement of

charged particles to oppositely charged electrodes. Oxygen gas can be produced at the anode in addition to chloride ions being oxidized to chlorine gas; however, the dominant oxidation reaction in non-inert anodes is the corrosion of the anode material. These gases are not produced in significant quantities in electrocoagulation treatment, therefore are not presented in Figure 5.

The adsorption of the solids and impurities on the metal hydroxides creates amorphous flocs that either sink as sediments, if the flocs are heavy enough, or float on the surface if the flocs are lighter. Amorphous nature of flocs formed can increase the surface area, hence increasing adsorption of suspended particles and colloids to the flocs and enhance solid-liquid separation (Gomes et al. 2007). However, light flocs float as a result of the upward force of hydrogen gas molecules and other gases that can be generated during the EC process; plenty gas generation can impede settling of the flocs.

A disadvantage of electrocoagulation though is the passivation of the anode, which occurs when an oxide layer covers the anode, decreasing the current efficiency and hence the overall process efficiency. Passivation of the anode gives a strong indication about the prolonged existence of an EC process (Holt et al. 1999). However, this passivation decreases with voltage decrease; and can be considered during the designing process. Another limitation can be the high price of energy in developing countries.

Some researcher (Canizares et al. 2006; Ni'am et al. 2007) concluded that EC produces denser flocs which have higher stability and are more readily separated from the solution. A reason for the denser floc production is electro-osmosis, a process that involves the movement of water out of the flocs under the influence of an electric field (Tuan et

al.2008). The following equation relates the velocity at which the water particles move due to electro-osmosis and to the potential gradient applied and zeta potential:

$$\boldsymbol{\upsilon_{H_2O} = \frac{\varepsilon\varepsilon_0\zeta}{\mu} E} \quad \textbf{(28)}$$

Where υ_{H_2O} is the flow of water due to electro-osmosis (m/s)

ζ is the zeta potential (V)

μ is electrolyte viscosity (kg/ms)

ε_0 and ε are the permittivity of vacuum and solvent respectively $C^2J^{-1}m^{-1}$

E is the potential gradient applied (V/m)

Therefore, apart from the fluid proerties, the electroosmotic flow is affected by the voltage applied and the spacing between the electrodes.

EC treatment systems are flexible, and that makes them ideal for treating a wide variety of effluents, e.g. seawater (Timmes et al. 2009), domestic effluents (Lin et al. 2005), dairy effluents (Tchamango et al. 2010), industrial effluents (Meas et al. 2010), heavy metal contaminated wastewaters (Hansen et al. 2005; Hansen et al. 2007), dye-polluted wastewaters (Kabdasli et al. 2007; Phalakornkule et al. 2010), textile effluents (Zongo, et al. 2009; Merzouk et al. 2010), restaurant food industry (Chen et al. 2000; Kobya et al. 2006), and oil industries (Bensadok et al. 2008).

All cited studies have shown that EC is effective in destabilizing charge and forming aggregates; however, each study investigated different parameters and operational conditions. Zongo et al. (2009) evaluated the efficiency of EC treatment in COD and turbidity removal from textile wastewater. They tested aluminum and iron anodes at

current densities in the range of 50 -200 A/m^2. A total turbidity removal and a COD removal rate 74-88% were achieved, starting from about 1500 mg/L. Removal efficiencies were not very different for both electrode materials; however, settling of aluminum formed gelatinous flocs that were better than the brown iron precipitates because the brown color contributed to changing the water quality. The process energy requirements were evaluated with respect to COD removal. The study found that 1.75 kWh/m^3 and 1.53 kWh/m^3 were consumed using iron and aluminum, respectively, to treat 1000 mg/L of COD; therefore using aluminum electrodes would reduce the energy requirements of the treatment. Nevertheless, the researchers found that energy consumption can be reduced by 30% if the solution conductivity was increased using sodium chloride.

Zodi et al. (2009) also investigated COD and turbidity removal from textile wastewater using both iron and aluminum anodes in the current density range of 50 – 200 A/m^2 to assess settling characteristics of sludge produced after treatment. A COD removal rate of 95% for initial COD concentration of 3200 mg/L was achieved in this investigation. The same COD removal efficiency was also reported by Meas et al. (2010), which was satisfactory for water recycling standards. Final COD concentrations achieved by the above-mentioned researchers were higher than standard effluent discharge limits; therefore, further treatment was required. At the current densities tested by Zodi et al. (2009), iron- treated wastewater had SVI values that were significantly lower than those of aluminum- treated wastewater, indicating better settling with iron treatment. The effect of treatment time on iron settling was not tangible, while settling characteristics of

aluminum-based flocs deteriorated as treatment time increased. This trend can be attributed to the gel-like hydroxides that form with aluminum.

Ni'am et al. (2007) investigated turbidity and COD removal using iron electrodes to treat synthetic wastewater at currents varying from 0.5- 0.8A. The effect of treatment time and settling time was also investigated. Similar results to the aforementioned investigations were observed with respect to turbidity removal; effluent turbidity was about 9 NTU. The highest observed COD removal rate was 75.5% starting with an initial concentration of 1140 mg/L. Findings proved that COD removal increases at higher currents, treatment times, and settling times.

COD removal efficiencies obtained by many researchers were mostly between 60 – 80%. Moises et al. (2010) designed a continuous electrocoagulation activated sludge system to improve color, turbidity and COD removal. The continuous system consisted of an electrocoagulation unit using aluminum electrodes, followed by a clarifier and a biological reactor. COD removal efficiency after EC treatment was 59%, but the overall removal efficiency was 80%. The pretreatment with EC can reduce the time needed in a biological reactor. The treatment duration applied was 45 minutes in the EC reactor and 6 hours in the biological reactor. The type of wastewater treated by Moises et al. (2010) had a conductivity of 6.7 ± 1.3 mS, making it a very good candidate for EC treatment, since energy requirements are very low at such a high conductivity. Although Moises et al. (2010) described their system as a combination system, the configuration applied served as a pretreatment to biological treatment.

The differences in COD removals can be explained by the fact that sugars, alcohols, phenols and other chemicals that do not react with the generated metallic cations remain in solution. These chemicals contribute to the COD measure if not absorbed into or adsorbed onto flocs; therefore, COD can remain unchanged after treatment (Moreno-Casillas et al. 2007). Municipal wastewater contains compounds of different sources; as a result, COD is only partially removed in most cases (Moreno-Casillas et al. 2007). After a coagulation treatment, the remaining COD portion is mainly the soluble COD (Bratby, 2006).

Research also expanded to investigate the performance of EC in eliminating coliform bacteria. Ghernaout et al. (2008) applied EC treatment to surface waters testing three anode materials: aluminum, steel and stainless steel. Four different current densities were tested: 20, 50 100 and 200 A/m^2 during 35 minutes of treatment. At current densities 20 and 50 A/m^2, decrease in *E.coli* culture was not observed rapidly; however, at 100 and 200 A/m^2, a significant decrease in bacterial count was noted. Thirty minutes were sufficient to completely eliminate *E.coli* and algae at all currents and treatment times tested; however, the study showed that aluminum electrodes were more efficient than steel and stainless steel electrodes on *E.coli* destruction (Ghernaout et al. 2008). Linares-Hernandez et al. (2009) also investigated the removal of coliforms using electrocoagulation, and a 99% coliform destruction rate was obtained using aluminum-iron electrodes at a current density of 45.45 A/m^2 and at pH 8. Coliform removal was coupled with 69%, 71%, 83% and 80% reduction of COD, BOD_5, color, and turbidity, respectively. Therefore, electrocoagulation can be used for disinfection at high current densities and long exposure durations.

One of the major environmental concerns for surface waters is eutrophication. A major factor in mitigating the effects of eutrophication is contaminant reduction at the source, by using phosphate-free detergents, for example. However, the presence of phosphates in domestic wastewaters is inevitable. Phosphorus is present in plants and animals, and finds its way to domestic wastewater through human waste (Sincero & Sincero, 2003). As described earlier, phosphorus removal can be carried out biologically by microorganisms, or by precipitating phosphates using metallic cations. EC can therefore be an alternative treatment mechanism for the removal of phosphorus from wastewater. Given that 60% of the phosphorus in domestic wastewater comes from urine, Zheng et al. (2009) ran EC experiments on male urine in order to assess the feasibility of reducing phosphorus at the source. Current densities tested were between 10 and 50 A/m^2, and the gaps between electrodes ranged from 5 to 40 mm. Removal efficiency of phosphorus increased as current density and treatment time increased. The optimal gap chosen was 5 mm, and at current density 40 A/m^2, 98% phosphorus removal was achieved after 20 minutes of treatment. Initial phosphorus concentration was 490.2 mg/L. Increasing the distance between the electrodes had no effect on phosphorus removal, but caused a significant increase in energy consumption. Despite obtaining such a high removal rate, using an iron electrode can lead to phosphates being released back into the wastewater. Under anaerobic conditions, iron (III) phosphate is reduced to soluble iron (II) phosphate. This problem can be avoided if aluminum electrodes are used for phosphorus removal, since aluminum has only one oxidation state.

If phosphorus levels in surface waters are not controlled, phosphorus can contaminate drinking water sources and ground waters. Vasudevan et al. (2008) studied the removal of

phosphates from drinking water by electrocoagulation using mild steel anode material. Five different current densities in the range of 0.01 to 0.05 A/dm^2 were tested. Removal efficiencies of phosphates increased as current density increased. Maximum removal for each current density was achieved after 20 minutes of treatment; any increase in treatment time after this period yielded no additional phosphate removal. The maximum removal efficiency was 98% and the lowest was 68%. The effect of pH change on removal efficiency was also assessed; the highest removal rate was noted at pH 6.5. Although similar removal efficiencies were observed in the two case studies, initial concentrations are much higher in the former experiment.

The dairy effluent treatment case by Tchamango et al. (2008) presented in section 2.2.2.2 included a comparison between the chemical treatment of dairy effluents and EC treatment using aluminum electrodes. Phosphorus, COD, nitrogen and turbidity results were almost identical for both treatment methods; phosphorus removal rate reached almost 90%. However, the researchers noted two major advantages of EC treatment over the conventional treatment: (i) treated wastewater showed lower conductivity and neutral pH, enabling its recycling for industrial purposes, (ii) the amount of aluminum released into solution was less than the salt amounts added in chemical coagulation.

As suggested by Tchamango et al. (2008), Ricordel et al. (2010) investigated treatment of surface waters using EC also for industrial uses. The experiments were run using aluminum anodes, and removal of phosphates, nitrates and bacteria were assessed. Oxygen levels decreased up to 90% during the experiments due to the deoxygenating effect of hydrogen gas produced.

$$O_2 + 2H_2O + 4e^- \rightarrow 4OH^- \quad (29)$$

The researchers related the nitrate reduction to the decrease in oxygen levels. However, phosphate removal was a result of the precipitation of phosphates to form insoluble aluminum phosphates.

In addition to EC's ability to improve effluent quality by eliminating contaminants, EC can be used as a pretreatment before membrane filtration units, in order to remove colloidal particles and decrease fouling. Bagga et al. (2008) studied pretreatment of surface water with EC using iron electrodes before microfiltration. Their research found that using iron as an anode was not recommended because soluble Fe^{2+} ions were also produced. They recommended using aluminum as anode material because it had only one oxidation state.

Electrocoagulation using aluminum electrodes has been tried, not as a pretreatment to membrane filtration, but as a combined system within submerged membrane reactor by Bani-Melhem & Elektorowicz, (2010). The researchers investigated the effect of electrocoagulation on mitigating membrane fouling in a submerged membrane electro-bioreactor (SMEBR). The anode material was aluminum, while the cathode was made of stainless steel. The investigation has shown that electrocoagulation can be combined with a membrane filtration unit to improve filtration operation and avoid fouling.

Although the treatment results achieved by the researches cited above were satisfactory, none of them carried out EC treatment on dilute wastewater with low initial COD, phosphorus and solids concentrations.

2.2.2.3 Electroflotation

As noticed in the previous section, electrocoagulation applications are very wide, but when applied on dilute wastewater, settling of the flocs formed could be a limitation. If proper settling is not achieved, the treated water could become turbid. Many municipalities and industries have strict regulations regarding the turbidity of discharged effluents. Coagulation, sedimentation, filtration, and flotation are examples of turbidity treatment methods.

Sedimentation by gravity is unfeasible in dilute systems if the density of the formed flocs is not significantly higher than the density of the solution. Settling problems could be solved by designing a flotation unit. Flotation as a technique for solid/liquid separation has been widely used; however, the technologies and applications vary. Flotation can be used for recovery of solids, water, oil, as well as wastewater/solid separation, sludge thickening, algae removal, and juice clarification (Lee et al. 2007; Araya-Farias et al. 2008; Shidong et al. 2009). Common types of flotation techniques are induced gas flotation (IGF), pressurized dissolved air flotation, non-pressurized entrapped air flotation, and biological flotation by gases produced by biological activities.

Dissolved air flotation (DAF) is used commonly in the industry. Pressurized gas is introduced into the system and carries the light particles to the surface. The particles could be light flocs, oils, suspended solids, or algae (Yang et al. 2008; Shidong et al. 2009). The flotation is achieved through the generation of many small gas bubbles, on which light particles adhere and get carried to the surface. Some researchers have tried

introducing ozone instead of air to achieve simultaneous separation and disinfection with promising results (Shidong et al. 2009).

Filtration and induced gas flotation processes require high energy input for pumping the wastewater or pressurizing and pumping the gases. Another type of flotation that is not commonly used in the industry, even if it has less energy requirements, is electroflotation (EF). Electroflotation is an electrocoagulation technique targeted to achieve solid/liquid separation in a reactor. Flotation occurs as the solids and flocs formed in the solution are carried to the surface by the hydrogen gas bubbles produced at the cathode as seen in equation 12.

The amount of hydrogen gas produced (moles) is related to the current density applied *(J)*, effective area of the electrode *(A)*, electrocoagulation time *(t)*, and number of hydrogen molecules generated per electron involved in redox reactions *(H)* (Phalakornkule et al. 2010):

$$n_{H_2} = \frac{J.A.t}{F} H \qquad \textbf{(30)}$$

In comparison to other flotation methods, electroflotation produces larger amounts of small gas bubbles, increasing the surface area for adsorption of contaminants on to gas bubble, thus carrying them to the water surface (Gao et al. 2005; Ge et al. 2004). The amount of gas produced depends on the amount of charge passing through the system. For each Faraday, or 26.8Ah, 0.0224 Nm^3 of hydrogen gas is produced, which surpasses the volume of gas in DAF methods explained above.

The fact that the gas bubbles generated during an EF treatment carry the solids and oils to the surface makes EF ideal for turbidity removal. Just like any other treatment, many parameters control the process. Current density, treatment time, wastewater characteristics, and choice of anode material are examples of controlling parameters. The flotation process is controlled by the current density, viscosity of the fluid and the surface tension. These parameters affect the bubble size, the bubble rise velocity, and the gas holdups (Ben Mansour et al. 2007; Sarkar et al. 2010). Sarkar et al. (2010) explained that the gas bubbles detach from electrode surface when surface tension forces (F_σ) are equal to the sum of buoyancy forces (F_B) and pressure forces (F_P):

$$\boldsymbol{F_\sigma = F_B + F_P} \tag{31}$$

Ben Mansour et al. (2007) experimentally related the bubble diameter (d_b), the bubble rise velocity (v_{rise}) and the gas hold ups (ε_{gas}) to the current density (J) and viscosity (μ) in the following equations:

$$\boldsymbol{d_b = 6.275\, x\, J^{0.46}\, x\, \mu^{0.48}} \tag{32}$$

$$\boldsymbol{v_{rise} = 0.568\, x\, J^{0.68}\, x\, \mu^{-1.07}} \tag{33}$$

$$\boldsymbol{\varepsilon_{gas} = 1.14x10^{-2}\, x\, J^{0.91}\, x\, \mu^{-0.77}} \tag{34}$$

The major controlling parameter in the electroflotation process is the current density, since it controls the amount and size of gas bubbles generated as seen from equations 30 and 32. As current density increases, more hydrogen gas is produced (Merzouk et al. 2010). Therefore, the treatment duration can be chosen based on the current density applied to control the amount and size of gas particles desired (Equation 30 & 32). It has

been shown that flotation is better with finer gas bubbles (Bagotsky, 2006; Jimenez et al. 2010).

The choice of anode material also affects flotation, since different anode materials produce varying hydroxides and formed flocs. For example, aluminum is a good choice for EF because aluminum hydroxides are usually light and get carried to the surface easily (Gao et al. 2005). Nevertheless, at high current densities and long exposure times, if excess aluminum is generated in-situ, excess aluminum hydroxide will form and accumulate in a polymer form, contributing to increasing the turbidity of the water rather than removing it (Merzouk et al. 2010).

Conductivity is one of the main wastewater characteristics that control EF treatment conditions and the amount of power supplied to the system. When the conductivity of the solution is high, lower potential is needed to reach to the desired current density. Conductivity in this context represents the ion concentration in the solution. Ions present in wastewater could be from dissolved salts, solids, acids or bases. The amount of ions present in a solution is important when using electrocoagulation, because it contributes to the electrical conductivity of the system.

Hydrogen production at the cathode can sometimes be a limitation to the settling of dense flocs in an EC reactor. A study targeting the removal of chromium from wastewater using electrocoagulation without filtration was conducted by Ping et al. (2006), where metal hydroxides were formed, but the hydrogen production hindered the settling of the flocs. The metal hydroxides formed were small and dense; therefore, they were not readily carried to the surface by the hydrogen bubbles.

Floc separation should be assured in order to obtain chromium levels that are safe for discharge, which is why a filtration unit is usually added. In order to solve the solid/liquid separation problem, the researchers added an EF unit after the EC reactor to separate the precipitates formed. Sodium chloride salt was added in the EF unit to increase the system conductivity, thereby increasing current and resulting in more hydrogen generation. Moreover, a surfactant was added to decrease the surface tension and enhance the rise of gas bubbles. The last addition to the system was alum, since aluminum hydroxides are large and have low densities, which makes them easier to carry to the surface. The use of two separate electrokinetic reactors, EC and EF would require high energy inputs in addition to additional space requirements. Modifications can be introduced to achieve simultaneous EC and EF in the same reactor.

The researchers also decided to try a hybrid Al-Fe electrode for flotation and removal of chromium without a filtration step or addition of surfactant. The hybrid system resulted in more than 97% removal of chromium at low power input, where the energy requirements were less than $1kWh/m^3$.

A study was conducted by Ge et al. (2004) to investigate EF effectiveness in treating laundry wastewater which contained surfactants, salts, and phosphates. The researchers studied the ability of EF to remove phosphates, COD, surfactant and turbidity. Three bipolar aluminum electrodes were places between two titanium electrodes. The titanium cathode and anode were dedicated for electrolysis of water, where oxygen gas was produced at the anode and hydrogen gas at the cathode. The three bipolar aluminum electrodes were in effect two-sided electrodes, one of which was connected to the positive terminal, making it the anode, and the other to the negative terminal, making it

the cathode. Having three sets placed in series increased the treatment efficiency, decreased the time and allowed better distribution of produced hydrogen gas.

As mentioned above, EF could be used for clarification purposes. A study was conducted by Farias et al. (2007) to investigate the effect of different current densities on the clarification of apple juice (decreasing the turbidity and improving the color of the juice). The current densities tested were 10, 20 and 40 A/m^2; and the treatment time was 30 minutes. The experiments were run with and without gelatin as a clarifying agent. Addition of gelatin helps in evaluating whether the desired results can be achieved by EF alone, or whether the addition of a clarifying agent is needed. Results showed that the best flotation was achieved at a current density of 20 A/m^2. Results of the study showed that EF alone, at a current density of 20 A/m^2, was efficient in reducing tannins and protein content of the juice. EF helped reduce turbidity from 436 NTU to 10 NTU at the above mentioned current density without a clarifying agent, and to 3.4 NTU with the addition of gelatin. Although EF proved to remove proteins in this case, results might not accurately describe the extent to which EF is responsible for protein reduction because a pectinase pretreatment was done before the EF unit.

Phalakornkule at al. (2010) looked at EF as a sustainable process from which energy can be recovered. The energy to be recovered is not in the form of electrical energy, but rather hydrogen recovery. Although hydrogen by itself is not a form of energy, it is a renewable energy source. The investigation involved hydrogen recovery from EC treatment of dye-containing wastewater. The treatment process was no longer regarded as a solid-liquid separation but rather a gas-liquid-solid separation. Results of the

investigation showed that the energy yield of collected hydrogen accounted to 8-13% of the energy requirements of the EC process.

Research continues to enhance the electrocoagulation and electroflotation processes; however, solutions should be aimed towards feasible technologies that are efficient, cost effective, and practical for a wide array of applications. Electroflotation is currently being considered as an extra unit following an EC treatment reactor; nevertheless, there is considerable potential in applying EF as a complete treatment unit with simultaneous treatment and solid-liquid separation in the same reactor, especially for dilute wastewater systems.

Chapter Three – Methodology

Failure of biological systems to effectively treat very dilute wastewater (e.g. less than 100 mg/L COD) , as well as the growing drive to limit the use of chemical coagulants and polymers in wastewater treatment, makes electrocoagulation (EC) an ideal alternative. This study was therefore initiated as a response to the lack of research into the applicability of EC when treating very dilute wastewater, with the interest of exploring a treatment process with the smallest economic and environmental footprint. This study aims to (i) investigate the effectiveness and feasibility of the EC process for the treatment of wastewaters with different initial characteristics to expand its applications to a wider gamut of industries; (ii) investigate different operational conditions of EC process in the interest of reducing operating costs to assess the feasibility of its application; (iii) evaluate EC performance as a pre-treatment, post-treatment and a standalone process. To achieve these objectives, the study was divided to four phases:

I. Phase I: Comparison of electrocoagulation and chemical coagulation
II. Phase II: Transformation of the electrocoagulation process into electroflotation
III. Phase III: Study of the effect of interrupted exposure to DC field on electrocoagulation and electroflotation
IV. Phase IV: Study of the effect of using different forms of electrodes on current efficiency

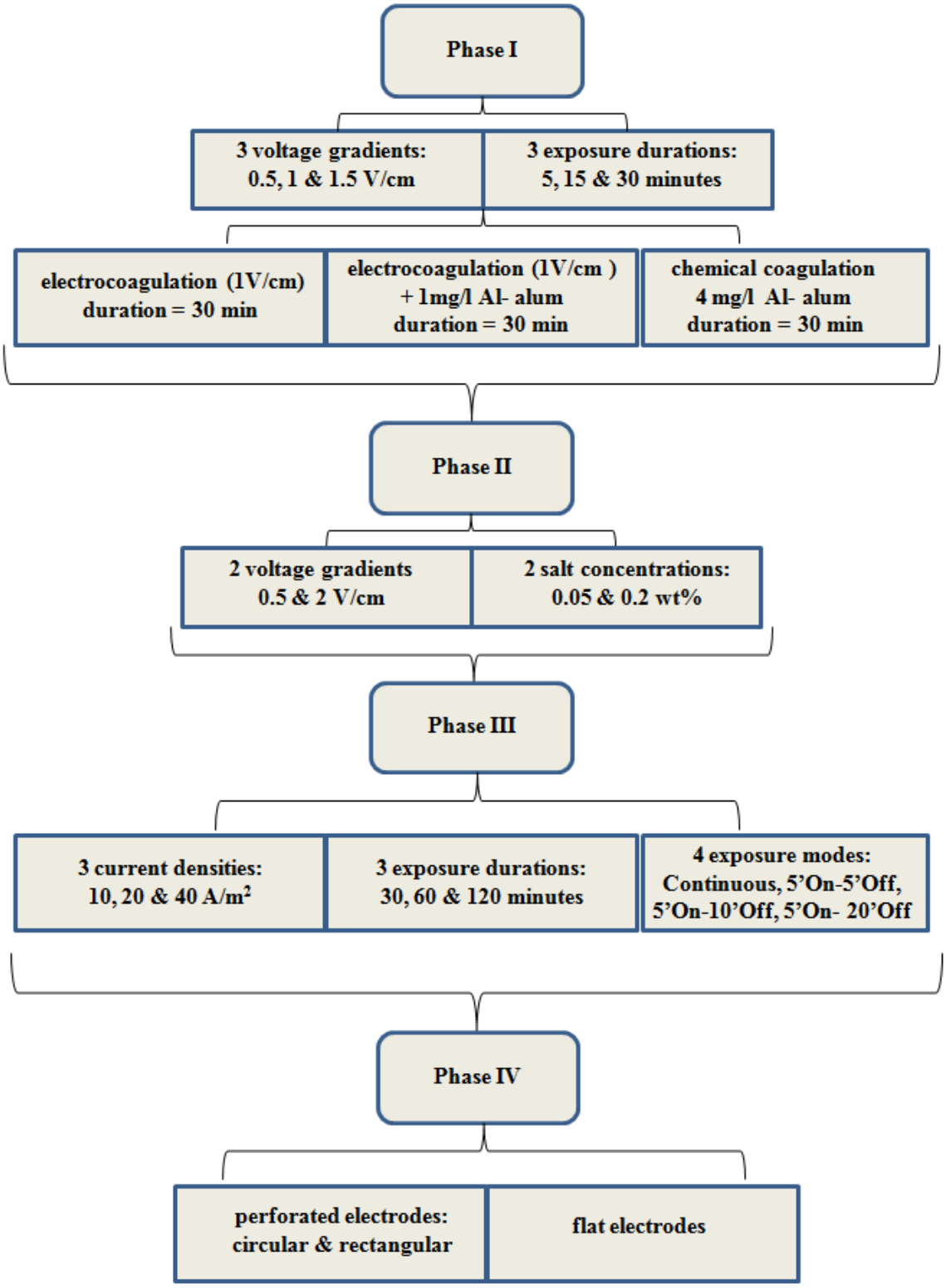

Figure 7 – Methodology of Phases I to IV

3.1 Phase I – Comparison between EC and chemical coagulation

The wastewater samples used for running the experiments were collected from a municipality in Quebec. Treated effluent samples were collected from the same plants in order to compare the removal efficiency by electrocoagulation in bench scale experiments with aerated primary treatment with usage of coagulants in the plant of concern. The tests conducted in this phase were run on 1.5 liter wastewater samples. The experimental work was divided into two stages: Stage I - investigation of adequate EC operating conditions, and Stage II - a comparative study between EC and chemical coagulation treatment.

EC Operating Conditions – Stage I

Based on previous of Bani-Melhem & Elektorowicz (2010), the following electrocoagulation experimental conditions were chosen for Phase I:

- Voltage gradients (0.5, 1 and 1.5 V/cm)
- Exposure times (5, 15 and 30 minutes)
- Aluminum (Al) anode dimensions (14.2cm x 11cm)
- Effective anode area: 156.2 cm^2 = 0.01562 m^2

In total, nine conditions were tested before choosing the optimal operating conditions for the second stage.

Comparative Experiments – Stage II (based on results from Stage I)

- Electrocoagulation (1V/cm)
- EC (1V/cm) + 1 mg/L Al
- Chemical Coagulation (4 mg/L) of Al *(alum)* $(Al_2(SO_4)_3.\ 18H_2O)$
- Duration: 30 min

Parameters studied:

- Phosphorus removal
- Chemical Oxygen Demand (COD) removal
- Filterability

Once the best electrocoagulation operating conditions for wastewater samples were chosen in the first stage, the second stage was initiated with the objective of comparing EC under these conditions with chemical coagulation treatment, using alum as the coagulant. Since the municipality involved in this study uses a dosage of 3-4 mg/L of aluminum, an aluminum concentration of 4 mg/L, in the form of alum, was chosen. An additional investigation was performed with the concentration of 1 mg/L of aluminum to complete the comparative study of chemical coagulation with electrocoagulation. Studies focused particularly on phosphorus compound, since it was the main concern for the municipality involved in this study. As discussed in the previous chapter, the presence of high concentrations of phosphorus in water bodies can lead to eutrophication. Phosphates are removed from water through a ligand exchange mechanism between the phosphate

group and hydroxides in solution (Golder et al. 2006). According to Mustafa et al. (1999) and Golder et al. (2006), phosphates are best sorbed on aluminum; consequently sacrificial aluminum anode was used in this study.

During the second stage of the experiment, three treatments were applied in parallel to the wastewater samples:

a) Electrocoagulation alone using aluminum anode ,
b) Chemical coagulation using aluminum coagulant (alum), and
c) Combination of electrocoagulation and chemical coagulation.

Electrocoagulation tests were operated based on optimal condition generated during Stage I.

Phosphorus and COD removal efficiencies, as well as time to filtration (TTF) were measured after each run. The time to filtration indicates the filterability of the flocs formed.

3.1.1 Experimental Apparatus

The experiments were run in 2 L cylindrical polyethylene reactor (with an effective volume of 1.5 L). The cathode material was stainless steel; meanwhile aluminum was the sacrificial anode. Stirring was done at a speed of 120 rpm throughout the experiment, using a Corning digital magnetic stirrer. No air was injected during all experiments. Figure 8 shows the setup for the electrocoagulation tests, which is identical to that of chemical coagulation tests, with the exception that the electrodes and the power supply are not used during the latter.

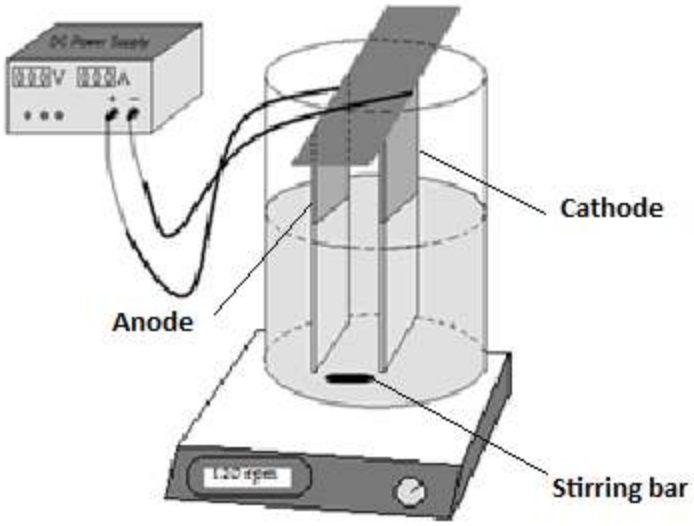

Figure 8- Experimental Setup- Phase I

3.1.2 Experimental Analysis

To study the effect of each operating condition on filterability of flocs, samples were taken before settling and 70 ml of each sample were filtered under vacuum using Ahlstrom-Grade 238 glass fiber filter paper. The time needed to filter the aforementioned volume of sample was noted, as the filtration time is directly proportional to the water retention of sludge, i.e. the longer the time needed, the higher the water retention.

After the experiment, a sedimentation time of one hour was allowed before supernatant samples were taken. However, conductivity and pH were directly measured before and after each run using HACH probe meters, methods 8160 and 8156, respectively. The samples were then filtered under vacuum filtration to test for TSS (APHA Method 2450D). After filtration, the filtrate was tested for orthophosphate and COD using HACH DR-2800 spectrophotometer methods 8178 and 8000, respectively.

3.2 Phase II – Electroflotation

Phase II is complimentary to phase I, with the aim of improving the solid/liquid separation in an electrocoagulation process. Since real wastewater was used in this study, the conductivity varied considerably with seasonal changes. When conductivity was low, the current passing at the fixed voltage gradients applied was very low. This causes the solid/liquid separation, or floc settling process, to slow down considerably, which in turn increased the retention time needed in the settling tanks. Electroflotation can solve the problem of weak floc settling, as it uses the bubbling of gases produced in-situ at the electrodes to carry the flocs up to the water surface as shown in equations 30, 33 and 34 in section 2.2.2.3.

Conductivity of the water collected for the Phase I experiments was found to be low; as a result, low current passed through at the voltage gradients applied. To increase the amount of current passing through the system, several screening tests were conducted to observe the effect of adding sodium chloride salt on conductivity. A combination of the salt concentrations of 0.05% w/w and 0.2% w/w, and voltage gradients of 0.5 V/cm and 2 V/cm were applied (Table 4). Two extreme values, lower and higher than optimal conditions applied in previous phase (1 V/cm), were chosen for studying the effect of salt even at lower voltage gradients to reduce the energy requirements of the process as noted by Zongo et al. (2009). The exposure duration was extended thirty minutes to a maximum of four hours in this set of screening tests to assess whether prolonged exposure has a significant effect on flotation.

Table 4 - Experimental Conditions Applied in Phase II

Conditions Applied	Duration	Volume	Anode Material	Cathode Material	Effective Anode Area cm^2
2V/cm-0.2% NaCl	4 hours	1.5 L	Aluminum	Stainless Steel	156.2
2V/cm-0.05% NaCl					
0.5V/cm-0.2% NaCl					
0.5V/cm-0.05% NaCl					

Dissolved oxygen, conductivity, pH, phosphorus, and COD were measured before and after each run. Electrodes were also washed, dried, and weighed after each experiment to measure the weight loss in the anode. The theoretical anode consumption was then calculated in order to compare it with the actual electrode consumption

Current was noted throughout the experiments, and the current density was calculated for each of the combinations chosen.

$$J = \frac{I}{A_{effective}} \quad \textbf{(35)}$$

Where J = current density (A/m^2)

I = current (Amps)

$A_{effective}$ = effective surface area (m^2)

Table 5 - Current Densities during Phase II

Conditions Applied	Average Current Density (A/m^2)
2V/cm-0.2% NaCl	150.1
2V/cm-0.05% NaCl	58.6
0.5V/cm-0.2% NaCl	16.0
0.5V/cm-0.05% NaCl	12.8

As seen from Table 5, the voltage gradients yielded different current densities, depending on the conductivity of the solution. Therefore, the EC-EF processes was operated at fixed current densities rather than fixed voltage gradients. The electric current represents the quantity of electrons passing through the system (Kobya et al. 2006; Drouiche et al. 2008), which has a direct influence on the anode dissolution as seen from Faraday's Law:

$$C_{electrode} = \frac{ItM_w}{zFV} \quad (36)$$

Where $C_{electrode}$ = electrode consumption (kg/m^3)

I = current (Amps),

M_w= molecular weight of the electrode material (g/mol)

z= valence number of electrons transferred by the anode

t= operating time (seconds),

V= volume of water treated (m^3)

F = Faraday's constant

Faraday's law measures the theoretical electrode consumption; however, actual electrode consumption was measured by weighing the electrodes before and after each experiment. When operating at a fixed current density, voltage will vary based on the conductivity of the system; therefore, the operating conditions won't be affected by the seasonal fluctuations of salt concentrations in wastewaters which are caused by road salt application, heavy rains and snow melts.

3.3 Phase III

The decision to work at fixed current densities instead of voltage gradients initiated a new set of experiments. The objective of this phase was to investigate the effects of different current densities, as well as modes and durations of exposure, on flotation and removal of phosphorus, nitrate, ammonia, COD and turbidity. Moreover, particle size distribution and zeta potential were measured.

Three variables were considered in this Phase III: treatment duration, current density, and electricity exposure modes. The current densities chosen were 10, 20 and 40 A/m^2 and the treatment durations were 30, 60, and 120 minutes per run. In each run, four 1.5 liter reactors were operated simultaneously, one reactor was continuously exposed to DC current and the other three were connected to pre-programmed timers to interrupt the exposure at various intervals throughout the experiment. A control reactor was also run without EC; mixing was applied throughout the experiment duration for comparison purposes. The power supply was connected to a control panel, enabling simultaneous power delivery to all the reactors and timers. The same interrupted modes were tested by Bani-Melhem & Elektorowicz (2010) and Ibeid et al. (2010); however, the wastewater used by the aforementioned researchers had much higher initial suspended solids and COD concentrations. The treatment runs and interval durations are summarized in Figure 9.

Figure 9- Operational conditions of Phase III

The combinations of experiments shown in Figure 9 were run on wastewater from two different municipalities in Quebec, designated as WWTP1 and WWTP2. Samples from WWTP1 were collected after ammonia removal, whereas WWTP2 samples were raw, and collected after screening. Both samples were collected during the winter season, but each had different initial characteristics. Having two different wastewaters was important to validate the flexibility of the system and its application on several types of wastewater. The initial characteristics of both wastewater samples are displayed in Table 6. All the values presented in Table 6 were measured in the lab before starting the treatment tests.

Table 6 – Phase III - Initial Wastewater Characteristics

	WWTP1	WWTP2
Conductivity (μS/cm)	2500 ± 250	1100 ± 300
TSS (mg/L)	42 ± 20	135 ± 50
PO_4^{-3} (mg/L)	1.5 ± 0.5	6.5 ± 3
COD (mg/L)	45 ± 8	165 ± 30
NO_3^- - N(mg/L)	12.2 ± 2.3	0.29 ± 0.11
NH_3 - N(mg/L)	0.04 ± 0.02	25 ± 5
Turbidity (NTU)	19 ± 4	40 ± 15

In Phase III, the treatment started for the samples from WWTP1; the resulting foam floating on the surface was skimmed off with a mesh spoon, as flotation was expected to occur during treatment. Skimming was necessary to allow sampling after treatment. However, this sampling method resulted in foam being broken and returned to solution; therefore, limitations in numerical turbidity readings occurred. A visual evaluation of turbidity removal was followed using comparison of pictures taken by a camera before and after the treatment. Consequently, for the experiments done on wastewater from WWTP2, a hole was drilled near the bottom side of each and a sampling tube was inserted in it. The purpose of the tube was not to disturb the accumulation of foam on the surface while sampling, therefore enabling a quantitative evaluation of the effect of treatment on turbidity.

Samples were collected from the reactors after each run and were tested for many characteristics and parameters to evaluate treatment efficiency. Since samples were taken directly after the experiment, some flocs were present in the solution; therefore, 30

minutes of settling in sample tubes were allowed before taking turbidity readings. The tested parameters, as well as the methods and devices used, are listed in Table 7.

Table 7 - Analyses applied in Phase III

Characteristic	Method/ Device
pH	Hach – HQ30D digital meter
Dissolved Oxygen	Hach – HQ30D digital meter
Conductivity	Hach – HQ30D digital meter
Zeta Potential	Zeta Meter
Turbidity	Turbidity meter
Particle Size Distribution	Horiba Particle Analyser
PO_4^{-3}	Hach DR-2800/ vials: TNT 843 + 844
NH_4^+	Hach DR-2800/ vials: TNT 832
NO_3^-	Hach DR-2800/ vials: TNT 835
COD	Hach DR-2800/ vials: TNT 821
TSS/ TVS	APHA 2540D and 2540E (1995)

3.4 Phase IV

Results from Phase III encouraged exploring the effect of electrode perforation to electrode consumption and operating cost. Therefore, two types of perforated anodes (having 46% of openings with circular and triangular forms) in addition to the flat anode used in the previous phases. Operation parameters applied based on the outcome from previous phases: current density of 20 A/m^2, a treatment time of 120 minutes, and two exposure modes (continuous and 5'ON- 20'OFF). All samples were tested for phosphorus, COD, ammonia, nitrate, and turbidity.

The perforation of electrodes resulted in reducing the effective area of the anode from 156.2 cm^2 to 84.35 cm^2. Flat electrodes and electrodes with triangular perforations had a thickness of 0.5 mm; the anode with circular perforation had a 1 mm thickness.

Table 8 - Phase IV - initial wastewater characteristics

Parameters	WWTP2
Conductivity (µS/cm)	890 ± 20
TSS (mg/L)	120 ± 5
PO_4^{-3} (mg/L)	12.8 ± 3
COD (mg/L)	415 ± 5
NO_3^- - N(mg/L)	0.62 ± 0.11
NH_3 - N(mg/L)	54 ± 0.5
Turbidity (NTU)	40 ± 15

3.5 Statistical Approach

In Phase III, after the treatment of wastewater from each WWTP, 45 samples were analyzed for each parameter; therefore more than 720 samples were tested. Repeating all the sample tests would have required an excessive number of sample vials, test kits and storage space. Nevertheless, in the interest of maintaining a high level of reliability, samples that did not fit within a certain trend were repeated; and at least 5 samples were repeated for each parameter. Overall zeta potential and turbidity values were averaged from six different readings, due to the difficulty in achieving accurate readings with the available equipment. In repeated samples for COD, phosphorus, ammonia and nitrate, errors were calculated and most results fitted within a margin error of 2%. Standard deviations in both zeta potential and turbidity were considerably high; therefore, the average of six samples was presented.

Chapter 4 – Results and Discussion

4.1 Phase I: Results

Assessment of the efficiency of electrocoagulation treatment in this phase was based on two main parameters: removal rates of phosphorus and COD. Operating costs at different operating conditions were also calculated.

4.1.1 Phase I - Stage I: Results

As mentioned in Chapter 3, Stage I consisted of choosing optimal conditions for treatment, namely durations and voltage gradients. Of the three durations tested 5, 15 and 30 minutes, the best treatment time chosen 30 minutes because it yielded the highest removal efficiencies (around 80% for phosphorus and close to 50% for COD) for all three voltage gradients tested (0.5, 1 and 1.5 V/cm).

Removal Rate (% Removal) was calculated using the following equation:

$$\%\ \boldsymbol{Removal} = \frac{\boldsymbol{Initial\ Concentration - Final\ Concentration}}{\boldsymbol{Initial\ Concentration}} \quad \textbf{(37)}$$

At treatment duration of 5 minutes and 15 minutes, the highest removal efficiencies were 31% and 58% for COD and phosphorus respectively. However, higher removal efficiencies were achieved after 30-minute exposure experiments; removal efficiencies of phosphorus and COD are presented in Figure 10.

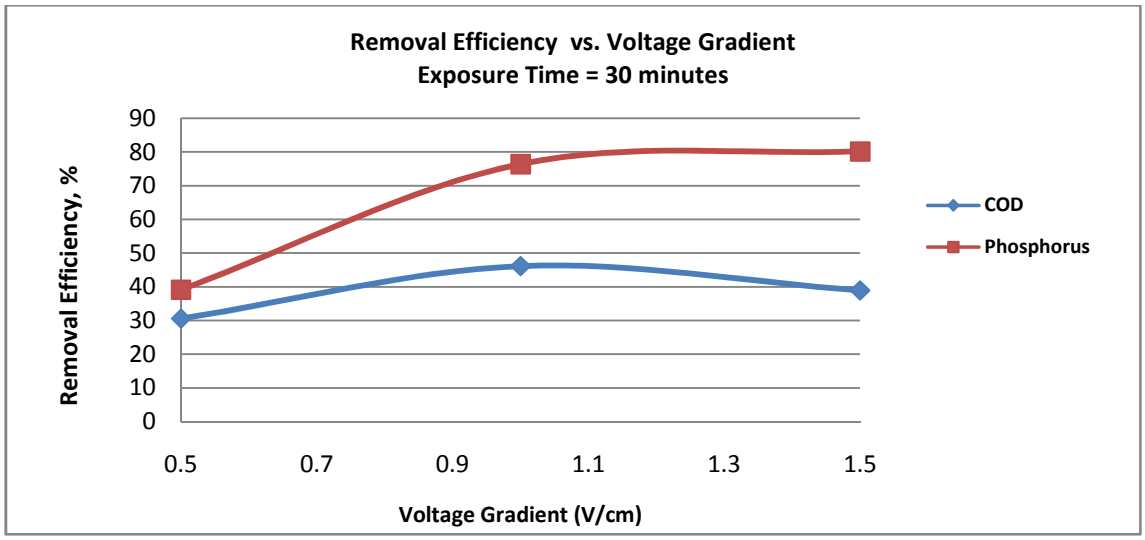

Figure 100 - Phase I - Stage I - Removal efficiency of phosphorus and COD

As seen in Figure 10, the rate of phosphorus removal increased nonlinearly with the increase of voltage gradient reaching 80% at 1.5V/cm. It is higher than removal of 68% obtained by Vasudevan et al. (2008) at 2 V/cm using a mild steel anode. Therefore, results obtained in this experiment demonstrate the superiority of aluminum anode in phosphorus removal.

Judging by the results shown in Figure 10, a voltage gradient of 1 V/cm and a 30 minute exposure time seem to be the optimal conditions, in terms of the obtained removal efficiency. However, a cost analysis was done in order to verify whether these conditions are also optimal from a financial perspective. In order to calculate the operating cost of an electrocoagulation process, two major parameters must be determined: electrode and energy consumptions.

The choice of material plays an important role in determining the overall cost. The theoretical electrode consumption $(C_{electrode},\ kg/m^3)$ is calculated using Faraday's law

(equation 36) to relate the mass of the anode consumed to the current passing through it *(I, Amps)*, the molecular weight of the electrode material *(M_w, g/mol)*, the valence number of electrons transferred by the anode *(z)*, the operating time *(t, seconds)*, the volume of water treated *(V, m^3)*, and Faraday's constant *(F, Coulomb/mole)* (Kobya et al. 2006; Drouiche et al. 2008).

$$C_{electrode} = \frac{ItM_w}{zFV} \quad (36)$$

Energy consumption *(C_{energy}, kWh/m^3)* is calculated using equation 38, where U is the voltage applied (Volts)

$$C_{energy} = \frac{UIt}{V} \quad (38)$$

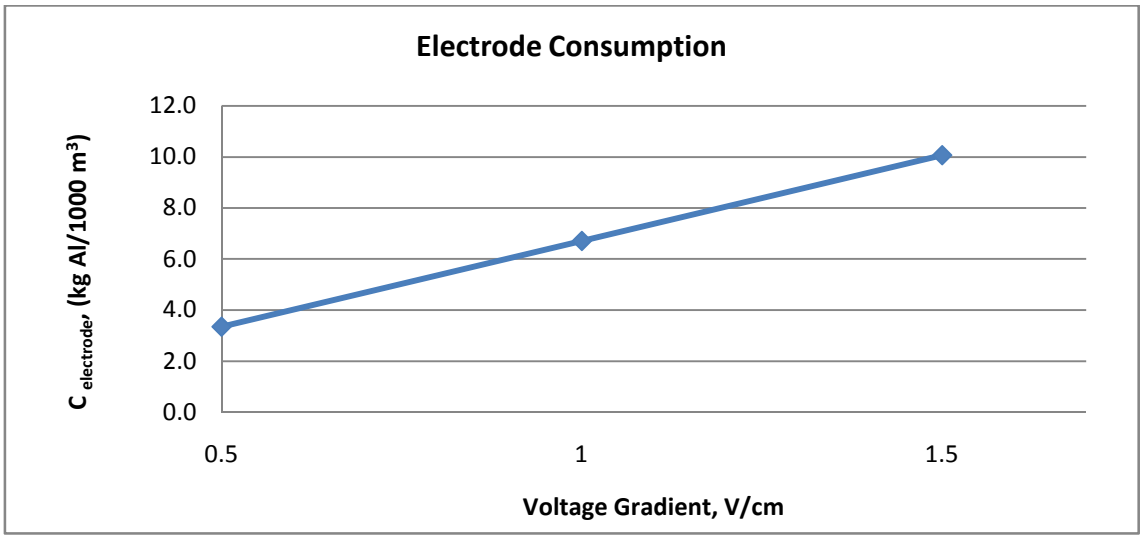

Figure 11 - Phase I - Stage I: Electrode consumption

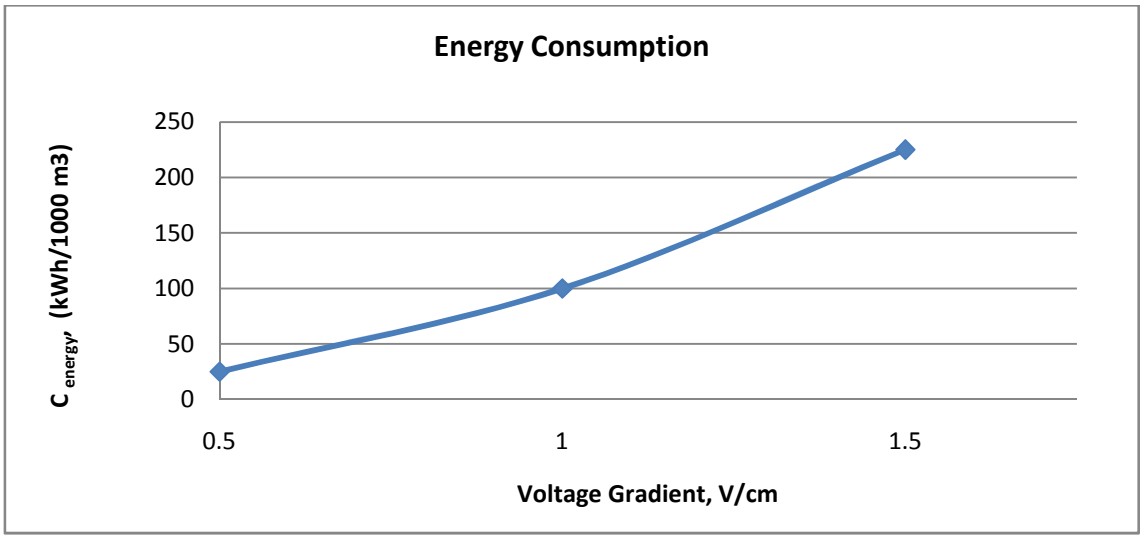

Figure 12 - Phase I - Stage I: Energy consumption

Results show an increase in electrode and energy consumption as voltage gradient increases. The electrode and energy consumption values are used to estimate the operating cost using the following equation (Kobya et al. 2006):

$$OperatingCost = aC_{energy} + bC_{electrode} \quad (39)$$

Where *a* and *b* are the price of energy (CAD/kWh) and electrode material (CAD/kg), respectively. The aluminum price used for calculations is 2.26 CAD/kg as per the London Metal Exchange (LME) on December 28th 2010. The price of electricity for industrial facilities, obtained from Hydro Quebec, was 0.05 CAD/kWh.

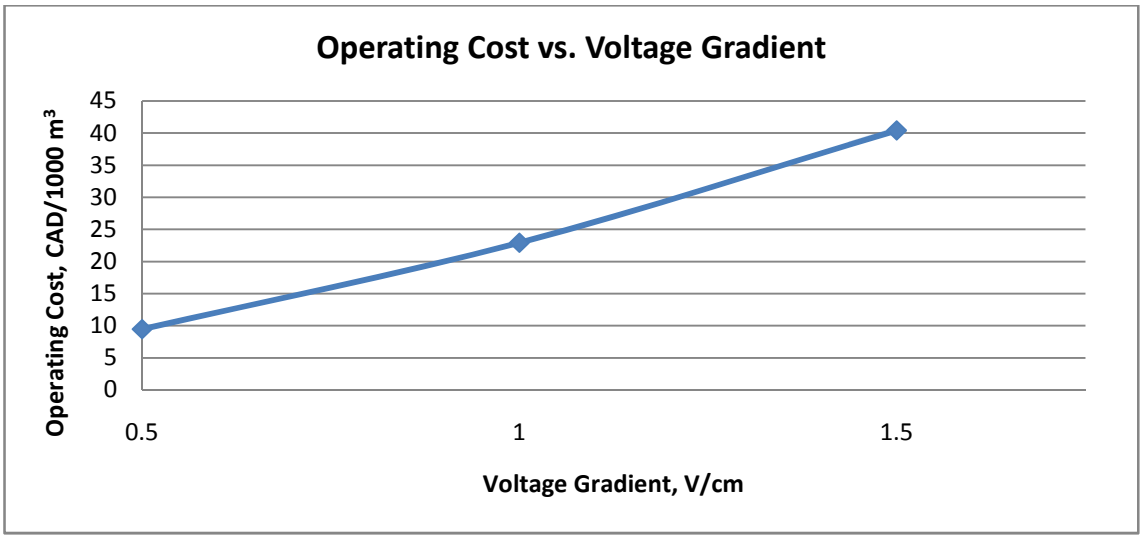

Figure 13 - Phase I - Stage I: Operating cost

The operating costs were 9, 23 and, 40 CAD per 1000 m^3 of treated water at 0.5, 1 and 1.5 V/cm, respectively (Figure 13). Since the operating cost for 1.5 V/cm was almost double that obtained at 1 V/cm, the latter value was chosen as the optimal operating condition, especially considering similar phosphorus removal efficiency for both voltage gradients as shown in Figure 10.

Table 9 – Operating Cost Summary

Voltage Gradient (V/cm)	Electrode Consumption (kg/1000 m^3)	Energy Consumption (kWh/1000 m^3)	Operating Cost (CAD / 1000 m^3)
0.5	3.36	25	9.5
1	6.71	100	22.9
1.5	10.07	225	40.4

4.1.2 Phase I – Stage II: Results

The best conditions (30 minutes exposure duration to 1V/cm) verified in Phase I Stage I were applied to comparative experiments in Stage II. In this stage, the TTF as well as removal efficiencies of phosphorus and COD were tested.

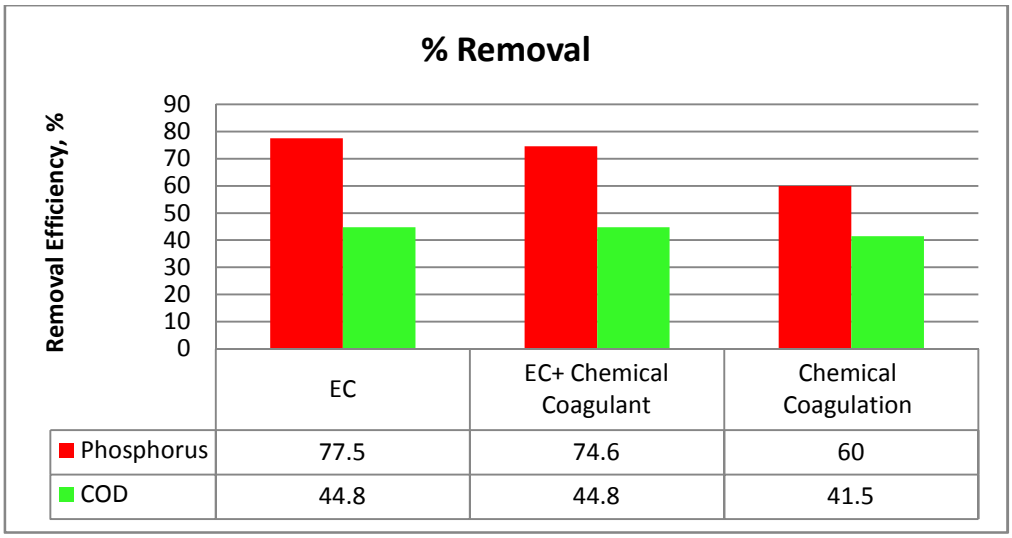

Figure 14 - Phase I - Stage II - Removal of phosphorous and COD in comparative experiments

Experimental results from Stage II (Figure 14) proved the advantage electrocoagulation provides over chemical coagulation treatment when removing phosphorus present in wastewater. Furthermore, it was noted that the addition of a chemical coagulant to an electrocoagulation treatment did not improve the phosphorus removal efficiency. Electrocoagulation treatment also removed an insignificantly higher amount of COD comparing to chemical coagulation.

When comparing water quality treated with EC and with a combination of EC and chemical coagulation treatment (Figure 14), the difference in results is negligible.

However, differences do emerge when comparing filtration times. Figure 15 illustrates the effect of all three treatments on floc filterability.

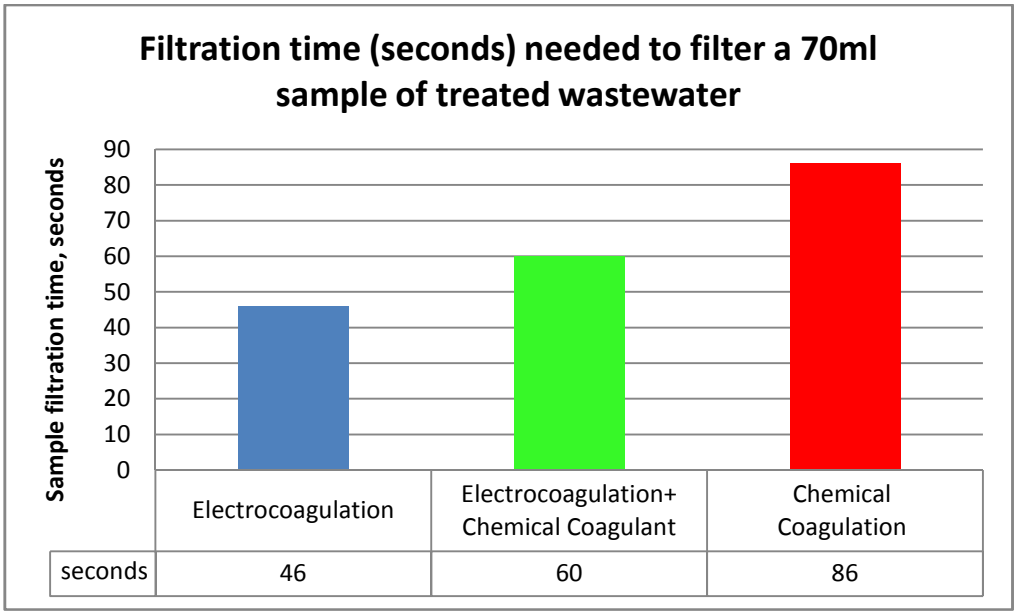

Figure 15 – Phase I - Stage II – TTF

The speed at which a wastewater sample is filtered gives an indication of the filterability of the formed flocs, as well as an idea about the water retention characteristics of the sludge. The higher the water retention, the more time it takes to filter a sample. As mentioned in Chapter 2, electrocoagulation produces flocs that are generally heavier and with lower water retention (Kobya et al. 2006); therefore, the time needed to filter samples treated by electrocoagulation should be considerably shorter. Results of this study, presented in Figure 15, show that filtration time for samples treated using electrocoagulation in Stage II was almost half of that required to filter the samples treated with chemical coagulation. The increase in time needed when combining EC and chemical coagulation can be attributed to the presence of sulphate ions in solution after coagulant salt hydrolysis. Trompette & Vergne (2009) explained that sulphate ions in

solution can hinder the EC process through their adsorption on to the aluminum hydroxide precipitate.

Equations 36, 38 and 39 (Section 4.1.1) were used to estimate the cost of EC; the cost of the chemical coagulant was also used for the combined EC-chemical coagulation experiment. Conventionally, an additional polymer cost is included in chemical treatment plants, but in this study, the coagulant material cost only was used for comparison. The chemical formula for the alum coagulant used was $Al_2(SO_4)_3.18H_2O$. Therefore, adding 4 mg/L of aluminum in the form of alum required using 50mg/L of coagulant. The price used for alum was 0.3 CAD/kg (Rossini et al. 1999). In order to accurately compare the cost of the coagulant in all three reactors, the consumed anode material was considered as the coagulant material in the electrocoagulation experiments.

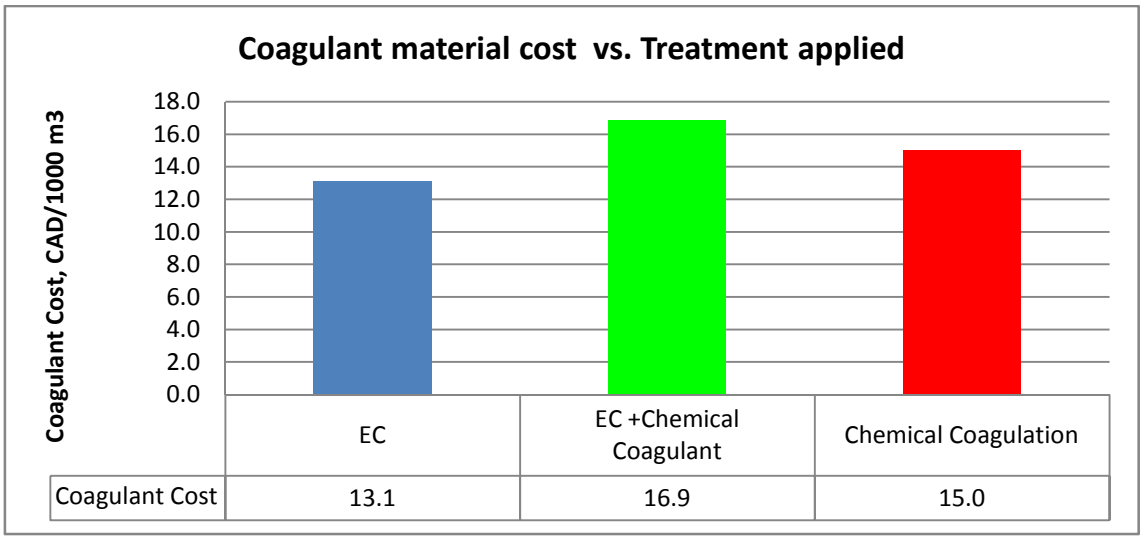

Figure 16 - Phase I - Stage II - Coagulating material costs

Figure 16 represents a comparison of the coagulant material cost between EC and chemical coagulation; the coagulating material in electrocoagulation treatment is the

anode material. The comparison in this study shows that anode material needed to treat 1000 m^3 of wastewater costs less than the chemical coagulant needed to treat the same volume of wastewater. EC was therefore shown to produce a higher effluent quality at an appreciably lower cost than chemical coagulation. Moreover, the additional costs of polymers, chemical storage and chemical transportation, if considered in this study, would have resulted in an even larger advantage for electrocoagulation, since these additional costs do not apply to EC treatments. Finally, better sludge quality can significantly decrease sludge management costs (Lin et al. 2005).

4.2 Phase II - Electroflotation with Conductivity Variation

Although results from the previous set of experiments were satisfactory with respect to phosphorus and COD removal, flocs' settling was slow in the reactors, leading to a longer retention time in the settling tanks. In Section 3.2, electroflotation was proposed as a potential solution for weak floc settling, since it uses gases produced at the electrodes to force flocs up to the surface (Equations 30, 33 and 34) where they can be skimmed off. As mentioned in Chapter 3, in Phase II, sodium chloride salt was added to increase the electrical conductivity of the wastewater. Meas et al. (2010) treated industrial wastewater with electrocoagulation and found that turbidity removal improves when conductivity increases. In Phase II experiments, flotation was achieved with the four conditions tested. Although the tests were run for four hours, complete flotation was achieved in the first 45 minutes for the four conditions (Table 4, Chapter 3). As seen in Figure 17, flotation was achieved, leaving the water column clean and carrying impurities to the water surface.

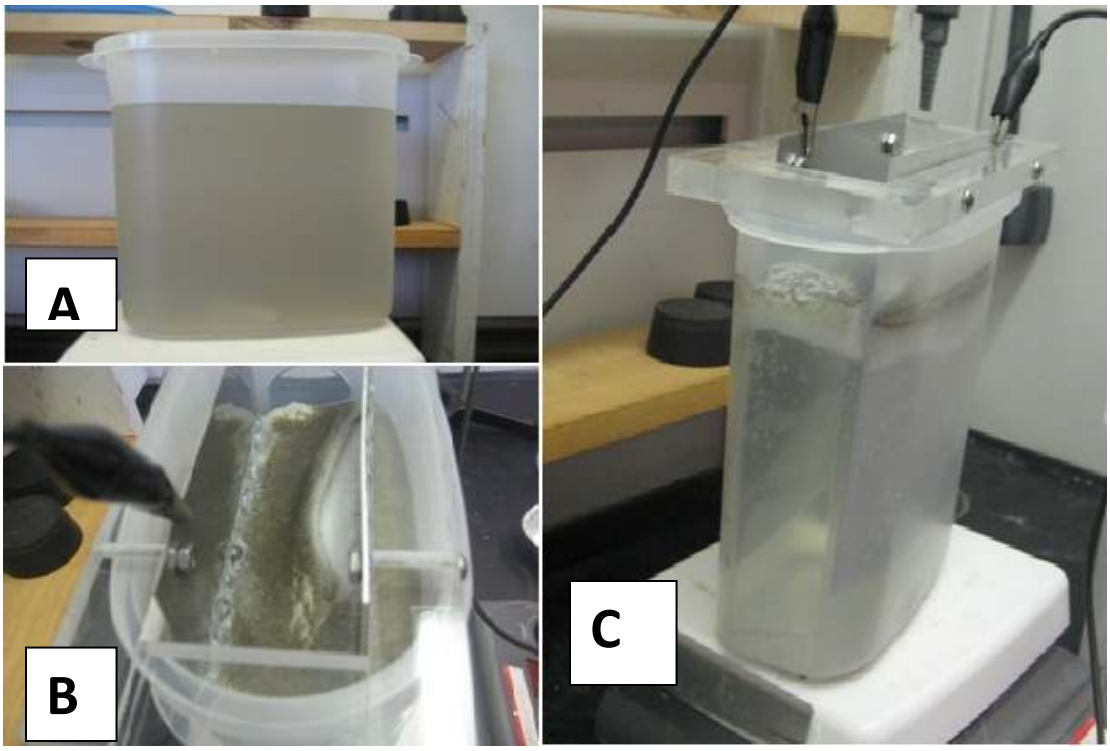

Figure 17 - Phase II – Electroflotation achieved after increase of conductivity of the wastewater:
A: before treatment, B: after treatment (top view), C: after treatment (side view)

Using high values for the salt concentration and voltage gradient (0.2% and 2 V/cm, respectively), current density was extremely high. Running the test for four hours resulted in excessive dissolution of the anode, causing the water to turn grey due to aluminum hydroxides (Appendix II). A temperature increase of 25^{o}C also occurred during this experiment; due to Joule's effect. Joule's effect is the heating that results upon the flow of current through a conductor (Kiehne, 2003). The generated heat leads to an increase in temperature of the conductor, which in turn heats the solution (Chambers' Encyclopedia, 1889).

$$\frac{dQ_{Joule}}{dt} = \Delta U x I \qquad (40)$$

Where Q_{Joule} is the heat generated (J)

t is the time (seconds)

ΔU is the voltage drop (V)

I is the current (Amps)

Finally, the water pH increased due to the excessive quantity of hydroxide ions produced.

Removal efficiencies were best presented in terms of current densities:

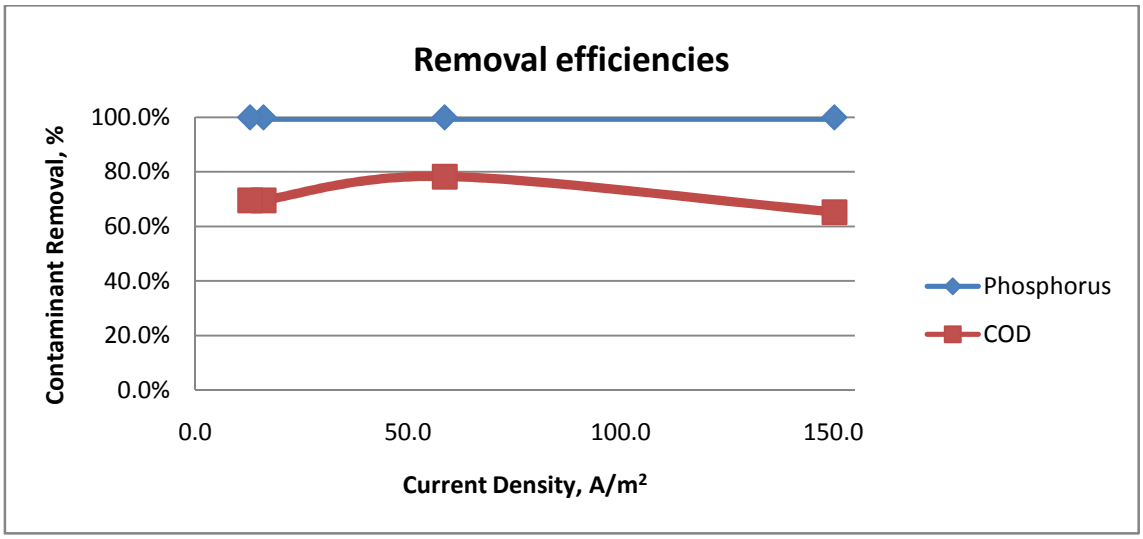

Figure 18 - Phase II – Removal efficiencies of phosphorus and COD

Removal efficiencies of phosphorus and COD were significantly higher in Phase II than in Phase I. Phosphorus removal was 100% for all the conditions tested, meanwhile COD removal ranged between 65% and 78%.

Table 10 - Phase II: Removal Efficiencies of Phosphorus and COD

Condition Number	Conditions Applied	Average Current Density (A/m^2)	PO_4^{-3} Removal	COD Removal
1	0.5V/cm-0.05% NaCl	12.8	100.0%	69.6%
2	0.5V/cm-0.2% NaCl	16.0	100.0%	69.6%
3	2V/cm-0.05% NaCl	58.6	100.0%	78.3%
4	2V/cm-0.2% NaCl	150.1	100.0%	65.2%

Table 10 shows a summary of the conditions, current densities and removal efficiencies. The COD removal efficiencies were almost 70% at low current densities. Merzouk et al. (2009) yielded results in the same range with respect to COD, achieving a 68% removal efficiency of COD at 11.55 A/m^2, which is very close to the 70% achieved at conditions 1 and 2 in Table 10 in the Phase II experiments. Moreno-Casillas et al. (2007) explained that COD removal rates decrease with increasing pH; in Phase II a considerable increase in pH was experienced at 150 A/m^2, due to the OH^- ion release in solution. This could explain the decrease in COD removal at 150 A/m^2 after it peaked at 58.6 A/m^2. Despite the differences in COD removal efficiencies, all concentrations after treatment in Phase II were within the acceptable discharge standard of < 35 mg/L.

Dissolved oxygen was monitored before and after each experiment to assess the effect of EC- EF treatment on oxidation processes particularly on nitrogenous compounds. As mentioned in Chapter 2, nitrogenous compounds also contribute to problems in receiving bodies and drinking water sources.

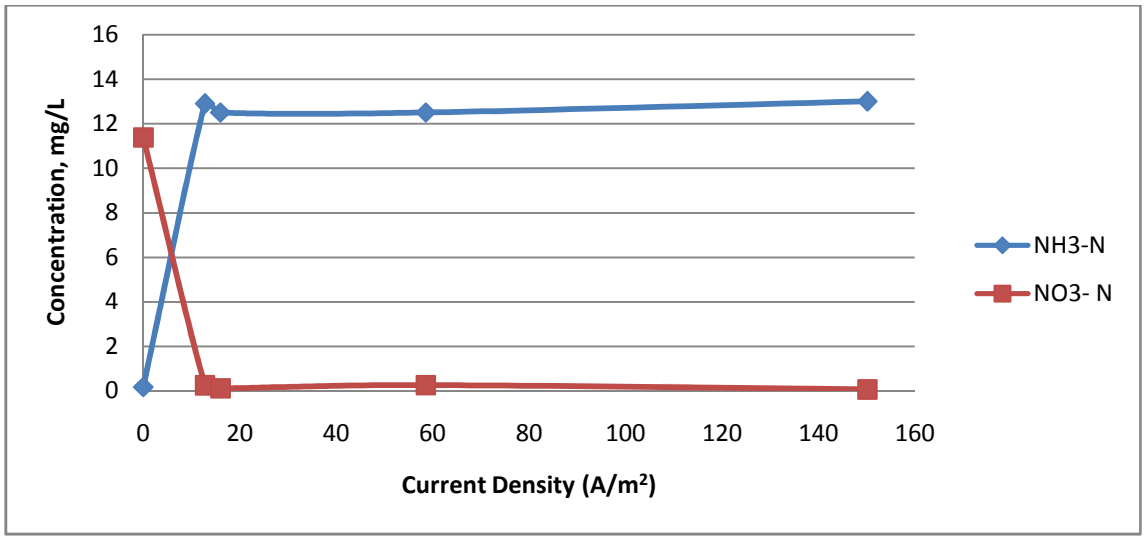

Figure 19 - Phase II - Ammonia and nitrate concentrations vs. Current density

The initial concentration of ammonia was almost zero and increased up to 75 fold after exposure to direct current for four hours. Nitrate concentration on the other hand, decreased to almost zero after the four- hour exposure. As can be seen in Figure 19, the difference between ammonia increase and nitrate decrease at different current densities is not significant indicating that the results obtained were the same at the lowest and the highest current densities.

The lack of oxygen resulted in anoxic conditions inside the reactor; the decrease in nitrate can be attributed to the anoxic conditions in the reactors. Dissolved oxygen (DO) decreases during the treatment, and the presence of anoxic conditions, coupled with the hydrogen gas production during the EC treatment, resulted in abiotic conversion of nitrates to ammonia (Equations 41 and 42). An et al. (2009) also observed abiotic conversion of nitrate to ammonia under anaerobic conditions, in addition to the presence of hydrogen and nano- scale zero-valent iron. A study conducted by Sorenson (1978)

explained that bacteria (e.g. Clostridium) in water can convert nitrates to ammonia if other nitrogen sources required for assimilation were in short supply. Although the explanation given by Sorensen seems to apply to the initial conditions where there was almost no ammonia present initially, studies by Ghernaout et al. (2008) and Linares-Hernandez et al. (2009) proved that the current densities tested affected the microorganisms, where complete removal of coliform bacteria was observed. Therefore, it is unlikely that the reduction was biological. Polatide and Kyriacou (2005) also investigated electrochemical nitrate reduction at the cathode and explained it the fate followed two different paths:

$$NO_3^- \rightarrow NO_2^- \rightarrow NH_3 \quad \textbf{(41)}$$

$$NO_2^- + 3H_2 \rightarrow NH_3 + OH^- + H_20 \quad \textbf{(42)}$$

And:

$$NO_3^- \rightarrow NO_2^- \rightarrow N_2 \quad \textbf{(43)}$$

$$2NO_3^- + 5H_2 \rightarrow N_2 + 4H_2O + 2OH^- \quad \textbf{(44)}$$

Polatide and Kyriacou (2005) tested different cathode material, but steel wasn't one of them, the results for aluminum cathodes showed that 98% of the nitrate reduced was in the forms of nitrite and ammonia, and only 2 % was converted to nitrogen gas.

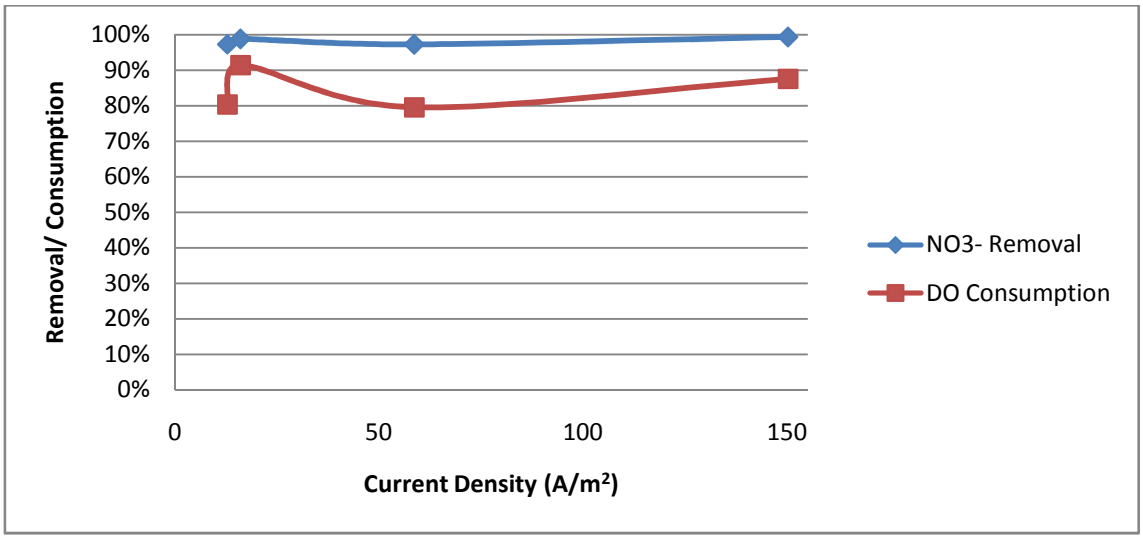

Figure 20 – Phase II - Nitrate Reduction and DO Consumption

Figure 20 shows that nitrate reduction follows the same trend as the decrease in dissolved oxygen levels. Therefore, confirming the relationship between anoxic conditions and nitrate removal. The decrease in dissolved oxygen levels was observed by Ricordel et al. (2010), where 90% of the dissolved oxygen was removed within 10 minutes of EC treatment.

$$O_2 + 2H_2O + 4e^- \rightarrow 4OH^- \quad (29)$$

DO removal is a reduction reaction, therefore occurring at the cathode. Ricordel et al. (2010) explained that the hydrogen evolved at the cathode had a deoxygenating effect resulting in reduced DO concentrations. The sudden increase in DO consumption observed at 16 A/m^2 in Figure 20 can be attributed to the variations in initial DO concentrations.

Electrode and energy consumptions were calculated using Equations 36 and 38 respectively, in order to observe the effect of the prolonged exposure period and high

current density on the consumptions; hence the operating cost. A comparison between actual and theoretical electrode consumption is presented in Figure 21.

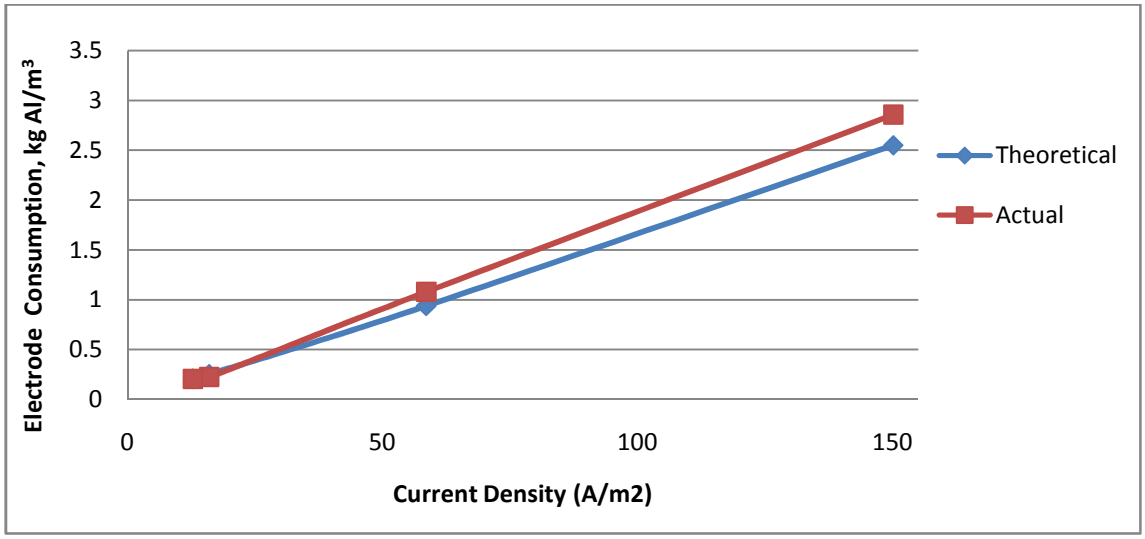

Figure 21 - Phase II – Actual and theoretical electrode consumption

At low current densities, there was almost no significant difference between the actual and theoretical consumption; however, actual consumption was higher at higher current densities. The difference observed between actual and theoretical consumptions at high current densities can be attributed to the temperature increase that took place during the treatment, thus increasing the rate of aluminum corrosion (Davis, 1999; Valenzuela et al. 2002; Mouedhen et al. 2008). Faraday's law was used to calculate the theoretical consumption. Since Faraday's Law does not take temperature into account (Figure 21), the calculated theoretical consumption was lower than the actual one. Another reason for increased corrosion rate can be the presence of chloride ions in solution, which are reported to cause pitting of the aluminum anode (Mouedhen et al. 2008).

Energy consumption is calculated using Equation 38, but to calculate operating cost Equation 39 was modified to include the price of salt added, yielding Equation 45:

$$OperatingCost = aC_{energy} + bC_{electrode} + cConcentration_{[NaCl]} \quad (45)$$

Where C is the price of salt in CAD/kg and $Concentration_{[NaCl]}$ is the salt concentration in kg/m^3. The price of salt used was CAD 50/ton (Environment Canada, 2006). Both theoretical and actual operating costs, based on the difference between actual and theoretical electrode consumption, are presented in Figure 23.

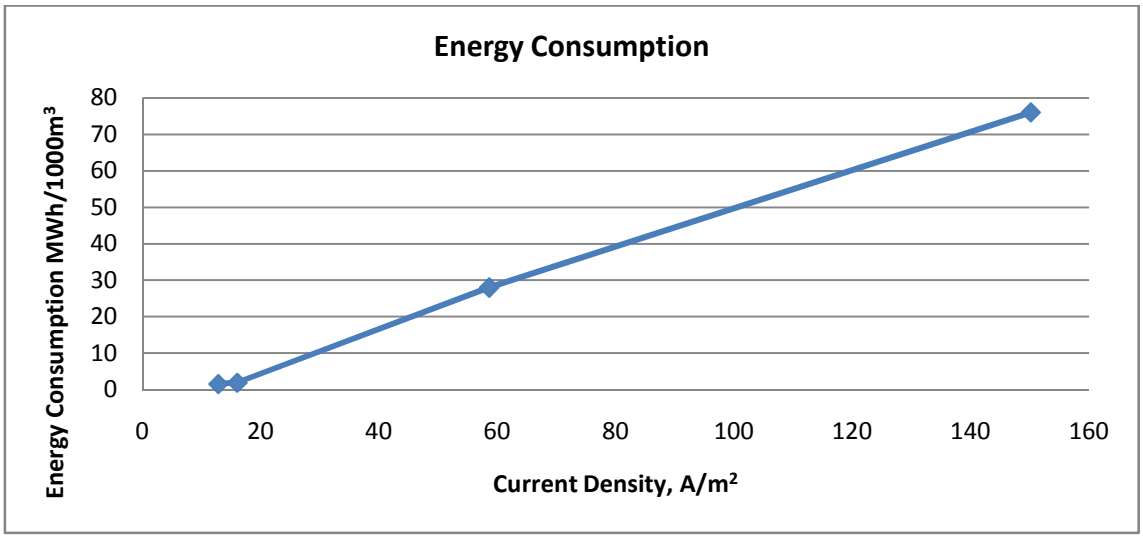

Figure 22 - Phase II - Energy Consumption

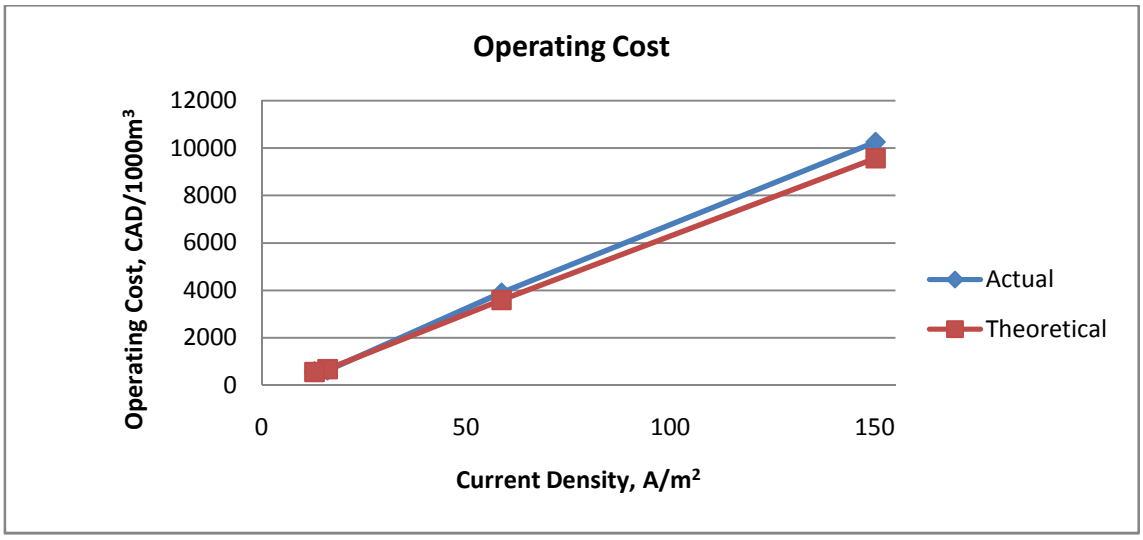

Figure 23 - Phase II - Operating cost

As seen from Figure 22 and Figure 23, energy consumption and operating cost are extremely high at the highest current densities, while effluent quality is not higher at these conditions than at the lower current densities tested. Therefore, very high current densities are undesirable due to the unnecessary high energy requirements and consequently high operating cost.

A comparison of Phase I and Phase II results highlights the importance of water conductivity in EC treatment. In Phase I, a voltage gradient of 0.5 V/cm did not yield more than a 50% phosphorus removal efficiency rate; using the same voltage gradient at a higher conductivity level, i.e. significantly higher current density, resulted in 100% removal efficiency. Furthermore, adding sodium chloride salt at the concentrations tested resulted in major reduction in energy consumption. In Phase I, 0.5 V/cm resulted in a current density of 1.9 A/m^2, whereas in Phase II, the same voltage gradient resulted in current densities 12.8 and 16 A/m^2 as seen in conditions 1 and 2 in Table 10. Mouedhen

et al. (2008) reported a decrease of over 83% in applied voltage when 100 mg/L of NaCl were added.

Continuous four-hour exposure resulted in extreme energy consumptions and undesirable operating costs. To verify if the same removal efficiencies can be achieved at shorter treatment durations and lower current densities than condition 2 in Table 10, a third phase was necessary.

4.3 Phase III - Effect of Interrupted Exposure on EC and EF

This phase examines the effects of three operating conditions on EC and EF: treatment time, current density, and exposure modes. Moreover, wastewaters were collected from two different wastewater treatment plants (WWTPs). Each WWTP had different initial characteristics; therefore, a comparison was also done between the two wastewaters in terms of treatment efficiencies, energy requirements, and operating cost. The figures for the results achieved in Phase III will be presented in removal efficiency versus treatment time in the text; however, removal efficiency versus current density is presented in Appendix I.

4.3.1 Fate of Nutrients

The change in nutrient concentrations during the experiments was studied to evaluate the effect of the chosen treatment conditions on the nutrients present in the wastewater. Considerable differences in the initial concentrations of phosphorus, nitrate, and ammonia (Chapter 3-Table 6) between the two wastewater tested could lead to different responses to the treatments applied.

4.3.1.1 Phosphorus Removal

Phosphorus removal efficiency for wastewater from WWTP1 was 100% for all the conditions tested, even with the shortest time and lowest current density. Meanwhile, WWTP2 wastewater, which had higher initial concentrations of phosphorus, experienced increased removal efficiency with longer treatment duration and current densities.

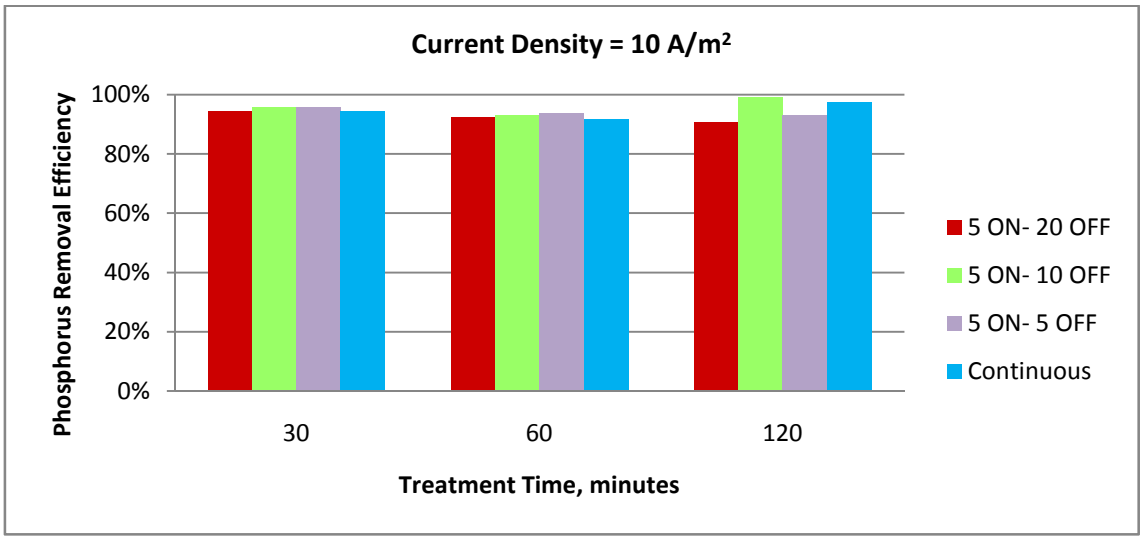

Figure 24 - Phase III - WWTP2 - Phosphorus removal – current density 10 A/m^2

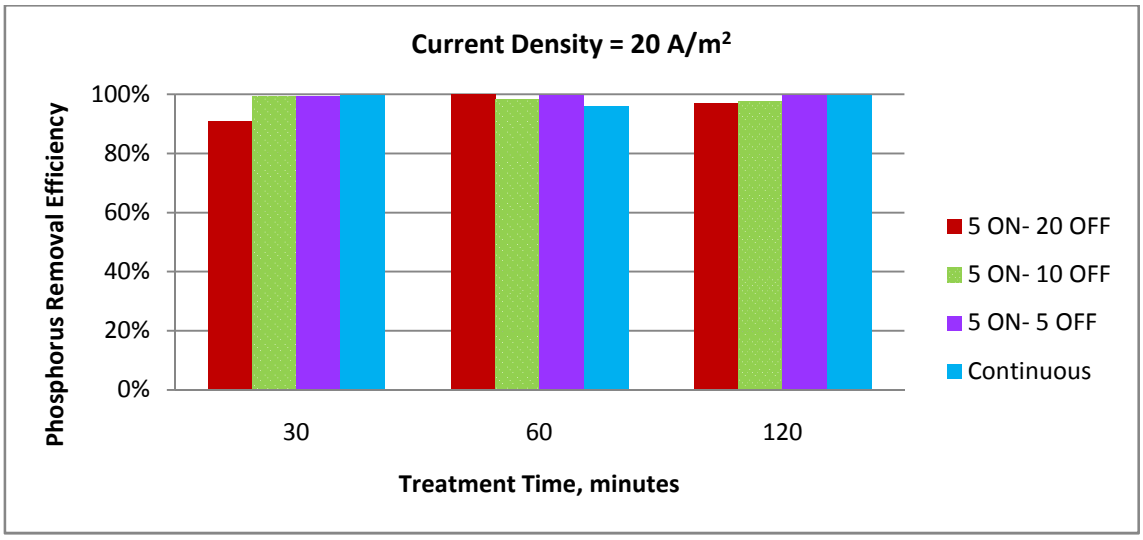

Figure 25 - Phase III - WWTP2 - Phosphorus Removal - Current Density 20 A/m^2

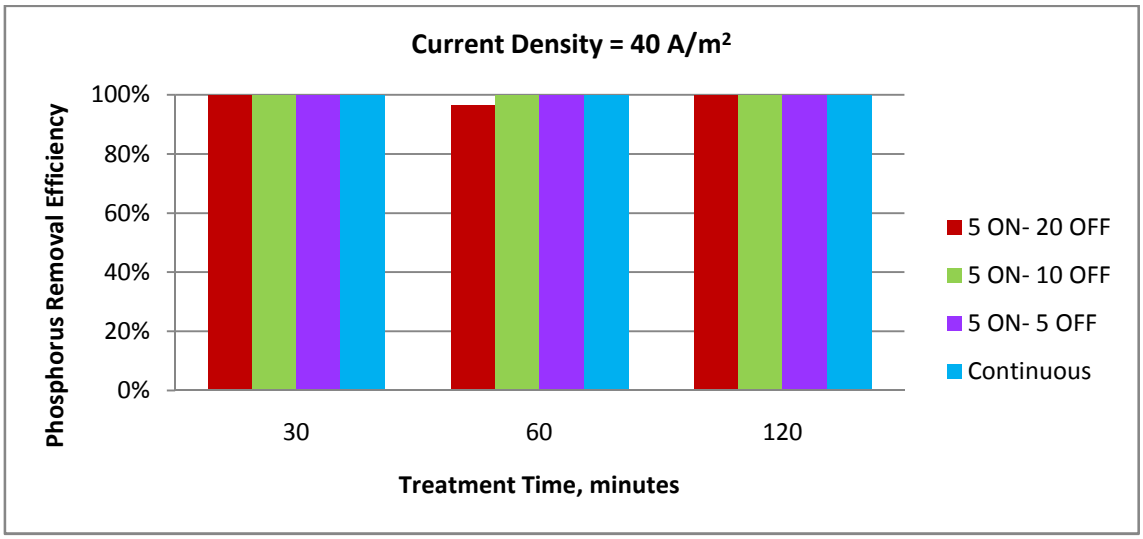

Figure 26 - Phase III - WWTP2 - Phosphorus Removal - Current Density 40 A/m^2

As seen in Figures 24-26, phosphorus removal efficiency at 10 A/m^2 ranged between 90 to 100% for all conditions, and increased at higher current densities (20 and 40 A/m^2), reaching 100% for most of the conditions. However, phosphorus removal was below 100% at current density 10 A/m^2, all the tested conditions resulted in the final phosphate concentrations below 0.5 mg/L. Phosphorus removal for current densities of 10, 20 and

$40A/m^2$ during a 30 minute treatment was also studied by Zheng et al. (2009); however, they achieved removal efficiencies of 40, 80, and 98% respectively. In this study (Phase III), the phosphorus removal from both WWTP1 and WWTP2 wastewater, using 30-minute runs and continuous exposure, was significantly higher. This divergence in results can be explained by their use of a 5mm gap between the iron electrodes.

4.3.1.2 Nitrogen Removal

While the wastewater from WWTP1 with sodium chloride conditioner was used in Phase II an investigation of nitrogen trends revealed a reduction of nitrates to ammonia. In phase III of nitrogen fate (a possibility of the same trends) was verified at lower treatment durations, lower current densities, and interrupted exposure. As it was mentioned in section 3.3, two types of wastewater, namely WWTP1 and WWTP2 were examined in this phase.

WWTP1 – low ammonia, high nitrate content:

In this experiment, the highest and lowest initial nitrate-nitrogen concentrations were 14.78 mg/L and 9.03 mg/L, respectively. After EC treatment, the lowest nitrate concentration in treated water was 2.96 mg/L. Figures 27- 29 illustrate nitrate removal at each current density as treatment time increases. A variation in the initial nitrogen concentrations gives an inaccurate indication about effluent quality, as higher removal efficiency does not necessarily result in the lower effluent concentration.

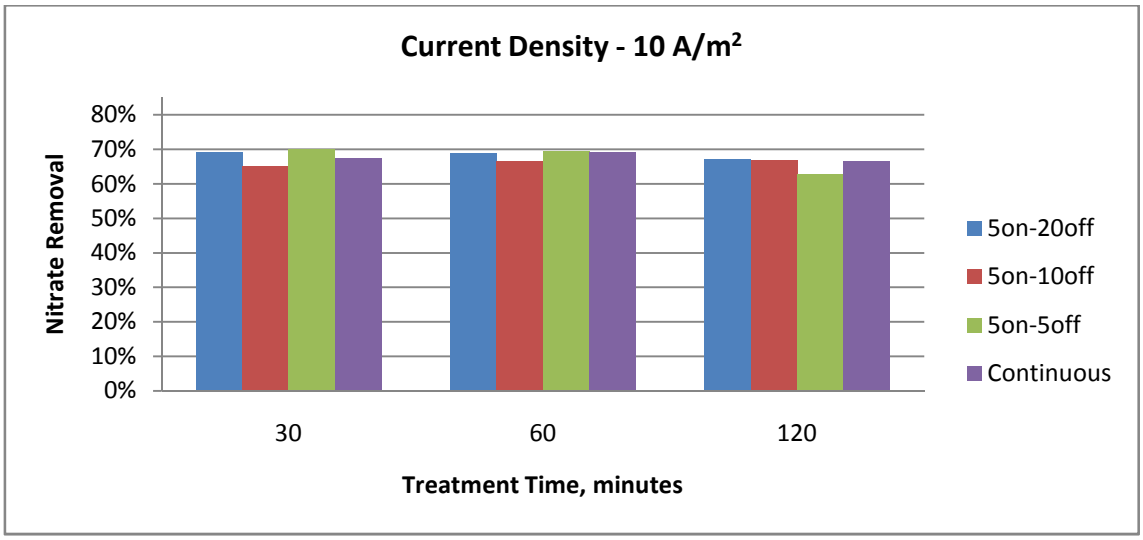

Figure 27 - Phase III - WWTP1 - Nitrate removal vs. exposure time and treatment duration at current density- 10 A/m^2

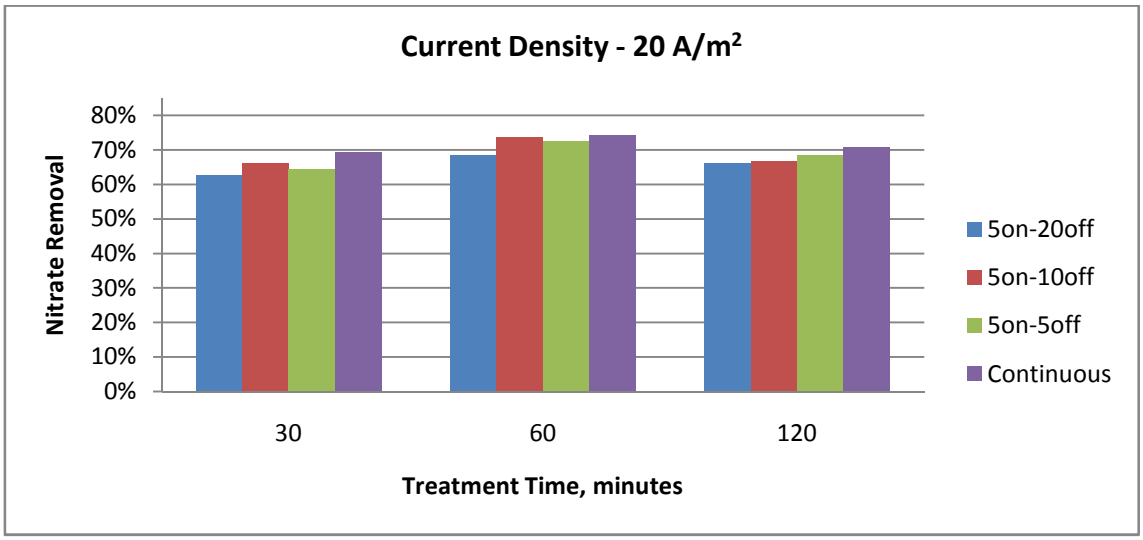

Figure 28 - Phase III - WWTP1 - Nitrate removal vs. exposure time and treatment duration at current density- 20 A/m^2

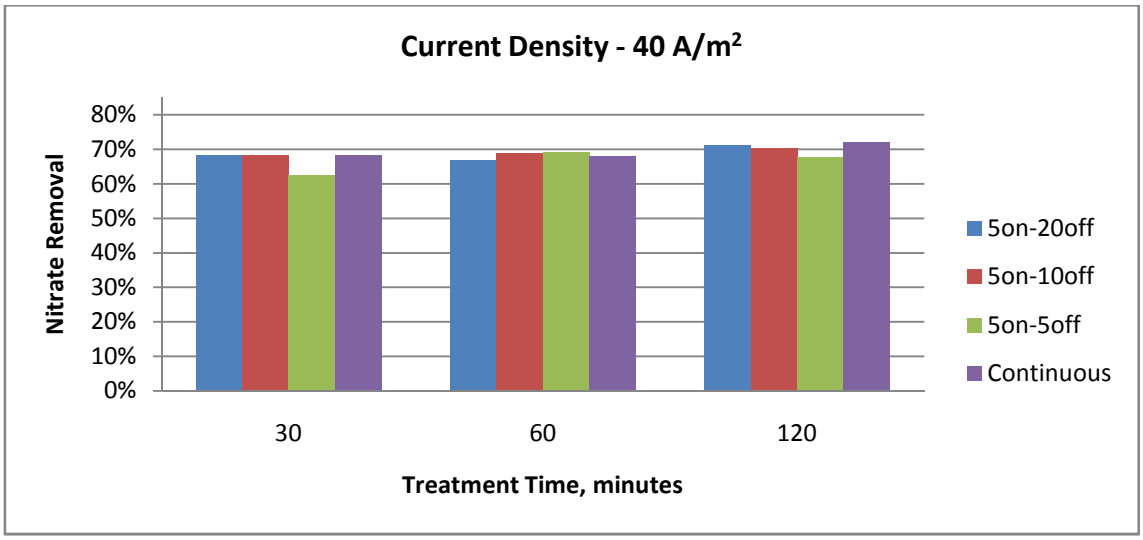

Figure 29 - Phase III - WWTP1 - Nitrate removal vs. exposure time and treatment duration at current density - 40 A/m^2

Shorter treatment durations did not seem to affect the trend found in Phase II with respect to nitrate reduction. In phase III, the nitrate removal ranged between 60% and 73% for all current densities and treatment durations.

As explained in Phase II, the nitrate reduction was stimulated by the presence of anoxic conditions; therefore, dissolved oxygen consumption are presented in Figures 30-32, and the same trend in nitrate removal and DO consumption confirms the relationship.

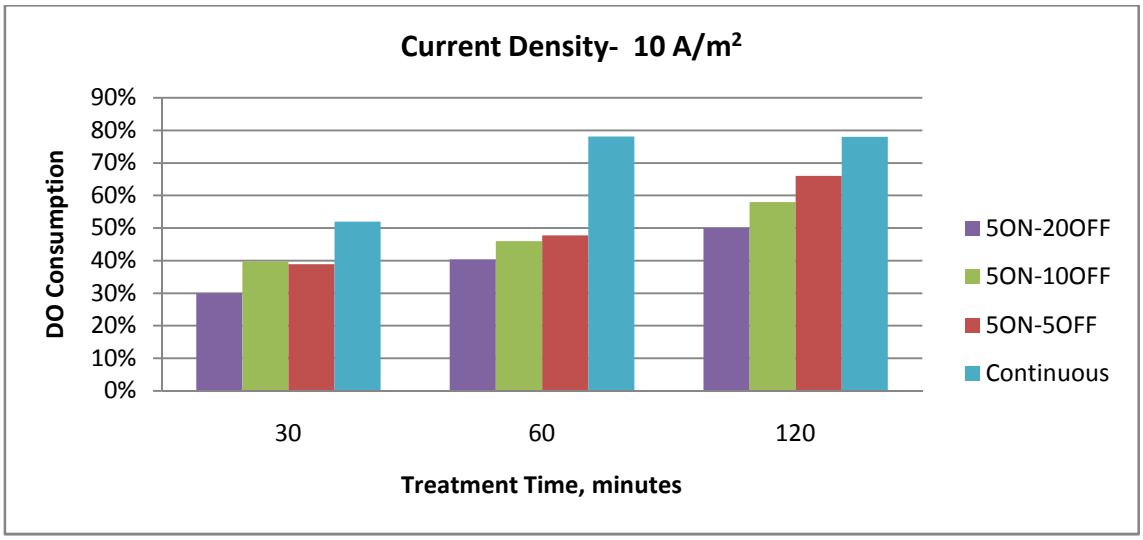

Figure 30 - DO consumption vs. exposure time and treatment duration at- Current density – 10 A/m^2

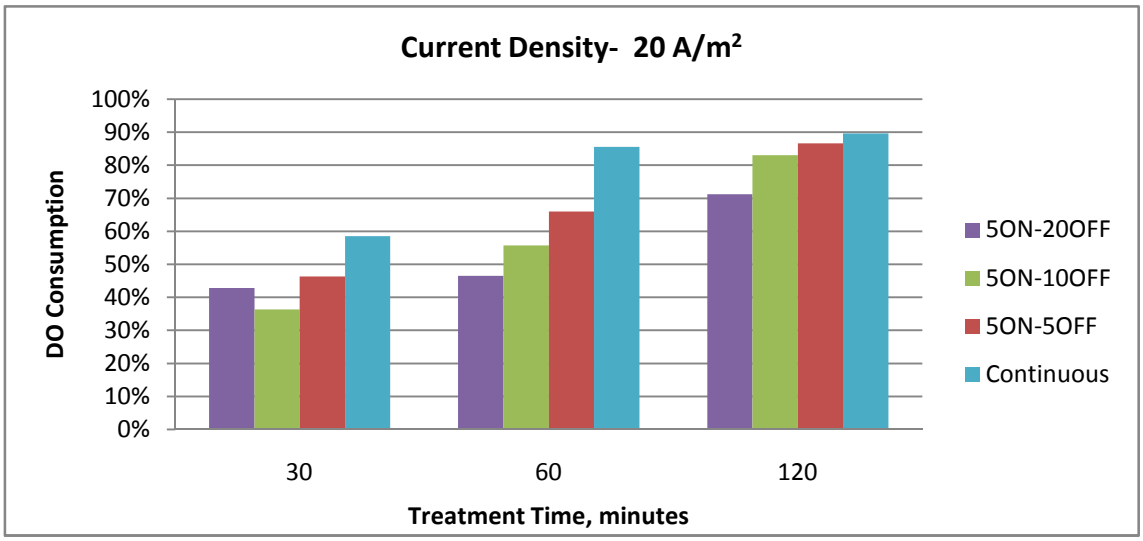

Figure 31 - DO consumption vs. exposure time and treatment duration at Current density – 20 A/m^2

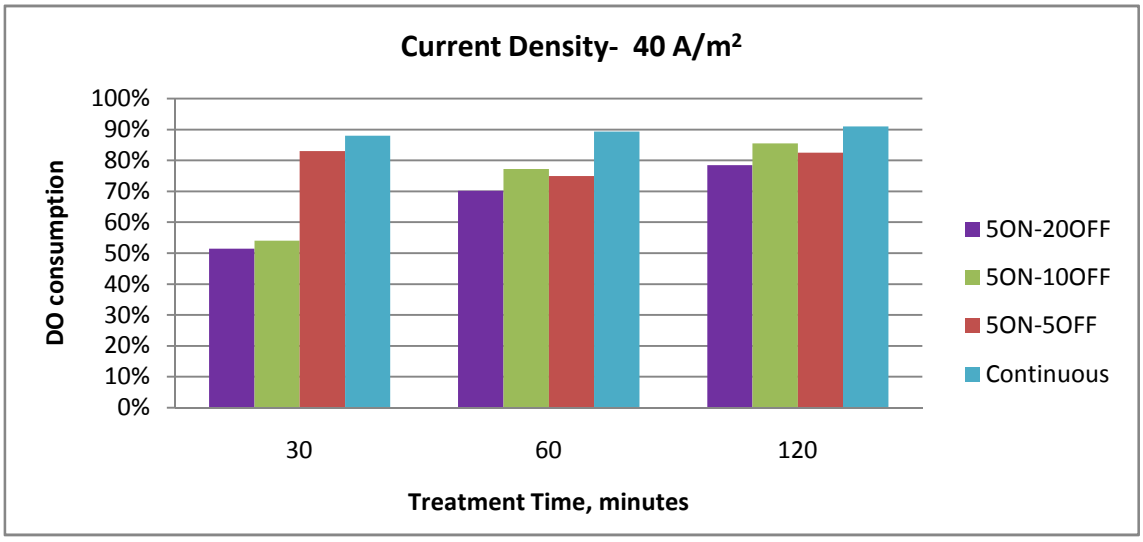

Figure 32 - DO consumption vs. exposure time and treatment duration at Current density – 40 A/m^2

The initial dissolved oxygen concentrations were different for all experiments, but final concentrations were always below 2 mg/L; therefore, anoxic conditions have been always generated during the EC treatment. An increase in current density and exposure duration to DC resulted in higher DO consumption.

Nitrate removal, anoxic conditions, and hydrogen gas generation during the experiments resulted in ammonia formation; the concentrations of ammonia increased as the nitrate concentration decreased. Figures 33-35 present nitrate and ammonia nitrogen concentrations during the EC treatment for the 60 minutes experiments.

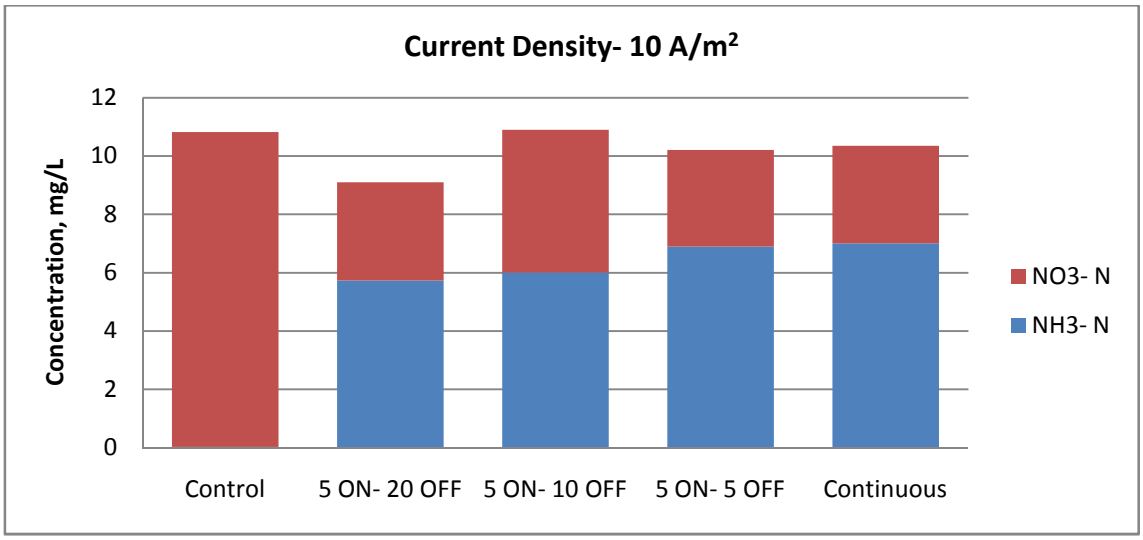

Figure 33 - Phase III - WWTP1 – Nitrate &ammonia concentrations vs. exposure time at treatment time - 60 minutes - current density - 10 A/m^2

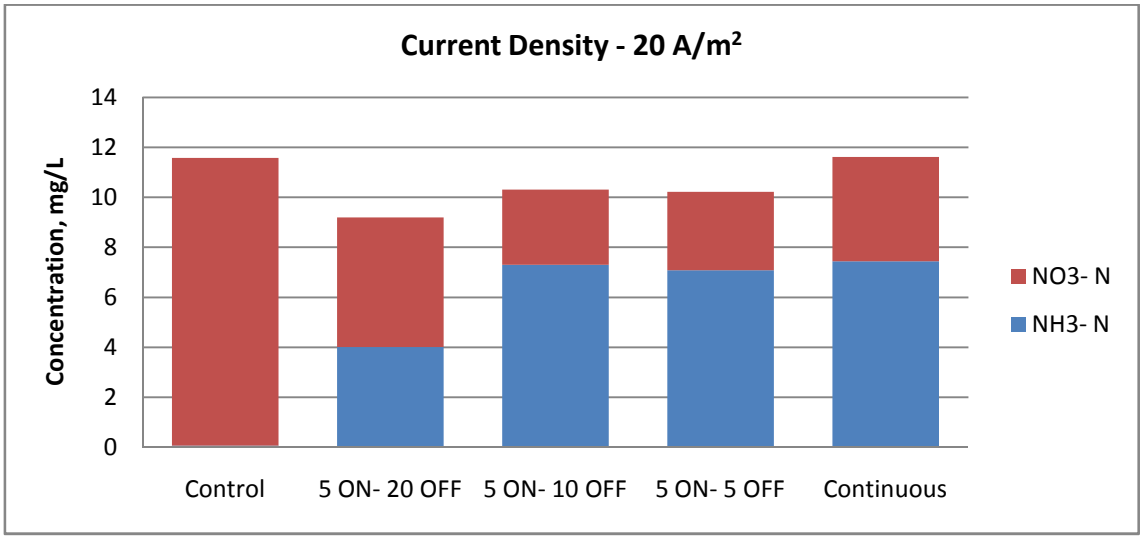

Figure 34 - Phase III - WWTP1 – Nitrate &ammonia concentrations vs. exposure time at treatment time - 60 minutes - current density - 20 A/m^2

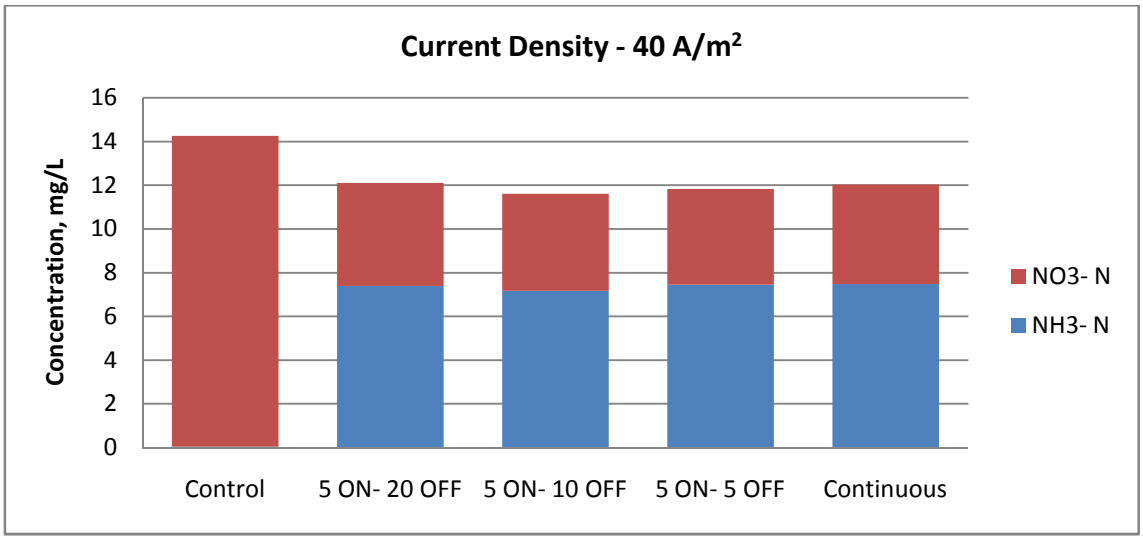

Figure 35 - Phase III - WWTP1 – Nitrate &ammonia concentrations vs. exposure time at treatment time - 60 minutes - current density - 40 A/m^2

A nitrogen balance for nitrate and ammonia indicates that some of the nitrate could have been converted to other forms of nitrogenous products along with ammonia. This is in agreement with the explanation provided by Polatide and Kyriacou (2005) concerning the reduction of nitrates to ammonia, nitrogen gas, or both (Equations 41-44).The biggest difference between the initial and final nitrogen concentrations was observed at 40 A/m^2; results can indicate that at higher current densities, nitrogen gas production rates increase.

WWTP2- high ammonia, low nitrate:

The initial nitrate concentrations in WWTP2 wastewater were 10 times lower than those of WWTP1, while ammonia concentrations were almost 75 times higher (Table 6). Therefore, nitrate reduction to ammonia was not expected to take place; however, ammonia and nitrate concentrations were monitored before and after each experiment.

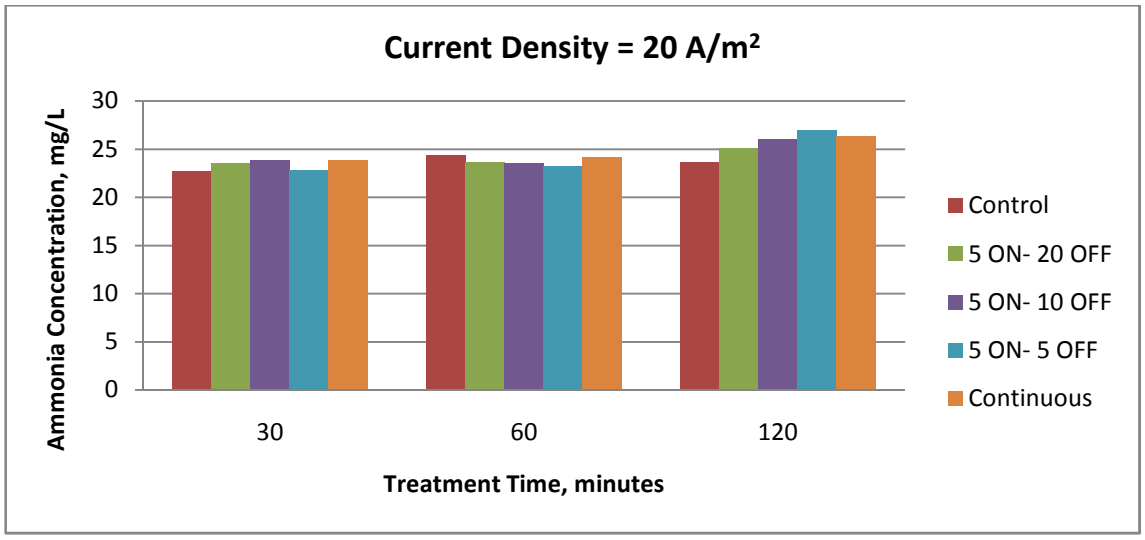

Figure 36 - Phase III - WWTP2 - Ammonia concentration vs. exposure time at current density - 20 A/m^2

No significant change was observed in ammonia and nitrate concentrations after treatment. This could be attributed to the relatively short treatment time, which was insufficient for biological nitrification- denitrification to take place. Nitrification did not therefore take place as there were only minor changes in ammonia concentrations, the lack of oxygen supply did not create the conditions to initiate the nitrification process.

$$NH_3 + O_2 \rightarrow NO_2^- + 3H^+ + 2e^- \quad (46)$$

$$NO_2^- + H_2O \rightarrow NO_3^- + 2H^+ + 2e^- \quad (47)$$

Despite the same dissolved oxygen consumption trends after the treatment of wastewaters of WWTP1 and WWTP2, and the resulting anoxic conditions, initial nitrogenous compounds concentrations led to different treatment results. The differences in trend could be in agreement with Sonerson's (1978) explanation of nitrates being reduced when other nitrogen sources are in short supply. Abiotic reduction of nitrates occurred in

WWTP1; meanwhile conditions for WWTP2's wastewater encouraged neither abiotic nor biological treatments.

4.3.2 COD Removal

The initial COD concentrations in the wastewater from WWTP1 were initially very low; therefore, high removal efficiencies of COD were not a priority. On the other hand, WWTP2 wastewater had high initial COD concentrations, and COD removal was important in order to achieve COD concentrations that were within the acceptable discharge limits.

WWTP1: low initial COD concentrations

COD removal efficiencies for wastewater from WWTP1 are presented in Figures 37-39;

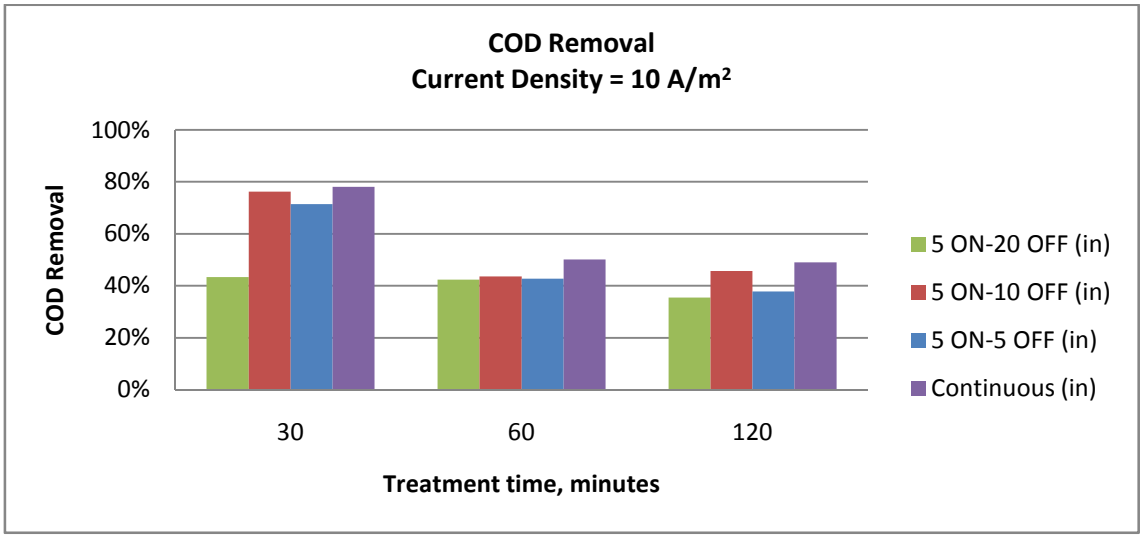

Figure 37 - Phase III - WWTP1 - COD removal, current density 10 A/m^2

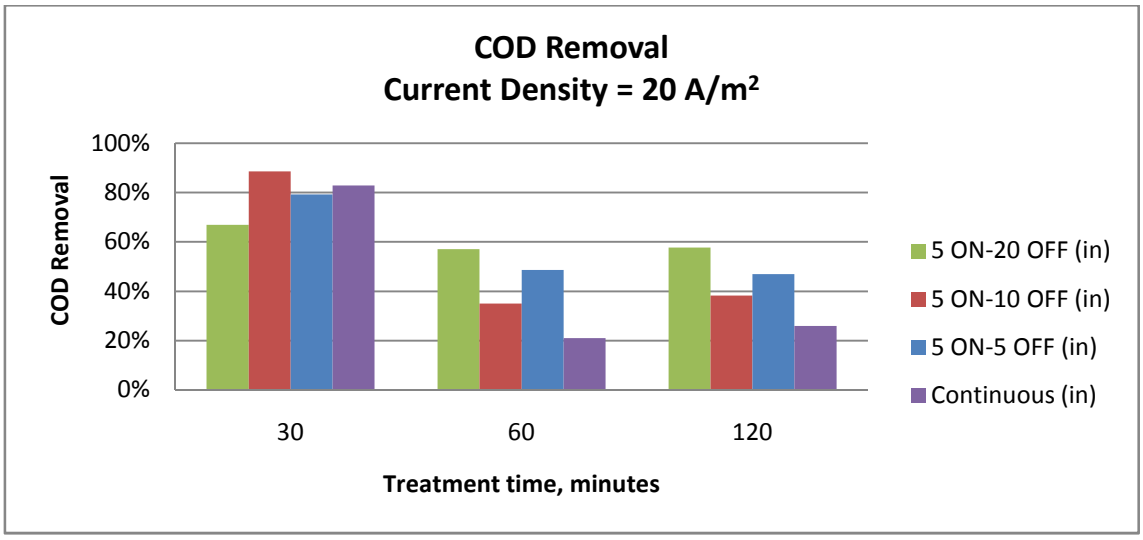

Figure 38 - Phase III - WWTP2 - COD removal - current density 20 A/m²

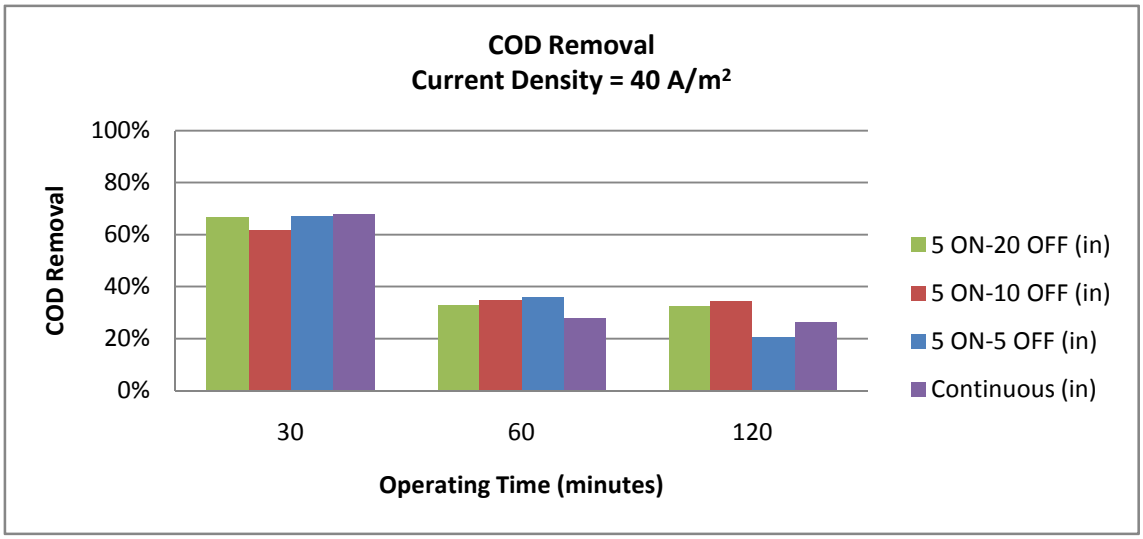

Figure 39 - Phase III - WWTP1 - COD removal - current density 40 A/m²

The trends of COD removal seen in Figures 37-39 for the wastewater of WWTP1 showed that COD removal efficiency increases as treatment time and current densities decrease reaching almost 70%. This behavior could be related to the decrease in anodic dissolution at shorter treatment times and lower current densities. Increase in anode dissolution

increases chemical sludge production, which can contribute to an increase of COD in the water, resulting in a decreasing overall COD removal efficiency.

However, it is important to note that initial COD concentrations were not identical for all tested conditions. Despite the differences in the removal efficiencies, all final COD concentrations were below 35 mg/L; and while some tests resulted in lower final COD concentrations that did translate into higher removal efficiencies since initial concentrations varied. The mode that showed a stable behavior for all the conditions tested was 5'ON- 20'OFF, where the removal efficiencies were in the same range at all current densities for each of the three treatment times, with the exception of 40 A/m^2, where efficiency was highest at 30 minutes while decreased at 60 and 120 minutes.

WWTP2: higher initial COD concentrations

Initial COD concentrations in WWTP2 wastewater were higher than those in WWTP1 wastewater, and the results for COD removal inevitably showed a different trend than in those from the first wastewater treatment plant.

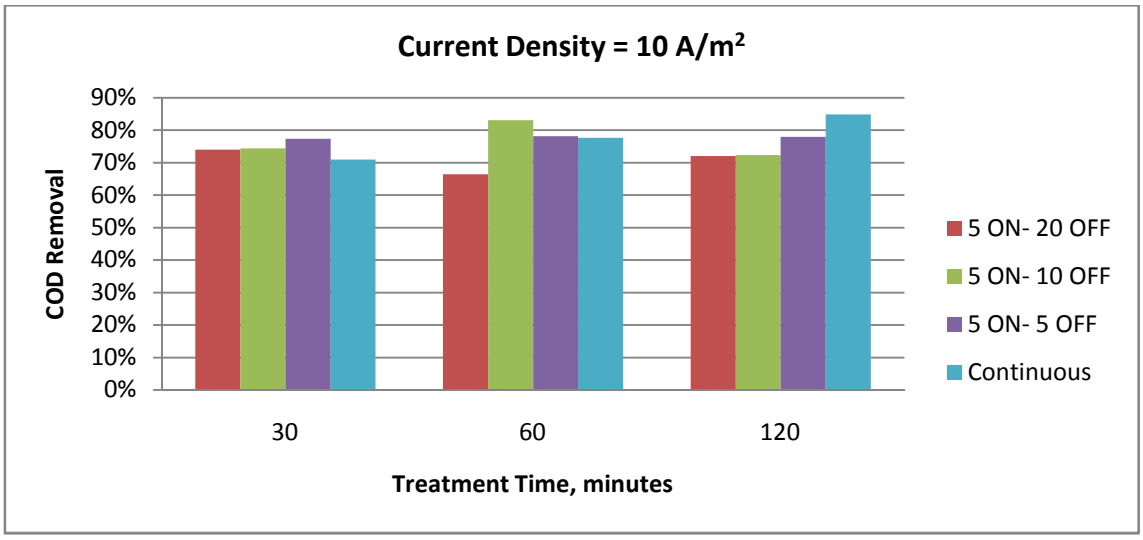

Figure 40 - Phase III - WWTP2 - COD removal - current density 10A/m^2

For the three durations tested at current density 10A/m^2 (Figure 40), most of the removal efficiencies ranged between 70% and 80%, and the efficiency differences between the different operating modes did not vary significantly.

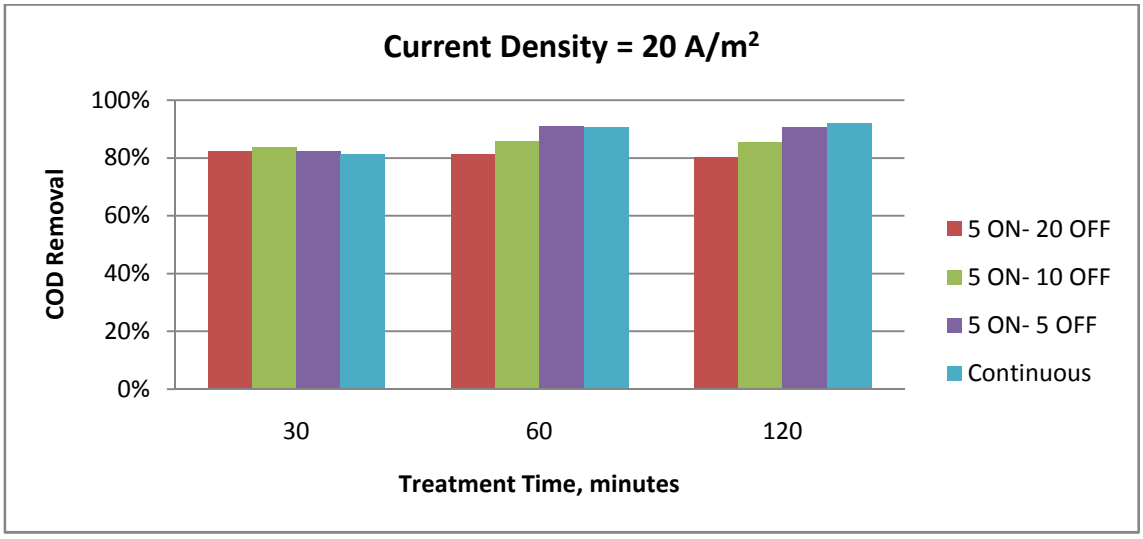

Figure 41 - Phase III - WWTP2 - COD removal - current density 20A/m^2

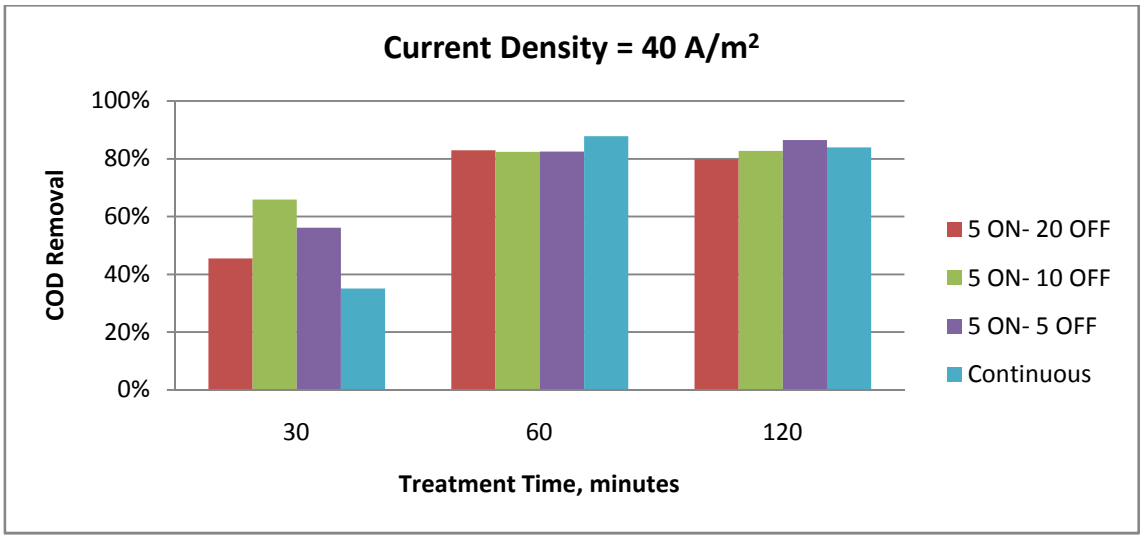

Figure 42 - Phase III - WWTP2 - COD removal - current density 40A/m^2

At 20 A/m^2 (Figure 41), removal efficiency increased, reaching values between 80% and 90%, and at 30 minutes, there was no discernible difference between the different operating modes. At 60 and 120 minutes, continuous and 5'ON-5'OFF modes produced slightly higher removal efficiencies than the other two operating modes. Removal efficiencies at 60 and 120 minutes were almost identical for the four modes tested.

At the highest current density (Figure 42), COD removal at 60 and 120 minutes was again almost identical for all tested modes, indicating that maximum removal efficiency, between 80% and 85%, had already been achieved, and that an increase in treatment duration would not improve the removal rate. No decrease in COD removal was noticed with increases to current density and treatment time, which was not the case for WWTP1 wastewater.

The wastewater used for the test conducted at 30 minutes and 40 A/m^2 was collected from the WWTP on a different day than the samples for the rest of experiments, and the initial COD concentrations were lower. Although the initial concentrations in both

wastewater treatment plants days varied drastically between days, final effluent concentrations were all in the same range (20-40 mg/L); the removal efficiency, as a percentage, was dependent on the initial COD concentration.

The inability to obtain final concentrations below 20 mg/L, most of them falling between 30 and 40 mg/L, could point to a limitation of physicochemical treatment with respect to COD removal. Given the above, additional treatment might be required to achieve 100% removal efficiency.

The results concerning removal efficiencies of COD can be misleading, whether in the experiments conducted in this research or other published studies. Higher removal efficiency is not always an indication of better treatment. Bratby (2006) tested the effect of coagulant dosage on COD removal, and results showed that a minimum concentration limit was achieved, with additional dosage producing no effect on COD removal. Results of COD removal for the three phases are therefore in agreement with Bratby's findings (2006), where maximum removal of COD was achieved even at the lowest exposure durations and current densities (Figures 40-42).

4.3.3 Zeta Potential

Zeta Potential readings for both types of wastewater did not change significantly with the treatments applied. Initial values were between -30 and -35 mV (Figures 43 – 45), and the highest value after treatment was -22 mV; therefore, some indication of floc formation was observed. Redox potential increased in negative values with the treatment (Appendix I- Figures 116-121), due to lack of oxygen supply, the release of hydroxide ions, and an increase in pH (Appendix I- Figures 104-109).

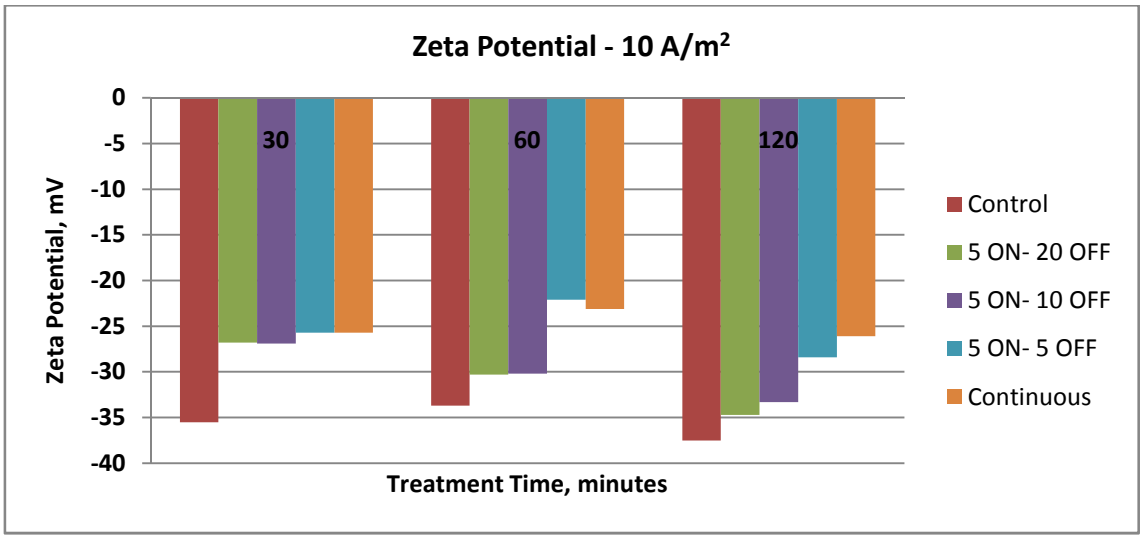

Figure 43 - Phase III - WWTP2 - Zeta potential - current density - 10 A/m^2

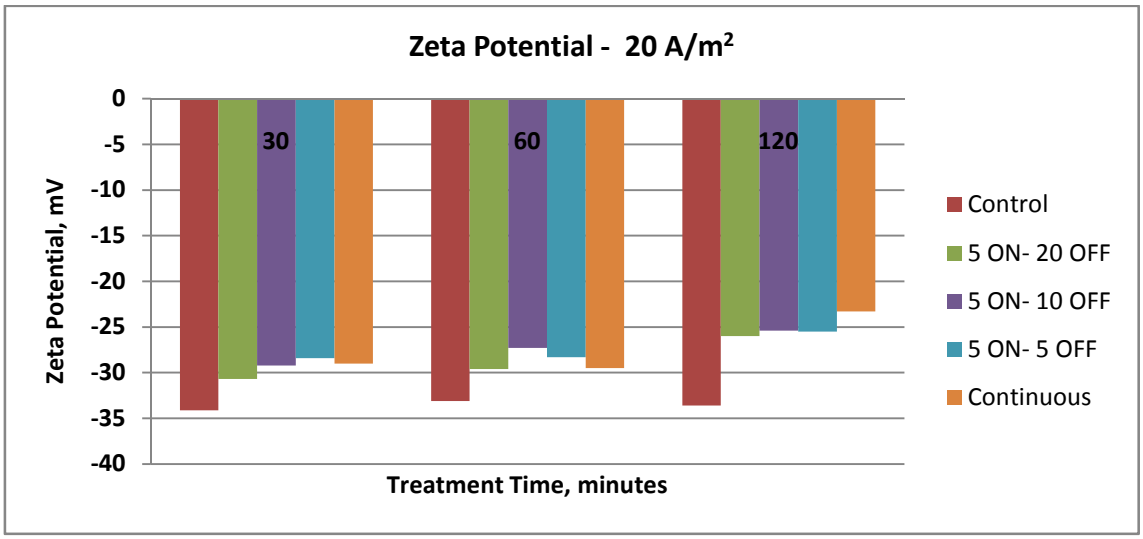

Figure 44 - Phase III - WWTP2 - Zeta potential - current density - 20 A/m^2

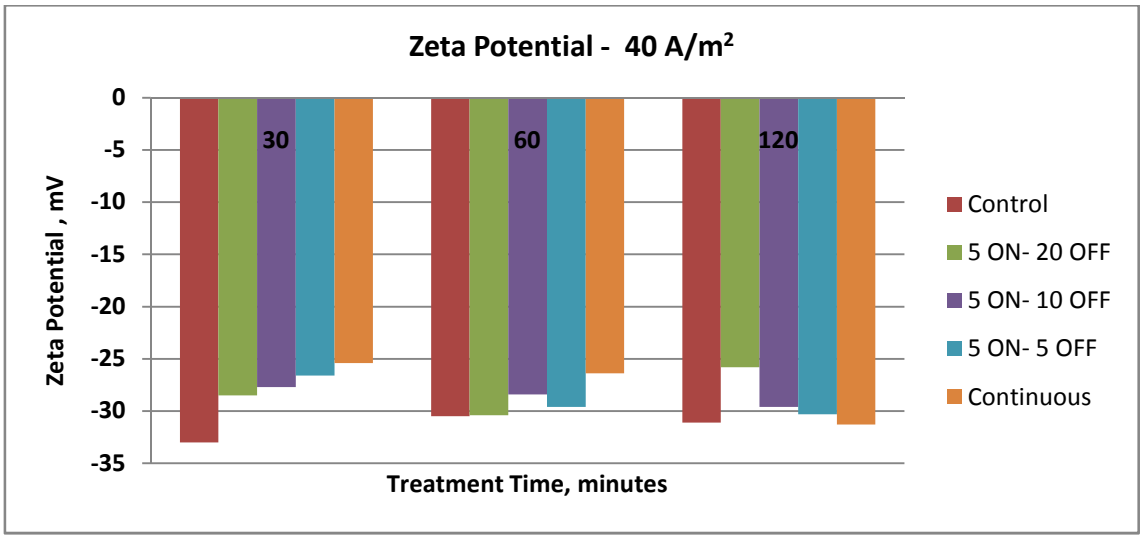

Figure 45 - Phase III - WWTP2 - Zeta potential - current density - 40 A/m^2

Figures 43-45 represent the zeta potential readings for WWTP2 samples, where a slight change was observed between initial and final conditions; however, in water from WWTP1, no difference was noted with respect to zeta potential. The zeta potential readings presented in Figures 43-45 were average results of six readings with standard deviations ranging from 1.7 to 3.2. The trend in zeta potential shows that the treatment times chosen and conditions applied promoted initiation of flocculation.

4.3.4 Average Particle Size

Particle size measurements were conducted to verify whether the tested exposure durations resulted in a difference in the average particle (flocs) sizes. Given that the wastewater of WWTP1 was extremely dilute, samples larger than 100 ml were needed to get one reading, and no significant difference was noted among runs for samples from WWTP1; the size range was always between 47 and 53 µm.

Measurements of particle size in wastewater WWTP2 showed increase with increase of exposure time in short tests. However, for longer tests, average particle size did not show

specific trend (Figure 46), since with increase in time other phenomena take place other than simple flocculation, e.g. electroosmosis.

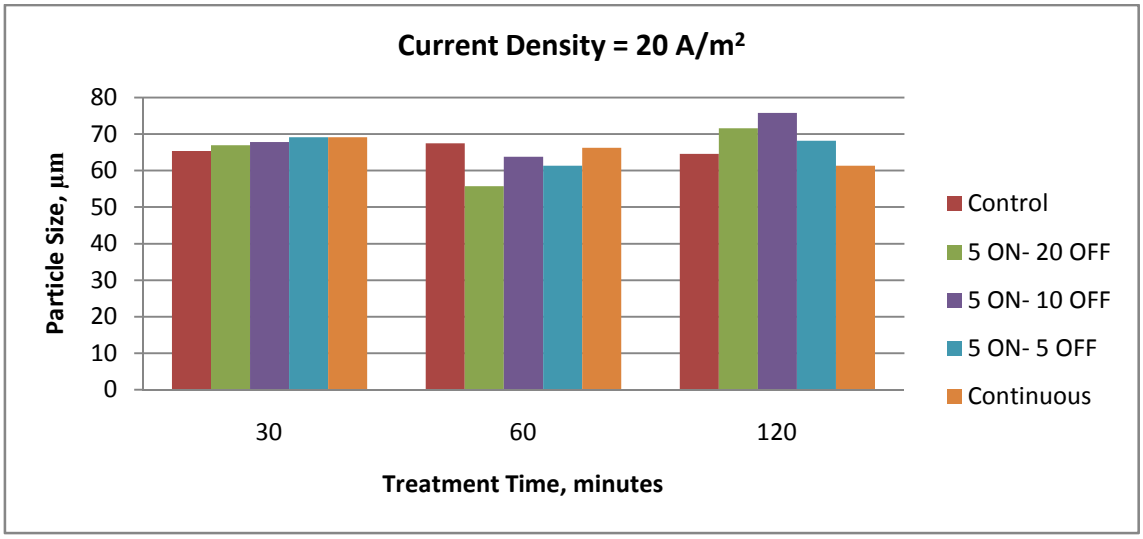

Figure 46 - Phase III - WWTP2 - Average Particle Size - Current Density - 20 A/m^2

Horiba Particle Size Analyzer gives a two dimensional estimate of the particle size; therefore, any variation in aggregate shape will be read as the diameter of a spherical particle. This creates a potential for misrepresentation of the actual morphology of the particle. Results of average particle size for treatments at current densities 10 and 40 A/m^2 are presented in Appendix I- Figures 122-124.

4.3.5 Turbidity Removal

WWTP1: Low suspended solids and high conductivity

As a result of the sampling method limitations mentioned in Chapter 3, a visual evaluation of turbidity removal is presented for WWTP1 wastewater in Figures 47– 49.

Current Density 10 A/m^2

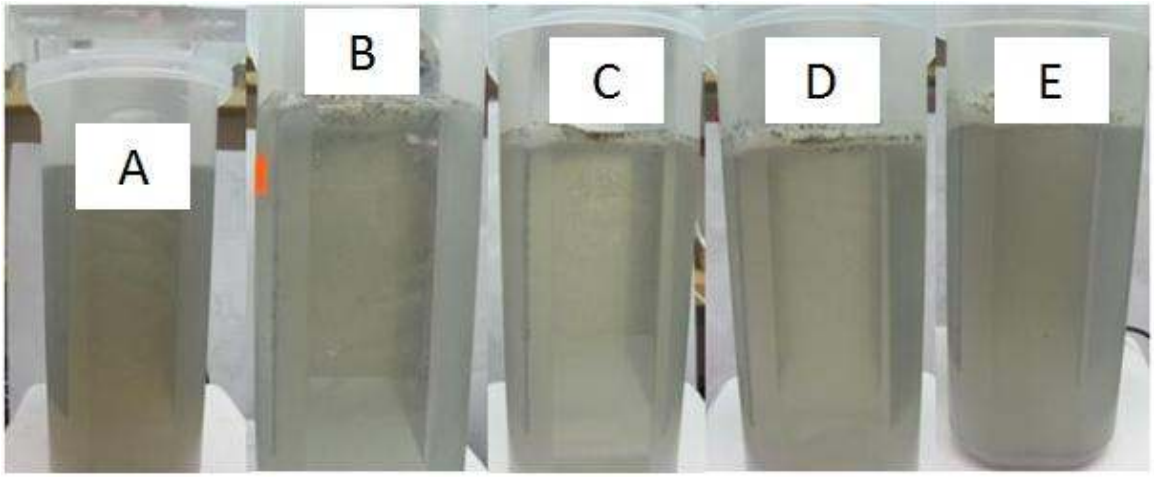

Figure 47 - Phase III - WWTP1 – Flotation - current density 10 A/m^2 - 120minutes
A: Control; B: 5'ON - 20'OFF; C: 5'ON - 10'OFF; D: 5'ON - 5'OFF;
E: Continuous

At a current density of 10A/m^2, flotation was weak, with no significant observed change in turbidity or color, as shown in Figure 47. However, some flotation was noticed after 120 minutes in the continuous exposure and 5'ON-5'OFF reactors (Figure 47 D & E).

Current Density- 20 A/m^2

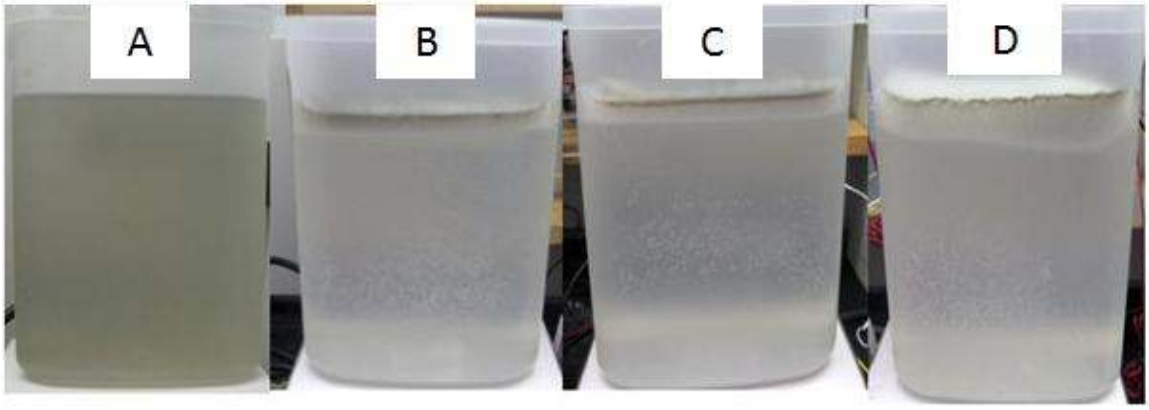

Figure 48 - Phase III - WWTP1 – Flotation - Current Density 20 A/m^2 - 120minutes
A: Control; B: 5'ON - 10'OFF; C: 5'ON - 5'OFF; D: Continuous

Using a current density of 20A/m^2, significantly better flotation was noted than at 10 A/m^2, with clear water columns at the end of the 120 minute experiment. Figure 48shows the reactors after treatment (Figure 48-B, C, D) in comparison to the control reactor (Figure 49-A). Visual interpretations indicate high turbidity removal, leaving a clear water column. The exposure mode 5'ON-20'OFF is not presented in Figure 48; however, the visual appearance was almost identical to the 5'ON-10'OFF mode (Figure 48-B). The remarks noted after the experiment stated that 5'ON-20'OFF resulted in the thinnest foam layer; nevertheless, it was stable and held tightly together. A very thick foam layer was formed in the continuous exposure and 5'ON- 5'OFF reactors (Figure 48- C&D) the layers were non-uniform and had a gel-like texture when skimmed due to aluminum species formation (Figure 49).

Figure 49 - Gelatinous aluminum hydroxide formation

As mentioned earlier, gel texture could be an indication of high water retention in the produced foam, which was later confirmed by water retention tests. At a current density of 20 A/m^2 and duration of 120 minutes, foam water retention values were higher for continuous and 5'ON-5'OFF exposure modes.

Current Density- 40 A/m^2

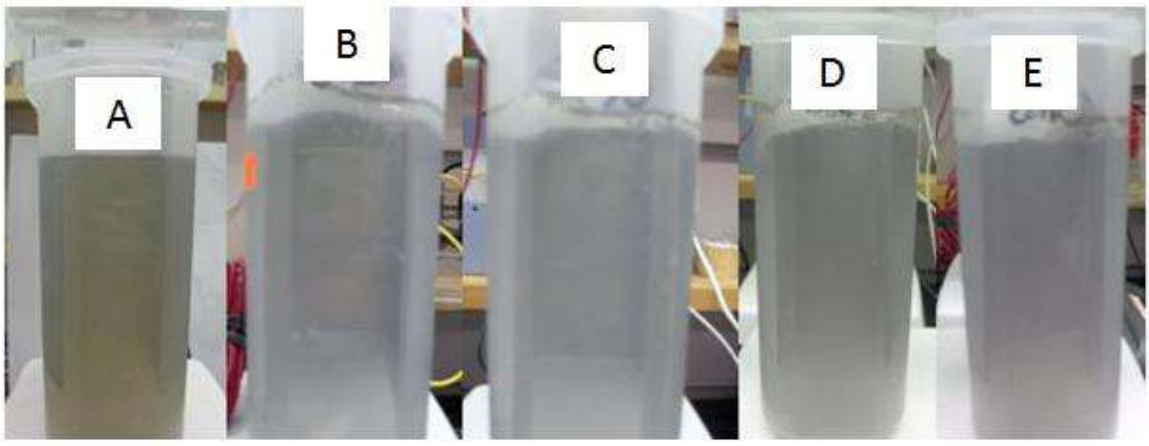

Figure 50 - Phase III - WWTP1 – Flotation - current density 40 A/m^2- 120minutes
A: Control; B: 5'ON- 20'OFF; C: 5'ON- 10'OFF; D: 5'ON- 5'OFF; E: Continuous

Doubling the current density from 20 to 40 A/m^2 resulted in an excessive release of aluminum ions into the solution. 5'ON-20'OFF and 5'ON-10'OFF modes involve longer "OFF" durations, resulting in fewer quantities of aluminum being released during the 120 minutes of treatment time. Figure 50 illustrates how turbidity decreases in 5'ON-20'OFF and 5'ON-10'OFF reactors (Figure 50- B&C), then increases again in the 5'ON-5'OFF and continuous exposure reactors (Figure 50- D&E). Water in the 5'ON-5'OFF and continuous exposure reactors turned grey after 60 minutes of treatment time due to the excess release of aluminum ions in solution.

Amongst three current densities and three treatment durations tested, the best solid/liquid separation conditions occurred with interrupted exposures at the current density of $20A/m^2$ and 120- minute treatment time (Figure 48- B&C). Continuous exposure at the same conditions also yielded a clear water column, but it produced a very thick foam layer (Figure 48-D).

Longer exposure allows for better mixing between the particles in wastewater and the aluminum ions released in solution. In cases of excess ion release, the OFF mode allows more time for mixing and flocculation, and the ON mode generates the hydrogen gas molecules that carry the flocs to the surface. Excess aluminum ions that remain in solution do not float to the surface, causing the water to turn grey and eventually settling at the bottom of the reactor when mixing stops. It was important to observe the flotation results in WWTP2 when the same operational conditions are applied.

WWTP2: high solid content

As mentioned in Chapter 3, turbidity measurements were read after allowing 30 minutes in the sampling vials to permit settling. Due to higher initial concentration of suspended solids in WWTP2 wastewater, not all of the flocs floated.

Settling occurs when the densities of the particles are higher than density of the carrying fluid, i.e $\rho_{2>}\rho_{1}$. However, in flotation, the particle moves upwards against gravity, with the help of an upward driving force (Equation 33). Flotation will occur only when the velocity of the rising particle is higher than the downward velocity of water (Chen et al. 2000). When suspended solid concentration increases, more hydrogen gas needs to be produced to carry them to the surface; controlling the amount of hydrogen gas production can be achieved by controlling current density and/or treatment time (Equation 30). Ben Mansour et al. (2007) applied electroflotation with waters of different weight concentrations of glycerine to measure uprise velocity of gas particles; the reactor with the highest weight percent had the lowest uprise velocity; thus confirming the differences in flotation between WWTP1 and WWTP2 in Phase II. Turbidity removal readings for WWTP2 samples are presented in Figures 52-54.

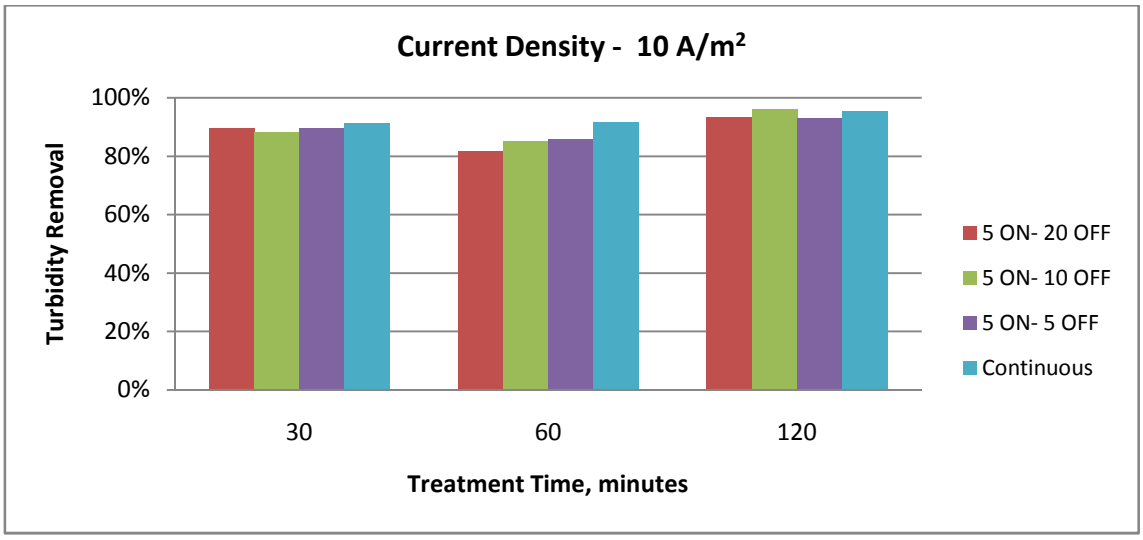

Figure 51 - Phase III - WWTP2 - Turbidity removal - current density 10 A/m²

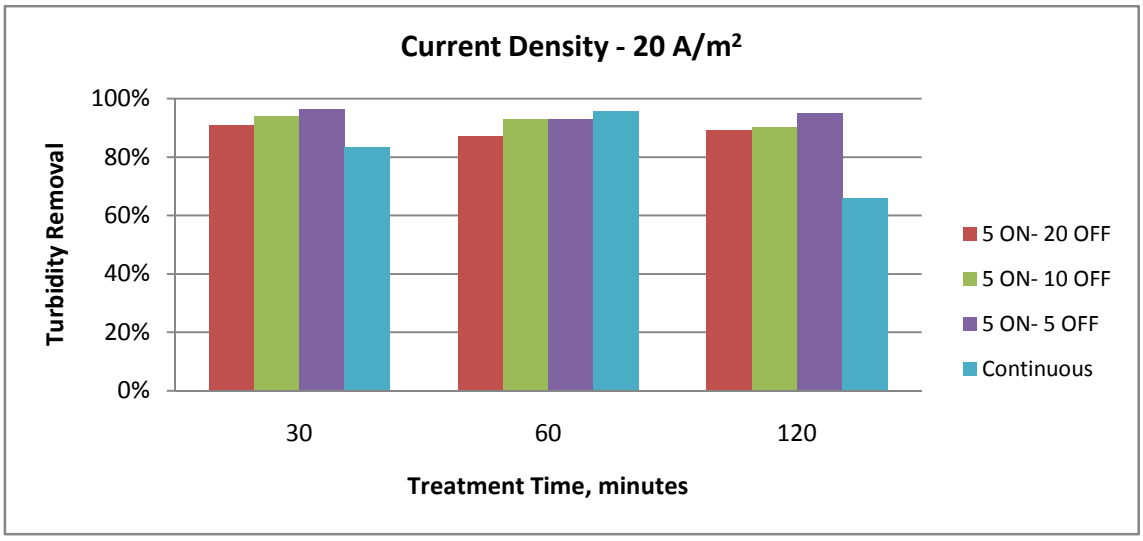

Figure 52 - Phase III - WWTP2 - Turbidity removal - current density 20 A/m²

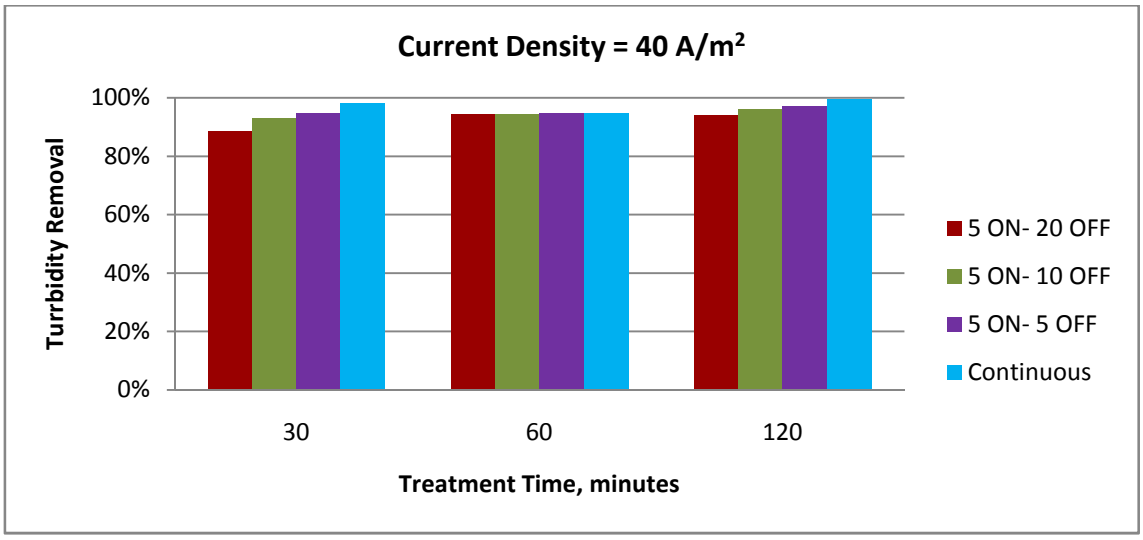

Figure 53 - Phase III - WWTP2 - Turbidity removal - current density 40 A/m^2

At 10 A/m^2 (Figure 51), a similar trend to the one observed for WWTP1 took place, where the highest turbidity removal was after the 2 hour experiment; however, 30 minutes after the end of the experiment, clear settling was observed in all of the reactors. The slowest settling occurred in the continuous mode reactor, where flocs started settling at the end of the 30 minute period.

Electroflotation was observed again at 20A/m^2, but the foam produced was not stable and it settled down in all reactors after electricity and mixing stopped. The foam formed by continuous exposure was the most stable and was the slowest to settle down. Excess aluminum was produced at current density of 40 A/m^2, and the foam formed after 120 minutes of treatment was very stable and very resistant to settling (Appendix II- Figure 147). This could be explained by the increased amount of hydrogen gas bubbles generated (Equation 30).

Figures 51 to 53 show that the treatment conditions and settling time chosen resulted in turbidity removal rate between 80 and 98%, except for the continuous mode at 20 A/m^2 and 120 minutes, where it was lower. It is important to note that the final turbidity values were due to combined electroflotation and settling.

The actual exposure time to electricity was proportional to the settling time needed; therefore, the fastest settling was observed at 5'ON-20'OFF mode; and the slowest was with continuous mode.

For a duration of 30 minutes, both 5'ON-10'OFF and 5'ON-20'OFF have a total of 10 minute exposure to electricity and 30 minutes of mixing time, and the rate of settling was almost the same for both modes. Thickness of settled layer is also related to actual exposure time to electricity, and the justification to this relationship is the amount of aluminum ions that are being produced in-situ; any excess ions settle to the bottom. Figures 54- 56 show the settling that resulted from 30 minutes of settling post to 30, 60 and 120 minutes of treatment at current density 20 A/m^2.

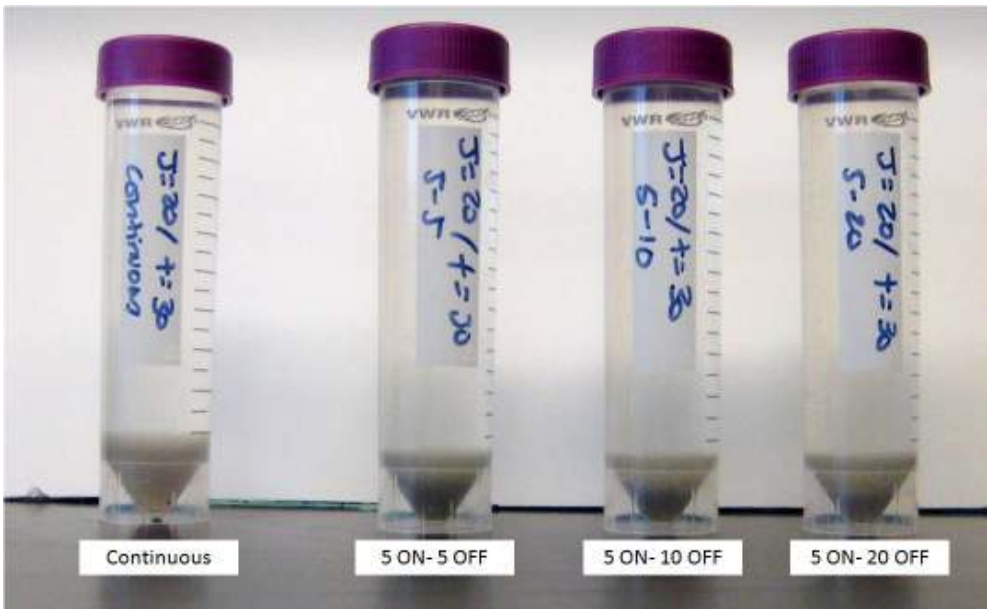

Figure 54 – Phase III - WWTP2 - Treatment time 30 minutes

Settling of solids after EC of WWTP2 samples for different exposure time

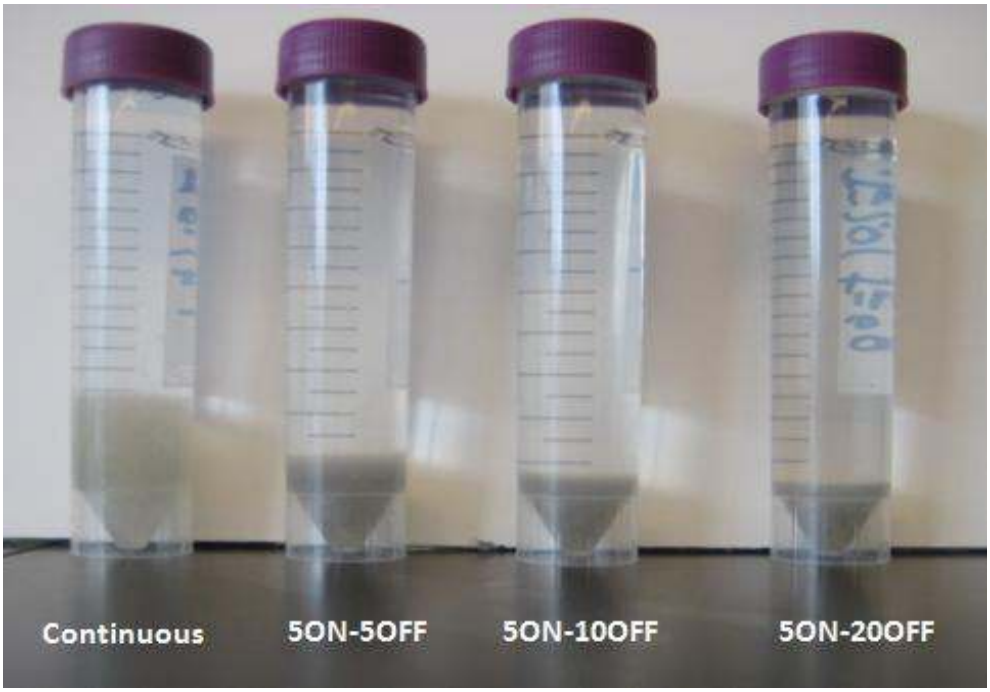

Figure 55 – Phase III - WWTP2 - Treatment time 60 minutes

Settling of solids after EC of WWTP2 samples for different exposure time

Figure 56 – Phase III - WWTP2 - Treatment time 120 minutes

Settling of solids after EC of WWTP2 samples for different exposure time

Calculating the change in anode weight after each experiment confirms the trend observed in Figures 54-56. The final stage evaluation of the best treatment conditions will be based on the electrode and energy consumptions, and consequently the operating cost.

4.3.6 Electrode Consumption

Electrode consumption was calculated theoretically using Faraday's Law, and compared to actual consumption (Chapter 3- Equation 36). The treatment time used for the calculation of interrupted exposure was based on the net exposure to electricity. Table 11 summarizes the net exposure durations for all the operation modes.

Table 11 - Phase III - Net Exposure to Electricity

Mode	Net Exposure (minutes)		
	30 min	60 min	120 min
5'ON-20'OFF	10	15	25
5'ON-10'OFF	10	20	40
5'ON-5'OFF	15	30	60
Continuous	30	60	120

Theoretical electrode consumption calculations are not affected by the applied voltage; therefore, the conductivity of the solution has no effect on the calculated electrode consumption. Despite the differences in initial conductivities between the waters of WWTP1 and WWTP2, calculated consumptions are the same.

WWTP1: high conductivity

** C.D – Current Density*

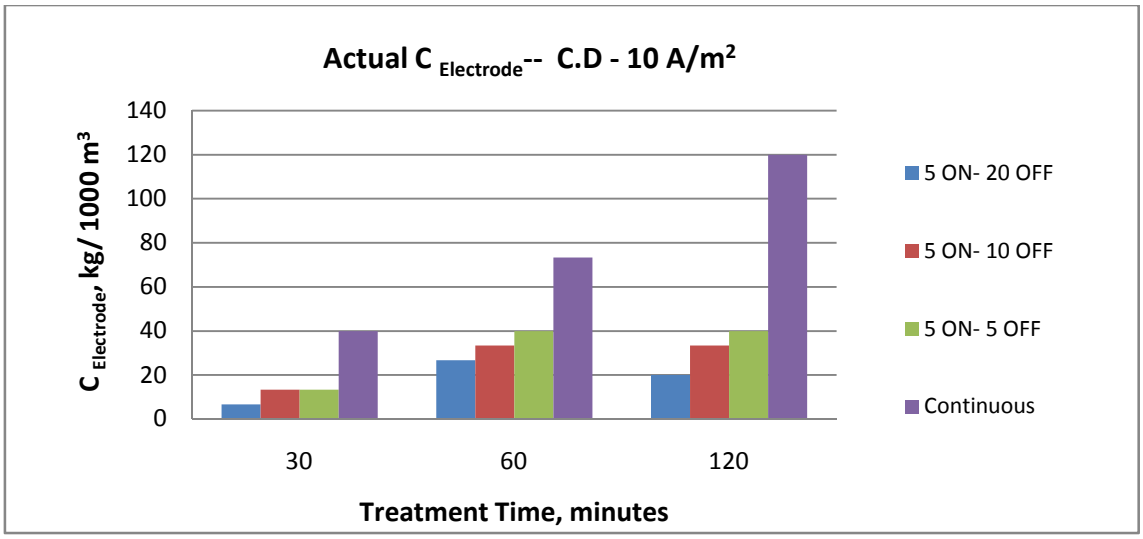

Figure 57 - Phase III - WWTP1 - Actual electrode consumption- current density 10 A/m^2

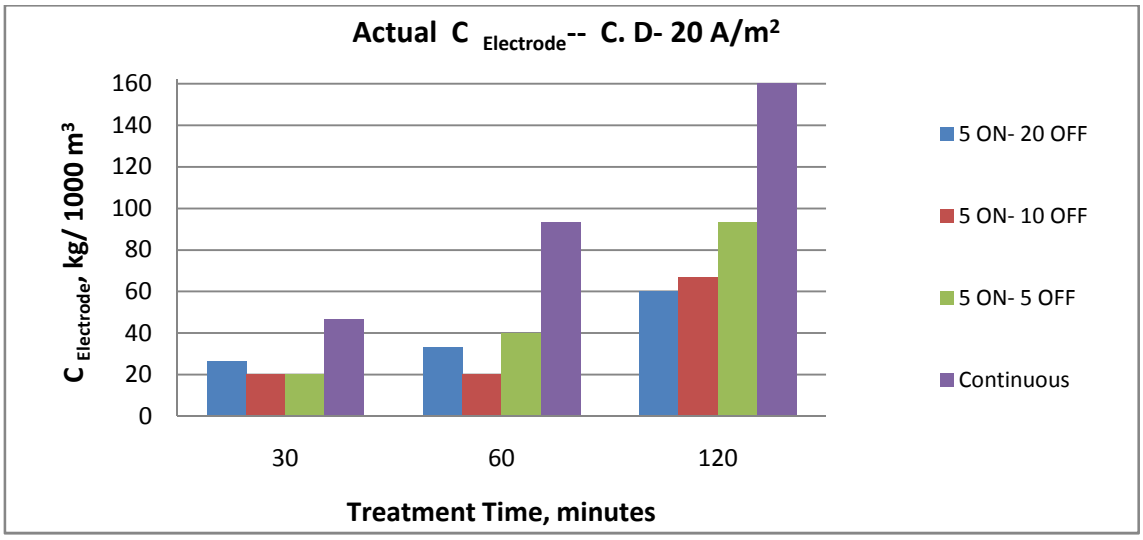

Figure 58 – Phase III - WWTP1 - Actual electrode consumption - current density 20 A/m²

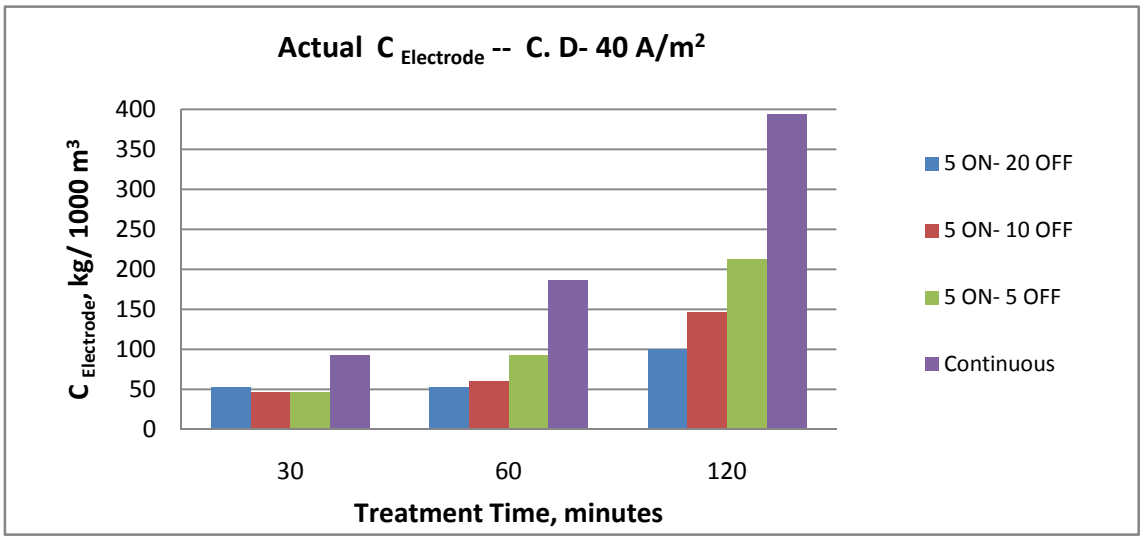

Figure 59 – Phase III - WWTP1 - Actual electrode consumption - current density 40 A/m²

Electrode consumption increases proportionally with the increase in treatment time, exposure time and current density (Figures 57 - 59). The highest anode dissolution occurs at continuous exposure, due to the rise in temperature that takes place with continuous exposure to electricity. Increase in temperature increases corrosion rate (Davis, 1999;

Valenzuela et al. 2002; Mouedhen et al. 2008), a factor that is not considered in Faraday's Law (Equation 36). Therefore, the actual consumption values are expected to be higher than theoretical values. Table 12 presents both actual and theoretical electrode consumptions.

Table 12 - Phase III- Actual and Theoretical Electrode Consumption – WWTP1

Electrode Consumption (kg/1000 m3)									
C.D A/m^2	**Time (min)**	**5'ON-20'OFF**		**5'ON-10'OFF**		**5'ON-5'OFF**		**Continuous**	
		T	A	T	A	T	A	T	A
10	30	6	7	6	13	9	13	18	40
	60	9	27	12	33	18	40	36	73
	120	15	20	24	33	36	40	72	120
20	30	12	27	12	20	17	20	35	47
	60	17	33	23	20	35	40	69	93
	120	29	60	46	67	69	93	139	160
40	30	23	53	23	47	35	47	69	93
	60	35	53	46	60	69	93	139	187
	120	58	100	92	147	139	213	277	393

T – Theoretical
A- Actual
C.D – Current Density

WWTP2: high conductivity

A comparison between actual electrode consumption when treating water from WWTP1 and WWTP2 will provide proof of the effect of solution conductivity on electrode consumption. Figures 60-62 present the actual electrode consumption versus treatment durations for current densities 10, 20 and 40 A/m^2.

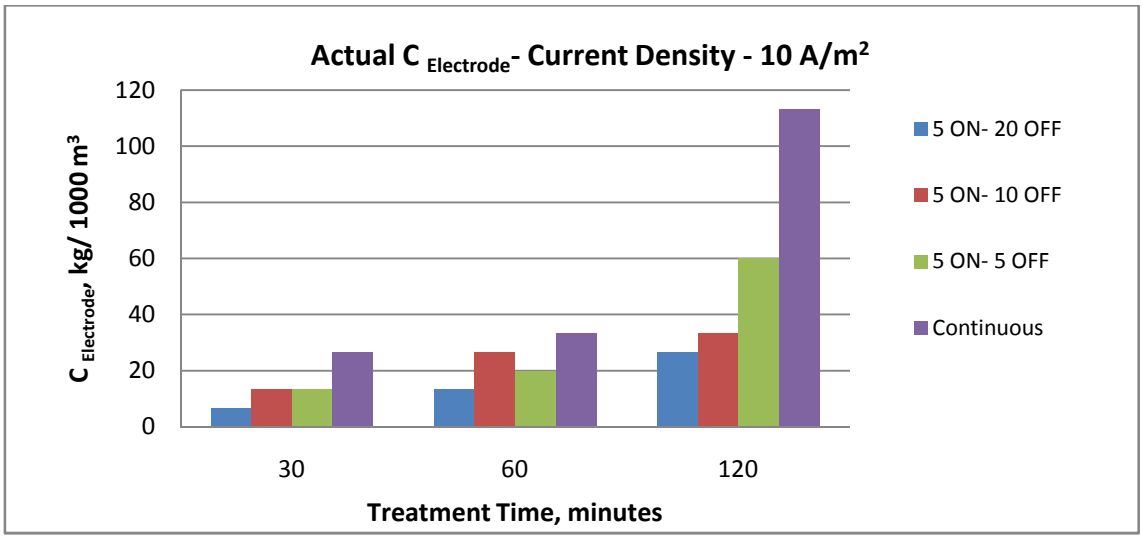

Figure 60 – Phase III - WWTP2 - Actual Electrode Consumption- Current Density 10 A/m^2

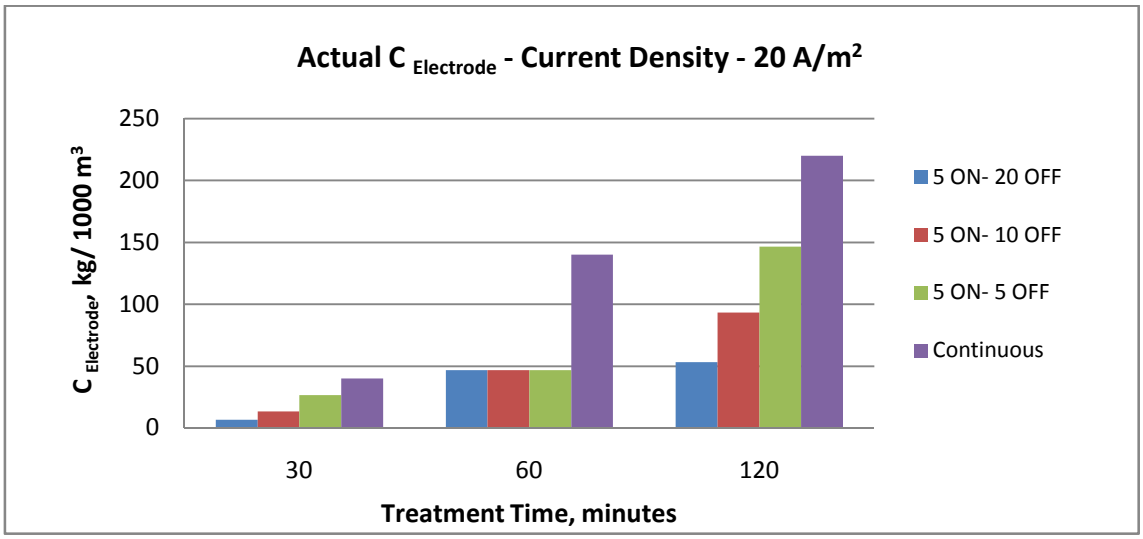

Figure 61 – Phase III - WWTP2 - Actual Electrode Consumption - Current Density 20 A/m^2

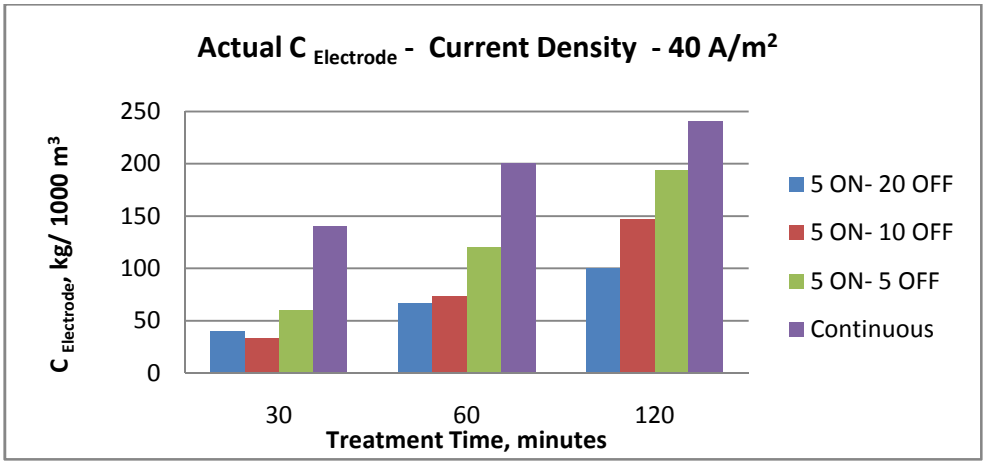

Figure 62 – Phase III - WWTP2 - Actual Electrode Consumption - Current Density 40 A/m^2

Table 13 – Phase III - Actual and Theoretical Electrode Consumption – WWTP2

Electrode Consumption (kg/1000 m3)									
C.D	Time (min)	5'ON-20'OFF		5'ON-10'OFF		5'ON-5'OFF		Continuous	
		T	A	T	A	T	A	T	A
10	30	6	7	6	13	9	13	18	27
	60	9	13	12	27	18	20	36	33
	120	15	27	24	33	36	60	72	113
20	30	12	7	12	13	17	27	35	40
	60	17	47	23	47	35	47	69	140
	120	29	53	46	93	69	147	139	220
40	30	23	40	23	33	35	60	69	140
	60	35	67	46	73	69	120	139	200
	120	58	100	92	147	139	193	277	240

C.D – Current Density (A/m^2)

The results of the electrode consumption for WWTP2 show the same trend with respect to increases in dissolution rate, as current density, treatment time, and temperature increase. As seen in Table 13, actual electrode consumption is higher than theoretical consumption; nevertheless, comparing the electrode consumption of WWTP1 and

WWTP2 treatments reveals significantly higher consumption when treating WWTP1 wastewater. The amount of cations released due to electrocoagulation represents the current efficiency of the dissolution; current efficiencies reported by researchers varied between 109 and 215% Mouedhen et al. 2008).

$$\boldsymbol{Current\ Efficiency} = \frac{\boldsymbol{Actual\ Electrode\ Consumption}}{\boldsymbol{Theoretical\ Electrode\ Consumption}}\ \boldsymbol{x\ 100\%} \qquad \textbf{(48)}$$

Actual electrode consumption was measured by weighing the electrodes before and after each treatment; theoretical treatment on the other hand, was a calculated using Faraday's law (Equation 36). Current efficiencies for treating both wastewaters were always greater than 100%, except for the test conducted using a current density of 40 A/m^2, 120 minute treatment time, and continuous mode, where the current efficiency was 86.6%. The decrease can be an indication that passivation of the anode took place during the experiment. High current densities and prolonged continuous exposure should be avoided to prevent passivation of the anode during treatment. Although treatment time was significantly longer in Phase II (4 hours), the difference between actual and theoretical electrode consumptions were not as important as those in Phase III; a possible explanation is that current efficiency was very high at the beginning before passivation occurred, rendering an overall difference that is slightly higher.

The increased anode dissolution with WWTP1's wastewater indicates that higher conductivity results in increasing corrosion rates of metals and increasing electrode consumption of EC treatment. On the other hand, higher conductivity requires lower power input; thus decreasing the energy consumption. Increased current efficiency or electrode consumption has been explained to be related to chloride ion concentrations.

Presence of chloride ions has been reported to decreased anode passivation and increase current efficiency (Bensadok et al. 2008).

Table 14 summarizes the consumptions at the different current densities, treatment times and exposure modes for wastewater obtained from both treatment plants. The increased anode dissolution with WWTP1's wastewater indicates that higher conductivity results in increasing corrosion rates of metals and increasing electrode consumption of EC treatment. On the other hand, higher conductivity requires lower power input; thus decreasing the energy consumption. Increased current efficiency or electrode consumption has been attributed to chloride ion concentrations. The presence of Cl^- has been reported to decrease anode passivation and increase current efficiency (Bensadok et al. 2008).

Table 14 – Phase III - Comparison of Actual Electrode Consumption for Treatment of WWTP1 and WWTP2 Samples

Electrode Consumption (kg/1000 m^3)									
C.D A/m^2	Time (min)	5'ON-20'OFF		5'ON-10'OFF		5'ON-5'OFF		Continuous	
		WWTP1	**WWTP2**	**WWTP1**	**WWTP2**	**WWTP1**	**WWTP2**	**WWTP1**	**WWTP2**
10	**30**	7	7	13	13	13	13	40	27
	60	27	13	33	27	40	20	73	33
	120	20	27	33	33	40	60	120	113
20	**30**	27	7	20	13	20	27	47	40
	60	33	47	20	47	40	47	93	140
	120	60	53	67	93	93	147	160	220
40	**30**	53	40	47	33	47	60	93	140
	60	53	67	60	73	93	120	187	200
	120	100	100	147	147	213	193	393	240

C.D – Current Density

4.3.7 Energy Consumption

The voltage potential needed to achieve the same current density for each type of wastewater varied due to the big differences in conductivity between the waters of both treatment plants. Energy consumption was calculated using Equation 38; and is based on the current, voltage applied, treatment duration, and volume of water treated. The values are presented in kWh/1000 m^3 in Figures 63-68.

WWTP1: high conductivity

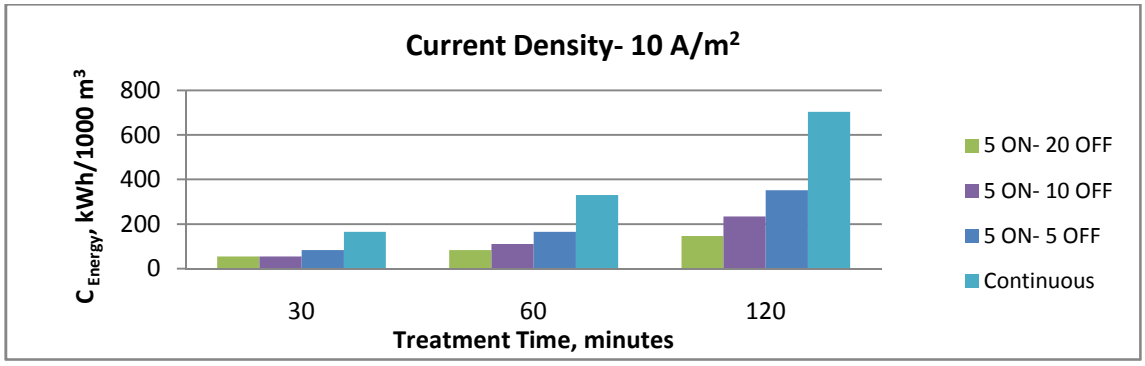

Figure 63 - Phase III - WWTP1 - Energy consumption - current density 10 A/m^2

Energy consumption at current density 10 A/m^2 was between 55 and 704 kWh/1000 m^3 of treated wastewater (Figure 63). However, doubling the current density from 10 to 20 A/m^2 (Figure 64) resulted in energy consumption more than three times higher, where consumption was between 189 -2232 kWh/1000 m^3 of treated wastewater.

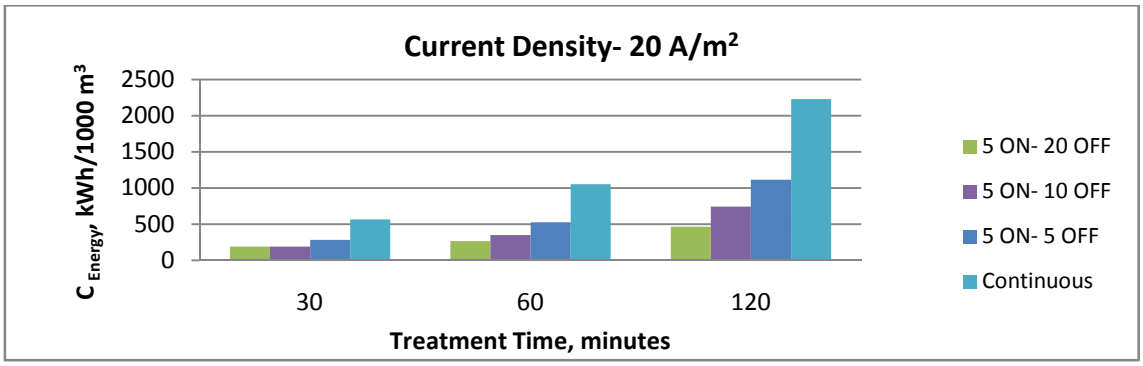

Figure 64 - Phase III - WWTP1 - Energy consumption - current density 10 A/m^2

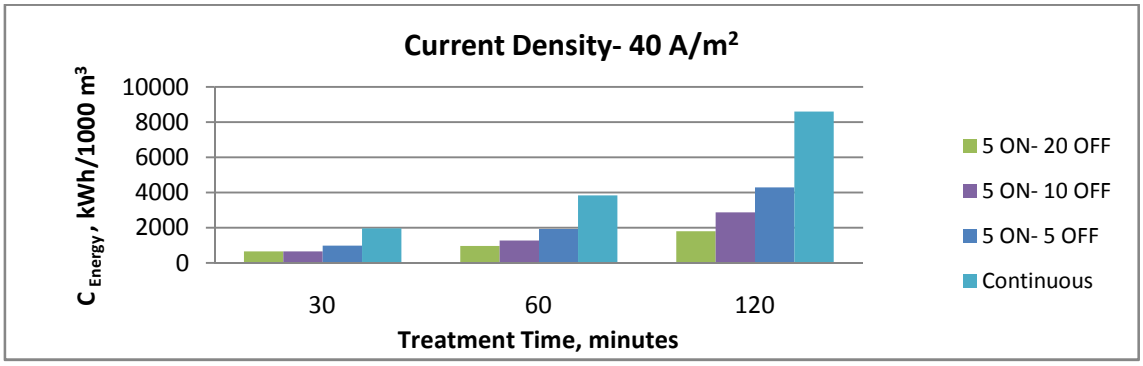

Figure 65 - Phase III - WWTP1 - Energy consumption - current density 40 A/m^2

The maximum energy consumption at current density 40 A/m^2 and continuous exposure for 120 minutes was 8600 kWh/m^3 of treated wastewater, almost 4 times the energy required for the same operational condition at 20 A/m^2, and more than 10 times the energy required at 10 A/m^2. Therefore, energy consumption and current density do not have a linear relationship.

WWTP2: low conductivity

Figures 66-68 present the energy consumption in kWh/1000 m^3 of treated wastewater from WWTP2. The same trend is observed for the same operational conditions with

WWTP1 (Figures 63-65); however, the lower conductivity of wastewater from WWTP2 resulted in higher energy requirements.

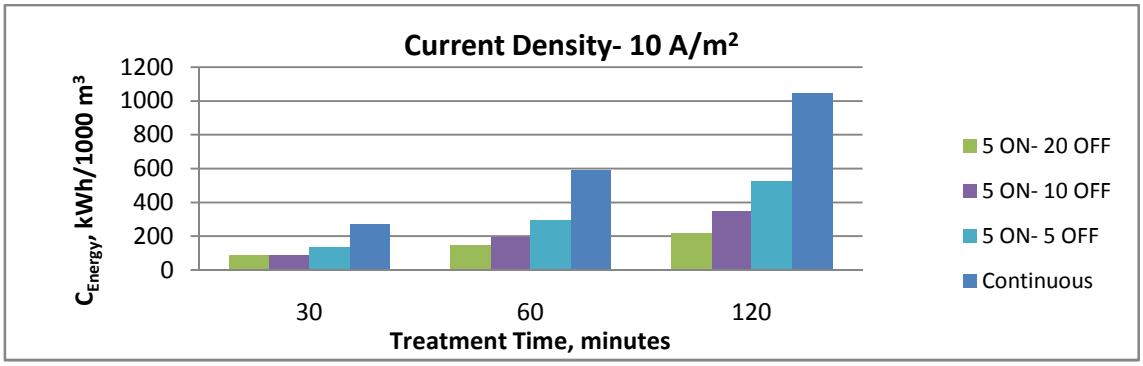

Figure 66 - Phase III- WWTP2 - Energy consumption - current density 10 A/m²

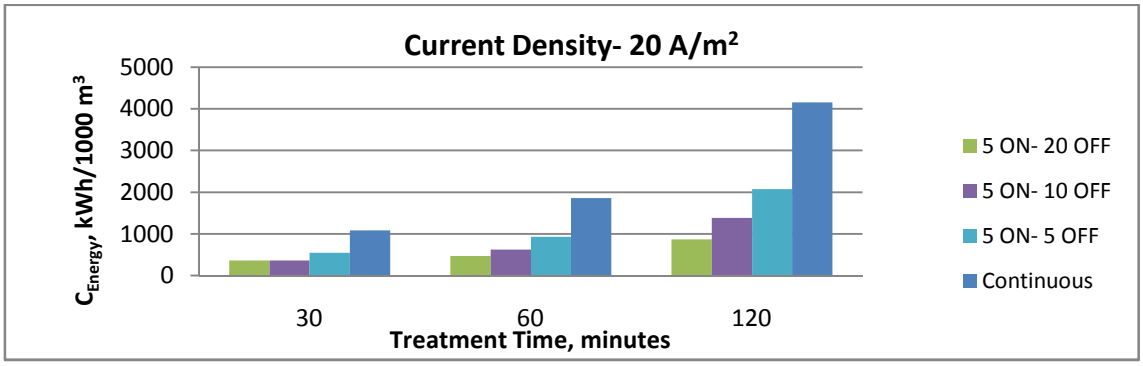

Figure 67 - Phase III- WWTP2 - Energy consumption - current density 20 A/m²

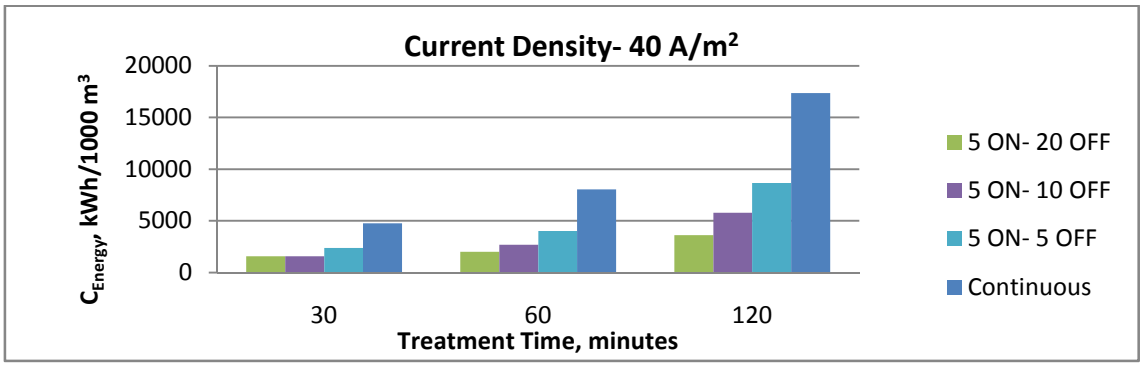

Figure 68 - Phase III - WWTP2 - Energy consumption - current density 40 A/m²

A substantial difference can be noticed from the graphical presentations of energy consumption during wastewater treatment of two plants (Figures 63-68). The voltage applied to achieve a certain current density when treating WWTP1's water was half that applied in treating WWTP2 water. Therefore, water conductivity is a very important parameter when evaluating the power requirements of an EC treatment process.

Table 15 – Phase III - Energy Consumption Comparison between WWTP1 and WWTP2

Energy Consumption (kWh/1000 m^3)									
C.D A/m^2	Time (min)	5'ON-20'OFF		5'ON-10'OFF		5'ON-5'OFF		Continuous	
		WWTP 1	**WWTP 2**	**WWTP 1**	**WWTP 2**	**WWTP 1**	**WWTP 2**	**WWTP 1**	**WWTP 2**
10	**30**	55	89	55	89	83	133	165	267
	60	83	147	110	196	165	293	331	587
	120	147	218	235	348	352	523	704	1045
20	**30**	189	362	189	362	284	543	568	1085
	60	264	465	351	620	527	930	1054	1860
	120	465	865	744	1385	1116	2077	2232	4154
40	**30**	654	1584	654	1584	982	2377	1963	4753
	60	961	2015	1281	2687	1922	4030	3844	8060
	120	1791	3617	2866	5787	4299	8680	8597	17360

CD – Current density

Table 15 summarizes the differences in energy consumption between the two wastewater samples (WWTP1 and WWTP2). Elevated conductivity values in wastewater can reduce the energy requirements of an EC process; hence, reducing the cost of energy. The relationship between conductivity and energy consumptions observed in phases II and III is in agreement with the studies of other researchers (Chen et al. 2000; Mouedhen et al. 2008; Ricordel et al. 2010).

4.3.8 Operating Cost

The two parameters controlling the operating cost of an EC treatment are the energy and electrode consumptions. Electrode consumption resulting from treating WWTP1 wastewater was higher than for WWTP2 wastewater; however, its energy consumption was significantly lower. To determine the major parameter contributing to operating cost, a comparison was necessary between operating costs of treating both wastewaters. The price of aluminum per kilogram (2.26 CAD/kg) is 45 times the energy cost per kWh (0.05 CAD/kWh); therefore a higher cost would be expected for treating the water that results in higher electrode consumption. The treatment that results in a higher operating cost will determine the main contributor to operating cost whether its energy or electrode consumption.

Table 16 - Phase III - Operating Costs (WWTP1 & WWTP2)

Operating Cost (CAD/1000 m^3)									
C.D A/m^2	Time (min)	5'ON-20'OFF		5'ON-10'OFF		5'ON-5'OFF		Continuous	
		WWTP 1	**WWTP 2**	**WWTP 1**	**WWTP 2**	**WWTP 1**	**WWTP 2**	**WWTP 1**	**WWTP 2**
10	**30**	16	18	16	18	24	27	49	54
	60	24	28	32	37	49	55	97	110
	120	41	45	66	71	98	107	197	214
20	**30**	36	44	36	44	53	66	107	132
	60	52	62	70	83	105	125	209	249
	120	88	108	141	173	212	260	424	520
40	**30**	85	131	85	131	127	197	255	394
	60	126	179	168	239	252	358	505	716
	120	220	311	352	498	528	747	1055	1494

CD- Current Density

Table 16 shows that operating cost of treating WWTP1's wastewater was 20-30% lower than the operating costs for WWTP2. Although the price of aluminum is much higher, the comparative results in Table 16 prove that the major contributor to the EC operating cost was not electrode consumption. Therefore, the controlling parameter in calculating the operating cost and the cost efficiency of an EC process is the energy consumption, or, in other words, the conductivity of the wastewater. The conductivity of wastewater from WWTP1 was 2500 ± 250 μS/cm, whereas for WWTP2 it was 1100 ± 300 μS/cm; therefore, doubling the conductivity of wastewater resulted in up to 30% reduction in operating costs.

4.4 Phase IV

The high electrode consumptions that resulted in Phase III led to an examination of the effect of anode design on electrode consumption and current efficiency. Results from this phase are a contribution to a pilot-scale electro-bioreactor design investigated by Elektorowicz et al. (2011). Phosphorus, COD, nitrate, ammonia and turbidity removals were also tested for comparative purposes. The wastewater used in Phase IV was from WWTP2.

4.4.1 Phosphorus Removal

No difference in removal efficiency was expected when changing the anode surface, because phosphorus removal is related to the amount of metallic cations released in solution. Removal efficiencies of phosphorus were between 99.3 and 100 % for the six combinations tested (Figure 69).

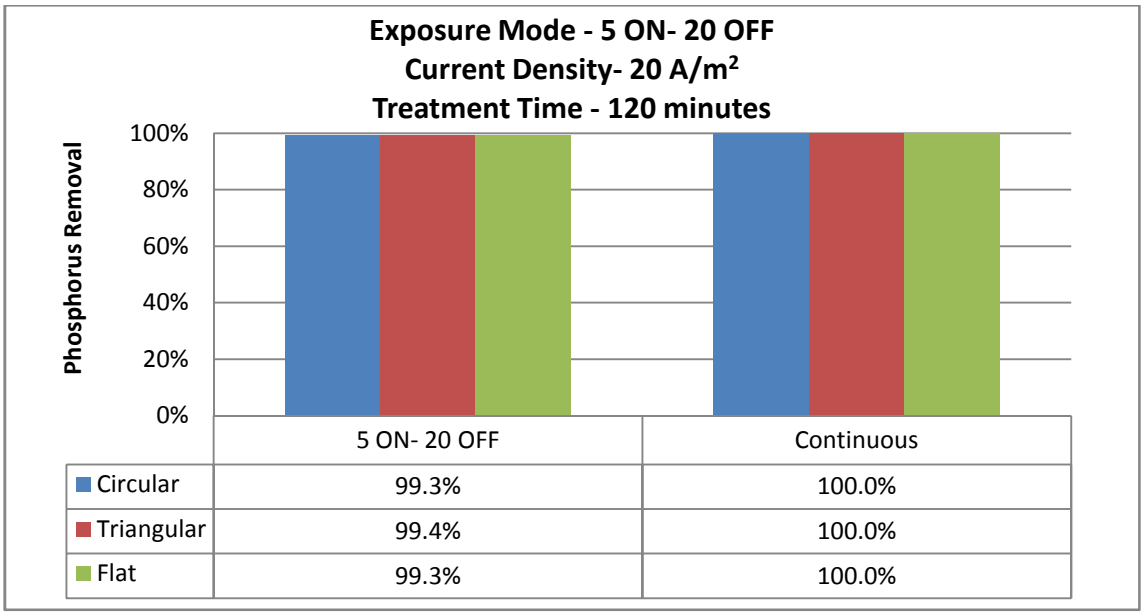

Figure 69 - Phase IV - Phosphorus removal

4.4.2 COD Removal

In Phase IV experiments, initial COD concentrations were higher than Phase III, therefore; final effluent concentrations were higher than the concentrations yielded in Phase III. Initial COD concentration in Phase IV was 415 ± 5 mg/L (Table 8).

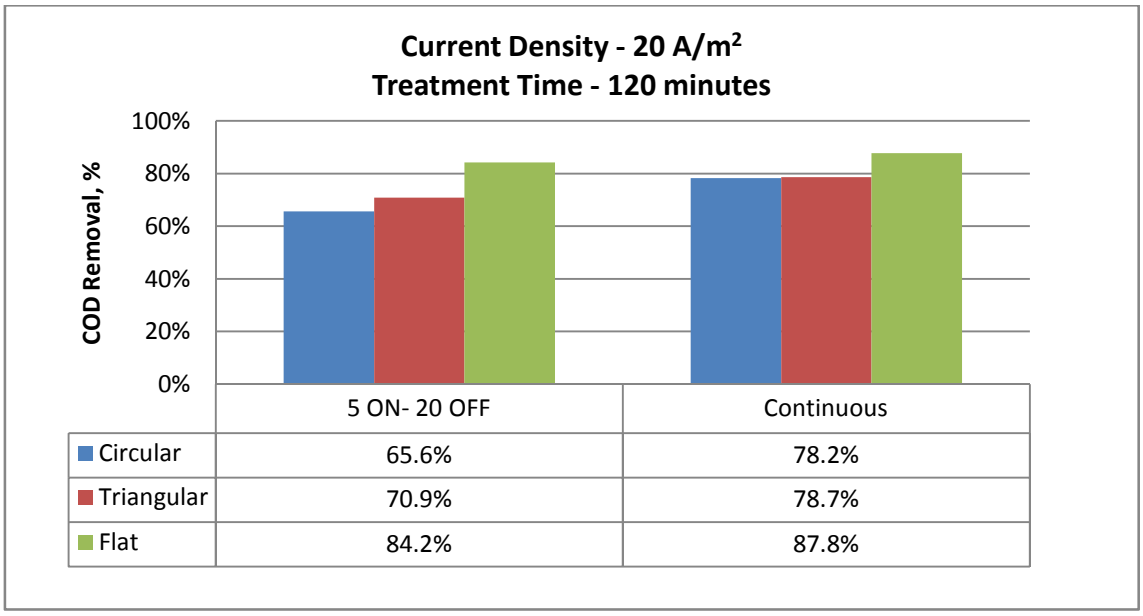

Figure 70 - Phase IV - COD removal

COD values were taken after half an hour of sample settling, similarly to Phase III. Despite the higher COD removal efficiencies achieved in Phase IV (Figure 70) when compared to Phase III, the lowest effluent concentration after treatment in Phase IV was 55 mg/L. Figure 71 presents the concentrations of COD after treatment in Phase IV starting from an initial concentration of 420 mg/L. Continuous exposure yielded better removal of COD than interrupted exposure (Figures 71 & 72).

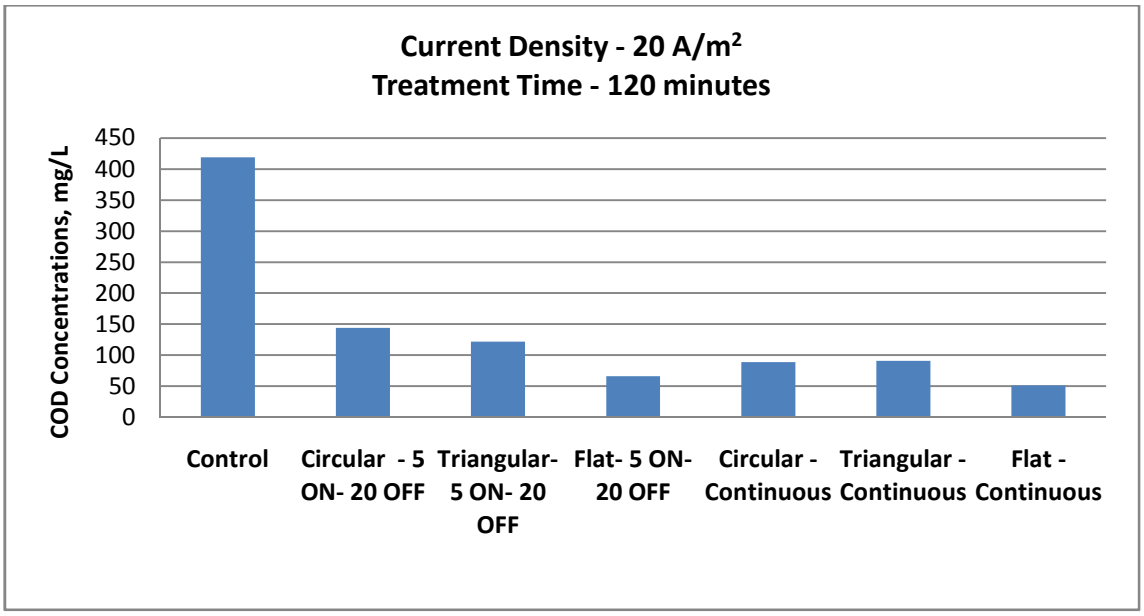

Figure 71 - Phase IV - COD concentrations of treated wastewater

4.4.3 Turbidity Removal

In this phase, turbidity readings were taken at the end of each experiment, and after 30 minutes of settling. Differences in turbidity removal for the three electrodes tested at the 5'ON-20'OFF modes were not very significant. After 120 minutes of continuous exposure, the electroflotation layer formed by the circular perforation had the most uniform thickness.

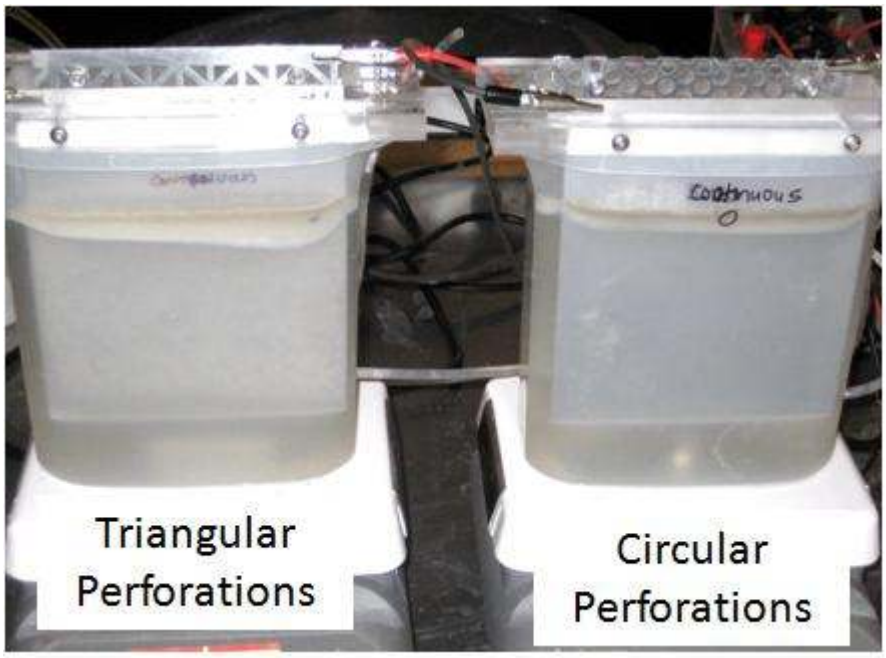

Figure 72 - Phase IV - Turbidity removal - perforated electrodes - continuous mode Uniform foam layer with circular perforations (right)

Towards the end of the two-hour experiments, the reactor with the triangular perforated anode and continuous exposure showed an increase in turbidity, indicating an excessive release of aluminum in solution. However, the reactor with circular perforation resulted in a clear column and good flotation. Consequently, turbidity was measured directly after the tests to evaluate the difference in turbidity removal if the tests were to be flotation treatments only (Figure 73).

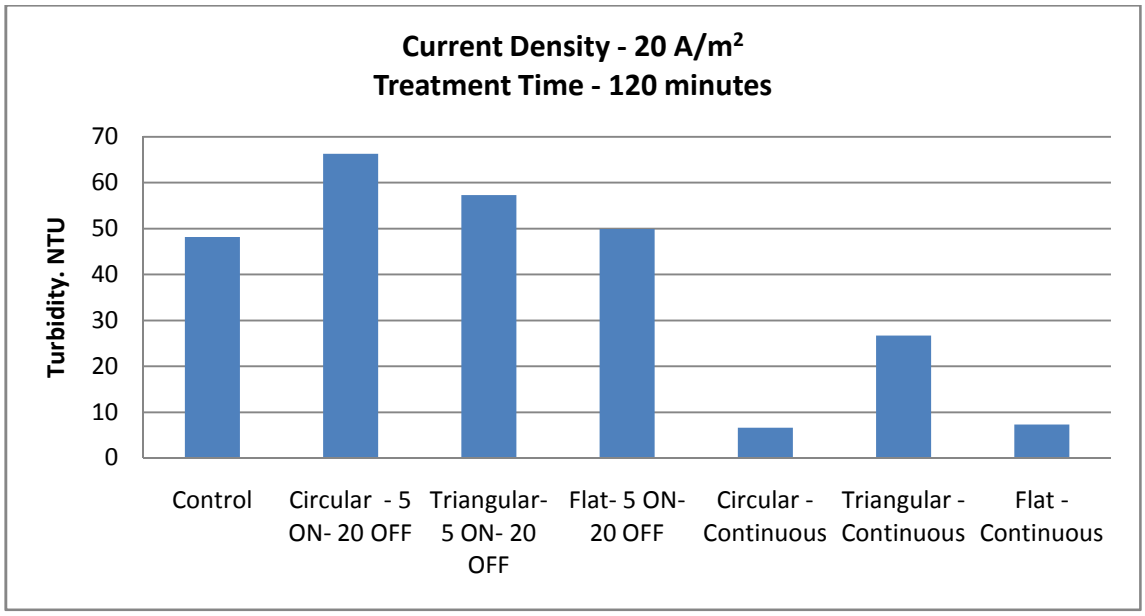

Figure 73 - Phase IV - Instantaneous turbidity measured directly at end of experiment

The increased turbidity at the interrupted modes in Figure 73 indicate that aluminum was being released in solution but the amount of hydrogen gas produced was not sufficient to carry the solids to the surface.

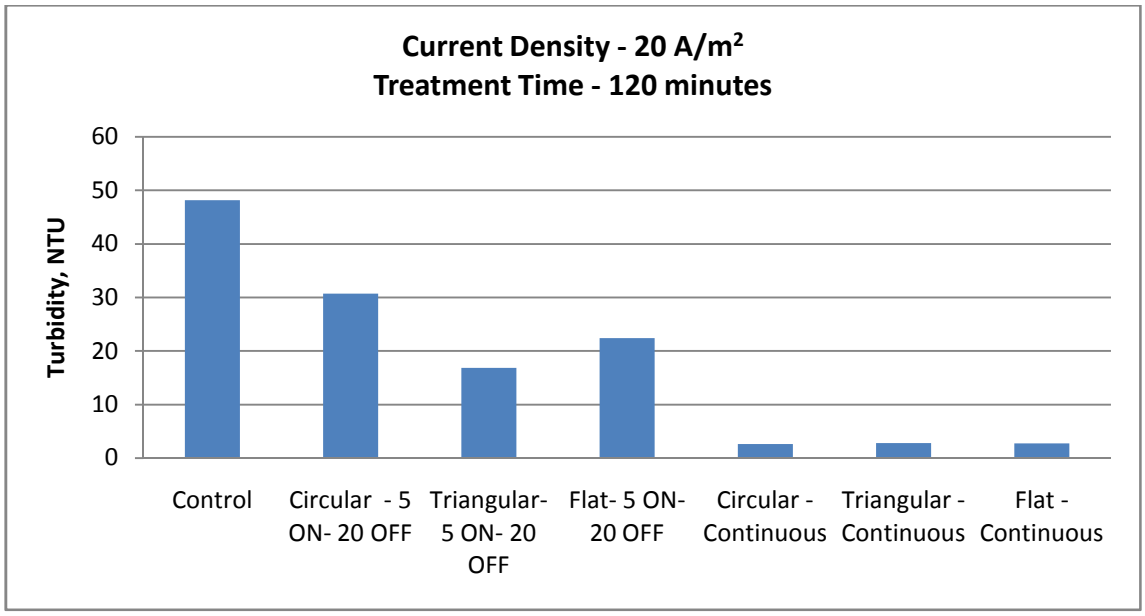

Figure 74 - Phase IV - Turbidity after 30 minutes of settling

Differences in turbidity after settling were not significant after 120 minutes of continuous exposure; however, the higher instantaneous turbidity reading for the triangular perforated electrodes confirm the aforementioned visual observation.

4.4.4 Electrode Consumption

To confirm if the increase in turbidity observed towards the end of the two-hour experiments with triangular perforated electrodes was due to an excessive release of aluminum, a comparison between electrode consumptions of the different electrodes was necessary.

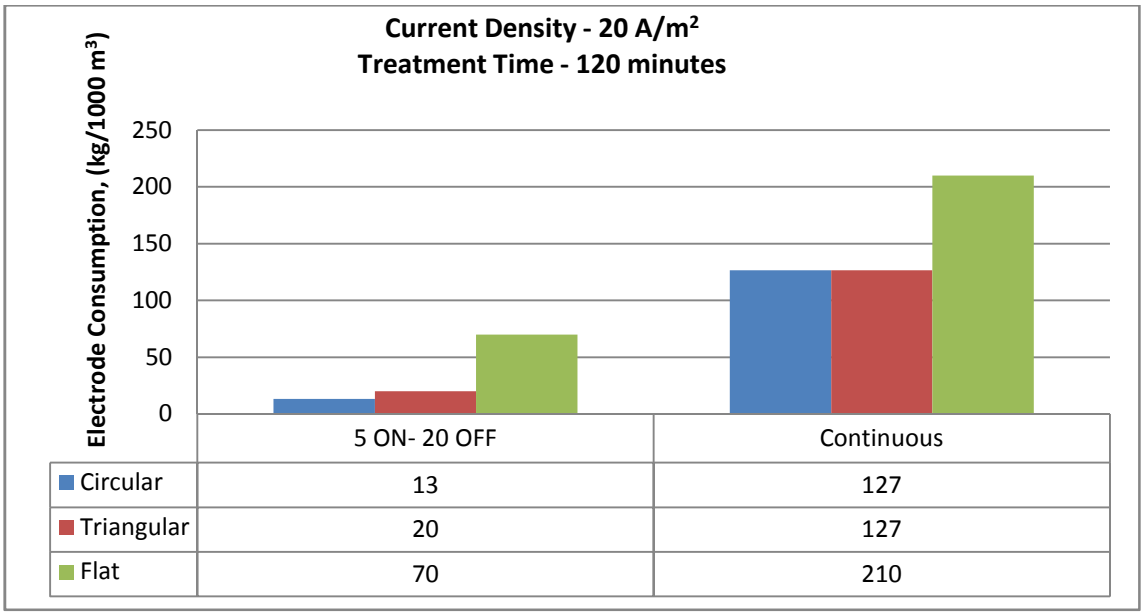

Figure 75 - Phase IV - Electrode consumption

Figure 75 shows that electrode consumptions of triangular perforated and circular perforated electrodes were identical at the continuous mode, but higher for triangular perforated electrodes at the 5'ON-20'OFF mode. Therefore, the turbidity increase noted earlier was not a result of excess aluminum release, but perhaps of a difference in electric field and flow distribution. Electrodes with circular perforation possessed a uniform pattern that might have helped in flotation and clarity of water column.

Flat electrodes resulted in significantly higher electrode consumptions at both modes. Differences between theoretical and actual electrode consumptions of perforated anodes were not very significant at the interrupted mode. However, at the continuous mode, actual electrode consumption significantly surpassed the actual consumption (Figure 76).

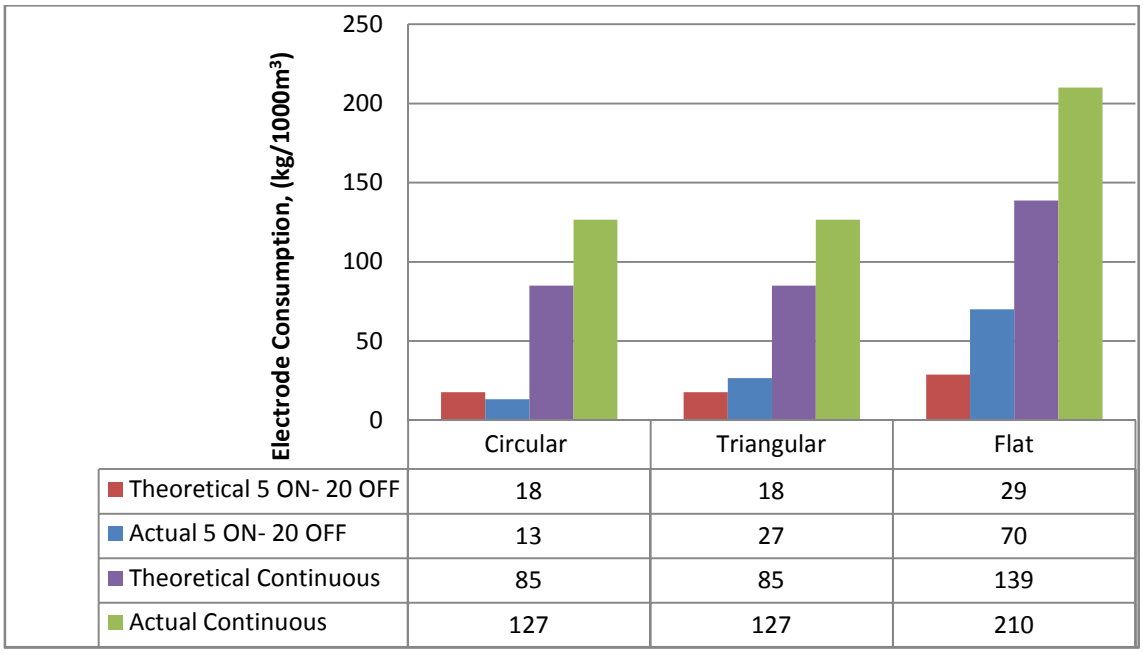

	Circular	Triangular	Flat
Theoretical 5 ON- 20 OFF	18	18	29
Actual 5 ON- 20 OFF	13	27	70
Theoretical Continuous	85	85	139
Actual Continuous	127	127	210

Figure 76 - Phase IV - Actual and theoretical electrode consumptions

When compared to perforated electrodes, flat electrodes require almost double the amount of anode material per cubic meter of wastewater treated, as seen from Figure 76; furthermore, no significant difference was observed with respect to the removal efficiencies of phosphorus, COD and turbidity. Therefore, perforated electrodes can help reduce material cost and hence overall operating cost.

4.4.5 Energy Consumption

Perforated electrodes have a lower effective surface area; therefore, lower current intensity is needed to deliver the same current density as flat electrodes. Subsequently, lower voltage input is required, and the overall energy consumption is expected to be lower. Figure 77 shows that energy consumption for the flat electrodes was more than double that of perforated electrodes.

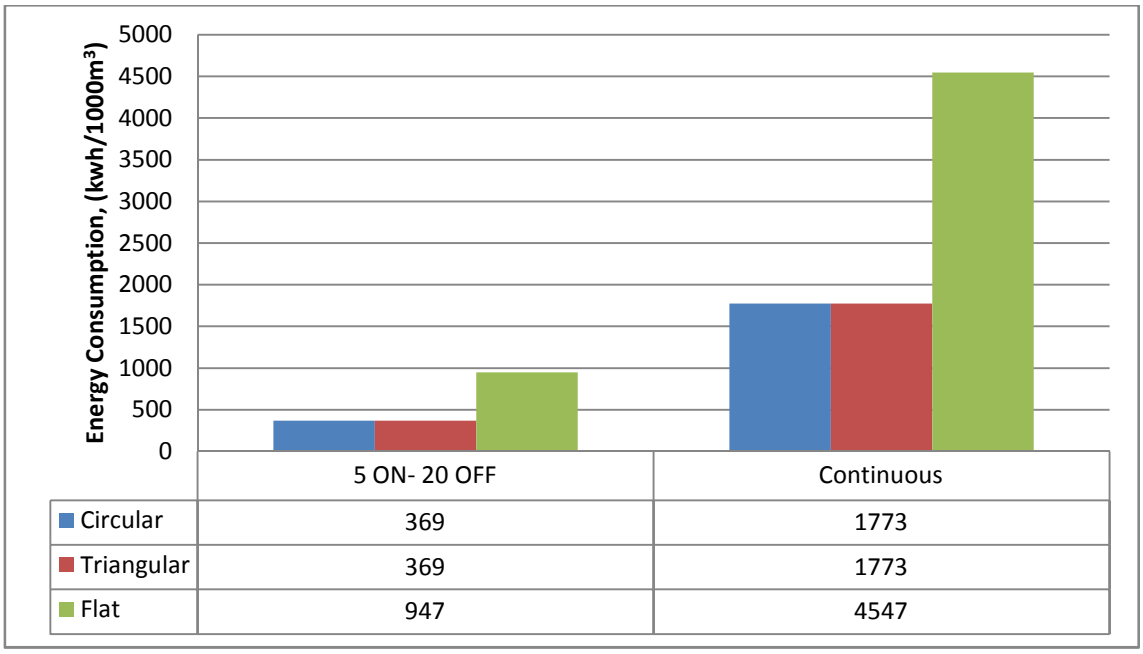

Figure 77 - Phase IV - Energy consumption of treating wastewater with perforated and non perforated anodes

4.4.6 Operating Cost

The reduction in energy and electrode consumption resulting from the use of perforated electrodes will consequently result in reduced operating costs. The operating costs for Phase IV experiments varied between 49 and 701 CAD/1000 m^3 of treated wastewater, as shown in Figure 78.

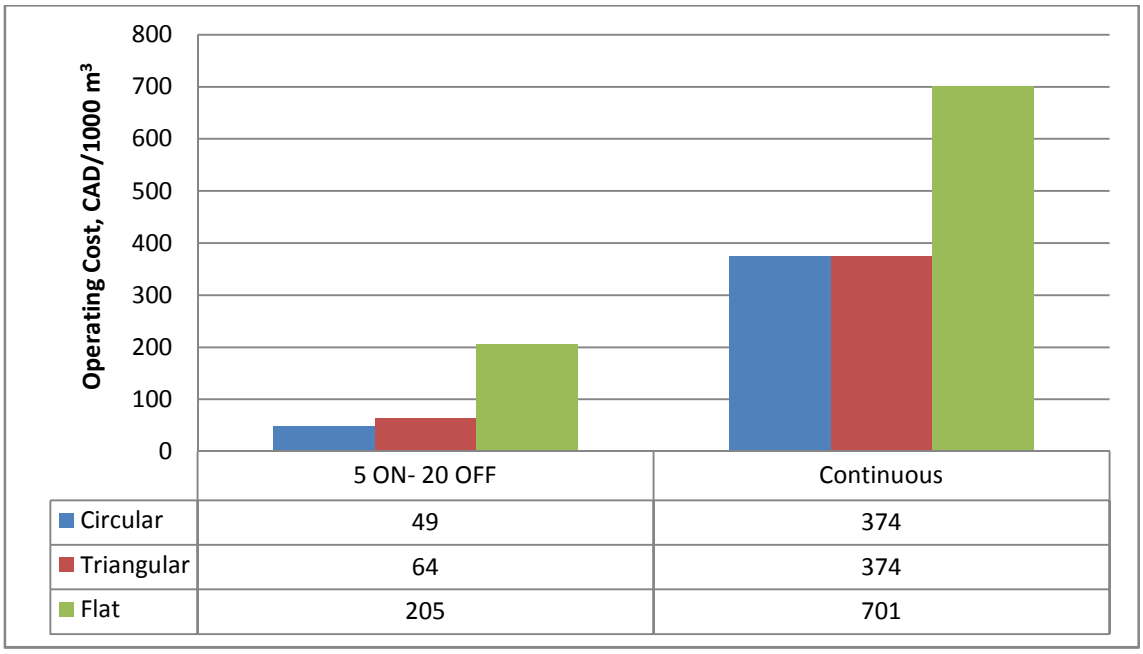

Figure 78 - Phase IV - Operating Cost of treating wastewater with flat and perforated anodes

Findings of this phase provided an alternative to reducing the operating cost of the EC process. The use of perforated electrodes not only resulted in lower electrode material requirements, but also in lower energy requirements; 61% lower energy consumption for perforated electrodes (Figure 77); hence, substantially improving the cost effectiveness of the EC process (Figure 78).

Chapter 5 – Conclusions & Recommendations

Wastewater treatment by electrocoagulation (EC) is an environment-friendly process that requires no addition of chemicals, yields high quality effluent, and requires short treatment times and simple operation. Given that this study is being conducted in Quebec, where hydroelectric power accounts for more than 95% of the total power of the province and is relatively inexpensive, applying electrocoagulation technology is an economical approach for wastewater treatment. However, the lack of research into the use of EC to treat very dilute wastewater motivated the present investigation into its effectiveness in treating real wastewater samples with distinct physical and chemical characteristics. The primary objectives of this study were to explore the flexibility of the EC process for the treatment of wastewaters with different initial characteristics, investigate different operational conditions of the EC process in the interest of reducing environmental and economic footprints, and evaluate the performance of EC as a pre-treatment, post-treatment, and a standalone process.

The wastewater used in this study was provided by two municipal wastewater treatment plants in Quebec. The wastewater samples from the two treatment plants, designated as WWTP1 and WWTP2, respectively, had distinctive overall characteristics which helped determine the treatment's effectiveness with varying initial conditions; such as different conductivities, suspended solid concentrations, COD, and nutrients concentrations.

Electrocoagulation experiments resulted in superior effluent quality when compared to chemical coagulation experiments. Moreover, the treatment proved far more cost-effective through the reduction of dewatering costs and the elimination of chemicals and

polymers, which, in turn, eliminates all costs related to the purchase, storage, and transportation of chemicals. Furthermore, the use of EC as an alternative treatment to chemical coagulation prevents the discharge of substantial amounts of undesired anions to receiving water bodies.

The ability to use EC to treat wastewater with different initial characteristics while easily modifying operating parameters proved the flexibility of the system. For highly diluted wastewater from WWTP1, all the tested operational conditions yielded satisfactory phosphorus removal rates, and the interruption of electrical exposure did not impede the treatment process. For the less diluted wastewater, obtained from WWTP2, phosphorus removal rates varied between 90% and 100%, and phosphorus levels after treatment at all tested conditions were lower than 0.5 mg/L.

Treating the WWTP1 wastewater, containing high initial nitrate concentrations and zero ammonia concentrations, showed that nitrate reduction is concentration-dependent. Despite the high initial ammonia concentrations in the wastewater from WWTP2, experimental operation conditions and lack of oxygen supply did not help initiate nitrification. Intermittent aeration can be applied to supply enough oxygen for the nitrification process while allowing anoxic periods for further nitrogen removal by denitrification. These findings show that the system can be applied to treat wastewater or groundwater with high initial nitrate content.

Solid-liquid separation using EC treatment was also observed with wastewater from both plants. Complete flotation resulted upon treatment of WWTP1 wastewater, leaving a clear water column. Meanwhile, flotation was very unstable when treating WWTP2

wastewater, and floated foam settled down readily once mixing stopped. Total treatment time is shorter when complete flotation is achieved; however, when settling is necessary, total treatment time increases in order to allow settling. It is therefore recommended to examine flotation with different initial concentrations of suspended solids in order to correlate electroflotation with initial suspended solid concentrations. Nevertheless, a solution to the problem of high initial TSS concentrations can be: (i) operating at lower current densities to avoid the generation of large amounts of hydrogen gas and obtain solid-liquid separation by settling, (ii) operating at one of the current densities tested, and adding inert electrodes for oxygen and hydrogen gas production by electrolysis, or (iii) combining EC treatment with a membrane filtration unit.

Adding salts to wastewater prior to treatment helped increase wastewater conductivity and initiate flotation. At the tested salt concentrations and voltage gradient combinations, electroflotation was observed in the first 45 minutes. The results confirmed that EC-EF treatment is ideal for wastewaters with high conductivity. However, operating at a fixed voltage gradient is not a practical approach due to the vast differences in current flowing through the system at different conductivities. A practical alternative is to operate at fixed current densities, where voltage will vary depending on the conductivity of the solution.

Electrode consumption was higher for wastewater with higher initial conductivity; therefore, the rate of anodic dissolution is proportional to the solution conductivity. Electrode consumptions for both wastewaters were higher than theoretically calculated values. To obtain more accurate consumption projections, Faraday's Law needs to be modified to include more factors that affect the rate of anodic dissolution, such as temperature and conductivity. It is highly recommended to conduct more EC tests on

wastewater with different initial conductivities to create a new relationship between electrode consumption and conductivity of wastewater. Improving electrode consumption calculations will greatly facilitate system scale-up and eventual applicability in industrial and municipal settings.

Long exposure to electricity can result in excessive amounts of aluminum ions release in the reactor. The interrupted exposure modes with the longest OFF period are therefore recommended to allow enough time for mixing and flocculation without the excessive release of metal into the solution. Energy consumption was considerably lower when treating WWTP1 wastewater, due to its very high initial conductivity. The amount of energy needed for treating WWTP2 wastewater was almost double that needed to treat WWTP1 wastewater. A comparison of operating costs for the treatment of wastewater from the two treatment plants led to the conclusion that the major contributing factor is energy consumption. Therefore, treating wastewater with high conductivity using EC is a cost effective approach. Furthermore, this demonstrates the flexibility of EC treatment, since its operating conditions can be altered based on initial wastewater characteristics and effluent standard requirements. Flexibility also extends to variations in electrode surfaces; the use of perforated electrodes produced a significant reduction in electrode and energy requirements; hence improving cost effectiveness.

Further modifications to operational conditions or reactor setup can be investigated to reduce the operating conditions of the treatment process; such as testing the effectiveness of longer current interruptions to avoid excess anode dissolution, as well as testing the effectiveness of leaving a smaller gap between electrodes to reduce energy requirements.

EC units are simple in design, operation, and construction; hence, it is recommended to install such units on-site in each industrial production facility, particularly in Quebec, where electricity is available at moderate prices. The test results presented above have demonstrated the system's flexibility and compatibility with other treatment units. When EC treatment is combined with a membrane filtration unit, for example, higher current densities and durations are not required. Furthermore, full or partial treatment of industrial effluents prior to discharge will reduce the load input to wastewater treatment facilities.

Biological conversion of organic phosphates to orthophosphates suggests the potential for EC as a promising post-treatment to biological treatment processes or as part of a combined treatment process, as studied by Bani-Melhem & Elektorowicz (2010), where EC was combined with a membrane bioreactor. In conclusion, the operating conditions tested and successful results yielded confirm that EC can be applied as a pre-treatment, in combination with other treatment units, or a standalone treatment.

References

Ahmad, A., Wong, S. S., Teng, T., and Zuhairi, A. 2007. Optimization of coagulation-flocculation process for pulp and paper mill effluent by response surface methodological analysis. Journal of Hazardous Materials. **145**(1-2): 162-168. doi:10.1016/j.jhazmat.2006.11.008.

Al-Amoudi, A., Williams, P., Mandale, S., and Lovitt, R. W. 2007. Cleaning results of new and fouled nanofiltration membrane characterized by zeta potential and permeability. Separation and Purification Technology. **54**(2): 234–240. doi:10.1016/j.seppur.2006.09.014.

An, Y., Li, T., Jin, Z., Dong, M., Li, Q., and Wang, S. 2009. Decreasing ammonia generation using hydrogenotrophic bacteria in the process of nitrate reduction by nanoscale zero-valent iron. Science of the Total Environment. **407**(21): 5465–5470. doi:10.1016/j.scitotenv.2009.06.046.

Araya-Farias, M., Mondor, M., Lamarche, F., Tajchakavit, S., and Makhlouf, J. 2008. Clarification of apple juice by electroflotation. Innovative Food Science and Emerging Technologies. **9**(3): 320–327. doi:10.1016/j.ifset.2007.08.002.

Artiga, P., Carballa, M., Garrido, J., and Mendez, R. 2007. Treatment of winery wastewaters in a membrane submerged bioreactor. Water Science & Technology. 56(2): 63-69. doi:10.2166/wst.2007.473.

Aylesworth-Spink, S. Walkerton Affects Today's Drinking Water System. http://www.suite101.com/content/walkerton-effects-todays-drinking-water-system-a96164. 2009, 02 28. (Accessed 09 2010)

Bagga, A., Chellam, S., & Clifford, D. A. 2008. Evaluation of iron chemical coagulation and electrocoagulation pretreatment for surface water microfiltration. Journal of Membrane Science. **309**(1-2): 82-93. doi:10.1016/j.memsci.2007.10.009.

Bagotsky, V. 2006. Fundementals of Elechtrochemistry. Pennington: John Wiley & Sons, Inc., Hoboken, N.J

Bani-Melhem, K., & Elektorowicz, M. 2010. Development of a Novel Submerged Membrane Electro-Bioreactor(SMEBR): Performance for Fouling Reduction. Environmental Science and Technology. **44**(9): 3298-3304. doi**:** 10.1021/es902145g.

Ben Mansour L., Chalbi S., Kesentini I. 2007. Experimental study of hydrodynamic and bubble size distributions in electroflotation process Indian Journal of Chemical Technology. **14**(3): 253-257.

Bensadok, K., Benammar, S., Lapicque, F., & Nezzal, G. 2008. Electrocoagulation of cutting oil emulsions using aluminum plate electrodes. Journal of Hazardous Materials. **152**(1): 423–430. doi:10.1016/j.jhazmat.2007.06.121.

Bratby, J. 2006. Coagulation and Flocculation in Water and Wastewater Treatment. London: IWA Publishing., London, Britain.

Can˜izares, P., Carmona, M., Lobato, J., Martı´nez, F., and Rodrigo, M. A. 2005. Electrodissolution of Aluminum Electrodes in Electrocoagulation Processes. Ind. Eng. Chem. Res. **44**(12): 4178-4185. doi: 10.1021/ie048858a.

Canizares, P., Martinez, F., Jimenez, C., Lobato, J., and Rodrigo, M. A. 2006. Coagulation and Electrocoagulation of Wastes Polluted with Dyes. Environmental Science and Technology. **40**(20): 6418-6424.doi: 10.1021/ie020951g.

Chambers's encyclopaedia: a dictionary of universal knowledge, Volume 4. J.B. Lippincott & Co., 1889(encycopedia)

Chen, G., Chen, X., and Yue, P. L. 2000. Electrocoagulation and Electroflotation of Restaurant Wastewater. Journal of Environmental Engineering. **26**(9): 858-863. doi: 10.1061/(ASCE)0733-9372(2000)126:9(858).

Conservation, M. D. Aquaguide- Clearing Ponds, from Pond Management Series. http://mdc4.mdc.mo.gov/Documents/9133.pdf (Accessed 27 December 2010)

Correll, J. 1998. The Role of Phosphorus in the Eutrophication of Receiving Waters. Environmental Quality. 27: 261-266.

Cosgrove, T. 2010. Colloids Science - Principles, Methods and Applications.: John Wiley and Sons.West Sussex, United Kingdom

Das, K., Raha, S., and Somasundaran, P. 2009. Effect of polyacrylic acid molecular weight on the floc stability during prolonged settling. Colloids and Surfaces. **351** (1-3): 1-8. doi:10.1016/j.colsurfa.2009.08.026.

Davis, J. R. 1999. Corrosion of aluminum and aluminum alloys. ASM International., Materials Park, OH

Den, W., and Huang, C. 2006. Electrocoagulation of Silica Nanoparticles in Wafer Polishing Wastewater by a Multichannel Flow Reactor: A Kinetic Study. Journal of Environmental Engineering. **132**(12): 1651-1658: doi:10.1061/(ASCE)0733-9372(2006)132:12(1651).

Drouiche, N., Ghaffour, N., Lounici, H., Mameri, N., Maallemi, A., and Mahmoudi, H. 2008. Electrochemical treatment of chemical mechanical polising wastewater: removal of

fluoride- sludge characteristics- operating cost. Desalination. **223**(1-3): 134-142. doi:10.1016/j.desal.2007.01.191.

Duan, J., and Gregory, J. 2003. Coagulation by hydrolysing metal salts. Advances in Colloid and Interface Science. **100-102:** 475-502. doi:10.1016/S0001-8686(02)00067-2.

El-Gohary, F., Tawfik, A., and Mahmoud, U. 2010. Comparitive study between chemical coagulation/ precipitation (C/P) versus coagulation/dissolved air flotation (C/DAF) for pre-treatment of personal care products (PCPs) wastewater. Desalination. **252**(1-3): 106-112. doi:10.1016/j.desal.2009.10.016.

Environment-Canada and G.L Limited. 2006. Development of Ecoregion Based Phosphorus Guidelines for Canada: Ontario as a Case Study. Gatineau: Canadian Council of Ministers of the Environment.

Environment-Canada. Road Salts. from Winter Road Maintenance Activities and the Use of Road Salts in Canada: A Compendium of Costs and Benefits Indicators. http://www.ec.gc.ca/nopp/roadsalt/reports/en/winter.cfm 26.05.2006 (Accessed 28 December 2010)

Environment-Canada. Phosphorus at the Mouths of Lake Saint-Pierre Tributaries. http://www.ec.gc.ca/stl/default.asp?lang=En&n=11281F1B-1 2007 (Accessed 12 January 2011)

Environmental Commisioner of Ontario 2010, 09 22. Sewage Treatment: Not Good Enough. Redefining Conservation, ECO Annual Report, 2009/10.The Queen's Printer for Ontario. Toronto, ON

Gao, P., Chen, X., Shen, F., and Chen, G. 2005. Removal of chromium(VI) from wastewater by combined electrocoagulation–electroflotation without a filter. Separation and Purification Technology. **43**(2): 117–123. doi:10.1016/j.seppur.2004.10.008.

Ge, J., Qu, J., Lei, P., and Liu, H. 2004. New bipolar electrocoagulation–electroflotation process for the treatment of laundry wastewater. Separation and Purification Technology. **36**(1): 33-39. doi:10.1016/S1383-5866(03)00150-3.

Ghernaout, D., Badis, A., Kellil, A., and Ghernaout, B. 2008. Application of electrocoagulation in Escherichia Coli culture and two surface waters. Desalination. **219**(1-3): 118-125**.** doi:10.1016/j.desal.2007.05.010.

Golder, A. K., Samanta, A. N., and Ray, S. 2006. Removal of phosphate from aqueous solutions using calcined metal hydroxides sludge waste generated from electrocoagulation. Separation and Purification Technology. **52**(1): 102-109. doi:10.1016/j.seppur.2006.03.027.

Gomes, A., Daida, P., Kesmez, M., Weir, M., Moreno, H., Parga,J., Irwin, G., McWhinney, Hylton., Grady, T., Peterson, E., and Cocke, D. 2007.Arsenic removal by electrocoagulation using combined Al–Fe electrode system and characterization of products. Journal of Hazardous Materials. **139**(2): 220-231. doi: 10.1016/j.jhazmat.2005.11.108.

Grimm, S. 2002. Aquafacts- Food To Microorganism Ratio. Newyork: National Rural Water Association Wastewater, Claverack, NY.

Gu, Z., Liao, Z., Schulz, M., Davis, J. R., Baygents, J., and Farrell, J. 2009. Estimating Dosing Rates and Energy Consumption for Electrocoagulation Using Iron and Aluminum Electrodes. Ind. Eng. Chem. Res. **48**(6): 3112-3117. d**oi:**10.1021/ie801086c.

Han, S.-S., Bae, T.-H., Jang, G.-G., and Tak, T.-M. 2005. Influence of sludge retention time on membrane fouling and bioactivities in membrane bioreactor system. Process Biochemistry. **40**(7): 2393-2400. doi:10.1016/j.procbio.2004.09.017.

Han, W.-Q., Wang, L.-J., Sun, X.-Y., and Li, J.-S. 2008. Treatment of bactericide wastewater by combined process chemical coagulation, electrochemical oxidation and membrane bioreactor. Journal of Hazardous Material. **151**(2-3): 306- 315. doi:10.1016/j.jhazmat.2007.05.088.

Hansen, H., Nu˜nez, P., and Grandon, R. 2005. Electrocoagulation as a remediation tool for wastewaters containing arsenic. Minerals Engineering. **19**(5): 521–524. doi:10.1016/j.mineng.2005.09.048.

Hansen, H., Nu˜nez, P., Raboy, D., Schippacasse, I., and Grandon, R. 2007. Electrocoagulation in wastewater containing arsenic: Comparing different process designs. Electrochimica Acta. **52**(10): 3464–3470. doi:10.1016/j.electacta.2006.01.090.

Holt, P., Barton, G. W., Wark, M., and Mitchell, C. 2002. A quantitative comparison between chemical dosing and electrocoagulation. Physiochemical Engineering Aspects. **211**(2-3): 233-248. doi:10.1016/S0927-7757(02)00285-6.

Holt, P., Barton, G., and Mitchell, C. 1999. Electrocoagulation as a wastewater treatment. In Proceedings of The Third Annual Australian Environmental Engineering Research Event. Castlemaine, Victoria., 23-26 November 1999. Department of Chemical Engineering, The University of Sydney

Ibeid, S., Elektorowicz, M., and Oleszkiewicz, J. A. 2010. Impact of electro-coagulation on the fate of soluble microbial products (SMP) in submerged membrane electro-bioreactor (SMEBR). Proceedings of the Annual Conference of the Canadian Society for Civil Engineering 2010, CSCE 2010. Winnipeg, Manitoba. Vol. 1, pp 634-640.

Ji, L., and Zhou, J. 2006. Influence of aeration on microbial polymers and membrane fouling in submerged membrane bioreactors. Journal of Membrane Science. **276** (1-2): 168-177. doi:10.1016/j.memsci.2005.09.045.

Jimenez, C., Talavera, B., Saez, C., Canizares, P., and Rodrigo, M. A. 2010. Study of the production of hydrogen bubbles at low current densities for electroflotation process. Journal Chem Technol Biotechnol. **85**(10): 1368-1373. doi: 10.1002/jctb.2442.

Kabdasli, I., Arslan-Alaton, I., Vardar, B., and Tunay, O. 2007. Comparison of electrocoagulation, coagulation, and the Fenton process for the treatment of reactive dyebath effluent. Water Science & Technology. **55**(10): 125-134. doi:10.2166/wst.2007.315.

Khor, S. L., Sun, D., Hau, C., and Leckie, J. 2006. Comparison of submerged membrane bioreactors in different SRT conditions. Water Practice & Technology. doi10.2166/wpt.2006.056.

Khoufi, S., Feki, F., Sayadi, S. 2007. Detoxification of olive mill wastewater by electrocoagulation and sedimentation processes. Journal of Hazardous Materials. **142**(1-2): 58-67. doi: 10.1016/j.jhazmat.2006.07.053.

Kiehne, H. A. 2003. Battery Technology Handbook. CRC Press (online)

Kobya, M., Hiz, H., Senturk, E., Aydiner, C., and Demirbas, E. 2006. Treatment of potato chips manufacturing wastewater by electrocoagulation. Desalination. **190**(1-3): 201-211. doi:10.1016/j.desal.2005.10.006.

LaGrega, M.D., Buckingham, P.L., Evans, J.C., and Environmental Resources Management. 2001. Hazardous Waste Management, McGraw-Hill INC., New York.

Lee, B. H., Song, W.-C., Manna, B., and Yang, H.-J. 2007. Removal of Color from Wastewater Using Ozonation. IEEE Xplore.

Lin, C., S.L.Lo, Kuo, C., and C.H.Wu. 2005. Pilot-scale electrocoagulation with bipolar aluminum electrodes for on-site domestic greywater reuse. Journal of Environmental Engineering. **131**(3): 491-495. doi 10.1061/(ASCE)0733-9372(2005)131:3(491).

Linares-Hernandez, I., Barrera-Diaz, C., Roa-Morales, G., Bilyeu, B., & Urena-Nunez, F. 2009. Influence of the anodic material on electrocoagulation performance. Chemical Engineering Journal. **148**(1): 97-105. doi:10.1016/j.cej.2008.08.007.

Liu, H., Zhao, X., & Qu, J. 2010. Electrocoagulation in Water Treatment. In C. C. Chen, Electrochemistry for the Environment. Lausanne: Springer. pp. 245-262. doi:10.1007/978-0-387-68318-8_10.

LME, L. M. (n.d.). LME Aluminium price graph. http://www.lme.com/aluminium_graphs.asp. 12 28, 2010.(Accessed 12 28,2010)

Mara, D., Mills, S., Pearson, H. W., and Alabaster, G. P. 1992. Waste Stabilization ponds: A viable alternative for small community treatment systems. Journal of Water and Environmental Management. **6**(1): 72-78.

Meas, Y., Ramirez, J. A., Villalon, M. A., and Chapman, T. W. 2010. Industrial wastewaters treated by electrocoagulation. Electrochimica Acta. **55**: 8165-8171.

Meng, F., Shi, B., Yang, F., and Zhang, H. 2007. New insights into membrane fouling in submerged membrane bioreactor based on rheology and hydrodynamics concepts. Journal of Membrane Science. **302**(1-2): 87 - 94. doi:10.1016/j.memsci.2007.06.030.

Merlo, R. P., Trussell, R. S., Hermanowicz, S. W., and Jenkins, D. 2004. physical, chemical and biological properties of submerged membrane bioreactors andconventional activated sludge. *In*Proceedings of the Water Environment Federation Weftec 2004. Water Environment Federation. pp. 625-642

Merz, C., Gildemeister, R., Hamouri, B. E., and Kraume, M. 2007. Membrane bioreactor technology for the treatment of greywater from a sports and leisure club. Desalination. **215**(1-3): 37-43.doi:10.1016/j.desal.2006.10.026.

Merzouk, B., Gourich, B., Sekki, A., Madani, K., and Chibane, M. 2009. Removal turbidity and separation of heavy metals using electrocoagulation–electroflotation technique A case study. Journal of Hazardous Materials. **164**(1):215–222. doi:10.1016/j.jhazmat.2008.07.144.

Merzouk, B., Madani, K., and Sekki, A. 2010. Using electrocoagulation–electroflotation technology to treat synthetic solution and textile wastewater, two case studies. Desalination. **250**(2):573–577. doi:10.1016/j.desal.2009.09.026.

Meunier, N., Drogui, P., Montane, C., Hausler, R., Mercier, G., and Blais, J.-F. 2006. Comparison between electrocoagulation and chemical precipitation for metal removal from acidic soil leachate. Journal of Hazardous Materials. **137**(1): 581-590. doi:10.1016/j.jhazmat.2006.02.050.

Ministry of Natural Resources- Quebec. La production d'électricité disponible par source d'énergie (1983-2008). http://www.mrnf.gouv.qc.ca/energie/statistiques/statistiques-production-electricite.jsp 2008 (Accessed December, 2010)

Ministère du Développement durable, de l'Environnement et des Parcs-Quebec. Critères de qualité de l'eau de surface au Québec. http://www.mddep.gouv.qc.ca/eau/criteres_eau/details.asp?code=S03932009 (Accessed 15 January 2011)

Mohammed, T. A., Birima, A. H., Noor, M. J., Muyibi, S. A., and Idris, A. 2008. Evaluation of using membrane bioreactor for treating municipal wastewater at different operating conditions. Desalination. **221**(1-3): 502-510. doi:10.1016/j.desal.2007.02.058.

Moisés, T.-P., Patricia, B. H., Barrera-Diaz, C., Gabriela, R.-M. and Natividad-Rangel, R. 2010. Treatment of industrial effluents by a continuous system: Electrocoagulation-Activated Sludge. Bioresource Technology. **101**(20): 7761-7766. doi:10.1016/j.biortech.2010.05.027.

Moreno-Casillas, H. A., Cocke, D. L., Gomes, J. A., Morkovsky, P., Parga, J., and Peterson, E. 2007. Electrocoagulation mechanism for COD removal. Separation and Purification Technology . **56**(2): 204–211.doi:10.1016/j.seppur.2007.01.031.

Morris, J. M., Fallgren, P. H., and Jin, S. 2009. Enhanced denitrification through microbial and steel fuel-cell generated electron transport. Chemical Engineering Journal. **153**(1-3): 37-42. doi:10.1016/j.cej.2009.05.041.

Mouedhen, G., Feki, M., Wery, M. D., and Ayedi, H. (2008). Behaviour of aluminum electrodes in electrocoagulation process. Journal of Hazardous Materials, **150**(1): 124-135. doi:10.1016/j.jhazmat.2007.04.090.

Mulligan, C. N. 2002. Environmental biotreatment: technologies for air, water, soil, and waste. Government Institutes, Michigan.

Mustafa, S., Naeem, A., Murtaza, S., Rehana, N., and Samad, H. Y. 1999. Comparatice sorption properties of metal (III) phosphates. Journal of Colloid interface Science. **221**(1): 63-74.

Newfoundland & Labrador, G. o. Lagoons - Operation and Management in New Brunswick. http://www.env.gov.nl.ca/env/waterres/training/aww/09_lagoons_operation_and_management_in_new_brunswick.pdf. 2009. (Accessed October 2010)

Ng, H. Y., Tan, T. W., and Ong, S. L. 2006. Membrane Fouling of Submerged Membrane Bioreactors: Impact of Mean Cell Residence Time and the contributing Factors. Environmental Science & Technology. **40**(8): 2706-2713.

Ni'am, M., Othman, F., Sohaili, J., and Fauzia, Z. 2007. Electrocoagulation technique in enhancing COD andsuspended solids removal to improve wastewater quality. Water Science & Technolog. **56**(7): 47-53.

Peavy, H.S., Rowe, D.R., and Tchobanglous, G. 1985. Environmental Engineering. McGraw-Hill, Inc., New York.

Phalakornkule, C., Sukkasem, P., and Mutchimasattha, C. 2010. Hydrogen Recovery from the electrocoagulation treatment of dye-containing wastewater. *International* Journal of Hydrogen Energy. **35**(20): 10934 - 10943. doi:10.1016/j.ijhydene.2010.06.100.

Polatide, C., Kyriacou, G. 2005. Electrochemical reduction of nitrate ion on various cathodes – reaction kinetics on bronze cathode. Journal of Applied Electrochemistry. **35**(5): 421–427. doi: 10.1007/s10800-004-8349-z.

Ricordel, C., Darchen, A., and Hadjiev, D. 2010. Electrocoagulation-electroflotation as a surface water treatment for industrial uses. Separation and Purification Technology. **74**(3): 342-347. doi:10.1016/j.seppur.2010.06.024.

Rossini, M., Garcia, G., and Galluzo, M. 1999. Optimization of the coagulation-flocculation treatment; influence of rapid mixing parameters. Water Research, **33**(8): 1817-1826. doi:10.1016/S0043-1354(98)00367-4.

Sabzali, A., Gholami, M., Yazdanbakhsh, A. R., Khodadadi, A., Musavi, B., and Mirzaee, R. 2006. CHEMICAL DENITRIFICATION OF NITRATE FROM GROUNDWATER VIA SULFAMIC ACID AND ZINC METAL. Iran. J. Environ. Health. Sci. Eng. **3**(3): 141-146.

Sarkar, M., Evans, G., and Donne, S. 2010. Bubble size measurement in electroflotation. Minerals Engineering. **23** (11-13): 1058-1065. doi: 10.1016/j.mineng.2010.08.015.

Shidong, Y., Lanhe, Z., Fengguo, C., and Jun, M. 2009. Preliminary Study on Enhanced Dissolved Air Floatation by Pulsed High Voltage Discharge. IEEE Xplore.

Sincero, A. P., and Sincero, G. A. 2003. Physical- Chemical Treatment of Water and Wastewater. IWA Publishing, London.

Sorensen, J. 1978. Capacity for Denitrification and Reduction of Nitrate to Ammonia in a Coastal Marine Sediment. Applied and Environmental Microbiology. **35**(2): 301-305.

Sperling, M.V. 2007. Basic Principles of Wastewater Treatment. IWA Publishing, London.

Sun, D. D., Khor, S. L., Hay, C. T., and Leckie, J. O. 2007. Impact of prolonged sludge

retention time on the performance of a submerged membrane bioreactor. Desalination. **208**(1-3): 101-112. doi:10.1016/j.desal.2006.04.076.

Taniguchi, Y., Stanley, H. E., and Ludwig, H. (2002) " Biological systems under extreme conditions. Structure and function." Springer, New York.

Tchabonglous, G., and Metcalf and Eddy. 1979. Wastewater engineering: treatment, disposal and reuse. McGraw-Hill, Newyork.

Tchamango, S., Nijki, C. P., Ngameni, E., Hadjiev, D., and Darchen, A. 2010. Treatment of dairy effluents by electrocoagulation using aluminum electrodes. Science of Total Environment. **408**(4): 974-952.

Texas A & M University. Active Learning in Chemical Engineering- Electrokinetics. http://alcheme.tamu.edu/?page_id=6823 2009. (Accessed November, 2010_

Thomann, R. V. and Mueller, J. A. (1987). " Principles of surface water quality modeling and control." Harper & Row., New York.

Tian, J.-y., Liang, H., Nan, J., Yang, Y.-l., You, S.-j., and Li, G.-b. 2009. Submerged membrane bioreactor (sMBR) for the treatment of contaminated raw water. Chemical Engineering Journal. **148**(2-3): doi:10.1016/j.cej.2008.08.032.

Timmes, T. C., Kim, H.-C., and Dempsey, B. A. 2009. Electrocoagulation pretreatment of seawater prior to ultrafiltration: Bench-scale applications for military water purification systems. Desalination. **249**(3): 895-901. doi:10.1016/j.desal.2009.07.002.

Trompette J.L., and Vergnes H. 2009. On the crucial influence of some supporting electrolytes during electrocoagulation in the presence of aluminum electrodes. Journal of Hazardous Materials. **163**(2-3): 1282-1288. doi:10.1016/j.jhazmat.2008.07.148.

Tuan P.-A., J. V. 2008. Electro-dewatering of sludge under pressure and nonpressure conditions. Environmental Technology. **29**(10): 1075-1084. doi:10.1080/09593330802180294.

Valenzuela, D. P., Dubey, S. T., and Dewan, A. K. 2002. Corrosion at Metal Interfaces - A Study of Corrosion Rate and Solution Properties, Including Conductance, Viscosity, and Density. Ind. Eng. Chem. Res. **41**(5): 914-921. doi: 10.1021/ie001027u.

Vasudevan, S., Sozhan, G., Ravichandran, S., Jayaraj, J., Lakshmi, J., and Sheela, S. M. 2008. Studies on the Removal of Phosphate from Drinking Water by Electrocoagulation Process. Ind. Eng. Chem. Res. **47** (6): 2018–2023. doi: 10.1021/ie0714652

Wang, L., Hung, Y.-T., and Shammas, N. 2005. Physicochemical Treatment Processes. In Handbook of Environmental Engineering **3**: 431-500. doi:10.1385/159259820x.

Wang, Z., Wu, Z., Yu, G., Liu, J., and Zhou, Z. 2006. Relationship between sludge characteristics and membrane flux determination in submerged membrane bioreactors. Journal of Membrane Science. **284**(1-2): 87-94. doi:10.1016/j.memsci.2006.07.006.

Water Quality Program Committee, Virginia Tech. Small Community Wastewater Treatment and Disposal Options. No.448404, July 1996.(report)

Yang, Q., Chen, J., and Zhang, F. 2006. Membrane fouling control in a submerged membrane bioreactor with porous, flexible suspended carriers. Desalination. **189**(1-3): 292-302. doi:10.1016/j.desal.2005.07.011.

Yang, W., Gao, H., Li, S., and Jian, X. 2008. Study on Advective Separation of Oil-Coagulation-Floatation-Slag Filtration Technology to Handle Oily. IEEE Xplore.

Zanello, P. 2003. Inorganic electrochemistry: theory, practice and application. Cambridge: Royal Society of Chemistry.

Zheng, X.-Y., Kong, H.-N., Wu, D.-y., Wang, C., and Yan Li, H.-r. Y. 2009. Phosphate removal from source separated urine by electrocoagulation using iron plate electrodes. Water Science & Technology. **60**(11): 2929-2938. doi:10.2166/wst.2009.309.

Zodi, S., Potier, O., Lapicque, F., and Leclerc, J.-P. 2009. Treatment of the textile wastewaters by electrocoagulation: Effect of operating parameters on the sludge settling characteristics. Separation and Purification Technology. **69**(1): 29-36. doi:10.1016/j.seppur.2009.06.028.

Zongo, I., Maiga, A. H., Wethe, J., Valentin, G., Leclerc, J.-P., Paternotte, G., and Lapicque, F. 2009. Electrocoagulation for treatment of textile wastewaters with Al or Fe electrodes: Compared variations of COD levels, turbidity and absorbance. Journal of Hazardous Materials. **169**(1-3): 70-76.

Appendix I – Additional results

Phase II

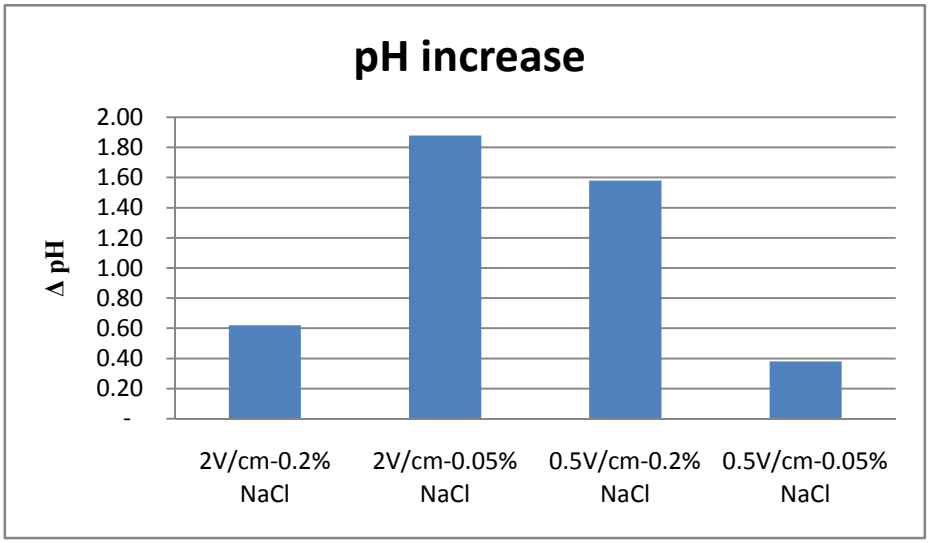

Figure 79 – Phase II - pH change after 4 hours of EC treatment

Phase III – WWTP1

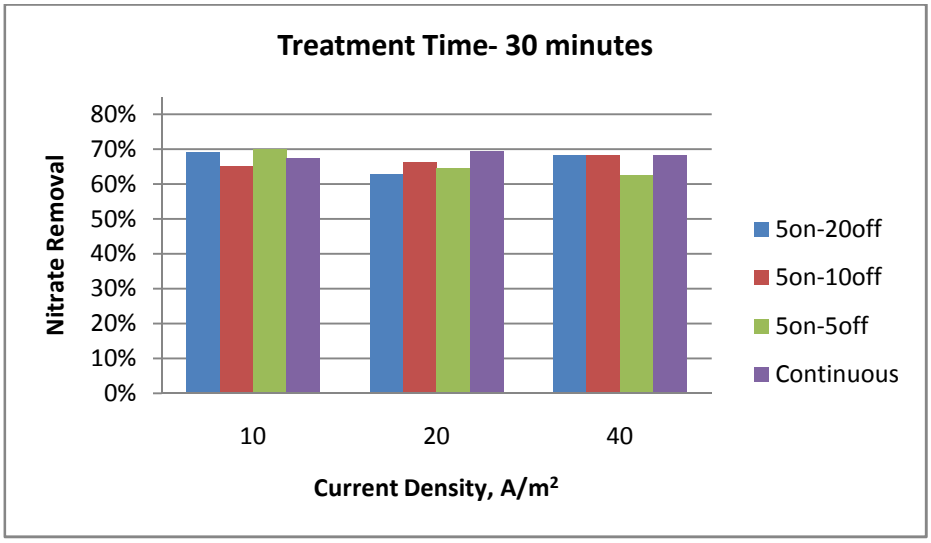

Figure 80 - Phase III - WWTP1 – Nitrate removal – treatment time - 30 minutes

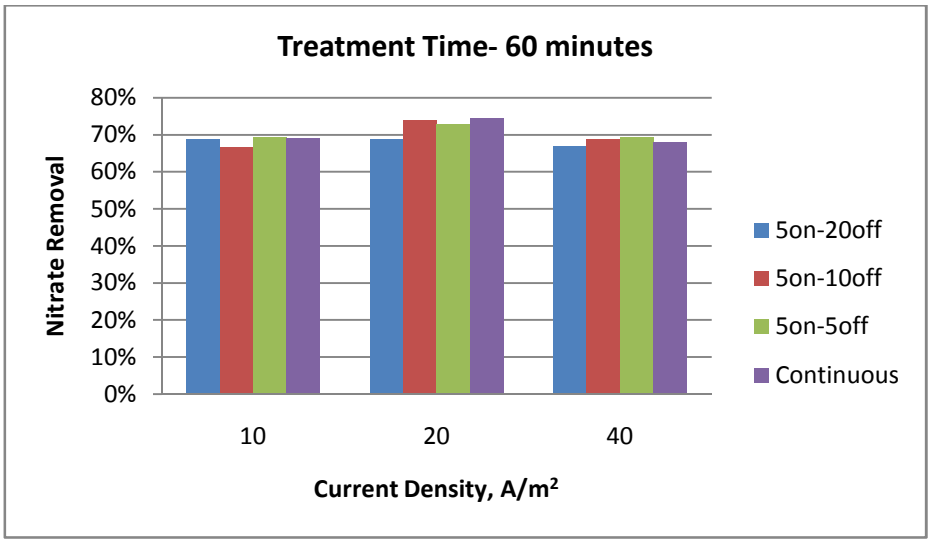

Figure 81- Phase III - WWTP1 – Nitrate removal – treatment time - 60 minutes

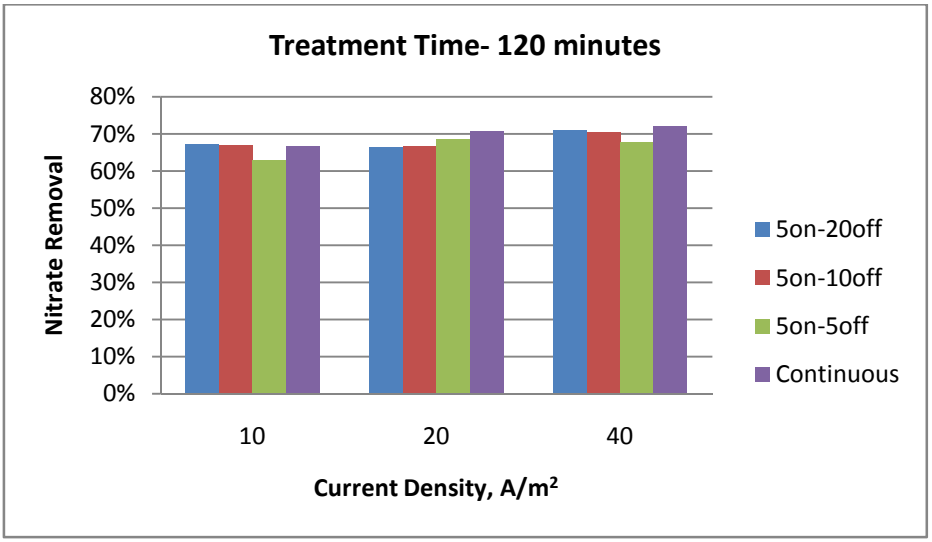

Figure 82 - Phase III - WWTP1 – Nitrate removal – treatment time - 120 minutes

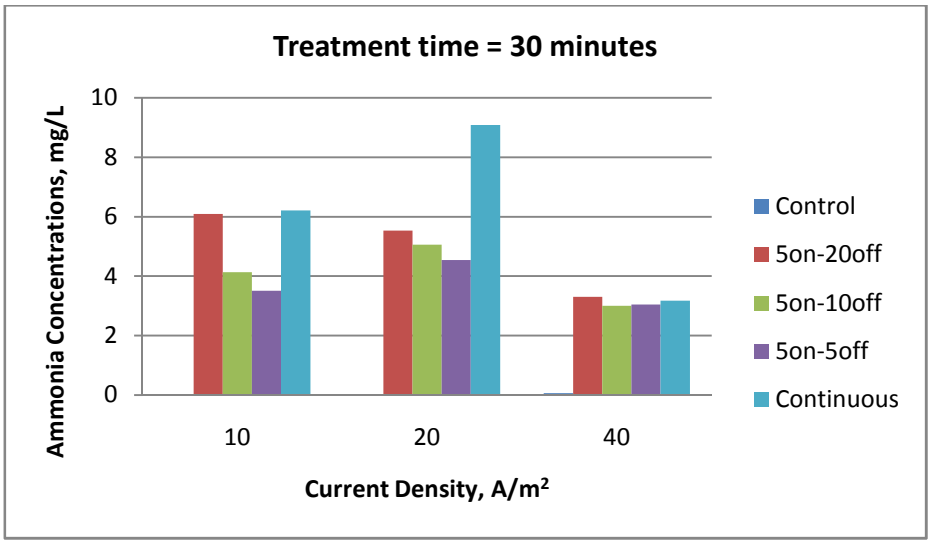

Figure 83 - Phase III - WWTP1 – Ammonia concentrations – treatment time - 30 minutes

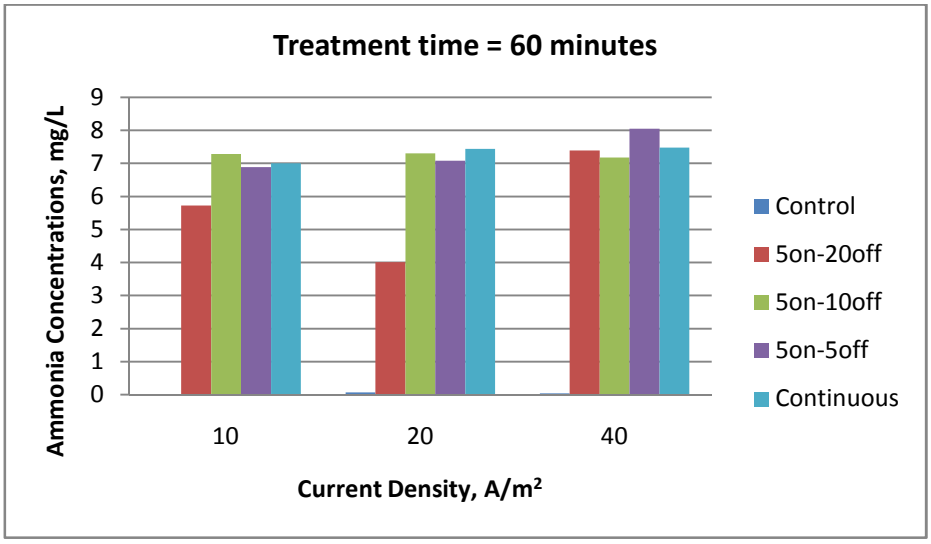

Figure 84 - Phase III - WWTP1 – Ammonia concentrations – treatment time - 60 minutes

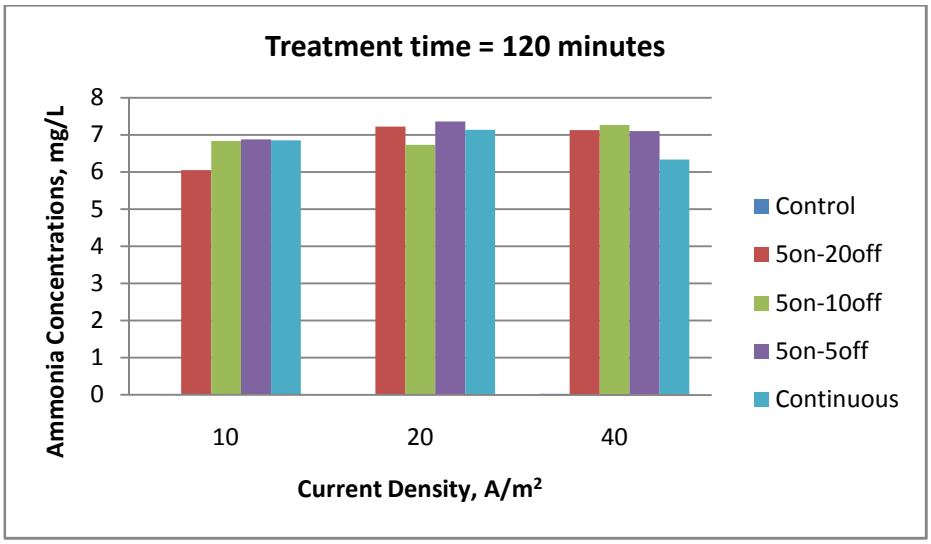

Figure 85 - Phase III - WWTP1 – Ammonia concentrations – treatment time - 60 minutes

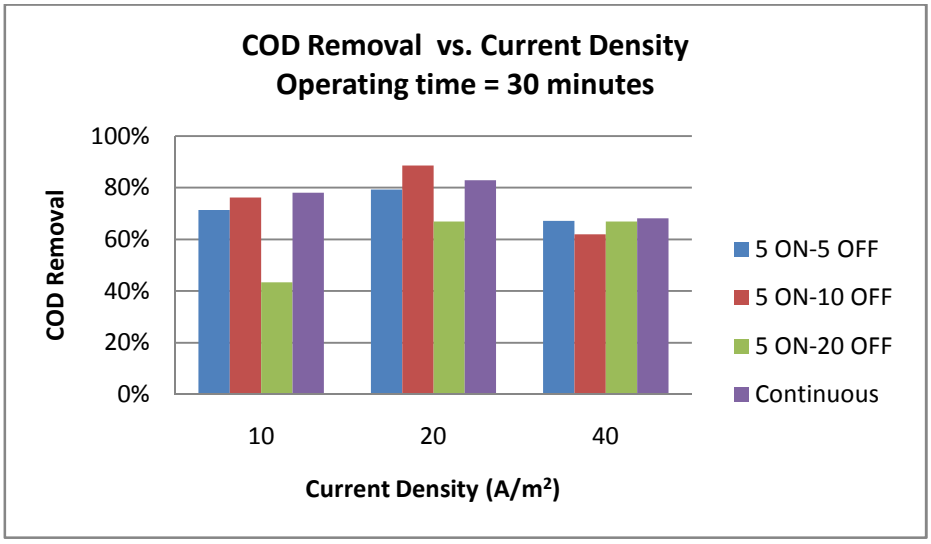

Figure 86 - Phase III - WWTP1 – COD removal – treatment time - 30 minutes

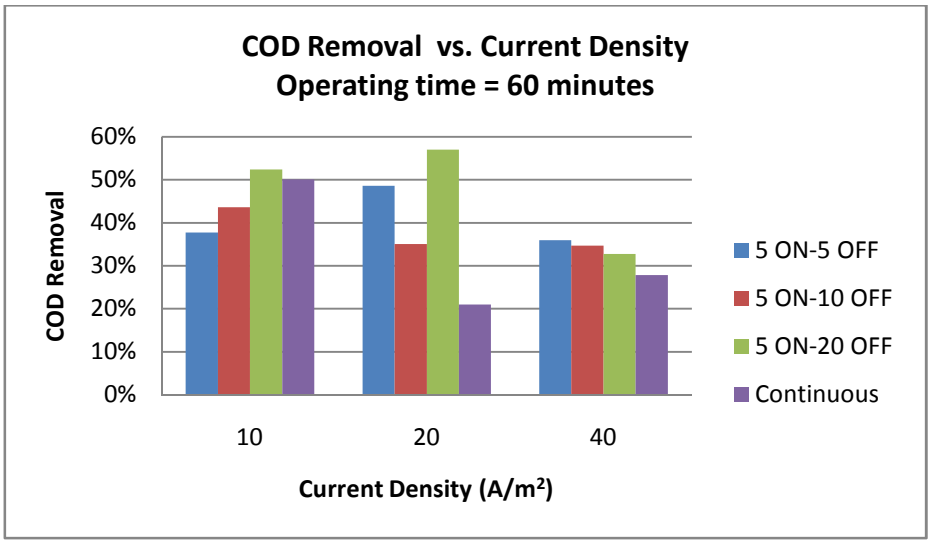

Figure 87 - Phase III - WWTP1 – COD removal – treatment time - 60 minutes

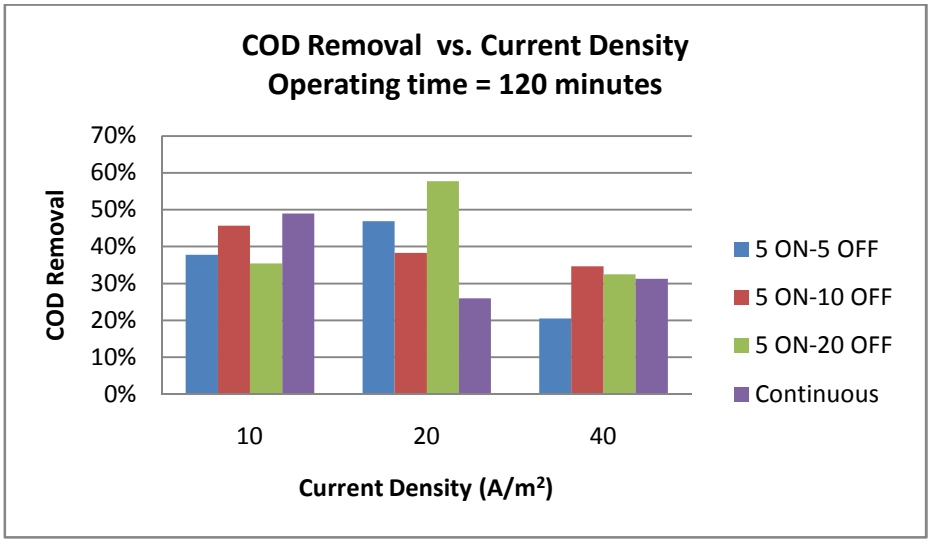

Figure 88 - Phase III - WWTP1 – COD removal – treatment time - 120 minutes

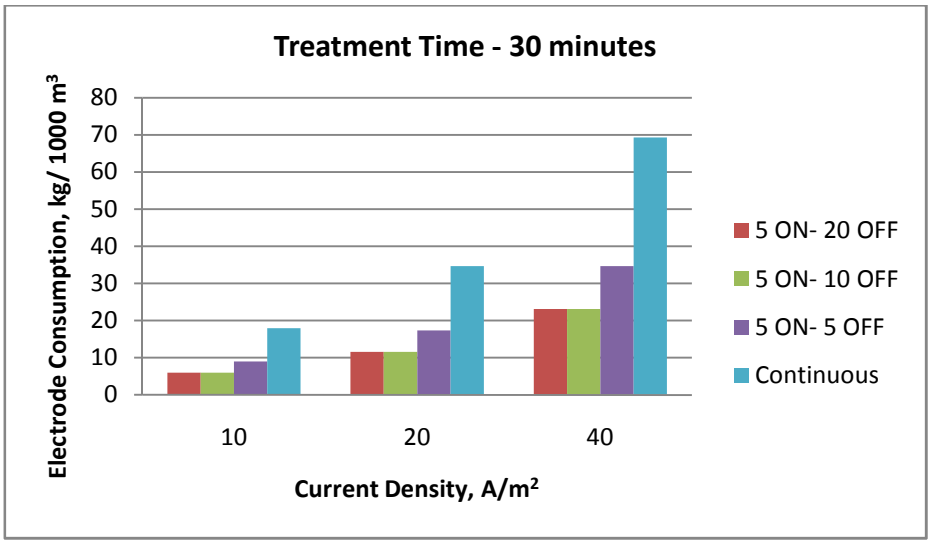

Figure 89 - Phase III - WWTP1 – Electrode consumption – treatment time - 30 minutes

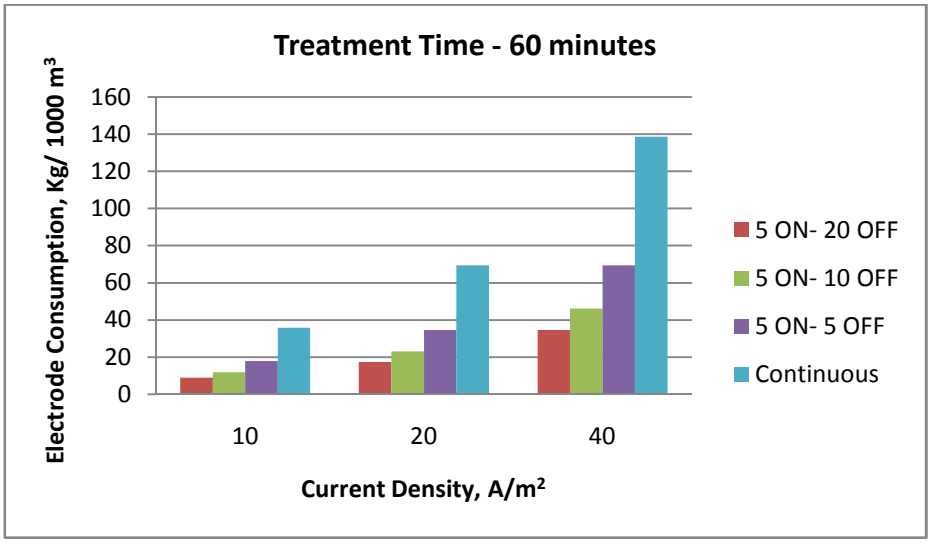

Figure 90 - Phase III - WWTP1 – Electrode consumption – treatment time - 60 minutes

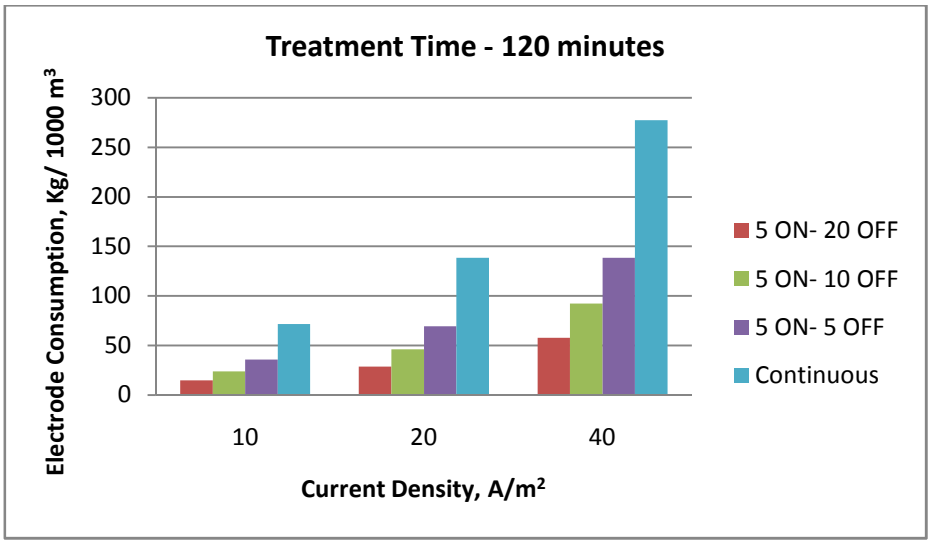

Figure 91 - Phase III - WWTP1 – Electrode consumption – treatment time - 120 minutes

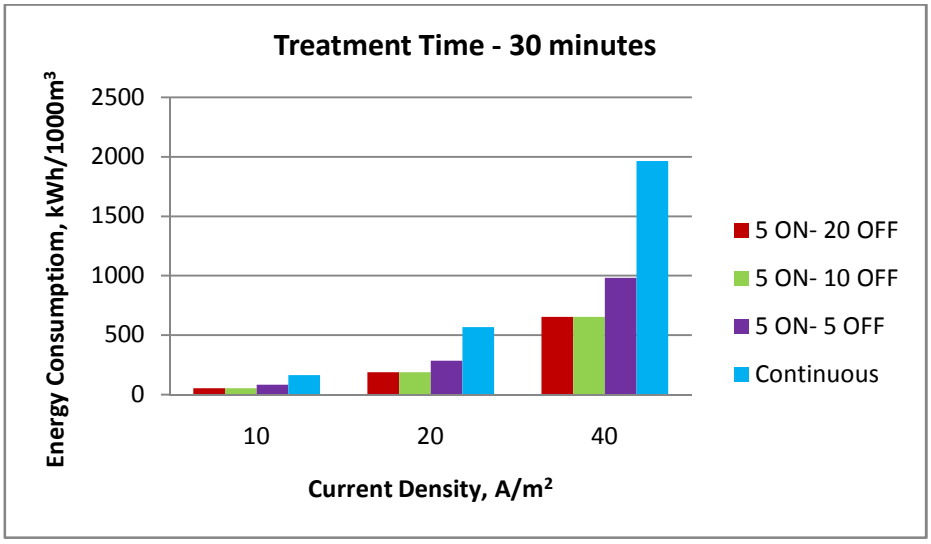

Figure 92 - Phase III - WWTP1 – Energy consumption – treatment time - 30 minutes

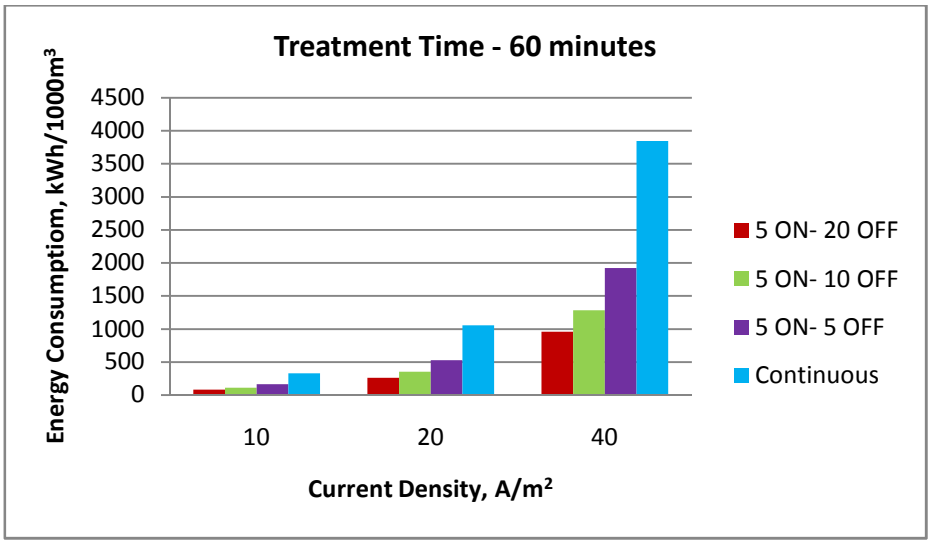

Figure 93 - Phase III - WWTP1 - Energy consumption – treatment time - 60 minutes

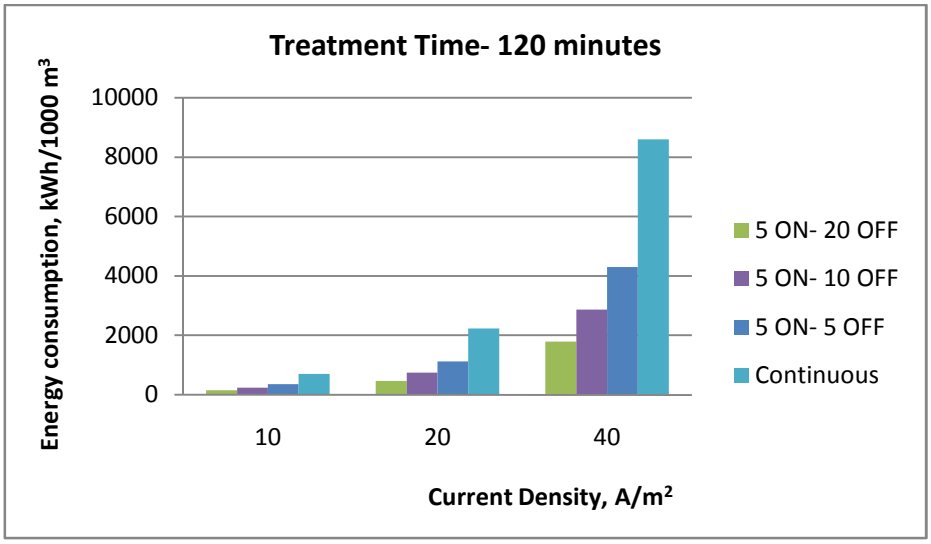

Figure 94 - Phase III - WWTP1 – Energy consumption – treatment time - 120 minutes

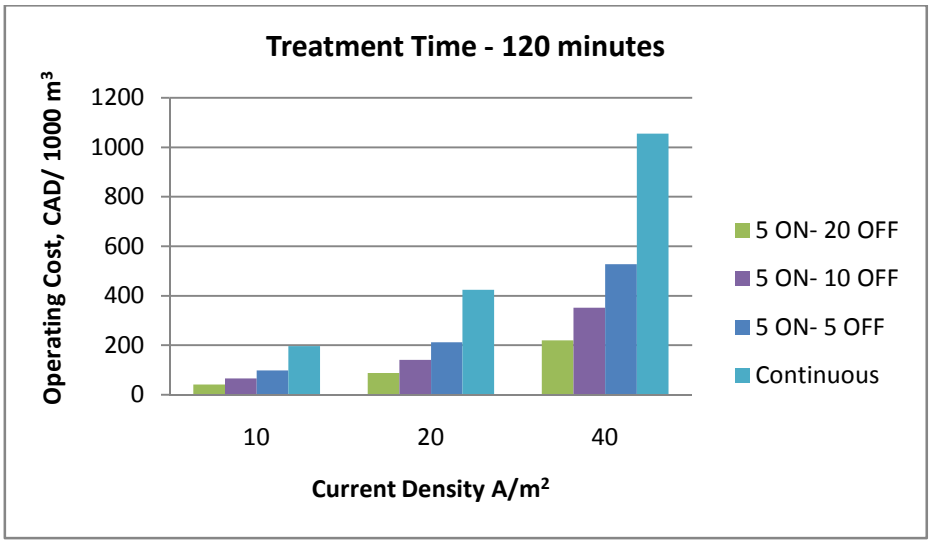

Figure 95 - Phase III - WWTP1 – Operating cost – treatment time - 120 minutes

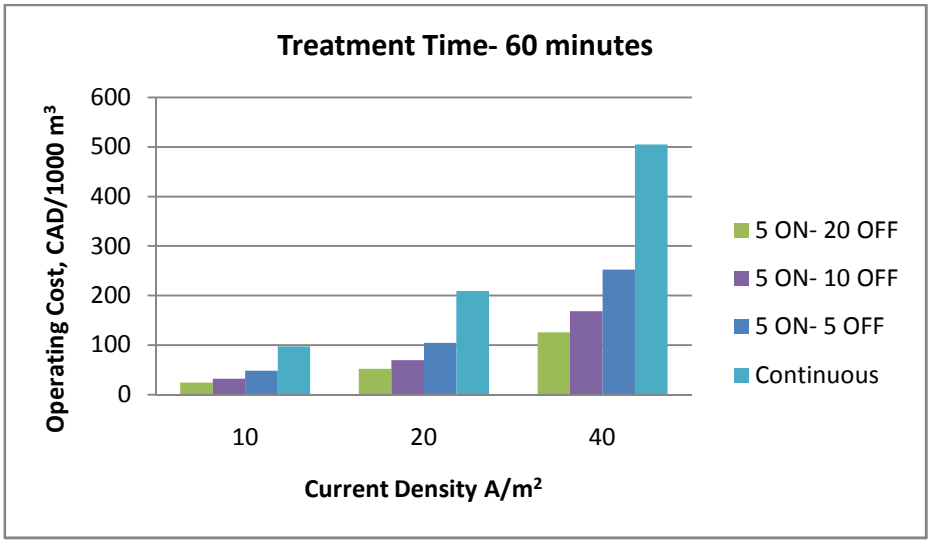

Figure 96 - Phase III - WWTP1 – Operating cost– treatment time - 60 minutes

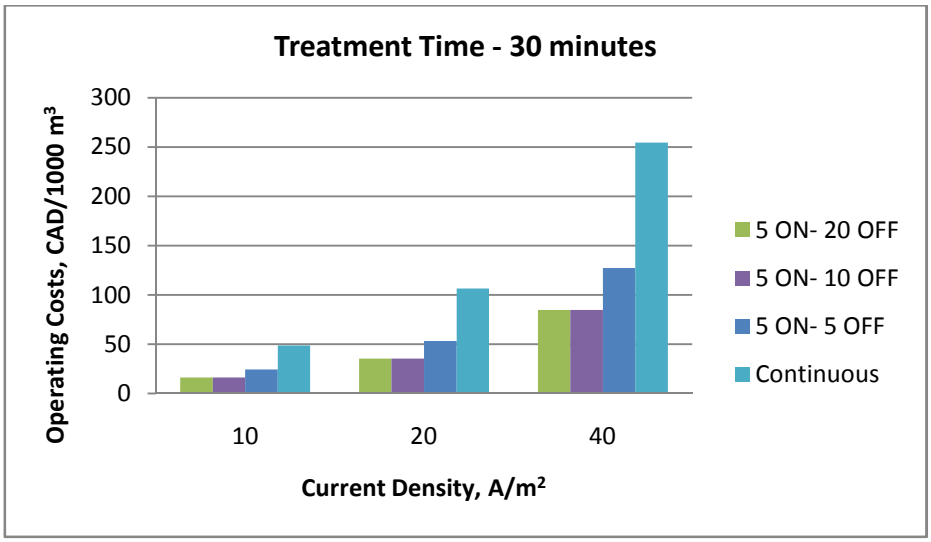

Figure 97 - Phase III - WWTP1 – Operating cost – treatment time - 30 minutes

Phase III - WWTP2

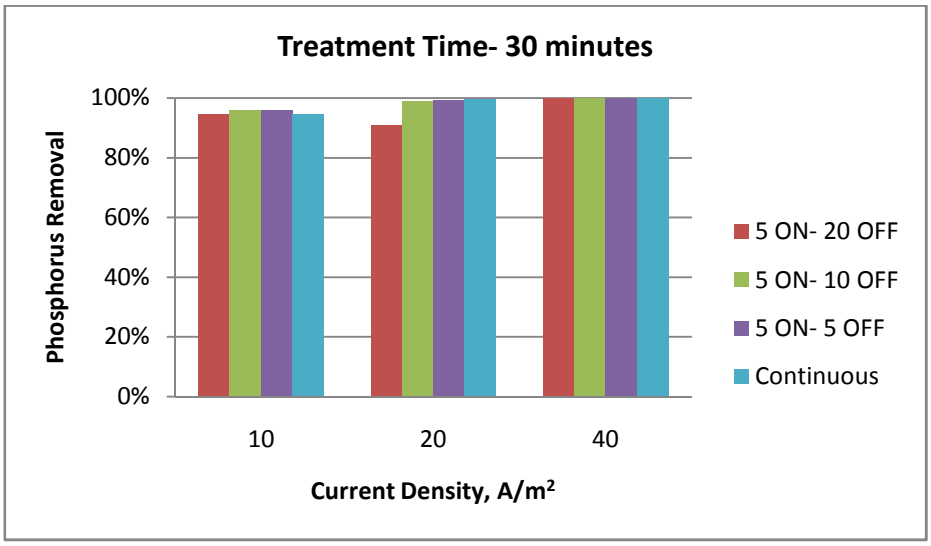

Figure 98 - Phase III - WWTP2 – Phosphorus removal – treatment time - 30 minutes

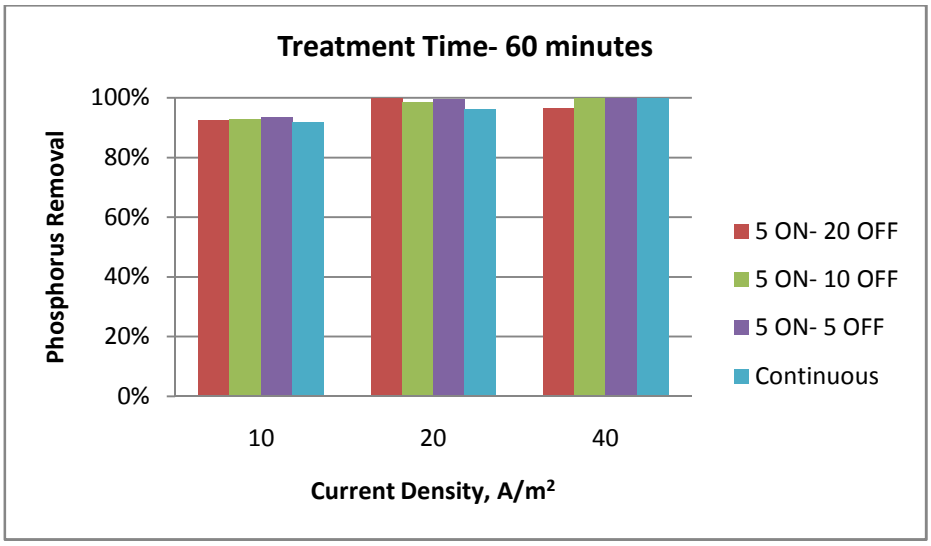

Figure 99 - Phase III - WWTP2 – Phosphorus removal – treatment time - 60 minutes

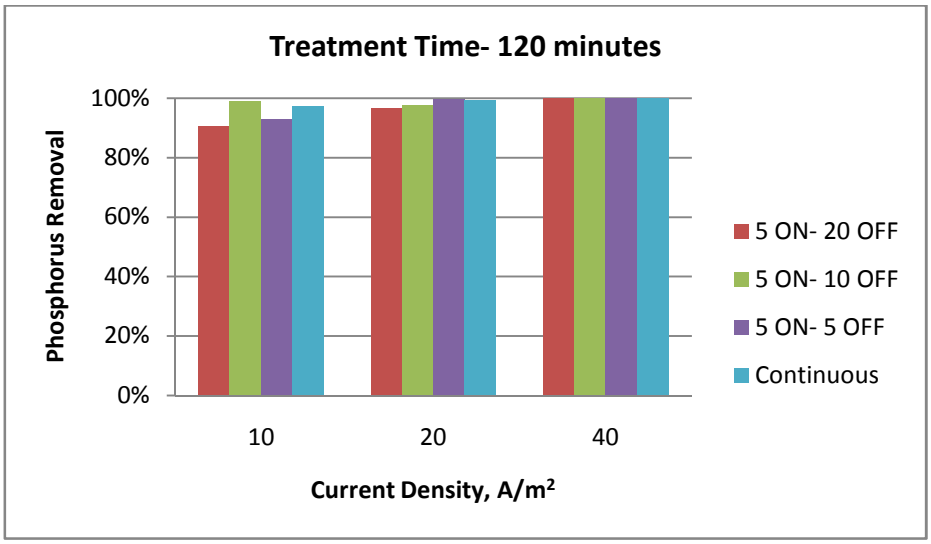

Figure 100 - Phase III - WWTP2 – Phosphorus removal – treatment time - 120 minutes

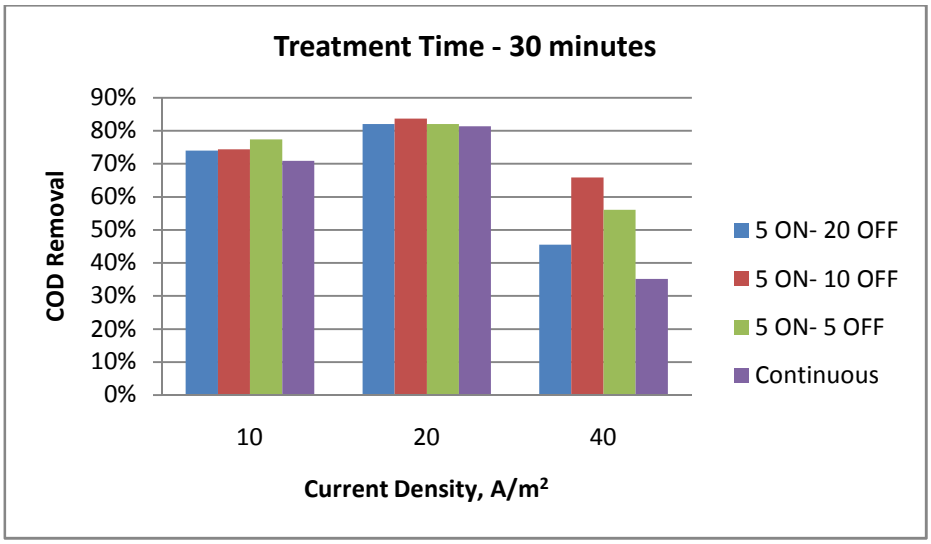

Figure 101 - Phase III - WWTP2 – COD removal – treatment time - 30 minutes

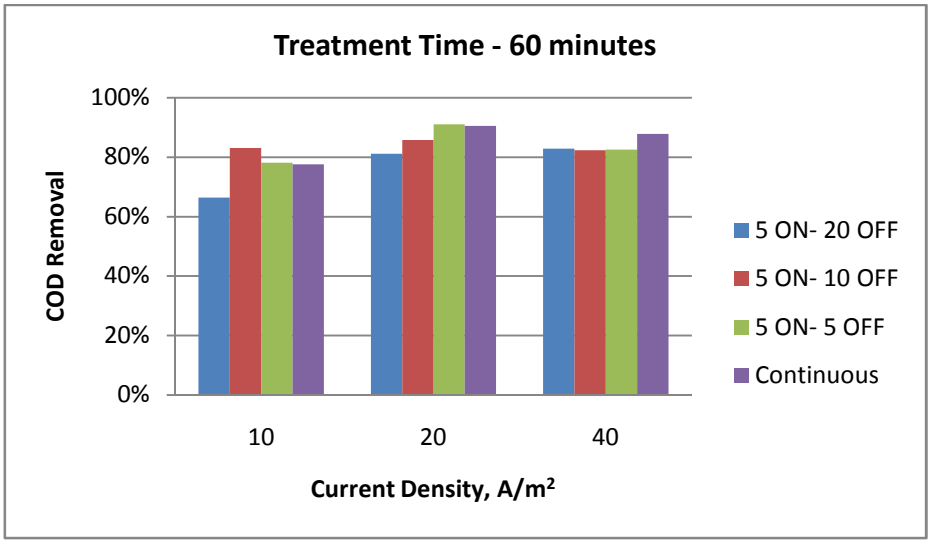

Figure 102 - Phase III - WWTP2 – COD removal – treatment time - 60 minutes

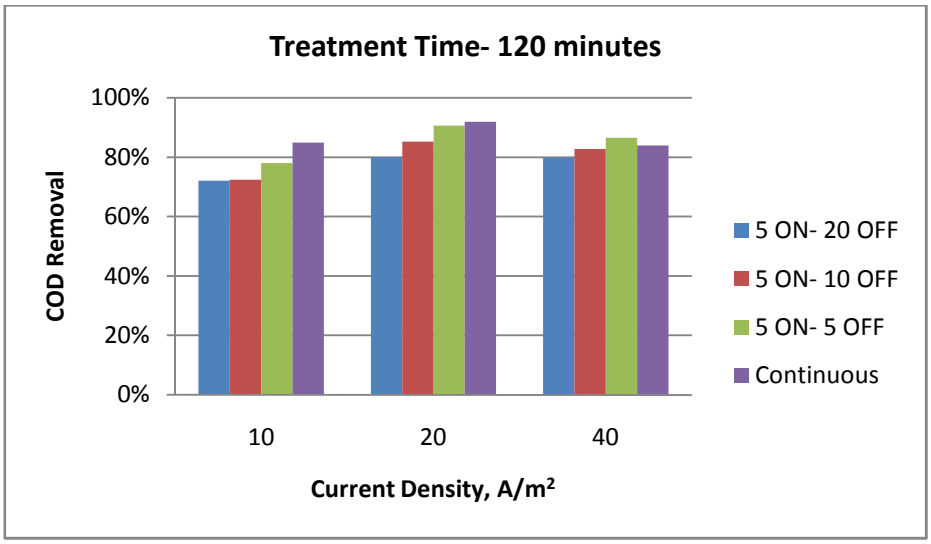

Figure 103 - Phase III - WWTP2 – COD removal – treatment time - 120 minutes

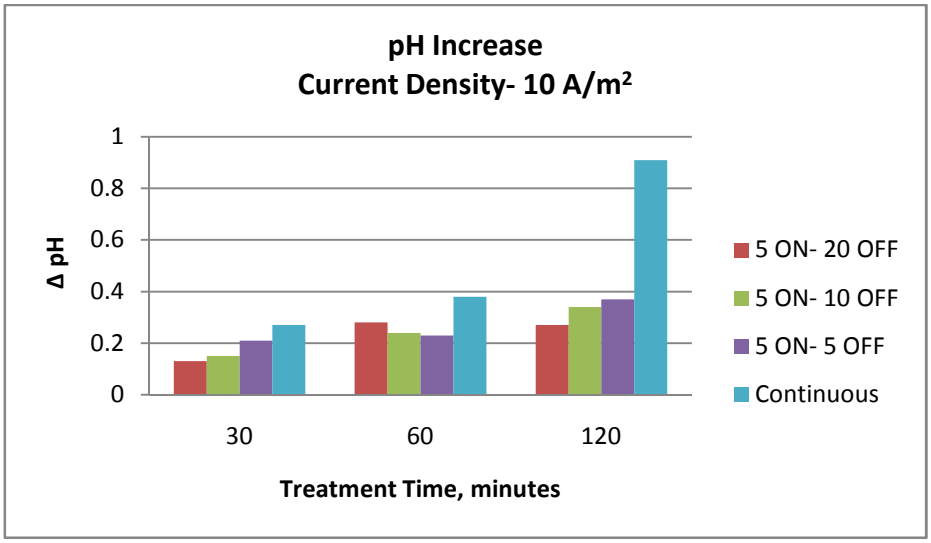

Figure 104 – Phase III - WWTP2 – pH increase – current density – 10 A/m^2

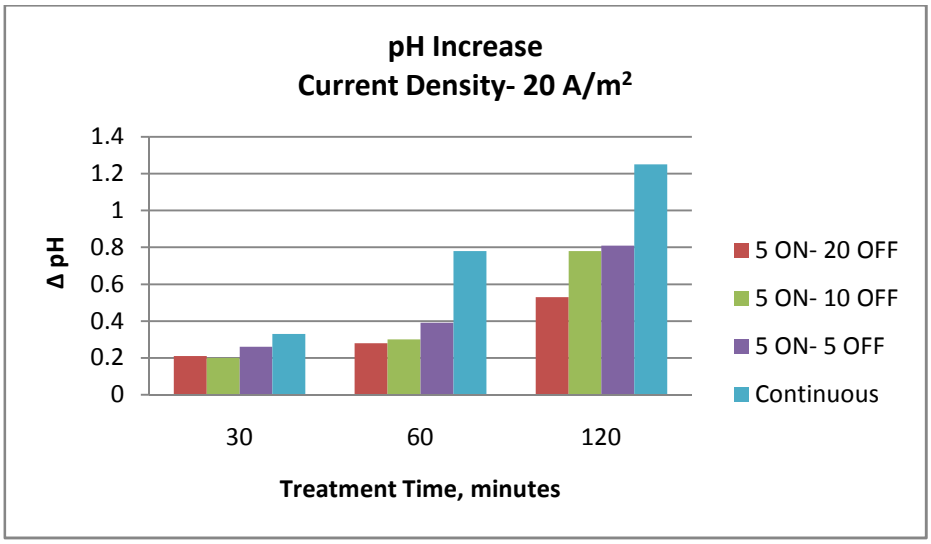

Figure 105 – Phase III - WWTP2 – pH increase – current density – 20 A/m^2

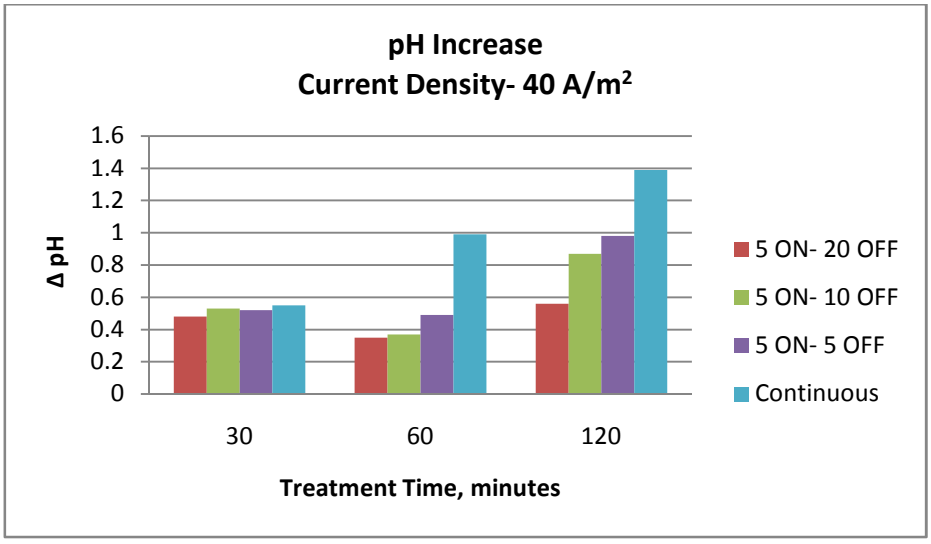

Figure 106 – Phase III - WWTP2 – pH increase – current density – 40 A/m^2

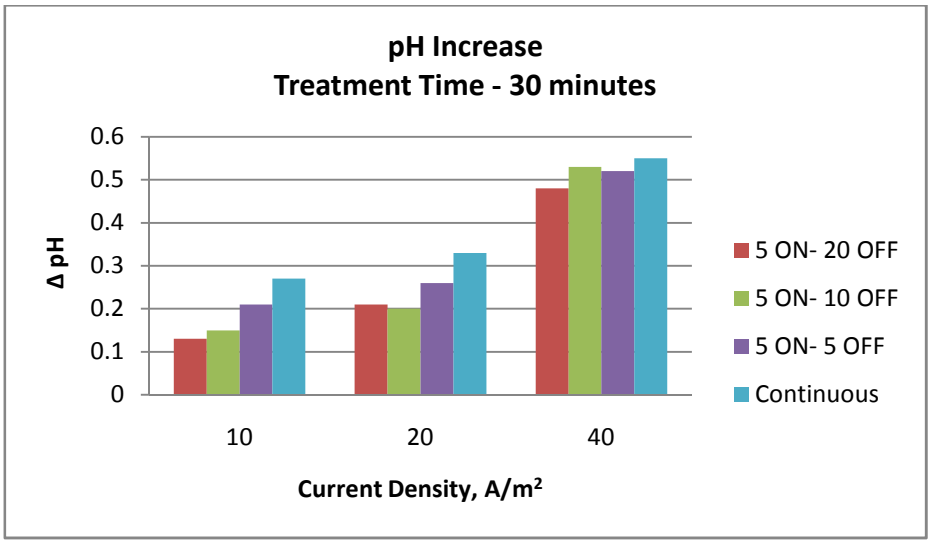

Figure 107 – Phase III - WWTP2 – pH increase – treatment time – 30 minutes

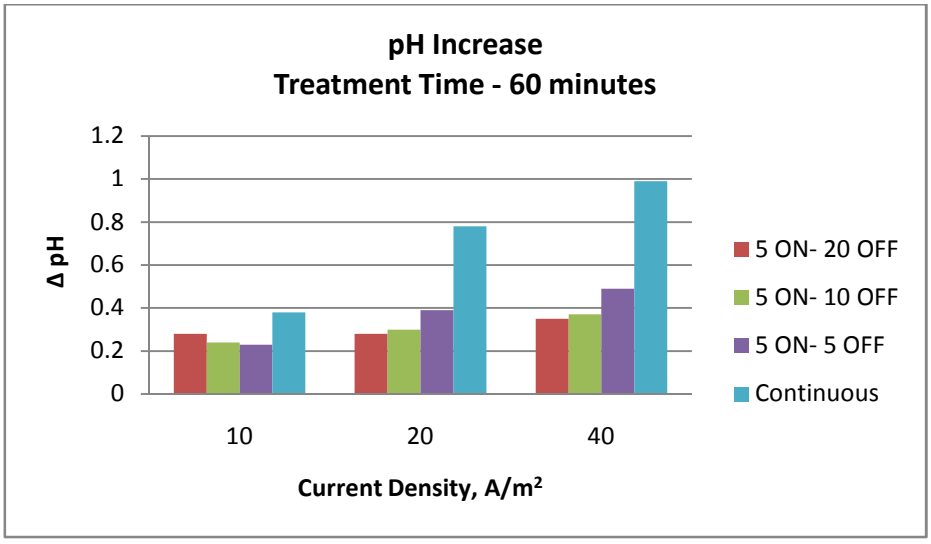

Figure 108 – Phase III - WWTP2 – pH increase – treatment time – 60 minutes

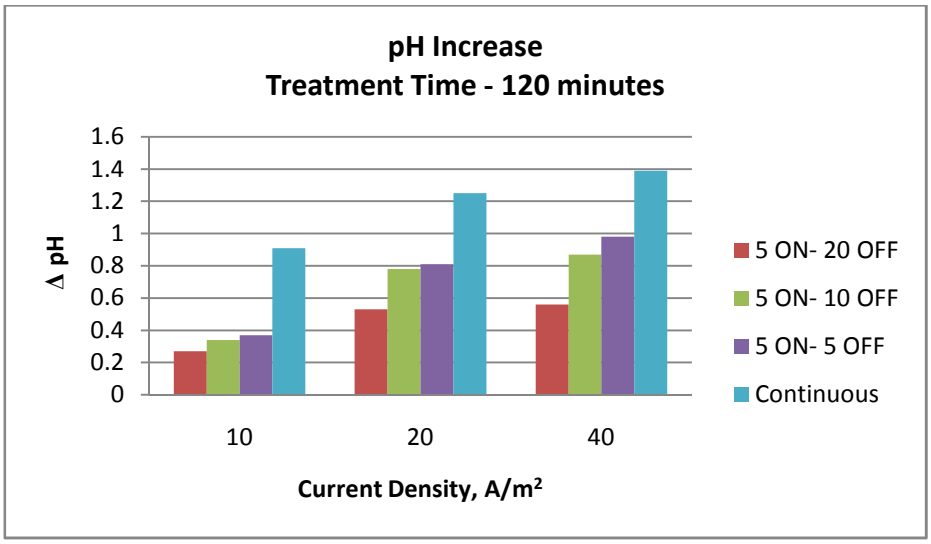

Figure 109 – Phase III- WWTP2 – pH increase – treatment time – 120 minutes

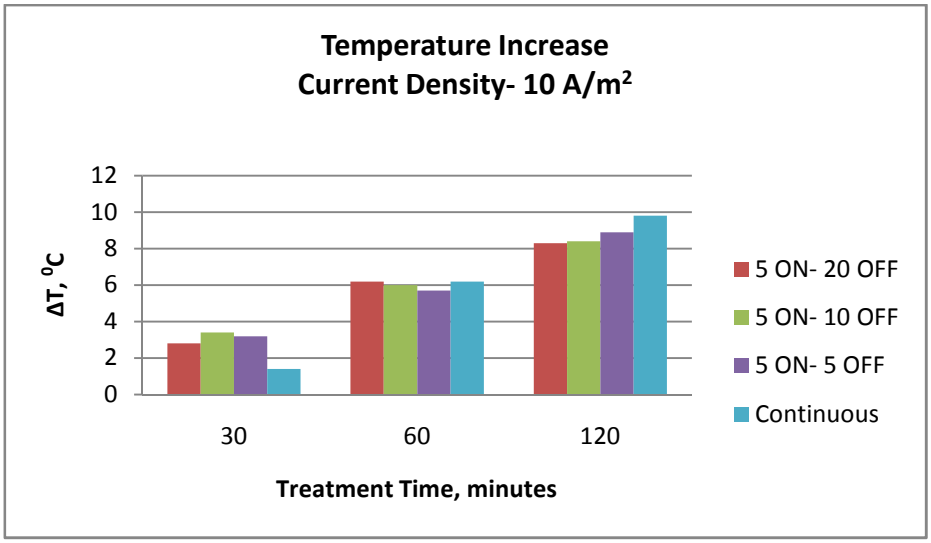

Figure 110 – Phase III - WWTP2 – Temperature increase – current density – 10 A/m²

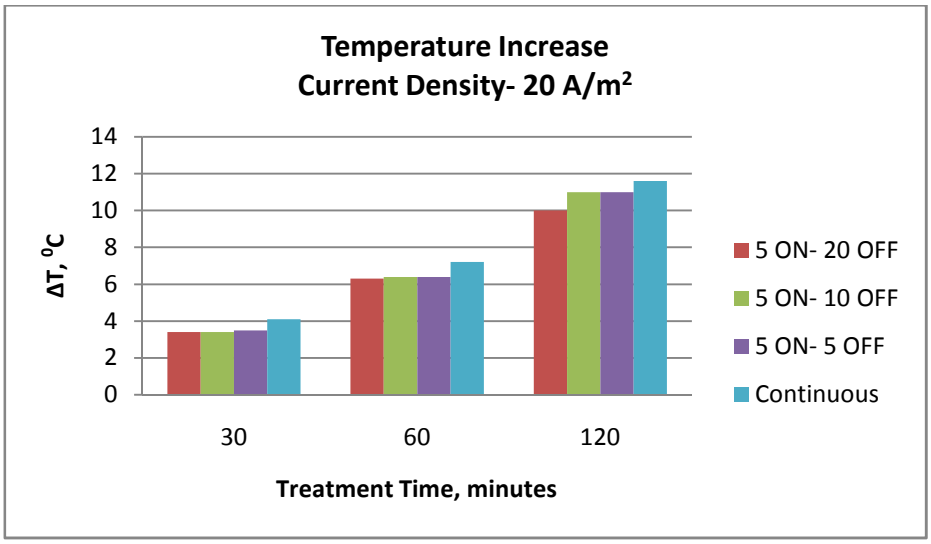

Figure 111 – Phase III - WWTP2 – Temperature increase – current density – 20 A/m^2

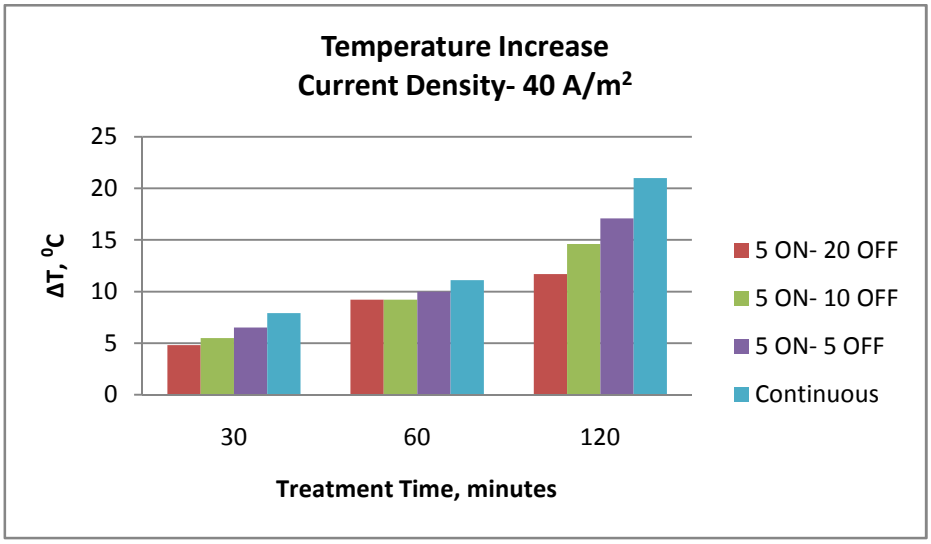

Figure 112 – Phase III- WWTP2 – Temperature increase – current density – 40 A/m^2

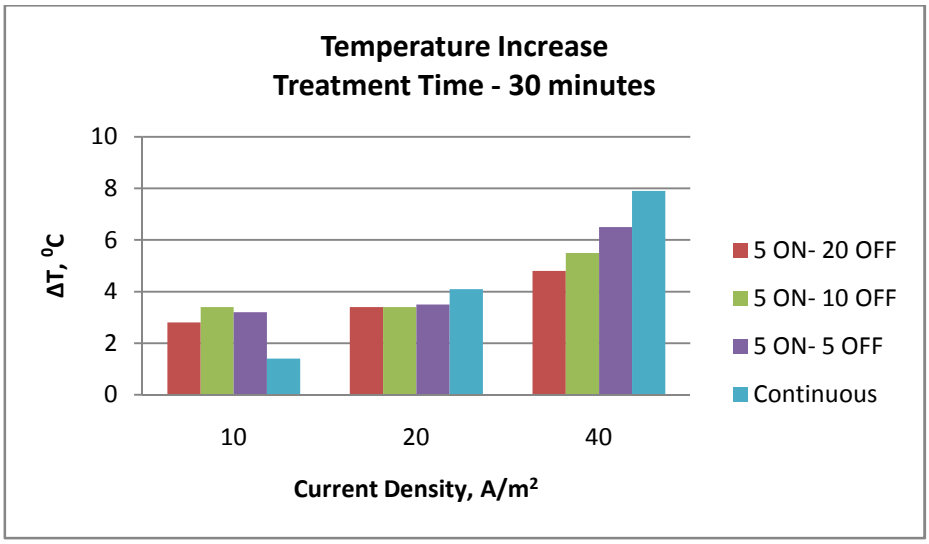

Figure 113 – Phase III - WWTP2 – Temperature increase – treatment time – 30 minutes

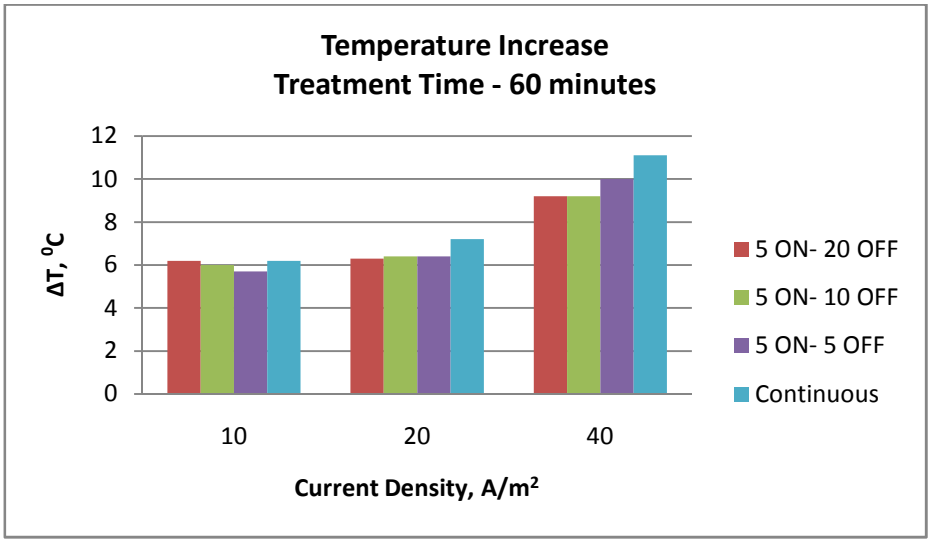

Figure 114 – Phase III - WWTP2 – Temperature increase – treatment time – 60 minutes

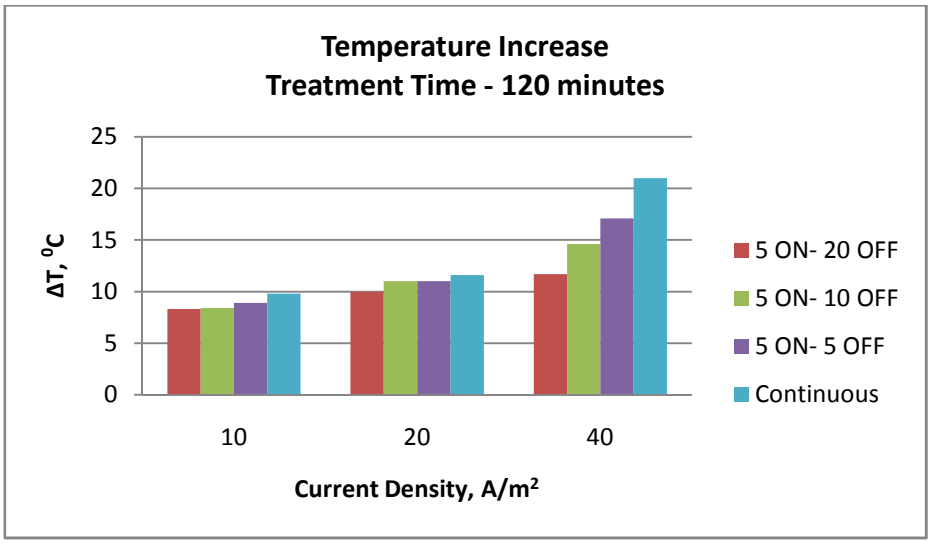

Figure 115 – Phase III - WWTP2 – Temperature increase – treatment time – 120 minutes

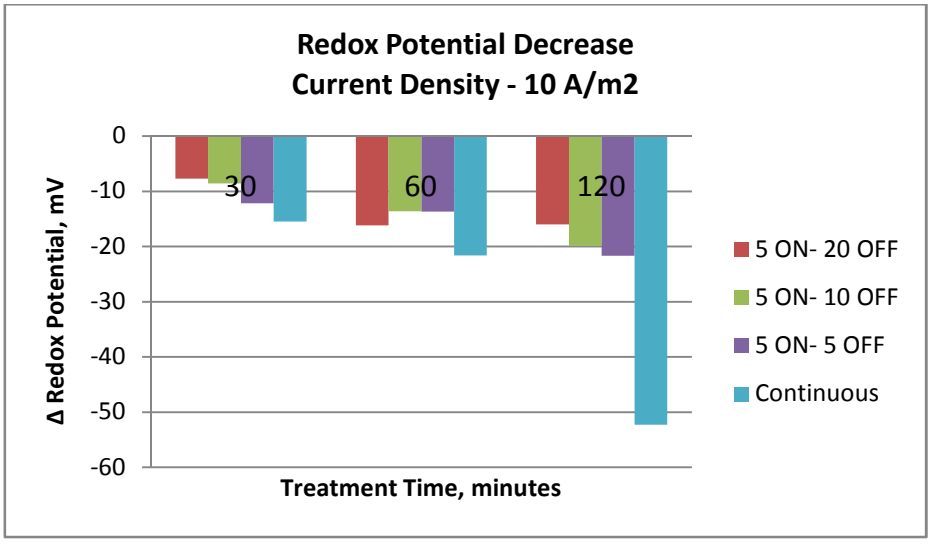

Figure 116 – Phase III - WWTP2 – Redox potential decrease – current density – 10 A/m^2

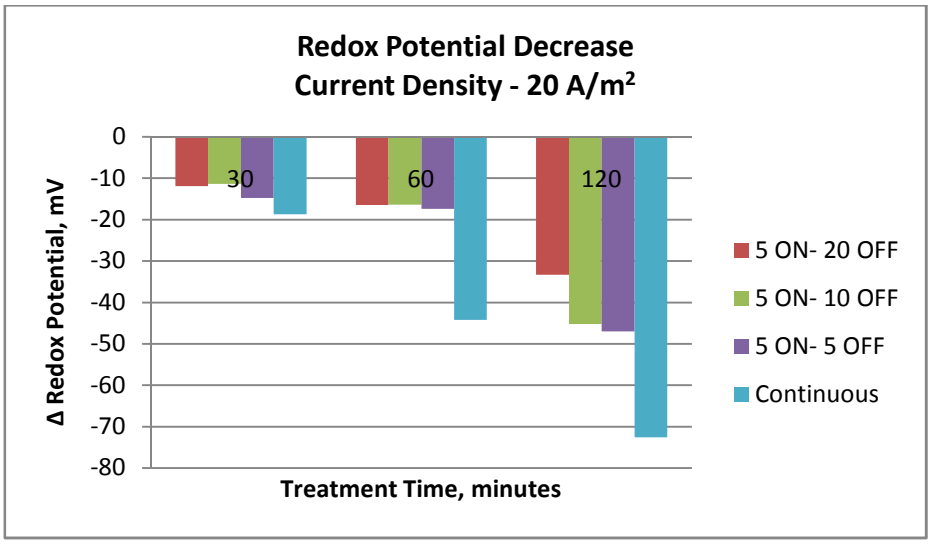

Figure 117 – Phase III - WWTP2 – Redox potential decrease – current density – 20 A/m²

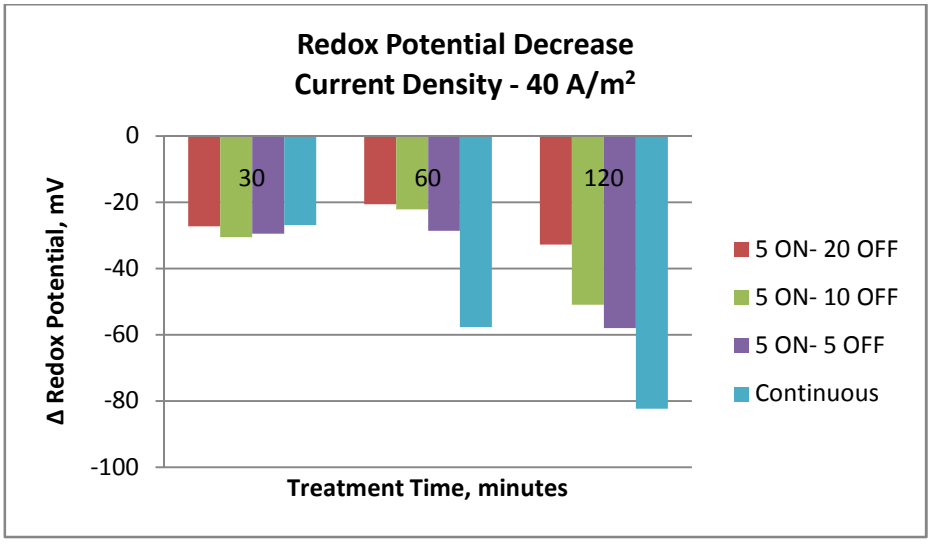

Figure 118 – Phase III - WWTP2 – Redox potential decrease – current density – 40 A/m²

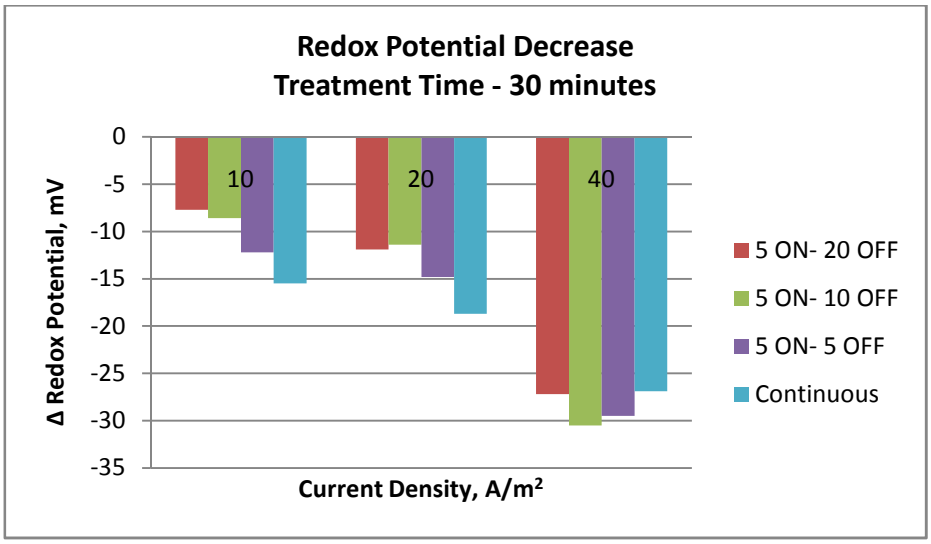

Figure 119 – Phase III - WWTP2 – Redox potential decrease – treatment time – 30 minutes

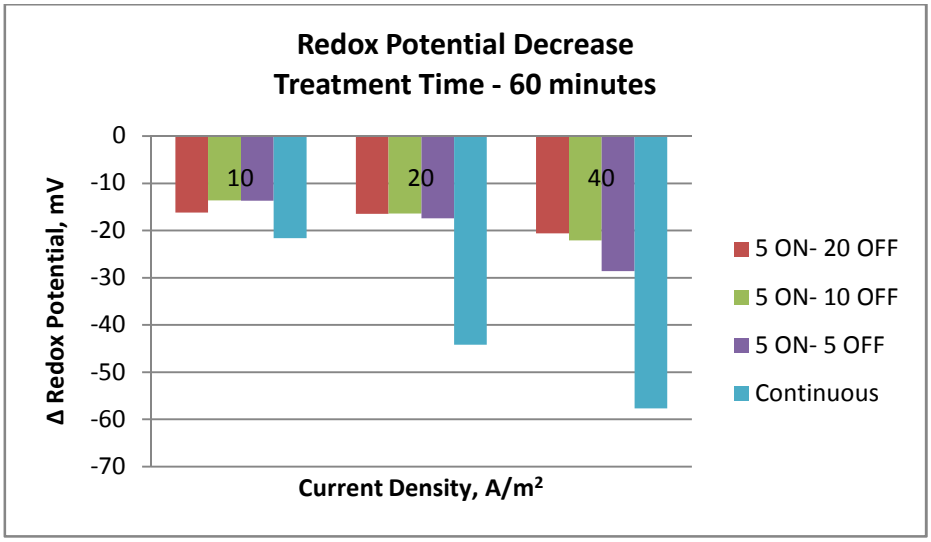

Figure 120 – Phase III - WWTP2 – Redox potential decrease – treatment time – 60 minutes

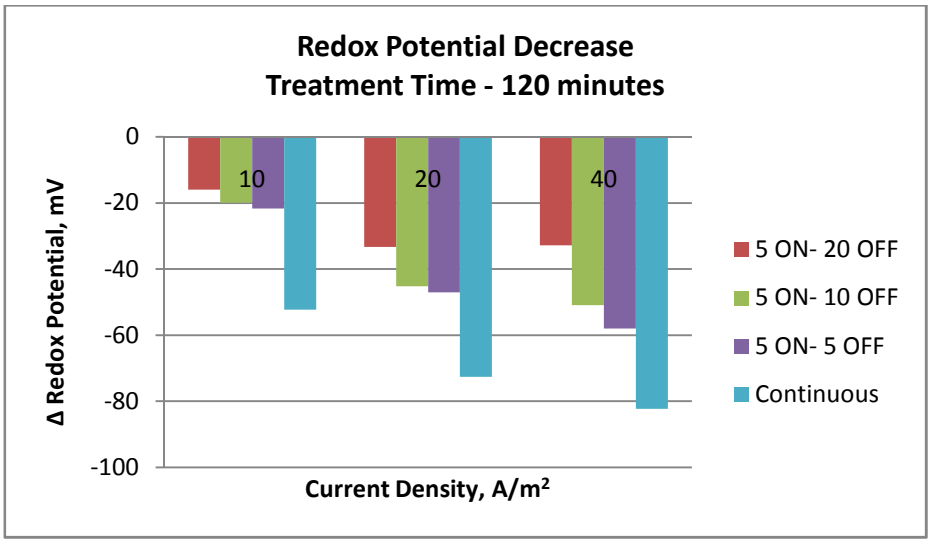

Figure 121 – Phase III - WWTP2 – Redox potential decrease – treatment time – 120 minutes

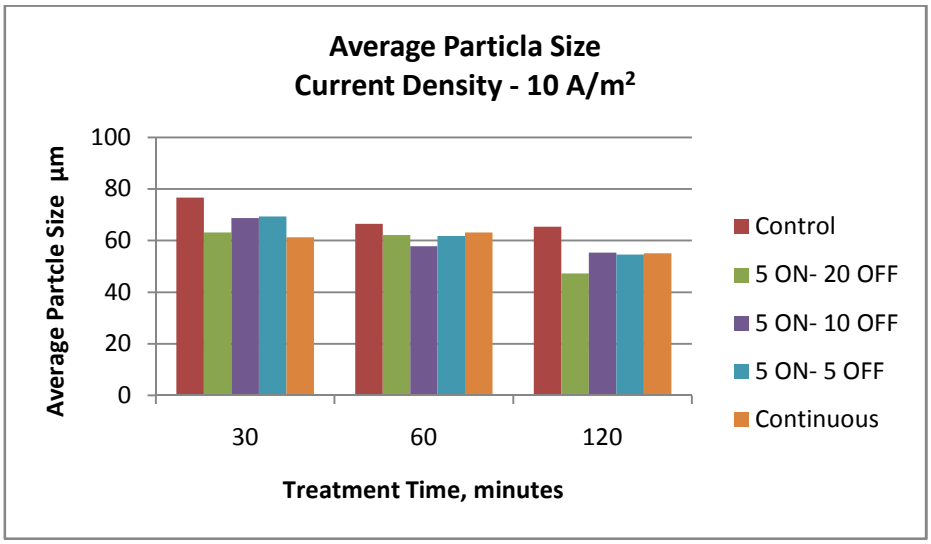

Figure 122 – Phase III - WWTP2 – Average particle size – current density – 10 A/m^2

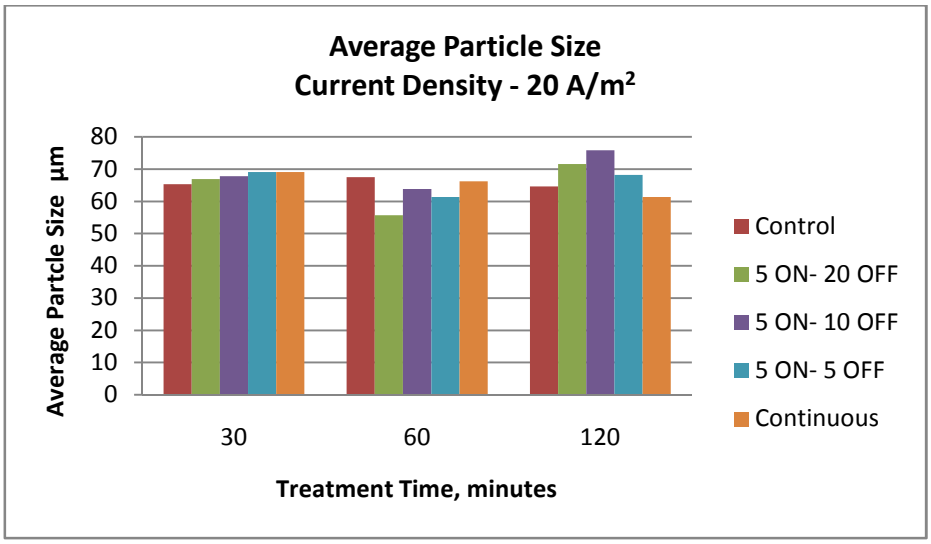

Figure 123 – Phase III - WWTP2 – Average particle size – current density – 20 A/m^2

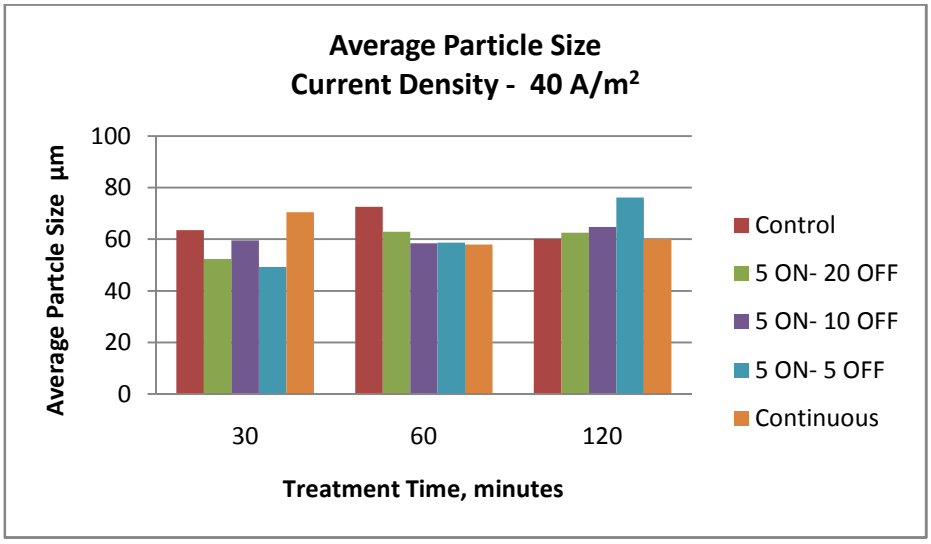

Figure 124 – Phase III - WWTP2 – Average particle size – current density – 40 A/m^2

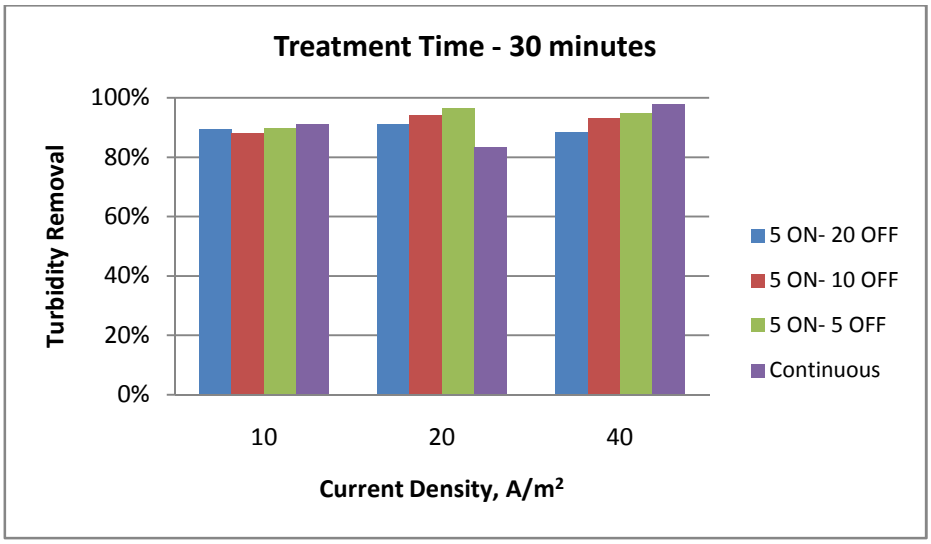

Figure 125 – Phase III - WWTP2 – Turbidity removal – treatment time – 30 minutes

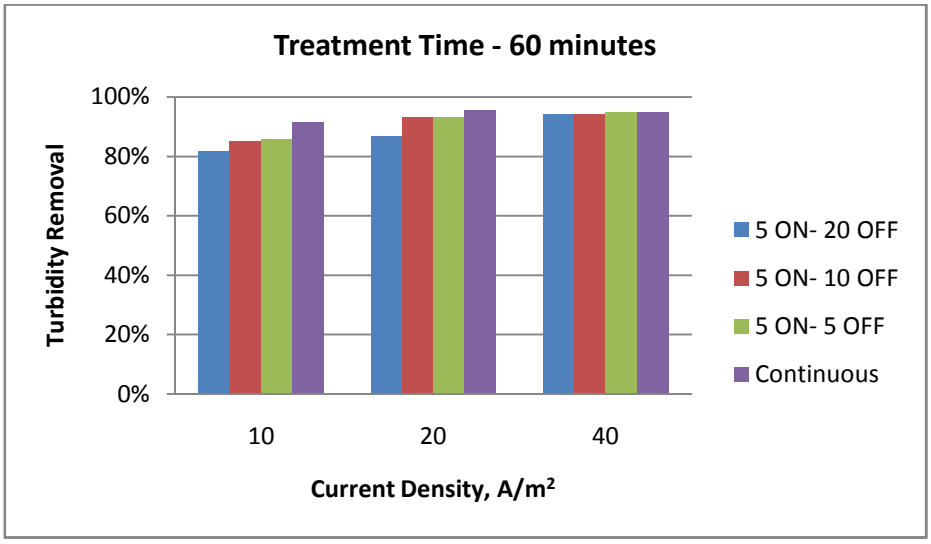

Figure 126 – Phase III - WWTP2 – Turbidity removal – treatment time – 60 minutes

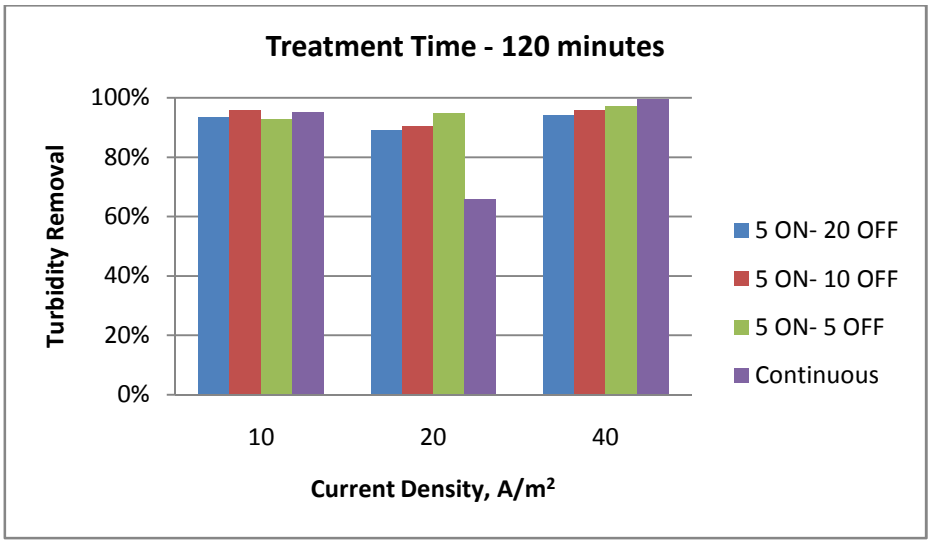

Figure 127 – Phase III - WWTP2 – Turbidity removal – treatment time – 120 minutes

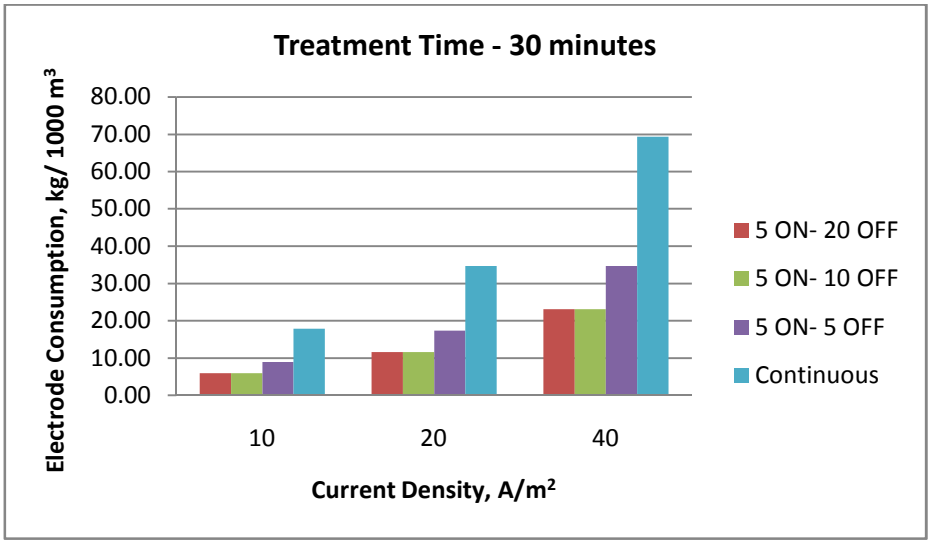

Figure 128 - Phase III - WWTP2 – Electrode consumption– treatment time - 30 minutes

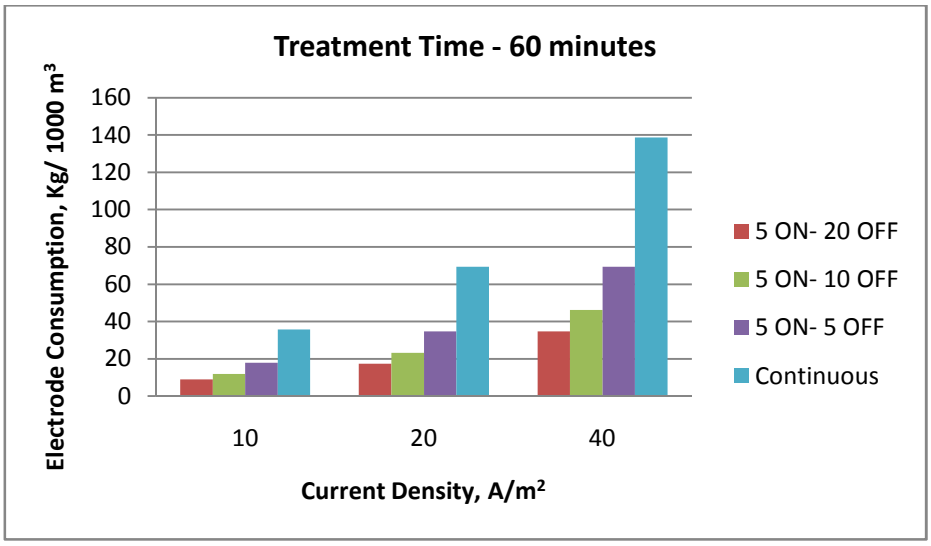

Figure 129 - Phase III - WWTP2 – Electrode consumption – treatment time - 60 minutes

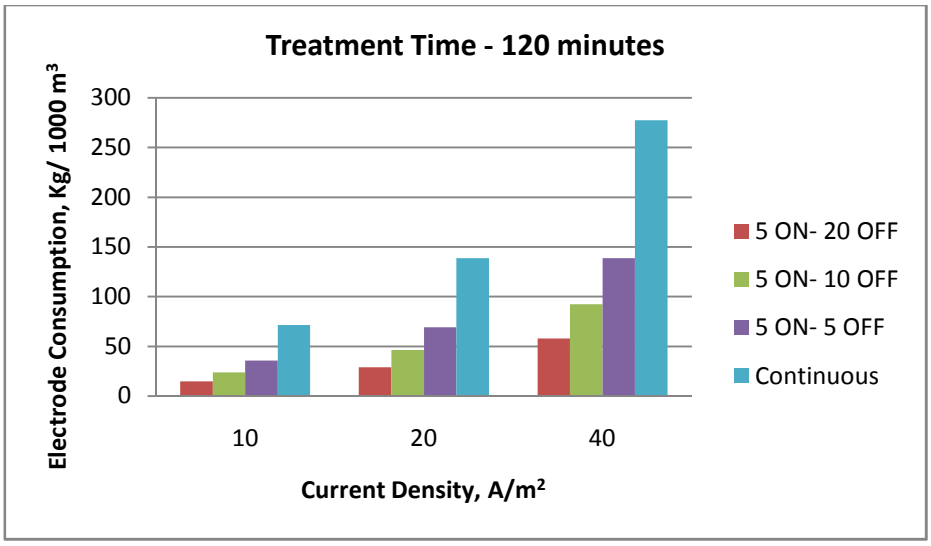

Figure 130 - Phase III - WWTP2 – Electrode consumption – treatment time - 120 minutes

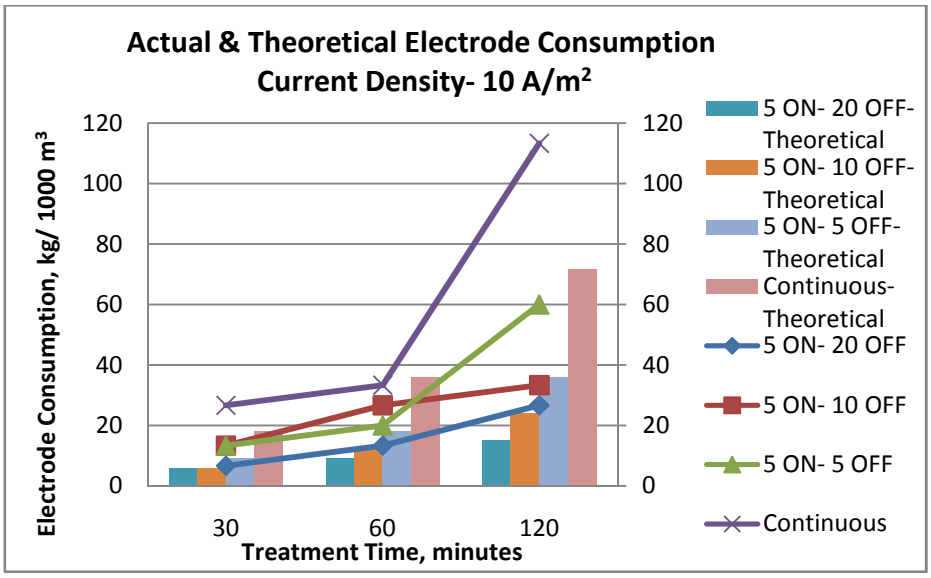

Figure 131- Phase III - WWTP2 – Actual and theoretical electrode consumption – Current Density- 10 A/m²

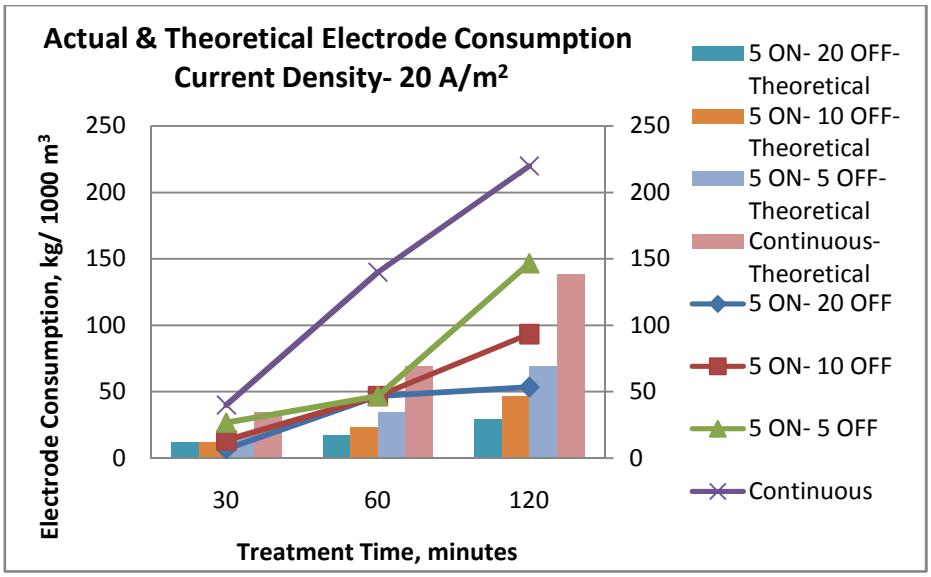

Figure 132 - Phase III - WWTP2 – Actual and theoretical electrode consumption – Current density - 20 A/m²

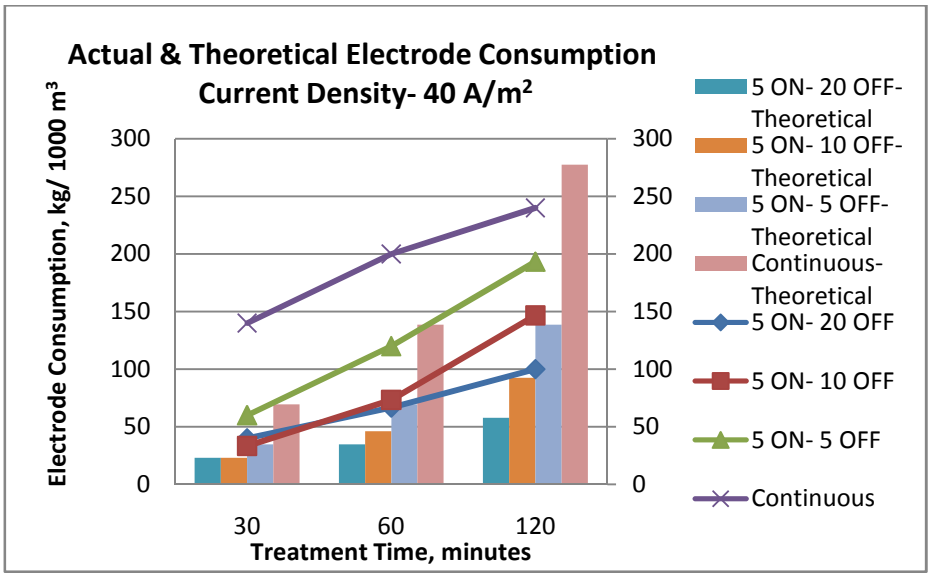

Figure 133 - Phase III - WWTP2 – Actual and theoretical electrode consumption – Current density - 40 A/m²

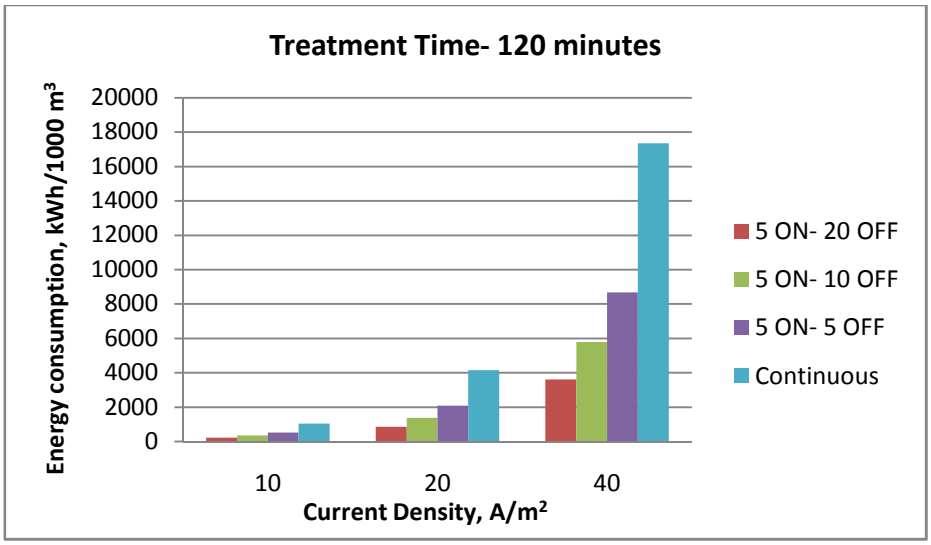

Figure 134 - Phase III - WWTP2 – Energy consumption – treatment time - 120minutes

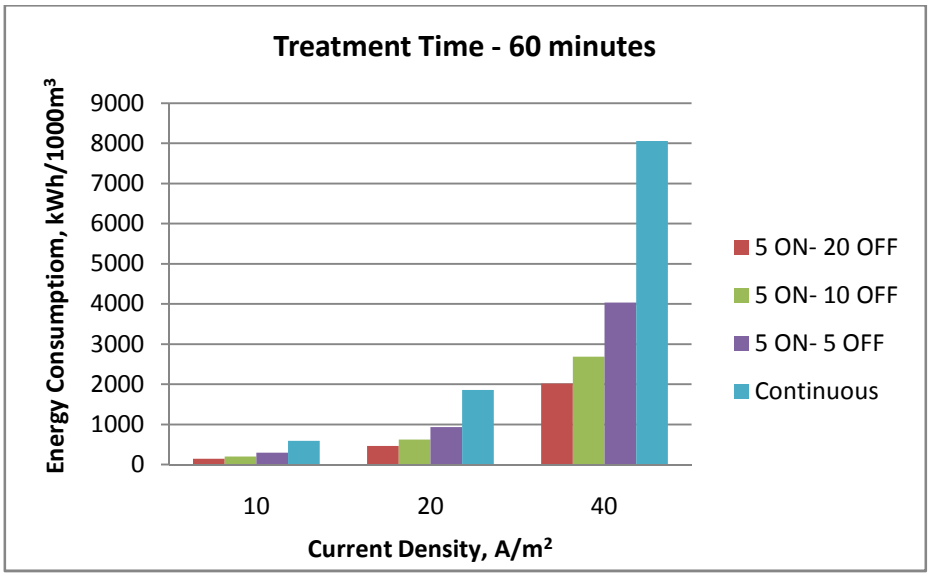

Figure 135 - Phase III - WWTP2 – Energy consumption – treatment time - 60 minutes

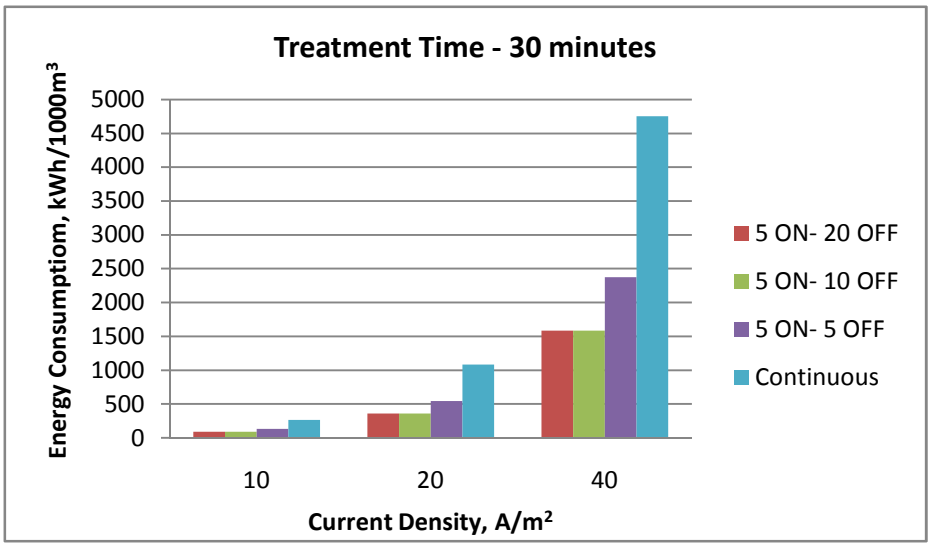

Figure 136 - Phase III - WWTP2 – Energy consumption – treatment time - 30 minutes

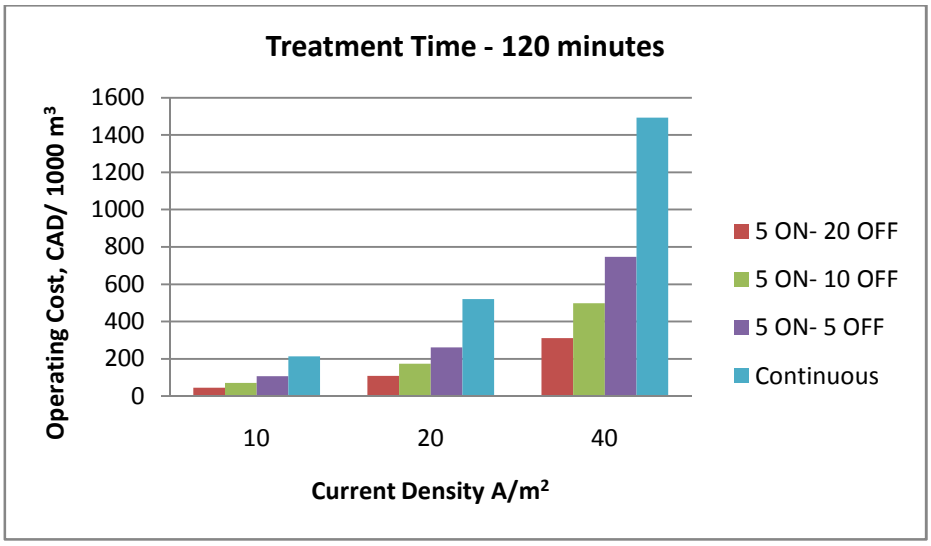

Figure 137 - Phase III - WWTP2 – Operating cost – treatment time - 120 minutes

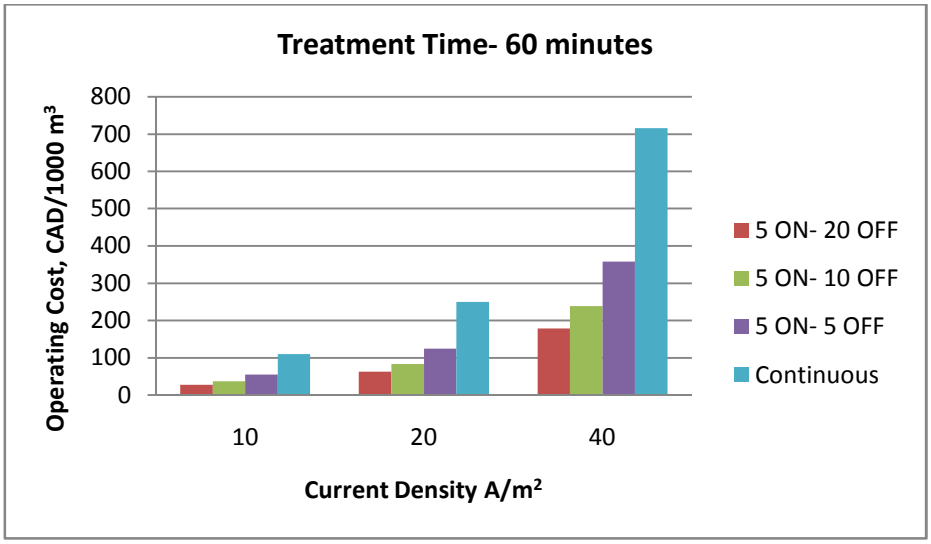

Figure 138 - Phase III - WWTP2 – Operating cost – treatment time - 60 minutes

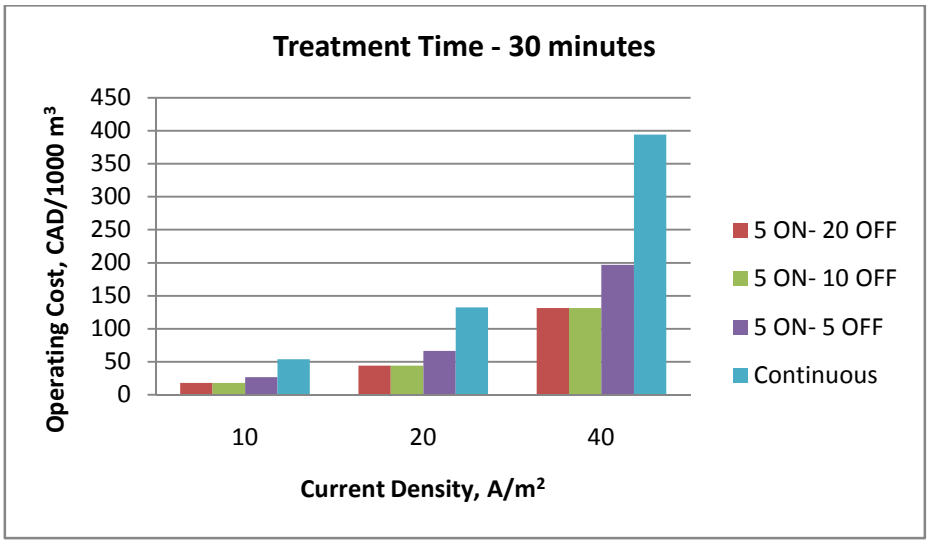

Figure 139 - Phase III - WWTP2 – Operating cost – treatment time - 30 minutes

Phase IV

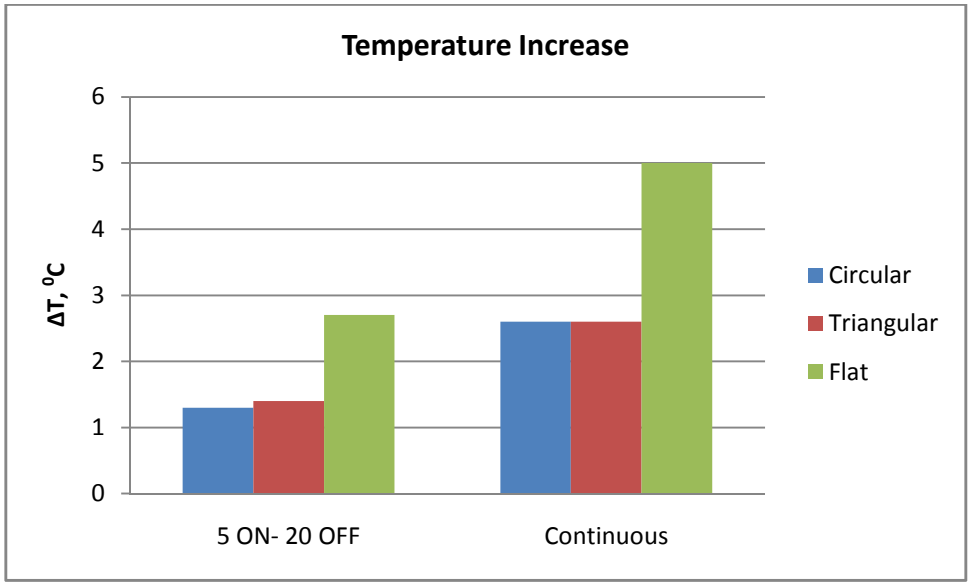

Figure 140 - Phase IV - Temperature increase - current density – 20 A/m^2

treatment time - 120 minutes

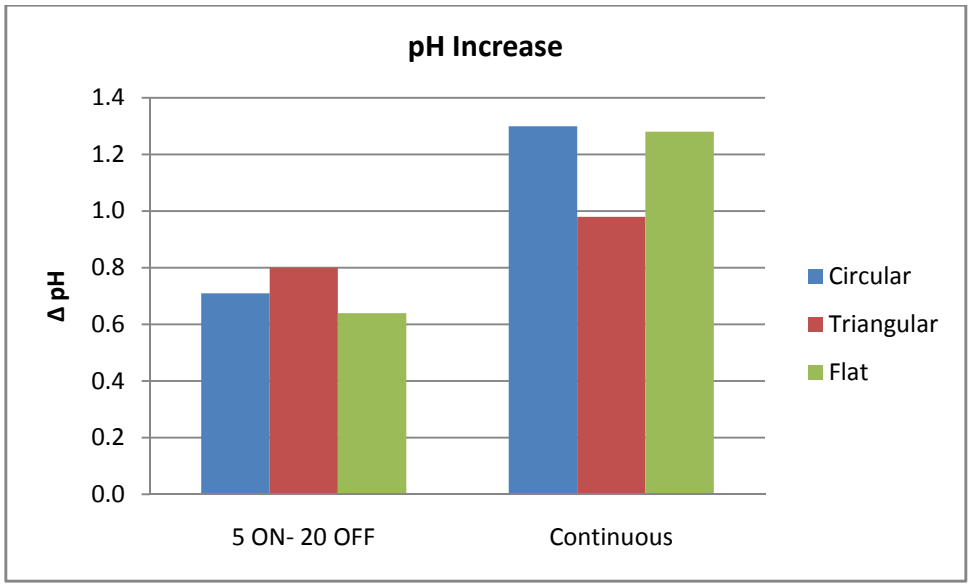

Figure 141 - Phase IV - pH increase - current density – 20 A/m^2 - treatment time - 120 minutes

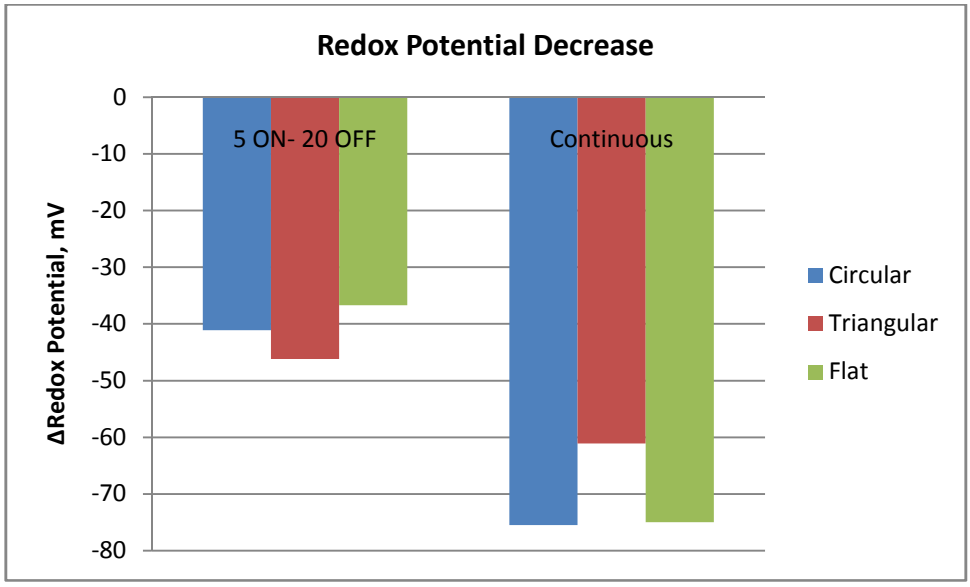

Figure 142 - Phase IV - Redox potential decrease - current density – 20 A/m^2 treatment time - 120 minutes

Appendix II - Additional photographs

Phase II

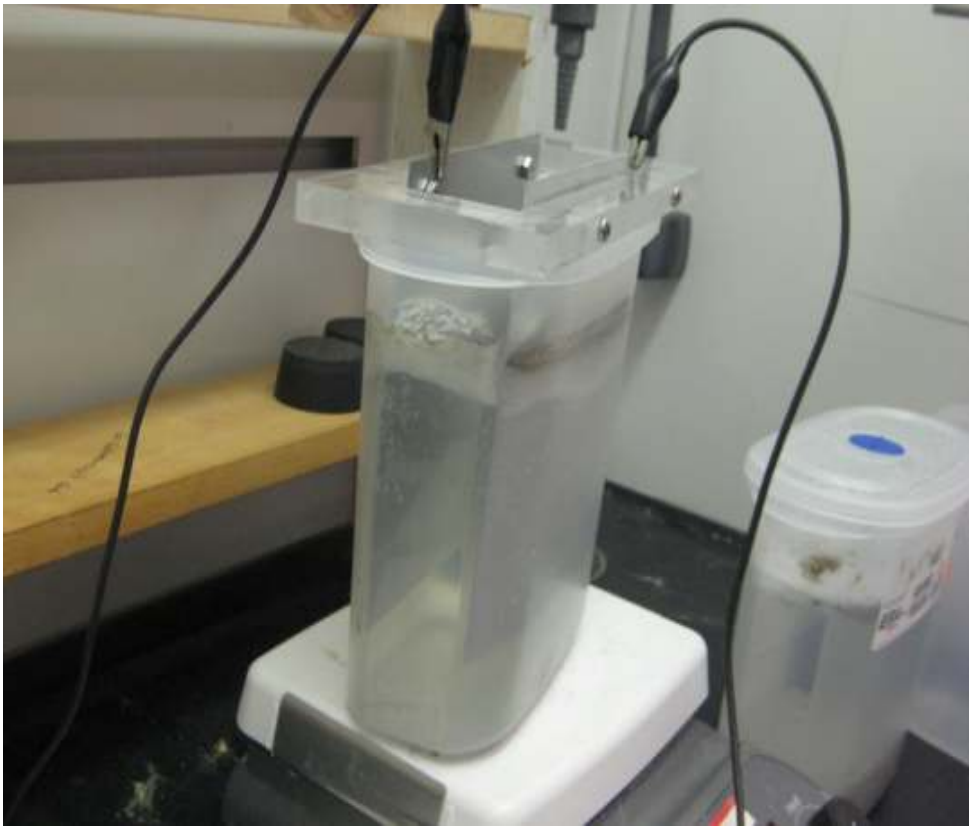

Figure 143 - Phase II - Flotation with salt addition - clear water column

0.5 V/cm & 0.05wt% NaCl

Figure 144 - Phase II - Thick and gelatinous flotation layer – clear water column

0.5 V/cm & 0.2 wt% NaCl

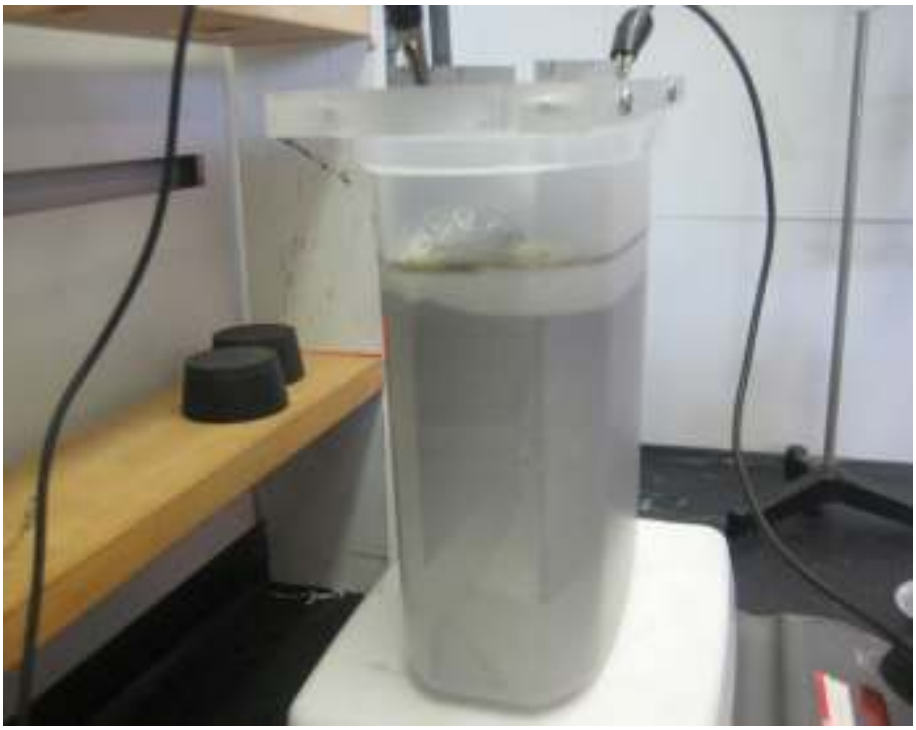

Figure 145 - Phase II - Excess aluminum release turns water turbid

2 V/cm & 0.2 wt% NaCl

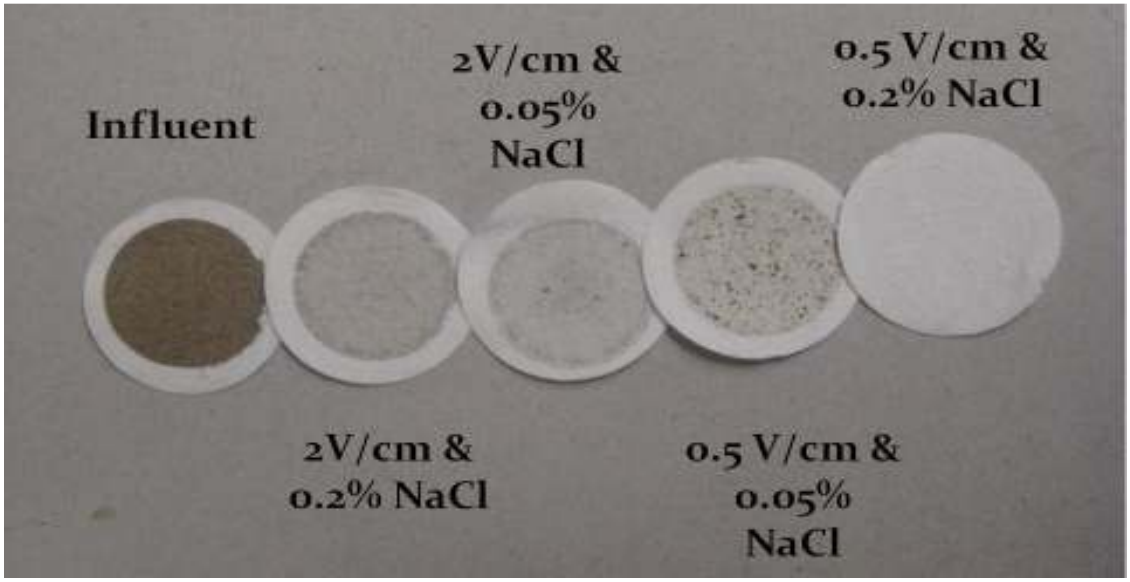

Figure 146 - Phase II- filter papers after filtering 50 ml of treated wastewater

Phase III

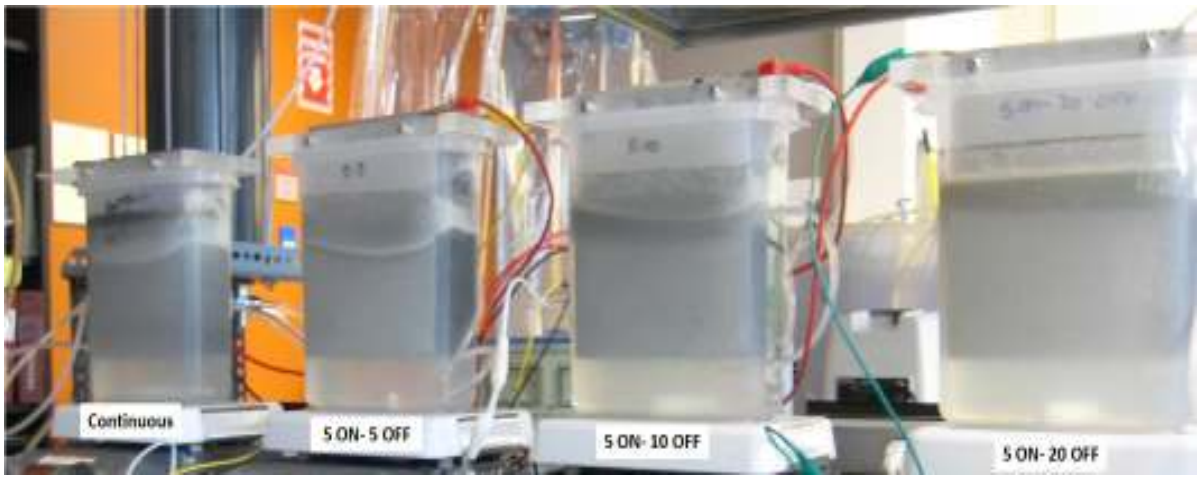

Figure 147 - Phase III - Flotation after 120 minutes of exposure to 40 A/m^2

Phase IV

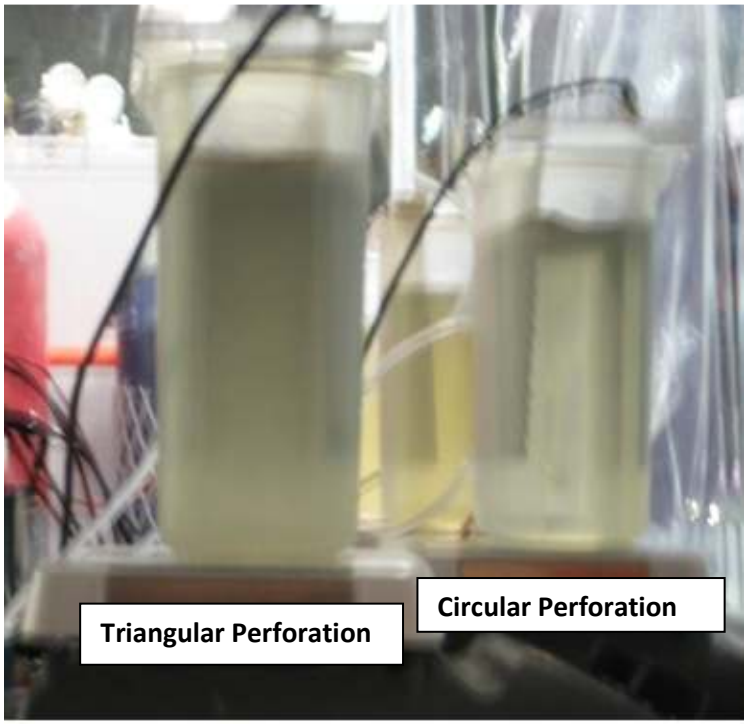

Figure 148 - Water column turning grey with triangular perforated anode - current density 20 A/m^2 - continuous mode - 120 minutes

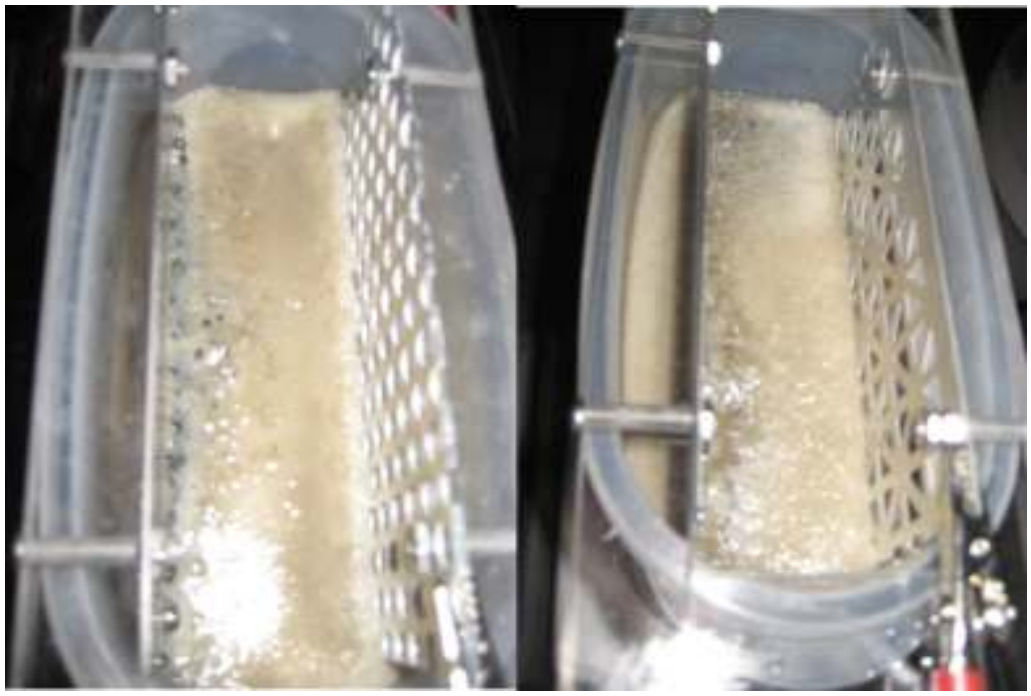

Figure 149 - Phase IV - Flotation at 120 minutes - continuous mode – 20 A/m^2

Circular (left), Triangular (right)

Appendix III - Sample calculations

Phase II

Table 17 - Phase II - Sample Calculations

Conditions Applied	ΔWt (g)	C_{Energy} (U*I*t)/v (kWh/m3)	C_{Salt} kg/m3	Salt CAD/kg	Energy CAD/kWh	Aluminum CAD/kg	Actual Operating CAD/m3
2V/cm- 0.2% NaCl	4.29	76.03	2	0.05	0.05	2.225	10.26
2V/cm- 0.05% NaCl	1.62	28.00	2	0.05	0.05	2.225	3.90
0.5V/cm- 0.2% NaCl	0.34	1.87	0.5	0.05	0.05	2.225	0.62
0.5V/cm- 0.05% NaCl	0.31	1.53	0.5	0.05	0.05	2.225	0.56

Phase III

Table 18 - Phase III - Sample Calculations- Current Density 10 A/m^2 - Treatment Duration - 30 minutes

J10t30								J10t30
	t (min)	U (V)	I (A)	z	$C_{electrode}$ (I*t*Mw)/(z*F*v)	Kg/m^3	C_{energy} (U*I*t)/v (kWh/m^3)	Operating Cost (CAD/m^3)
5'ON- 20'OFF	10	5	0.16	3	5.97	0.005965	0.089	0.018
5'ON- 10'OFF	10	5	0.16	3	5.97	0.005965	0.089	0.018
5'ON- 5'OFF	15	5	0.16	3	8.95	0.008948	0.133	0.027
Continuous	30	5	0.16	3	17.90	0.017896	0.267	0.054

Table 19 - Phase III - Sample Calculations- Current Density 10 A/m^2- Treatment Duration- 60 minutes

J10t60								J10t60
	t (min)	U (V)	I (A)	z	$C_{electrode}$ (I*t*Mw)/(z*F*v)	Kg/m^3	C_{energy} (U*I*t)/v (kWh/m^3)	Operating Cost (CAD/m^3)
5'ON- 20'OFF	15	5.5	0.16	3	8.95	0.008948	0.147	0.028
5'ON- 10'OFF	20	5.5	0.16	3	11.93	0.011931	0.196	0.037
5'ON- 5'OFF	30	5.5	0.16	3	17.90	0.017896	0.293	0.055
Continuous	60	5.5	0.16	3	35.79	0.035793	0.587	0.110

Table 20 - Phase III - Sample Calculations - Current Density 10 A/m^2- Treatment Duration- 60 minutes

J10t120								J10t120
	t (min)	U (V)	I (A)	z	$C_{electrode}$ (I*t*Mw)/(z*F*v)	Kg/m^3	C_{energy} (U*I*t)/v (kWh/m^3)	Operating Cost (CAD/m^3)
5'ON- 20'OFF	25	4.9	0.16	3	14.91	0.014914	0.218	0.045
5'ON- 10'OFF	40	4.9	0.16	3	23.86	0.023862	0.348	0.071
5'ON- 5'OFF	60	4.9	0.16	3	35.79	0.035793	0.523	0.107
Continuous	120	4.9	0.16	3	71.59	0.071585	1.045	0.214